

Mechanisms of GABA_A and Glycine Receptor Analgesia in the
Spinal Dorsal Horn: *In Vitro* Models as Translational Platforms for
Drug Discovery

Natalie Helen Griffiths

Submitted in accordance with the requirements for the degree of

Doctor of Philosophy

University of Leeds

School of Biomedical Sciences

November 2015

Declaration

The candidate confirms that the work submitted is her own and that appropriate credit has been given where reference has been made to the work of others.

This copy has been supplied on the understanding that is copyright material and that no quotation from the thesis may be published without proper acknowledgement.

© 2016 The University of Leeds and Natalie Helen Griffiths

Acknowledgements

Firstly I would like to thank my supervisor Professor Anne King for her support and guidance throughout my PhD, during the ups and downs of the past 4 years. Thank you to my industrial supervisor Dr Sarah Nickolls for her expert guidance on the research I completed at Pfizer, Cambridge.

I could not have managed without the excellent knowledge and technical expertise of Stuart Prime during my Pfizer placement, thank you Stuart. Thank you also to the other researchers at Pfizer who assisted me during my placement, including Sian Humpherys, Clara Stead, Peter Cox and Gordon McMurray.

Thank you to those who helped me at the University of Leeds, particularly Dr Chris Kay and all those from the Gamper Lab. You all helped to provide some sanity over the years and some much needed friendship.

I would like to give a special thank you to my parents, who have provided so much emotional support and guidance from the very beginning of this PhD despite the distance apart. Finally, I am forever grateful to Tommaso Iannitti for helping me in every way possible to complete my thesis. I could not have met a more supportive boyfriend.

Abstract

Available analgesics do not always provide adequate pain relief and are often associated with a significant side-effect profile. Following reports of a loss of inhibitory signalling in the spinal dorsal horn (DH) network in persistent pain conditions, γ -amino butyric acid type A (GABA_A) and glycine receptors have been identified as promising targets. The present study assesses two *in vitro* models for their suitability for screening novel analgesics targeting GABA_A and glycine receptors. Firstly, the embryonic cultured spinal DH cell model and secondly an acute rat spinal cord slice model.

Immunofluorescence characterisation of the spinal DH culture illustrated that this model displays many similarities with the *in vivo* spinal DH. Immunofluorescence and RT-PCR demonstrated the presence of GABA_A and glycine receptor subunits in the spinal DH culture. Calcium imaging and extracellular multi-electrode array (MEA) recording techniques were utilised to study the effect of GABA_A, GABA_B and glycine receptor drugs on the spinal DH culture network activity. All drugs tested significantly modulated the culture's spontaneous firing. A further study assessed whether lentivirus and Accell siRNA mediated glycine receptor α subunit gene silencing modulates calcium responses in the DH culture model. The lentiviruses had low transfection efficiencies and caused cell death, however Accell siRNA transfection was successful and significantly decreased baseline spontaneous activity compared to untreated cultures.

Single electrode and MEA extracellular recordings were performed with the acute spinal cord slice model. GABA_A, GABA_B and glycine receptor drugs modulated 4-aminopyridine-induced hyperexcitability in the *substantia gelatinosa* lamina of the slices. The MEA recordings illustrated that 4-aminopyridine-induced activity manifested more prominently in the DH than the ventral horn (VH) and that the DH

network activity was highly synchronous. Taken together, these findings demonstrate that these *in vitro* models provide suitable platforms to test novel analgesics targeting GABA_A and glycine receptors in the spinal DH network.

Table of Contents

1	Introduction.....	1
1.1	Pain and Nociception.....	2
1.2	Loss of Inhibition in the Superficial Spinal Dorsal Horn in Chronic Pain Conditions.....	4
1.2.1	Spinal Dorsal Horn Inhibitory Interneuron Cell Death in Pain Conditions.....	4
1.2.2	Decrease in GABA and Glycine Synthesis and Release in Pain Conditions.....	5
1.2.3	Modulation of GABA and Glycine Receptor Activity.....	6
1.2.4	Altered Chloride Homeostasis in the Spinal Dorsal Horn.....	7
1.3	Classification of Spinal Dorsal Horn Cell Types.....	8
1.3.1	Spinal Dorsal Horn Cell Classification.....	9
1.3.2	GABA _A Receptor Expression in the Spinal Dorsal Horn.....	13
1.3.3	Glycine Receptor Expression in the Spinal Dorsal Horn.....	17
1.4	GABA _A Receptor Pharmacology.....	20
1.5	Glycine Receptor Pharmacology.....	22
1.6	Rhythmic Oscillations in Central Nervous System Networks.....	22
1.7	Investigating the Spinal Dorsal Horn Neuronal Network: <i>In Vitro</i> Models.....	28
1.7.1	In Vivo Spinal Cord Recordings.....	28
1.7.2	In Vitro Spinal Cord Slices.....	29
1.7.3	Primary Cell Culture of the Spinal Dorsal Horn.....	31
1.8	Objectives.....	32
2	Characterisation of the Embryonic Spinal Dorsal Horn Cell Culture Model.....	34

2.1	Introduction.....	35
2.1.1	Aims	36
2.2	Methods.....	37
2.2.1	Embryonic Dorsal Horn Primary Cell Culture	37
2.2.2	Fluorescent Calcium Imaging with Cultured Dorsal Horn Cells	41
2.2.3	Culture Dorsal Horn Cell Immunofluorescence	42
2.2.4	Imaging and Analysis.....	43
2.2.5	Quantitative Real-Time PCR.....	46
2.2.6	Analysis of Relative Quantification RT-PCR	50
2.2.7	Absolute Quantification of Glycine Receptor Subunits	51
2.2.8	Analysis of the Absolute Quantification RT-PCR Data	52
2.3	Results	53
2.3.1	Optimisation of the Embryonic Rat Spinal Dorsal Horn Culture.....	53
2.3.2	Characterisation of the Spinal Dorsal Horn Cell Culture Model: Neuronal and Non-Neuronal Cells	57
2.3.3	Excitatory and Inhibitory Interneurons in the Spinal Dorsal Horn Cell Culture Model	57
2.3.4	Neurochemically Defining Neuronal Cell Populations in the Dorsal Horn Culture	61
2.3.5	GABA _A Receptor α Subunit Expression in the Embryonic Dorsal Horn Culture	63
2.3.6	Glycine Receptor α Subunit Expression in the Dorsal Horn Culture..	66
2.3.7	Quantitative Real-Time PCR with Human Spinal Cord and Culture Dorsal Horn Cells.....	68

2.4	Discussion	74
2.4.1	The Spinal Dorsal Horn Culture has a High Proportion of Neuronal Cells	74
2.4.2	Excitatory and Inhibitory Interneurons in the Spinal Dorsal Horn Culture	74
2.4.3	The Spinal Dorsal Horn Culture Contains Parvalbumin and nNOS Neuronal Cells	75
2.4.4	Inhibitory Interneurons in the Spinal Dorsal Horn Culture Express KCC2	77
2.4.5	All GABA _A Receptor α Subunits are Expressed in the Spinal Dorsal Horn Culture	78
2.4.6	Differences in Glycine Receptor α Subunit Expression in the Spinal Dorsal Horn Culture Compared to Human Spinal Cord	79
2.4.7	Conclusions	80
3	Calcium Response as a Measure of the Embryonic Spinal Dorsal Horn Network	82
3.1	Introduction	83
3.1.1	Neuronal Primary Cell Culture	83
3.1.2	Calcium Imaging Techniques to Measure Neuronal Network Activity	84
3.1.3	Aims	85
3.2	Methods	86
3.2.1	Embryonic Dorsal Horn Primary Cell Culture	86
3.2.2	Flexstation Calcium Imaging with Cultured Dorsal Horn Cells	86
3.2.3	Flexstation Data Analysis	88

3.3	Results	90
3.3.1	Optimisation of the Flexstation Calcium Imaging with the Cultured Embryonic Spinal Dorsal Horn Cells	90
3.3.2	The Role of GABA _A Receptor Signalling in Dorsal Horn Activity	93
3.3.3	The Role of the Glycine Receptor in the Dorsal Horn Activity	93
3.4	Discussion	102
3.4.1	GABA _A and Glycine Receptor Agonists and Antagonists Modulate the Spinal Dorsal Horn Culture Activity	103
3.4.2	Conclusions.....	106
4	siRNA Knockdown of Glycine Receptor α Subunits in the Dorsal Horn Cell Culture Model.....	107
4.1	Introduction.....	108
4.1.1	RNA Interference Mechanism.....	108
4.1.2	Glycine Receptor Subunit Gene Silencing	110
4.1.3	Aims	112
4.2	Methods.....	113
4.2.1	Lentiviral shRNA Preparation.....	113
4.2.2	Lentiviral Transfection.....	114
4.2.3	Accell siRNA Preparation and Transfection	116
4.2.4	Calcium Imaging Assay of the Dorsal Horn Culture Transduced with Lentivirus or Accell siRNA.....	118
4.2.5	Real-Time PCR with Accell siRNA Transfected Dorsal Horn Cells..	120
4.2.6	Real-Time PCR Analysis	120
4.3	Results	121

4.3.1	Lentivirus Transfection.....	121
4.3.2	Activity of the Dorsal Horn Cultures Transfected with Lentivirus	127
4.3.3	Accell siRNA Transfection	137
4.3.4	Activity of the Dorsal Horn Cultures Transfected with Accell siRNA	142
4.4	Discussion	155
4.4.1	Glycine Receptor α Subunit Gene Silencing Reduces Dorsal Horn Network Activity	156
4.4.2	Conclusions.....	158
5	Extracellular Single Electrode Spinal Cord Slice Recordings.....	159
5.1	Introduction.....	160
5.1.1	4-Aminopyridine-Induced Rhythmic Activity in the Central Nervous System	160
5.1.2	Aims	161
5.2	Methods.....	163
5.2.1	Spinal Cord Slices	163
5.2.2	Single-Electrode Extracellular Slice Recordings	165
5.2.3	Spike 2 Data Analysis.....	172
5.2.4	Statistics.....	173
5.2.5	Materials.....	176
5.3	Results	177
5.3.1	GABA _A Receptor Agonist and Antagonist Effects on Spinal Dorsal Horn Activity	177
5.3.2	GABA _B Receptor Compound Effects on Spinal Dorsal Horn Activity.....	192

5.3.3	Glycine Receptor Agonist and Antagonist Effects on Spinal Dorsal Horn Activity	198
5.4	Discussion	207
5.4.1	4-AP Activity and LTP.....	207
5.4.2	GABA _A Receptor Agonists Decrease Rhythmic Activity and Population Spikes with the Exception of GABA	208
5.4.3	GABA _A Receptor Antagonists Decrease 4-AP-Induced Rhythmic Activity and Population Spikes in the SG of the Spinal Cord	215
5.4.4	GABA _B Receptor Agonist Inhibits and Antagonist Enhances 4-AP-Induced Rhythmic Activity and Population Spikes.....	219
5.4.5	Glycine receptor compound effects on spinal dorsal horn activity ...	220
5.4.6	Extracellular Recordings from Spinal Cord Slice Dorsal Horn as a Model for Investigating the Network.....	221
6	Multi-Electrode Array with Spinal Cord Slices and Cultured Dorsal Horn Cells.....	223
6.1	Introduction.....	224
6.1.1	Aims	226
6.2	Methods.....	228
6.2.1	Multi-Electrode Extracellular Spinal Cord Slice Recordings	228
6.2.2	MC Rack MEA Data Analysis	230
6.2.3	Culturing Embryonic Dorsal Horn Cells on the MED64 Arrays	234
6.2.4	MED64 Recordings with Cultured Dorsal Horn Cells	234
6.2.5	Analysis of MED64 Recordings with Cultured Dorsal Horn Cells	237
6.3	Results	238

6.3.1	MEA Recordings Show 4-AP Induces Population Spikes throughout the Dorsal Horn and Ventral Horn of Spinal Cord Slices	238
6.3.2	MEA Recordings with Cultured Dorsal Horn Cells Detect Spontaneous Activity	256
6.4	Discussion	265
6.4.1	MEA Spinal Cord Slice Recordings Detected 4-AP-Induced Activity Throughout all Laminae of the Dorsal and Ventral Horns Hyperexcitability ...	265
6.4.2	4-AP-Induced Activity in Spinal Cord Slices is Modulated by GABA _A Receptor Agonists and Antagonists	267
6.4.3	4-AP Activity in Spinal Cord Slices is Modulated by GABA _B Receptor Agonist Baclofen and Antagonist 2-Hydroxysaclofen	269
6.4.4	4-AP Activity in Spinal Cord Slices is Modulated by Glycine Receptor Agonist and Antagonists	270
6.4.5	KCC2 Inhibitor VU0240551 Increases 4-AP Spike Amplitude in the Spinal Cord.....	272
6.4.6	Cultured Dorsal Horn Cells on the MEA Detects Synchronous and Non-Synchronous Electrical Activity	273
6.4.7	Comparing the Potential of the Spinal Cord Slice and Spinal Dorsal Horn Culture Models.....	274
7	General Discussion.....	276
7.1	Outline.....	277
7.2	Primary Cell Culture of the Spinal Dorsal Horn	277
7.2.1	Characterisation of the Spinal Dorsal Horn Culture.....	277
7.2.2	GABAergic and Glycinergic Neurotransmission Regulate Spinal Dorsal Horn Culture Rhythmic Oscillations	280

7.2.3	Glycine Receptor siRNA Gene Silencing in the Spinal Dorsal Horn Culture	281
7.3	Spinal Cord Slice Recordings	282
7.3.1	GABA _A and Glycine Receptors Modulate the 4-AP-Induced Rhythmic Activity	282
7.4	Conclusions.....	286

List of Figures

Chapter 1

Figure 1.1	The anatomy of the pain pathway	3
Figure 1.2	A figure of a transverse spinal cord section with the laminae defined, and a list of some of the classified neurons and interneurons present in laminae I and II. The significant properties of each of the classes of neurons and interneurons in these laminae are included.	11
Figure 1.3	The structure of the GABA _A receptor	16
Figure 1.4	The glycine receptor structure	19
Figure 1.5	Two proposed mechanisms for the generation of neuronal network oscillations. (A) The ING mechanism involves interconnected inhibitory interneurons which mutually inhibit each other and generate a summated IPSP. This synchronises the activity of the postsynaptic excitatory interneurons and subsequently the network. (B) The PING oscillation mechanism requires an excitatory interneuron with a reciprocally inhibiting inhibitory interneuron. This generates rhythmic oscillations from an asynchronous input by restraining the output of the excitatory interneuron to the time in which the excitatory interneuron is recovered from the IPSP generated from the stimulation of the inhibitory interneuron.	27

Chapter 2

Figure 2.1	Flow diagram of the spinal DH cell culture protocol	40
Figure 2.2	IF control experiment images	44
Figure 2.3	Embryonic rat spinal DH cell culture at 14 DIV before and after optimisation	54
Figure 2.4	Progression of the rat embryonic spinal DH cell culture from day 0, immediately after plating the cells, to 1 DIV, 8 DIV and 14 DIV.	55
Figure 2.5	An example of the spontaneous, synchronous firing of the embryonic spinal DH cell culture	56
Figure 2.6	NeuN, GFAP and Iba1 staining in the rat embryonic DH cell culture	58
Figure 2.7	Embryonic DH culture stained with NeuN and vGluT2	59

Figure 2.8	The embryonic DH culture stained for NeuN and GAD 65 and 67	59
Figure 2.9	Double immunolabelling of the spinal DH culture with NeuN and GlyT2	60
Figure 2.10	The cultured rat embryonic spinal DH cells co-stained with (A) GAD65-67 and PV, and (B) GlyT2 and PV	62
Figure 2.11	The embryonic rat spinal DH culture double labelled with nNOS and gephyrin	62
Figure 2.12	The embryonic rat spinal DH culture stained for KCC2 and gephyrin	63
Figure 2.13	The embryonic DH cell culture with double immune-labelling of NeuN and the GABA _A receptor α 1 subunit	64
Figure 2.14	The rat embryonic spinal DH cell culture stained with GABA _A receptor α 2 subunit antibody and NeuN	64
Figure 2.15	Staining of the embryonic DH culture for GABA _A receptor α 3 subunit and NeuN	65
Figure 2.16	The embryonic rat DH culture stained with the antibody for GABA _A receptor α 4 subunit and NeuN	65
Figure 2.17	Staining of the spinal DH culture for the GABA _A receptor α 5 subunit and NeuN	65
Figure 2.18	The rat embryonic DH culture stained with the GABA _A receptor α 6 subunit antibody and NeuN	66
Figure 2.19	The embryonic DH culture stained with NeuN and the glycine receptor α 1 subunit	67
Figure 2.20	The DH culture stained with NeuN and the glycine receptor α 2 subunit	67
Figure 2.21	The DH culture stained with NeuN and glycine receptor α 3 subunit	68
Figure 2.22	The relative expression of each of the GABAA receptor α subunits (GABRA1-6) in the rat spinal DH culture (A) and in the adult human spinal cord (B)	70
Figure 2.23	The relative expression of each of the glycine receptor α subunits (Glr1-4) and β subunit (Glrb) in the rat spinal DH culture (A) and in the human spinal cord (B)	71

Figure 2.24	The standard curves from each of the absolute quantification RT-PCR experiments	72
Chapter 3		
Figure 3.1	The effect of DMSO on the embryonic spinal DH culture baseline spontaneous activity	91
Figure 3.2	Spontaneous firing of the DH culture detected by using two different calcium imaging systems	92
Figure 3.3	Inhibition of the DH culture spontaneous activity by GABA _A receptor agonists	94
Figure 3.4	GABA _A receptor PAM, diazepam decreases the spontaneous activity of the spinal DH culture	95
Figure 3.5	The effects of GABA _A receptor antagonists' bicuculline and gabazine on the DH culture activity	96
Figure 3.6	The actions of GABA _B receptor agonist and antagonist on the DH cell culture spontaneous activity	97
Figure 3.7	Glycine receptor agonist effects on the DH culture spontaneous activity	98
Figure 3.8	The effect of the GlyT1 antagonist CP-802079 addition on the DH culture spontaneous activity	99
Figure 3.9	The effect of strychnine and gelsemine on the spontaneous activity of the spinal DH culture	100
Figure 3.10	The effect of blocking the KCC2 co-transporter in the spinal DH culture	101
Chapter 4		
Figure 4.1	Gene silencing by transfection of shRNA using a lentiviral vector	110
Figure 4.2	Image of the DH culture infected with the glycine receptor $\alpha 3$ lentivirus shRNA with TurboGFP tag	116
Figure 4.3	Images taken of DH cultures at 13 DIV transfected with lentivirus and untreated	122

Figure 4.4	Images of a DH culture transfected with the control lentivirus with scrambled shRNA	123
Figure 4.5	Images of a DH culture transfected with the lentivirus with <i>Gira1</i> shRNA	124
Figure 4.6	Images of a DH culture transfected with the lentivirus with <i>Gira2</i> shRNA	125
Figure 4.7	Images of a DH culture transfected with the <i>Gira3</i> lentivirus shRNA	126
Figure 4.8	Comparison of the baseline activity of the cultures transfected with each of the lentiviruses to the untreated DH culture	130
Figure 4.9	The activity of the DH culture not transfected with lentivirus, analysing both the area under the curve and the spike frequency of the baseline activity, the activity in presence of strychnine and glycine	131
Figure 4.10	The activity of the DH cultures transfected with the control scrambled lentivirus at baseline and in the presence of strychnine and glycine	132
Figure 4.11	The activity of the DH cultures transfected with the <i>Gira1</i> lentivirus, and their responses to strychnine and glycine	133
Figure 4.12	The activity of <i>Gira2</i> lentivirus transfected DH cultures and their responses to strychnine and glycine	134
Figure 4.13	The activity of <i>Gira3</i> lentivirus transfected DH cultures and their responses to addition of strychnine and glycine	135
Figure 4.14	The primary DH culture transfected with the control Accell siRNA with encoded RFP at 12 DIV	137
Figure 4.15	The expression of <i>Gira1</i> mRNA in each of the four DH cultures relative to the untreated DH culture	139
Figure 4.16	The relative expression of <i>Gira2</i> mRNA in each of the four different DH cultures relative to the untreated DH culture	140
Figure 4.17	The relative expression of the <i>Gira3</i> mRNA in each of the DH cultures relative to the untreated DH culture	141
Figure 4.18	The baseline activity of the DH cultures transfected with each of the Accell siRNAs compared with the baseline activity of the untreated cultures	143

Figure 4.19	The activity of the untreated DH cultures to illustrate the normal activity of the cultures and their responses to the addition of strychnine and glycine	144
Figure 4.20	The activity of the DH cultures transfected with the non-targeting negative control siRNA, and their responses to the application of strychnine and glycine	146
Figure 4.21	The activity of the DH cultures transfected with the non-targeting negative control Accell siRNA with an RFP tag, and their responses to the application of strychnine and glycine	147
Figure 4.22	The activity of the cultured DH cells transfected with the positive control Accell siRNA encoding cyclophilin B, and their responses to the application of strychnine and glycine	148
Figure 4.23	The activity of the cultured DH cells transfected with the positive control Accell siRNA encoding GAPDH, and their responses to the application of strychnine and glycine	149
Figure 4.24	The activity of the DH cultures transfected with the Accell siRNA encoding the <i>Glr1</i> gene for the knockdown of the glycine receptor α 1 subunit	151
Figure 4.25	The activity of the DH cultures transfected with the Accell siRNA encoding the <i>Glr2</i> gene for the knockdown of the glycine receptor α 2 subunit	152
Figure 4.26	The activity of the DH cultures transfected with the Accell siRNA encoding the <i>Glr3</i> gene for the knockdown of the glycine receptor α 3 subunit	153

Chapter 5

Figure 5.1	Photograph of the spinal cord slice holder	168
Figure 5.2	Photograph of the interface chamber used for the single electrode slice recordings	169
Figure 5.3	A schematic diagram of the circuit used for the single electrode recordings from the spinal cord slices	170
Figure 5.4	An example of a recording from the SG of a spinal cord slice using the single electrode extracellular recording technique	171
Figure 5.5	Processing of extracellular recordings from the SG region of a rat spinal cord slice for analysis of the rhythmic oscillations	174

Figure 5.6	A Power Spectra generated from FFT Power Spectrum analysis of the rhythmic oscillations recorded from the SG region of the spinal cord slices	175
Figure 5.7	The effects of GABA on the 4AP-induced rhythmic activity in the SG region of rat spinal DH	179
Figure 5.8	GABA _A receptor agonist muscimol effects on the 4-AP-induced activity in the SG of rat spinal cord slices	180
Figure 5.9	The effects of GABA _A agonist THIP on the 4-AP-induced rhythmic activity in the spinal DH SG	181
Figure 5.10	The effects of the GABA _A receptor positive allosteric modulator L-838,417 on the 4-AP-induced rhythmic activity of the SG	182
Figure 5.11	GABA _A receptor antagonist bicuculline effects on 4AP-induced rhythmic activity in the SG	183
Figure 5.12	The effects of gabazine on the 4-AP-induced rhythmic activity in the SG of spinal cord slices	184
Figure 5.13	The changes in population spike frequency and amplitude by GABA recorded in the SG of the spinal cord slices using single electrode extracellular recordings	186
Figure 5.14	The changes in population spike frequency and amplitude by muscimol recorded in the SG of the spinal cord slices using single electrode extracellular recordings	187
Figure 5.15	The changes in population spike frequency and amplitude in the SG of spinal cord slices by GABA _A receptor agonist THIP	188
Figure 5.16	The changes in population spike frequency and amplitude in the SG of spinal cord slices by GABA _A receptor PAM L-838,417	189
Figure 5.17	The changes in 4-AP-induced population spike frequency and amplitude in the SG of spinal cord slices by GABA _A receptor antagonist bicuculline	190
Figure 5.18	The changes in 4-AP-induced population spike frequency and amplitude in the SG of spinal cord slices by GABA _A receptor antagonist gabazine	191
Figure 5.19	The effects of GABA _B receptor agonist baclofen on the 4-AP-induced rhythmic activity in the SG of spinal cord slices	193
Figure 5.20	The effects of GABA _B receptor antagonist 2-hydroxysaclofen	194

	on 4-AP-induced activity in the SG of spinal cord slices	
Figure 5.21	The changes in 4-AP-induced population spike frequency and amplitude in the SG of spinal cord slices by GABA _B receptor agonist baclofen	196
Figure 5.22	The changes in 4-AP-induced population spike frequency and amplitude in the SG of spinal cord slices by GABA _B receptor antagonist 2-hydroxysaclofen	197
Figure 5.23	The effects of glycine on 4-AP-induced rhythmic activity in the SG of spinal cord slices	200
Figure 5.24	The effects of glycine receptor antagonist strychnine on 4-AP-induced activity in the SG of spinal cord slices recorded from using single electrode extracellular recording technique	201
Figure 5.25	The changes in 4-AP-induced population spike frequency and amplitude in the SG of spinal cord slices by glycine	202
Figure 5.26	The changes in 4-AP-induced population spike frequency and amplitude in the SG of spinal cord slices by glycine receptor antagonist strychnine	203
Figure 5.27	A schematic diagram of the switch in direction of chloride ion flux between immature and mature neurons as a result of a change in the expression of the transporters KCC2 and NKCCs	211
Figure 5.28	Hypothetical models to account for the effects observed with the GABA _A receptor agonists and antagonists	218
 Chapter 6		
Figure 6.1	A photograph of a perforated MEA probe	231
Figure 6.2	Photographs of the MEA rig setup	232
Figure 6.3	A photograph of a lumbar spinal cord slice and harp grid	233
Figure 6.4	A photograph of a MED64 probe used to culture the DH cells	236
Figure 6.5	A section of a recording from a MED64 probe with the DH culture at day 12	239
Figure 6.6	4-AP-induced activity in the SG, deep DH and VH of spinal cord slices on the MEA	240

Figure 6.7	Image to illustrate the synchronous DH activity detected with the MEA and acute spinal cord slice model	242
Figure 6.8	The average spike amplitudes and frequencies in the SG, deep DH and VH regions of the spinal cord slices determined from MEA recordings during the perfusion of 4-AP and 4-AP with GABA	243
Figure 6.9	The average spike amplitudes and frequencies in the SG, deep DH and VH regions of the spinal cord slices determined from MEA recordings during the perfusion of 4-AP and 4-AP with THIP	244
Figure 6.10	The average spike amplitudes and frequencies in the SG, deep DH and VH regions of the spinal cord slices determined from MEA recordings during the perfusion of 4-AP and 4-AP with muscimol	245
Figure 6.11	The average spike amplitudes and frequencies in the SG, deep DH and VH regions of the spinal cord slices determined from MEA recordings during the perfusion of 4-AP and 4-AP with bicuculline	246
Figure 6.12	The average spike amplitudes and frequencies in the SG, deep DH and VH regions of the spinal cord slices determined from MEA recordings during the perfusion of 4-AP and 4-AP with gabazine	249
Figure 6.13	The average spike amplitudes and frequencies in the SG, deep DH and VH regions of the spinal cord slices determined from MEA recordings during the perfusion of 4-AP and 4-AP with baclofen	250
Figure 6.14	The average spike amplitudes and frequencies in the SG, deep DH and VH regions of the spinal cord slices determined from MEA recordings during the perfusion of 4-AP and 4-AP with 2-hydroxysaclofen	251
Figure 6.15	The average spike amplitudes and frequencies in the SG, deep DH and VH regions of the spinal cord slices determined from MEA recordings during the perfusion of 4-AP and 4-AP with glycine	252
Figure 6.16	The average spike amplitudes and frequencies in the SG, deep DH and VH regions of the spinal cord slices determined from MEA recordings during the perfusion of 4-AP and 4-AP with strychnine	253

Figure 6.17	The mean population spike amplitudes and frequencies recorded from spinal cord slices using the MEA during perfusion of 4-AP and 4-AP with gelsemine	254
Figure 6.18	The mean population spike amplitudes and frequencies recorded from spinal cord slices using the MEA during perfusion of 4-AP and 4-AP with VU 0240551	258
Figure 6.19	An image of the embryonic spinal DH culture on a MED64 probe after 13 DIV	259
Figure 6.20	Embryonic spinal DH culture recording on the MED64, with GABA receptor agonist and antagonist application	260
Figure 6.21	A MED64 recording with the spinal DH culture where muscimol and bicuculline are applied to the culture	261
Figure 6.22	The effect of glycine and gelsemine on the spinal DH culture electrical activity using the MED64	262
Figure 6.23	The effect of taurine and strychnine on the DH cultures on the MED64	263

List of Tables

Chapter 2

Table 2.1	Culture medium 1 components	39
Table 2.2	Culture medium 2 components	39
Table 2.3	List of the primary antibodies used for IF	45
Table 2.4	List of the secondary antibodies used for IF	46
Table 2.5	The contents for 20 μ l of mastermix for cDNA production	48
Table 2.6	A list of the RT-PCR rat assay probes used, with their assay ID number from Applied Biosystems (Thermoscientific, UK).	49
Table 2.7	A list of the RT-PCR human assay probes used, with their assay ID number from Applied Biosystems (Thermoscientific, UK).	49
Table 2.8	The TaqMan mastermix reagents for RT-PCR	50
Table 2.9	A summary of the number of molecules of the glycine receptor α 1 subunit and α 3 subunit variants K and L in the adult human spinal cord	73
Table 2.10	A list of the results from the absolute quantification RT-PCR experiment to show the number of molecules of each of the glycine receptor α subunits in the spinal DH culture	73
Table 2.11	A summary of the comparisons in expression of the antibodies utilised for characterisation of the spinal DH culture, between the spinal DH culture and the <i>ex vivo</i> spinal cord from published sources. The percentage values indicate the expression of the first antibody staining out of the total number of positive cells counted for the second antibody. Quantification of the expression of KCC2 and GAD65-67 has not been defined in the <i>ex vivo</i> spinal cord.	81

Chapter 3

Table 3.1	A list of the compounds and their range of concentrations applied to the spinal DH culture in the Flexstation calcium imaging assay. Supplier information and solvent utilised for each compound is also provided.	89
-----------	--	----

Chapter 4

Table 4.1	A summary of the effects on the area under the curve following application of strychnine and glycine on each of the DH cultures transfected with lentivirus and the untreated culture	136
Table 4.2	A summary of the effects on the spike frequency with the addition of strychnine and glycine on each of the DH cultures transfected with lentivirus and the untreated DH culture	136
Table 4.3	A summary of the area under the curve data illustrating the effects of each of the Accell siRNAs on the DH culture baseline activity compared to the untreated DH culture and the responses of the cultures to strychnine and glycine	154
Table 4.4	A summary of the spike frequency data illustrating the effects of each of the Accell siRNAs on the DH culture activity and its responses to strychnine and glycine compared to the untreated DH culture	154

Chapter 5

Table 5.1	List of compounds used in the single electrode extracellular recordings	176
Table 5.2	A summary of the effects of the GABA _A receptor compounds on the 4-AP-induced rhythmic activity parameters investigated	178
Table 5.3	A summary of the effects of the GABA _A receptor compounds on the 4-AP-induced population spikes in the SG of the spinal cord slices recorded using single electrode extracellular recordings	192
Table 5.4	A summary of the effects of the GABA _B receptor agonist baclofen, and antagonist 2-hydroxysaclofen (2-OH-S) on the 4-AP-induced rhythmic activity in the SG	195
Table 5.5	A summary of the effects of the GABA _B receptor agonist baclofen, and antagonist 2-hydroxysaclofen (2-OH-S) on the 4-AP-induced population spikes	198
Table 5.6	A summary of the effects of the glycine and strychnine on the 4-AP-induced rhythmic activity	204
Table 5.7	A summary of the effects of the glycine and strychnine on the	204

4-AP-induced population spike activity

Table 5.8	Summary of the actions of each compound applied on the 4-AP-induced rhythmic activity in the SG of the spinal cord slices	205
-----------	---	-----

Table 5.9	Summary of the actions of each compound applied on the 4-AP-induced population spike amplitude and frequency in the SG of the spinal cord slices	206
-----------	--	-----

Chapter 6

Table 6.1	List of compounds applied to the spinal cord slices during MEA recordings	229
-----------	---	-----

Table 6.2	A summary of the effects on the 4-AP induced activity by the GABA _A and GABA _B receptor agonists and antagonists applied to the spinal cord slices on the MEA	255
-----------	---	-----

Table 6.3	A summary of the effect of the glycine receptor agonist and antagonists and the KCC2 inhibitor on the 4-AP-induced population spikes in the SG, deep DH and VH of the spinal cord slices recorded from using the MEA	255
-----------	--	-----

Table 6.4	A summary table of the effects of the GABA _A receptor agonist and antagonists applied to the spinal DH cultures on the MED64 probes	264
-----------	--	-----

Table 6.5	A summary table of the effects of the glycine receptor agonists and antagonists on the spinal DH culture activity recorded using the MED64	264
-----------	--	-----

Chapter 7

Table 7.1	A summary of the overall effect of each of the compounds tested on the spinal DH cell culture model and the acute spinal cord slice model for each technique. S.E. stands for the single electrode recording technique, ↑ indicates a significant increase in activity, ↓ indicates a significant decrease in activity, NA = not applicable or not tested and ND = not defined.	288
-----------	---	-----

Abbreviations

5-HT ₃	5-hydroxytryptamine receptor 3
ACTB	β-actin
AMPA	α-amino-3-hydroxyl-5-methyl-isoxazole-propionate
Ara-C	Cytosine β-D-arabinofuroside
CCI	Chronic constriction injury
cGMP	Cyclic guanosine monophosphate
Cl ⁻	Chloride ion
CNS	Central nervous system
DH	Dorsal horn
DIV	Days <i>in vitro</i>
DMSO	Dimethyl sulfoxide
Dnase	Deoxyribonuclease 1
DRG	Dorsal root ganglion
E14	Embryonic day 14
E _{GABA}	Reversal potential of GABA
E _{Glycine}	Reversal potential of glycine
EP2	Prostaglandin E2 receptor 2
GABA	γ-aminobutyric acid
GAD 65/67	Glutamic acid decarboxylase 65/67
GAPDH	Glyceraldehyde-3-phosphate dehydrogenase
GFP	Green fluorescent protein
GlyT2	Glycine transporter 2
GPCR	G-protein coupled receptor
HBSS	Hanks' Balanced Salt Solution
HCO ₃ ⁻	Bicarbonate ion
IF	Immunofluorescence

ING	Interneuron gamma oscillations
IPSC	Inhibitory postsynaptic current
KCC2	Potassium-chloride co-transporter 2
K _{ir}	Inward-rectifying potassium channels
LGIC	Ligand-gated ion channels
LTP	Long term potentiation
MEA	Multi-electrode array
MOI	Multiplicity of infection concentration
NDMA	N-methyl-D-aspartate
NK1r	Neurokinin 1 receptor
NKCC1	Sodium-potassium-chloride cotransporter 1
nNOS	Neuronal nitric oxide synthase
NO	Nitric oxide
PAM	Positive allosteric modulator
PBS	Phosphate-buffered saline
PGE ₂	Prostaglandin E ₂
PING	Pyramidal interneuron network gamma oscillations
PKA	Protein kinase A
PV	Parvalbumin
RFP	Red fluorescent protein
RFU	Relative fluorescence units
RISC	RNA induced silencing complex
RNAi	RNA interference
ROI	Region of interest
RT-PCR	Real-time polymerase chain reaction
S.E.M	Standard error of the mean
SG	<i>Substantia gelatinosa</i>

shRNA	Short hairpin RNA
siRNA	Short interference RNA
SNL	Spinal nerve ligation
THIP	4,5,6,7-tetrahydroisoxazolo[5,4-c]pyridine-3-ol
vGluT	Vesicular glutamate transporter
VH	Ventral horn

1 Introduction

1.1 Pain and Nociception

The primary afferents which innervate the skin and deeper tissues of the body detect and respond to specific types of noxious and innocuous stimuli. There are defined classes of sensory primary afferents, which include the A β , A δ and C fibres (Baron, 2006). The A β afferents respond to innocuous stimuli such as touch or hair movement, while A δ and C fibres are nociceptors, responding to noxious mechanical, chemical and thermal stimuli. These primary afferents terminate in specific laminae of the spinal dorsal horn (DH), determined by their functional class (Figure 1.1) (Light and Perl, 1979). The spinal cord grey matter has been divided into ten lamina; the A δ and C fibres innervate lamina I and II (Rexed, 1952). Lamina II is also known as the *substantia gelatinosa*. The neurons of the superficial spinal DH modulate the sensory information from the periphery before it is propagated to several brain regions (Ruscheweyh and Sandkuhler, 2005, Zheng et al., 2010, Smith et al., 2015). In periaqueductal grey matter (PAG) of the brainstem the second order neuron synapses, and via other brainstem regions, including the rostral ventromedial medulla, there is a descending pathway back to the spinal DH (Antal et al., 1996, Lau and Vaughan, 2014). This descending pathway is known to further modulate the spinal DH network activity (Koutsikou et al., 2007). The second order neurons terminate in the thalamus, from where neurons project to the somatosensory cortex which is involved with the discrimination of the sensory stimuli (Todd, 2010). Projections to other brains regions result in the emotional, cardiovascular and autonomic responses to pain stimuli (Treede et al., 1999).

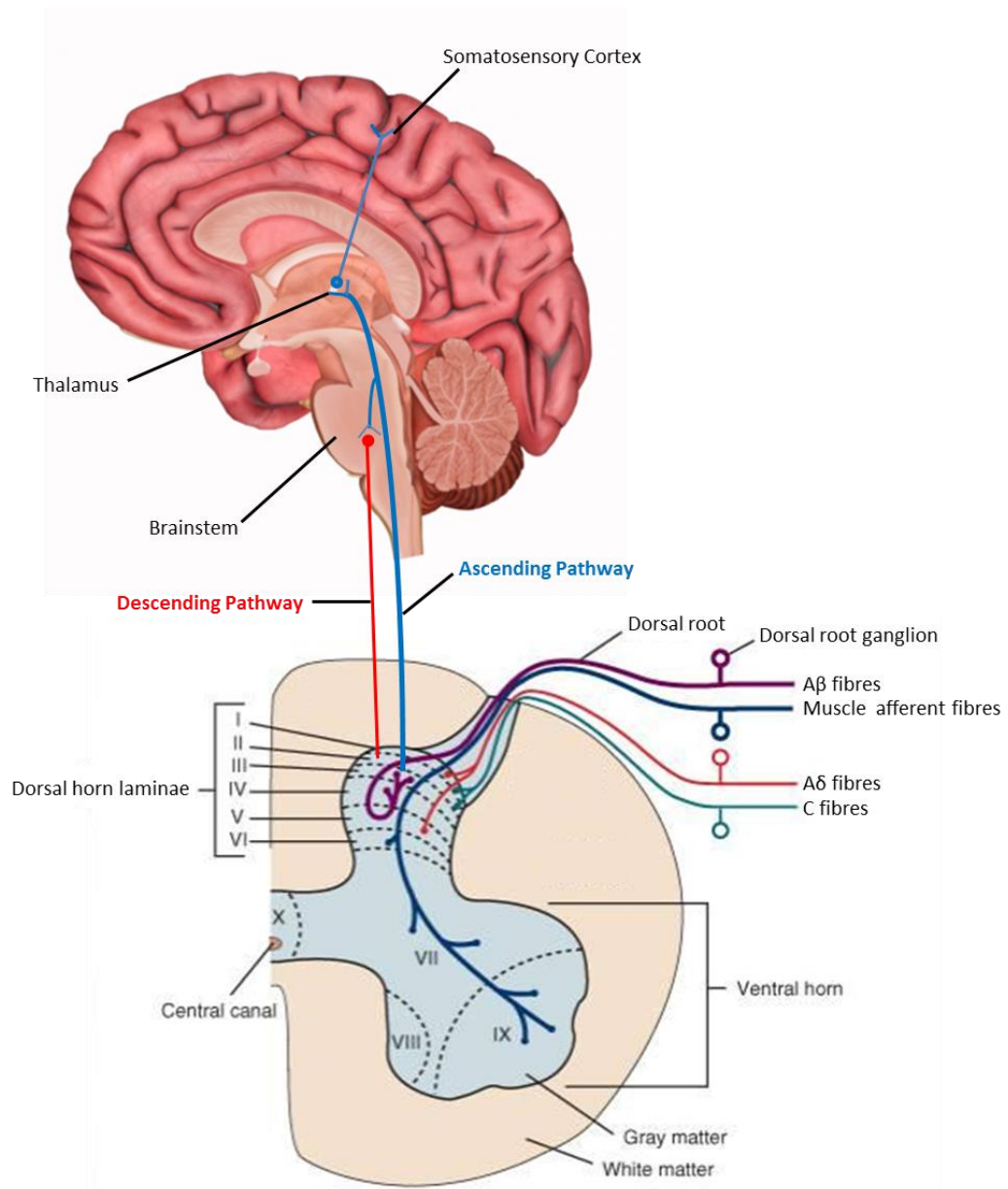


Figure 1.1 The anatomy of the pain pathway. The classes of primary afferents are indicated with the locations of their termination within the spinal dorsal horn laminae. The second order neurons first cross the midline and then ascend to the thalamus where they terminate. Third order neurons subsequently project from the thalamus to the somatosensory cortex, and other brain regions to process the stimuli. There is also a feedback loop from the brainstem where a branch of the second order neurons synapse with neurons of the descending pathway which project back to the spinal dorsal horn to regulate output. Adapted from www.studyblue.com.

1.2 Loss of Inhibition in the Superficial Spinal Dorsal Horn in Chronic Pain Conditions

Since the Gate Control Theory was proposed by Melzack and Wall (1965) there have been countless examples of the significance of inhibitory transmission in the development of pathological pain and the loss of inhibitory signalling in the spinal DH in pain conditions. For example, *in vivo* studies utilising antagonists of the γ -aminobutyric acid (GABA) and glycine receptors induce hyperalgesia and allodynia (Yaksh, 1989, Sherman and Loomis, 1994, Sivilotti and Woolf, 1994). Conversely, GABA_A agonists and positive allosteric modulators (PAMs) have an analgesic effect (Clavier et al., 1992, Eaton et al., 1999, Knabl et al., 2008). A number of potential causes of the changes in inhibitory neurotransmission in the spinal DH in chronic pain have been investigated, and discussed in detail below, including: (i) inhibitory interneuron cell death, (ii) a decrease in the synthesis of GABA and glycine, (iii) modulation of GABA and glycine release from presynaptic terminals, (iv) modulation of GABA and glycine receptor activity and (v) altered chloride ion homeostasis in the spinal DH.

1.2.1 Spinal Dorsal Horn Inhibitory Interneuron Cell Death in Pain Conditions

Several studies have investigated GABAergic cell death in models of neuropathic pain. There have been reports of a reduction in the number of GABAergic cells in the spinal DH following sciatic nerve transection (Castro-Lopes et al., 1993). Castro-Lopes et al. (1993) suggested this resulted from a loss of sensory input to the DH GABAergic neurons. In addition, there is a selective loss of GABA_A receptor-mediated inhibitory postsynaptic currents (IPSCs) in lamina II of the spinal DH in peripheral nerve lesion rodent models of chronic pain (Ibuki et al., 1996, Moore et

al., 2002). Caspase-3, a protease playing a key role in apoptosis, has also been identified in the ipsilateral spinal DH neurons of rats with peripheral nerve lesions being expressed in glutamatergic and GABAergic interneurons (Scholz et al., 2005). In this study, the onset of apoptosis coincided with the observed decrease in IPSCs in DH lamina II. The loss of IPSCs and interneurons in the spinal DH was prevented with the local application of a caspase-3 inhibitor, which also reduced peripheral nerve injury-induced hypersensitivity (Scholz et al., 2005). However, other studies have not identified a loss of GABA or GABAergic neurons in the spinal DH in chronic constriction injury (CCI) or spared nerve injury models (Polgar et al., 2003, Polgar et al., 2005). These conflicting results may be due to the staining of GABA being associated with the cell bodies as shown by Scholz and co-workers (2005) and Moore and collaborators (2002) which may have a lower retention of GABA, as opposed to the axon terminals which were analysed by Polgar and co-workers (Polgar et al., 2003, Polgar et al., 2005).

1.2.2 Decrease in GABA and Glycine Synthesis and Release in Pain Conditions

A decrease in the synthesis of GABA has been identified as another potential aspect of the loss of inhibition observed in pain conditions. A lower level of GABA was detected in the spinal DH in the CCI model (Somers and Clemente, 2002). A decrease in the GABA synthesising enzyme glutamic acid decarboxylase (GAD) 65 has also been shown in the ipsilateral spinal DH following peripheral nerve injury (Eaton et al., 1998, Moore et al., 2002). The release of inhibitory neurotransmitters GABA and glycine can be regulated by pre-synaptic GABA_B receptor signalling on A δ or C fibre terminals (Chéry and De Koninck, 2000, Choi et al., 2008). Activation of the GABA_B receptor causes inhibition of the presynaptic terminal through

coupling with potassium and calcium ion channels (Hinckley et al., 2005). Increasing cell membrane permeability to potassium ions causes hyperpolarisation, and decreasing permeability to calcium ions prevents further release of neurotransmitters (Chen and Johnston, 2005). Therefore, presynaptic GABA_B receptors are involved in the negative feedback for the release of GABA and glycine from the presynaptic terminals (Yang et al., 2015). Consequently this modulation of GABA release by GABA_B receptors could contribute to the inhibitory regulation of glutamatergic signalling within the spinal DH, which is relevant to nociception.

1.2.3 Modulation of GABA and Glycine Receptor Activity

Naturally occurring neurosteroids can modulate GABA_A receptor kinetics, prolonging synaptic inhibition (Cooper et al., 1999, Keller et al., 2004). The production of neurosteroids is upregulated in the spinal DH in peripheral inflammation, therefore slowing the GABA_A receptor kinetics resulting in an anti-nociceptive action (Poisbeau et al., 2005). Therefore, these neurosteroids can work as endogenous analgesics (Belelli and Lambert, 2005, Kibaly et al., 2008). The production of prostaglandin E2 is also upregulated in inflammatory pain (Samad et al., 2001). Prostaglandin E2 phosphorylates α 3-containing glycine receptors in the spinal DH through prostaglandin E2 receptor 2 (EP2) -mediated activation of protein kinase A (PKA) (Ahmadi et al., 2002, Harvey et al., 2004). Phosphorylation of the α 3-containing glycine receptors results in a conformational change in the glycine binding site on the receptor which prevents activity of the glycine receptor and thus glycinergic inhibition (Han et al., 2013). Consequently, this loss of glycinergic inhibition would result in increased excitability in the spinal DH and thus increase nociceptive signals.

1.2.4 Altered Chloride Homeostasis in the Spinal Dorsal Horn

GABA_A and glycine receptor ion channels are both permeable to chloride ions (Cl⁻) and bicarbonate ions (HCO₃⁻) (Lynch, 2004, Hubner and Holthoff, 2013). Cl⁻ ions are fourfold more permeable than HCO₃⁻ and are more readily available, therefore the reversal potential for GABA (E_{GABA}) and glycine (E_{glycine}) are dependent on the intracellular concentration of Cl⁻ ions. In the adult central nervous system (CNS), neurons have a low intracellular Cl⁻ ion concentration, therefore E_{GABA} and E_{glycine} are more negative than the resting membrane potential. Consequently the opening of the GABA_A or glycine receptor ion channels results in an influx of Cl⁻ ions which hyperpolarises the cell membrane preventing the generation of action potentials. The Cl⁻ ion electrochemical gradient is therefore fundamental in maintaining inhibition in the spinal DH. A shift in the reversal potential for anions (Cl⁻ and HCO₃⁻) to a more positive potential is known as shunting inhibition (Mitchell and Silver, 2003). Shunting inhibition arises as a result of a small cell membrane depolarisation, which can activate some voltage-dependent ion channels. This can cause the resting membrane potential to become more positive, which can decrease or completely prevent hyperpolarisation induced by GABA_A and glycine receptor channel opening resulting in disinhibition (Prescott et al., 2006). Consequently, shunting inhibition is believed to contribute to the development of central sensitisation as a consequence of the lack of inhibitory signalling in the spinal DH (Prescott et al., 2006).

The potassium-chloride co-transporter 2 (KCC2) is required to maintain a low intracellular Cl⁻ ion concentration, while the sodium-potassium-chloride cotransporter 1 (NKCC1) accumulates Cl⁻ ions inside the cells (Watanabe and Fukuda, 2015). During early development there is a high expression of NKCC1 and a low expression of KCC2 causing GABA to be depolarising in immature neurons (Lee et al., 2005). However, during development NKCC1 expression decreases and

the KCC2 expression increases, which changes the electrochemical gradient of Cl⁻ ions. Thus GABA switches from being depolarising to hyperpolarising in mature neurons (Rivera et al., 1999). In animal models of peripheral nerve injury, E_{GABA} is more positive in spinal lamina I neurons, which leads to a reduction in GABA-induced hyperpolarisation. The shift in E_{GABA} was demonstrated to be the result of a downregulation of KCC2 (Coull et al., 2003, Rivera et al., 2004). Furthermore, rat models of peripheral inflammatory pain have a reduced KCC2 expression in the spinal DH and develop hypersensitivity (Zhang et al., 2008c). There is evidence that pharmacologically increasing KCC2 extrusion of Cl⁻ ions in models of neuropathic pain restores spinal inhibition (Kahle et al., 2014). Therefore, the KCC2 transporter is a key target for the development of novel analgesics (Kahle et al., 2014).

1.3 Classification of Spinal Dorsal Horn Cell Types

The spinal DH is comprised of 90% interneurons, which synapse locally and are believed to be involved in the processing of sensory inputs, including pain (Basbaum et al., 2009, Sandkühler, 2009, Zeilhofer et al., 2012). The spinal DH physiology has been intensively investigated in order to understand how the circuitry controls the propagation of nociceptive inputs to higher brain centres. Understanding this circuitry could lead to the development of novel analgesics and improve treatment for a multitude of pain conditions. While progress has been made in this field, the circuitry of the DH remains elusive due to difficulty in defining functional interneuron populations (Graham et al., 2007, Todd, 2010). Inhibitory interneurons make up 25-40% of the neurons in laminae I-III of the rat spinal DH (Polgar et al., 2003). The remaining 60-75% is believed to be comprised of glutamatergic interneurons (Todd and Spike, 1993, Todd et al., 2003). Immunocytochemical studies have indicated that all the inhibitory interneurons in

the spinal DH are GABAergic, with 96 to 99% of these also being glycinergic in laminae I-II and III, respectively (Polgar et al., 2003, Todd, 2010, Polgar et al., 2013). Many research investigations have suggested that the loss of function of inhibitory interneurons in the spinal DH leads to the development of central sensitisation and neuropathic pain conditions (Moore et al., 2002, Coull et al., 2003, Coull et al., 2005, Scholz et al., 2005). Blockade of GABA_A and glycine receptors in the spinal DH *in vivo* induces symptoms of neuropathic and inflammatory pain illustrated by behavioural tests (Yaksh, 1989, Sherman and Loomis, 1994, Sivilotti and Woolf, 1994). These findings illustrate that DH inhibitory interneurons are involved in the processing of nociceptive signals.

1.3.1 Spinal Dorsal Horn Cell Classification

Classification of interneurons in the spinal DH has been based on cell morphology, electrophysiological properties and neurochemistry. Grudt and Perl (2002) provided one of the most comprehensive studies, where they identified at least nine categories of neurons in the spinal DH based on a combination of location, cellular geometry, distribution of neurites, connectivity and excitability. In lamina I two types of neurons were identified; projection neurons with axons that project ventromedially to the contralateral ventrolateral column and those which are non-projecting and have numerous neurites branching within the superficial DH (Grudt and Perl, 2002). Evidence suggests that the larger projection neurons all express the substance P receptor neurokinin 1 receptor (NK1r) while the smaller non-projecting neurons are interneurons (Al Ghamdi et al., 2009).

In lamina II of the hamster spinal DH five distinct classes of interneurons were identified by Grudt and Perl (2002): islet, radial (stellate), vertical, central and medial-lateral cells (Figure 1.2). These have since been confirmed in rat and mouse

studies (Heinke et al., 2004, Maxwell et al., 2007, Yasaka et al., 2010). Islet cells have been identified as GABAergic and/or glycinergic (Todd and McKenzie, 1989, Todd and Sullivan, 1990). Electrophysiological recordings from islet cells have revealed that these cells display a tonic firing pattern throughout the duration of depolarisation (Grudt and Perl, 2002). Excitatory and inhibitory synaptic inputs to lamina II islet cells have been detected from cells also located within lamina II (Kato et al., 2007). Furthermore, C fibres were found to synapse with virtually all islet cells (Grudt and Perl, 2002), which demonstrates these inhibitory interneurons receive direct nociceptive input from the periphery.

Vesicular glutamate transporters (vGluT) 1, 2 and 3 are glutamatergic neuronal markers. The majority of spinal glutamatergic neurons express vGluT2 (Oliveira et al., 2003, Todd et al., 2003, Malet et al., 2013, Punnakkal et al., 2014). vGluT2-positive cells have a morphology similar to that described for vertical cells (Punnakkal et al., 2014). Vertical cells are non-GABAergic (Todd and McKenzie, 1989) and account for a third of all the excitatory neurons found in the DH lamina II (Yasaka et al., 2010). There is evidence that vertical cells synapse with projection neurons in lamina I of the DH and therefore potentially provide a major output pathway from lamina II (Lu and Perl, 2005, Maxwell et al., 2007).

Vertical cells are almost exclusively glutamatergic, while islet cells are exclusively GABAergic and/or glycinergic interneurons. The other cell types identified in the spinal DH have been more difficult to classify in terms of being excitatory or inhibitory. Central neurons were named based on their location in the 'mid-zone' of lamina II by Ramon y Cajal (1909) and they represent approximately a quarter of the cells in the DH. Grudt and Perl (2002) reported that central cells can be split into two groups: those displaying a tonic firing response to a step depolarisation and those only producing action potentials during the initial phase of the depolarisation (Hantman et al., 2004). Many of the tonically firing central cells are GABAergic and

receive monosynaptic input from C-fibres (Grudt and Perl, 2002). The group of the transiently firing central cells were identified as glutamatergic and receive input from A δ -fibres. Radial cells identified by Grudt and Perl (2002) were located at the border between inner lamina II and outer lamina II, and had dendrites which extended in all directions, with some extending as far as lamina I in a dorsal-lateral direction but many projecting in the rostro-caudal axis. These are considered the same as “stellate” cells previously identified in the human spinal DH (Schoenen, 1982). Most radial cells have been labelled as glutamatergic, however, some GABAergic radial cells have also been identified (Maxwell et al., 2007, Yasaka et al., 2010). Medial-lateral cells were identified as the only interneurons of lamina II which has dendrites which do not extend in a rostral-caudal direction, and therefore have been suggested to play a role in connecting the other interneurons of lamina II (Grudt and Perl, 2002).

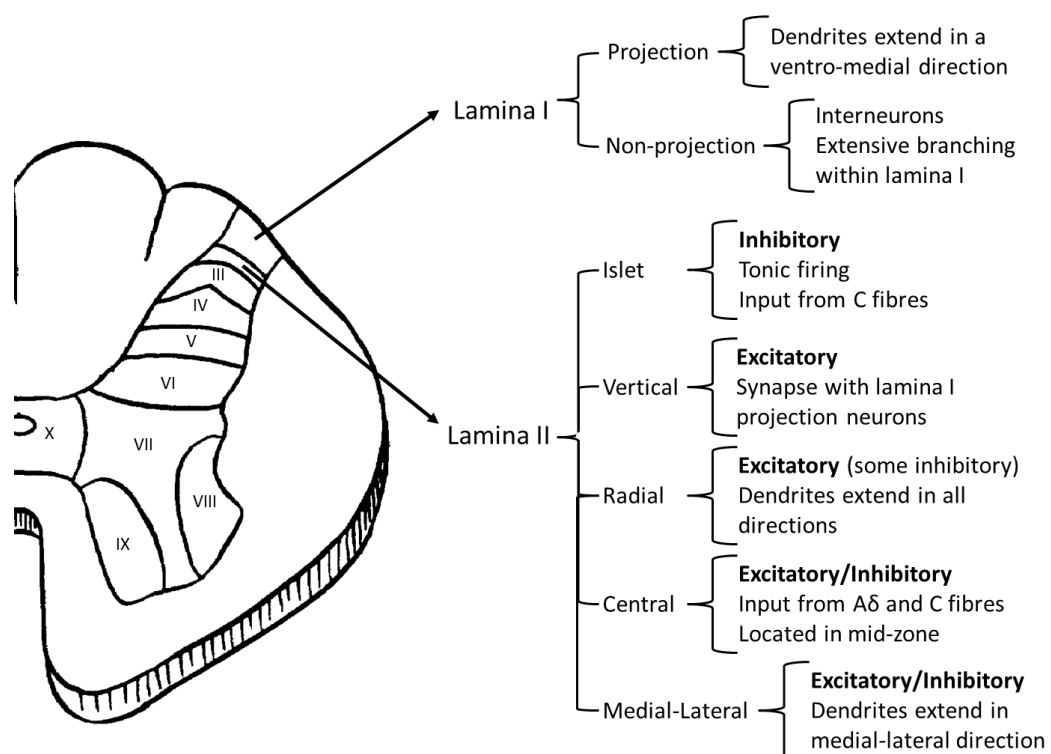


Figure 1.2 A figure of a transverse spinal cord section with the laminae defined, and a list of some of the classified neurons and interneurons present in laminae I and II. The significant properties of each of the classes of neurons and interneurons in these laminae are included.

A high density of parvalbumin (PV) positive interneurons in lamina II of the spinal DH have been identified from immunohistochemical studies, with some also found in lamina III but almost none in lamina I (Hughes et al., 2012). PV is a calcium-binding protein, which can transiently bind calcium and transport it to intracellular calcium stores (Celio and Heizmann, 1982, Celio, 1990). Therefore, there is evidence that PV is involved in regulating neurotransmitter release in the presynaptic terminal, which is dependent on a calcium trigger for synaptic vesicle exocytosis (Augustine, 2001, Neher and Sakaba, 2008). Consequently PV affects the firing properties (Albéri et al., 2013) and short-term synaptic plasticity at inhibitory synapses in the brain (Caillard et al., 2000). GABAergic interneurons in the brain and spinal cord have been identified as PV-immunoreactive (Celio, 1990, Baimbridge et al., 1992), however a population of glutamatergic interneurons in the spinal DH are also PV-positive (Grudt and Perl, 2002).

Neurochemically defining populations of cells within the spinal DH has indicated a significant expression of neuronal nitric oxide synthase (nNOS) (Sardella et al., 2011, Polgár et al., 2013). DH lamina II was found to have a higher expression of nNOS-positive cells compared to laminae I and III (Sardella et al., 2011). Excitatory and inhibitory interneurons of the spinal DH express nNOS, although the majority (90%) of nNOS-positive cells are GABAergic (Valtschanoff et al., 1992, Sardella et al., 2011). Nitric oxide (NO) is produced by nNOS which subsequently produces cyclic guanosine monophosphate (cGMP) (Garthwaite, 2008, Schmidtko et al., 2009). An NO-cGMP signalling pathway in the spinal DH has been linked with development of spinal hyperalgesia in the formalin inflammatory pain model (Tao et al., 1999). Inhibition of NO synthesis in the spinal cord and nNOS knockout mice have been used to illustrate that NOS is involved in the development and maintenance of inflammatory and neuropathic pain (Chu et al., 2005, Guan et al., 2007). Furthermore, nNOS-positive cells respond to formalin injection and noxious

heat stimulation by an up-regulation of Fos (Polgár et al., 2013). Fos is currently used as a marker for demonstrating the occurrence of central sensitisation in pain conditions (Ahmad and Ismail, 2002, Gao and Ji, 2009, Hsieh et al., 2015).

1.3.2 GABA_A Receptor Expression in the Spinal Dorsal Horn

The GABA_A receptors are members of the Cys-loop pentameric ligand gated ion channel (LGIC) receptor family (Schofield et al., 1987). There is at least 30% homology between all members of the Cys-loop LGIC family (Collingridge et al., 2009), and they all form from five subunits with each subunit consisting of four transmembrane-spanning domains (Nayeem et al., 1994) (Figure 1.3). Together these subunits form a central pore, which for GABA_A receptors is permeable to anions; particularly Cl⁻ and HCO₃⁻. The binding of an agonist to the GABA_A receptor causes a conformational change that leads to the opening of the ion channel pore. Depending on the electrochemical gradient of Cl⁻ ions, when the channel pore is open there is either a net influx or efflux of Cl⁻ ions across which can cause hyperpolarisation or depolarisation, respectively.

There have been nineteen different human GABA_A receptor subunits identified: six α , three β , three γ , one δ , one ϵ , one π , one θ , and three ρ , with splice variants identified for a number of these subunits (Simon et al., 2004, Olsen and Sieghart, 2008). Not all combinations of subunits are thought to occur partly due to restrictions of subunit assembly, the most common combination in the brain contain two α , two β and one γ subunit (Chang et al., 1996, Tretter et al., 1997, Farrar et al., 1999). However, multiple GABA_A receptor subtypes have been found in a single neuron (Mangan et al., 2005). Synaptic GABA_A receptors are predominantly composed of α 1, α 2 and/or α 3 with β 2/3 and γ 2 subunits (Olsen and Sieghart, 2008). These GABA_A receptors have fast synaptic GABA transient current (Olsen

and Sieghart, 2009). Extrasynaptic GABA_A receptors often contain the δ subunit (Mortensen and Smart, 2006). For example, the subtypes $\alpha 4\beta\delta$, $\alpha 6\beta\delta$ and $\alpha 5\beta\gamma 2$ have all been detected extrasynaptically (Mortensen and Smart, 2006). These subtypes are more sensitive to low concentrations of GABA with some also having a higher affinity for GABA, and furthermore they are less likely to desensitise (Rossi and Hamann, 1998, Brickley et al., 1999, Mangan et al., 2005). Extrasynaptic GABA_A receptors produce a tonic Cl⁻ current, which is believed to be involved in shunting inhibition (Mitchell and Silver, 2003). The synaptic GABA_A receptors produce a phasic current which allows for these receptors to function at high frequency for efficient information transfer (Brickley et al., 1996, Wisden et al., 2002).

In the brain the GABA_A receptor $\alpha 1$ subunit is the most abundant subunit, particularly in the cerebral and cerebellar cortex (Fritschy and Mohler, 1995, Korpi et al., 1999). The $\alpha 2$ subunit is most prominently expressed in the amygdala, hippocampus and striatum (Fritschy and Mohler, 1995). The GABA_A receptor $\alpha 3$ subunit is found primarily in the thalamus, basal forebrain and brainstem neurons (Fritschy and Mohler, 1995). The most prominent expression of the $\alpha 4$ subunit is in the thalamus and dentate gyrus of the hippocampus, with moderate expression in the cortex (Jia et al., 2007). The $\alpha 5$ subunit is most highly expressed in the hippocampus, and finally the $\alpha 6$ subunit is exclusively expressed in cerebellar granule cells (Fritschy and Mohler, 1995, Korpi et al., 1999). The expression of the $\gamma 1$, $\gamma 3$, ϵ , θ and π subunits is scarce throughout the CNS, which has limited their characterisation (Olsen and Sieghart, 2008). However, there is evidence for their expression in non-neuronal cells, including the pancreas, lung, breast and uterus (Jin et al., 2005, Zafra et al., 2006, Takehara et al., 2007). There are GABA receptors which are formed entirely from ρ subunits, which are termed GABA_{A-rho} receptors (also known as GABA_C receptors) (Barnard et al., 1998, Bormann, 2000,

Olsen and Sieghart, 2009). Additionally, ρ subunits have been found to assemble with the GABA_A receptor $\gamma 2$ subunit to form functional GABA_A receptors (Pan et al., 2000). The GABA_{A- ρ} receptors are primarily expressed in the retina (Cutting et al., 1991), although have also been detected in the brainstem, hippocampus and other brain regions at lower levels of expression (Sieghart and Sperk, 2002, Milligan et al., 2004). It has been shown that there is a laminar distribution of specific GABA_A receptor α subunits in the spinal DH (Paul et al., 2012). In the superficial spinal DH the GABA_A receptor $\alpha 1$, $\alpha 2$, $\alpha 3$, $\alpha 5$, $\beta 2/3$ and $\gamma 2$ subunits have all been detected in the superficial spinal DH (Bohlhalter et al., 1996, Zeilhofer et al., 2009). The $\alpha 2$ and $\alpha 3$ GABA_A receptor subunits have been shown in rats to have a higher expression in lamina II of the spinal DH, while $\alpha 1$ and $\alpha 5$ subunits are more prominent in lamina III (Bohlhalter et al., 1996).

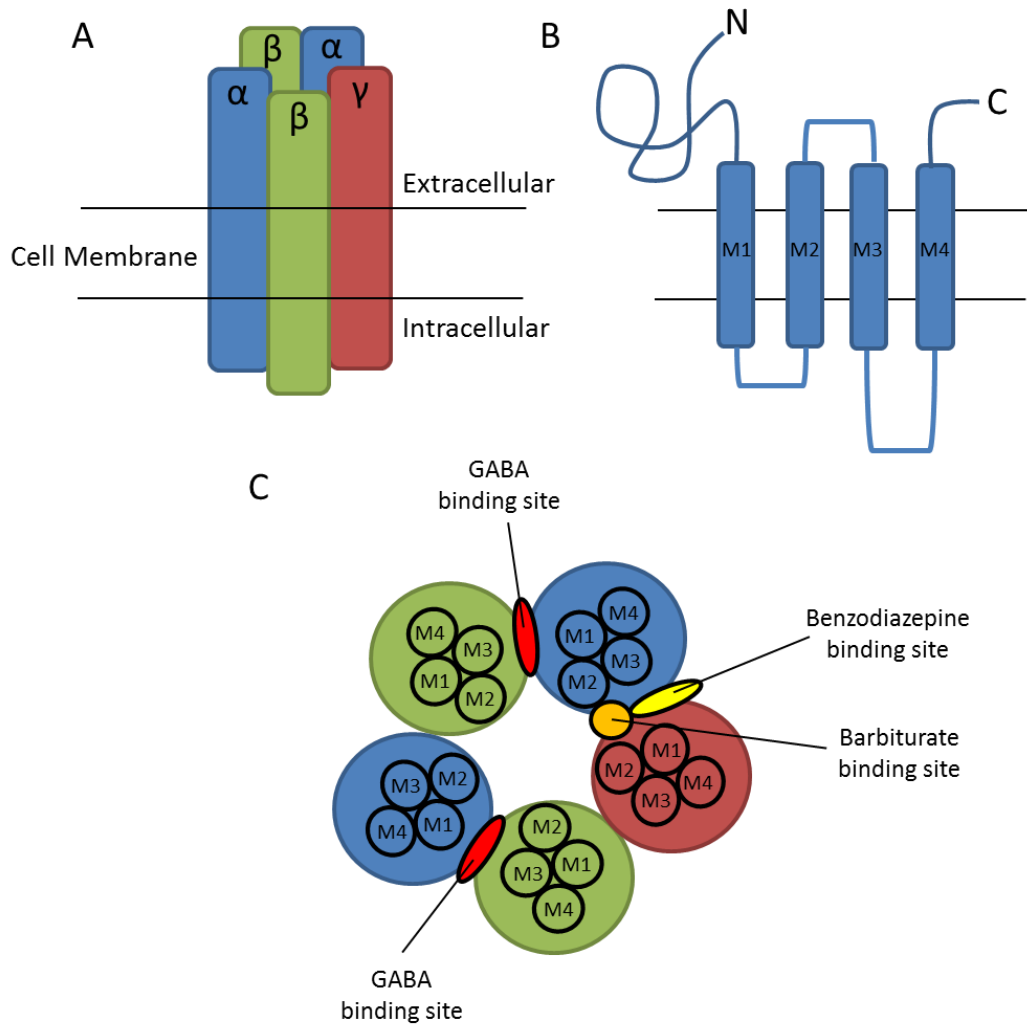


Figure 1.3 The structure of the GABA_A receptor. (A) The GABA_A receptor is formed from five subunits, with the most typical stoichiometry of two α, two β and a γ subunit. (B) Each subunit is composed of four transmembrane spanning domains (M1-M4), with a long extracellular N-terminal domain and a shorter extracellular C-terminal domain. (C) The M2 domains of each subunit line the GABA_A receptor channel pore. The GABA binding site is located at the interface between the α and β subunits. The benzodiazepine and barbiturate binding sites are located at the interface between the α and γ subunits.

1.3.3 Glycine Receptor Expression in the Spinal Dorsal Horn

Glycine receptors, like the GABA_A receptors, are pentameric LGICs. There are five glycine receptor subunits which have been identified, α 1-4 and β and typically glycine receptors have a 2 α :3 β stoichiometry (Grudzinska et al., 2005) (Figure 1.4). Homomeric receptors consisting of only one α subtype can form functional glycine receptors *in vitro* (Griffon et al., 1999), but the β subunit alone does not form receptors (Bormann et al., 1993). Splice variants of each of the α subunits have been identified, the α 1^{ins} splice variant has an eight amino acid insert in the large intracellular loop (Malosio et al., 1991a). The α 2 subunit has three splice variants: α 2A and α 2B, which have two amino acid substitutions, while the α 2* splice variant has a single amino acid substitution which makes glycine receptors with this splice variant insensitive to strychnine (Kuhse et al., 1990). The glycine receptor α 3 subunit has two splice variants: α 3L and α 3K (Nikolic et al., 1998). The α 3K variant is lacking 15 amino acids in the cytoplasmic loop between transmembrane spanning regions 3 and 4 compared to the other α subunits. The α 3K-containing glycine receptors display faster desensitisation kinetics compared to those receptors containing the α 3L subunit. The glycine receptor α 4 subunit was first identified in the mouse, but is not found in humans (Matzenbach et al., 1994).

The glycine receptor α 1 subunit is expressed most prominently in the spinal cord and retina, but is also detected in the brainstem, thalamus and hypothalamus (Malosio et al., 1991b, Sato et al., 1991, Harvey et al., 2004). The α 2 subunit is highly expressed during early development but decreases postnatally to very low levels in the mature CNS while the opposite is true for α 1 and α 3 subunits (Akagi et al., 1991, Watanabe and Akagi, 1995). The α 3 subunit is strongly expressed in lamina II of the spinal DH, while the α 1 subunit in the spinal DH is predominantly expressed in lamina III and deeper DH laminae (Harvey et al., 2004). A low expression of the α 3 subunit has also been detected in the hippocampus and

hypothalamus (Malosio et al., 1991b). While the $\alpha 4$ subunit is a pseudo gene in humans, it is found as a protein in the sympathetic ganglia, spinal cord, dorsal root ganglia (DRG) and genital ridge of mice, chick, zebrafish and rat (Harvey et al., 2000). The β subunit is expressed throughout the CNS, from early development through to the mature adult CNS (Grenningloh et al., 1990, Fujita et al., 1991, Malosio et al., 1991b). The β subunit in heteromeric glycine receptors anchors the receptor to the post-synaptic cytoskeleton through binding gephyrin (Meyer et al., 1995b, Kneussel and Betz, 2000). Gephyrin has also been shown to cluster GABA_A receptors at the post-synaptic membrane (Maric et al., 2011). Additionally, there is evidence that the glycine receptor β subunit is involved in ligand binding (Grudzinska et al., 2005).

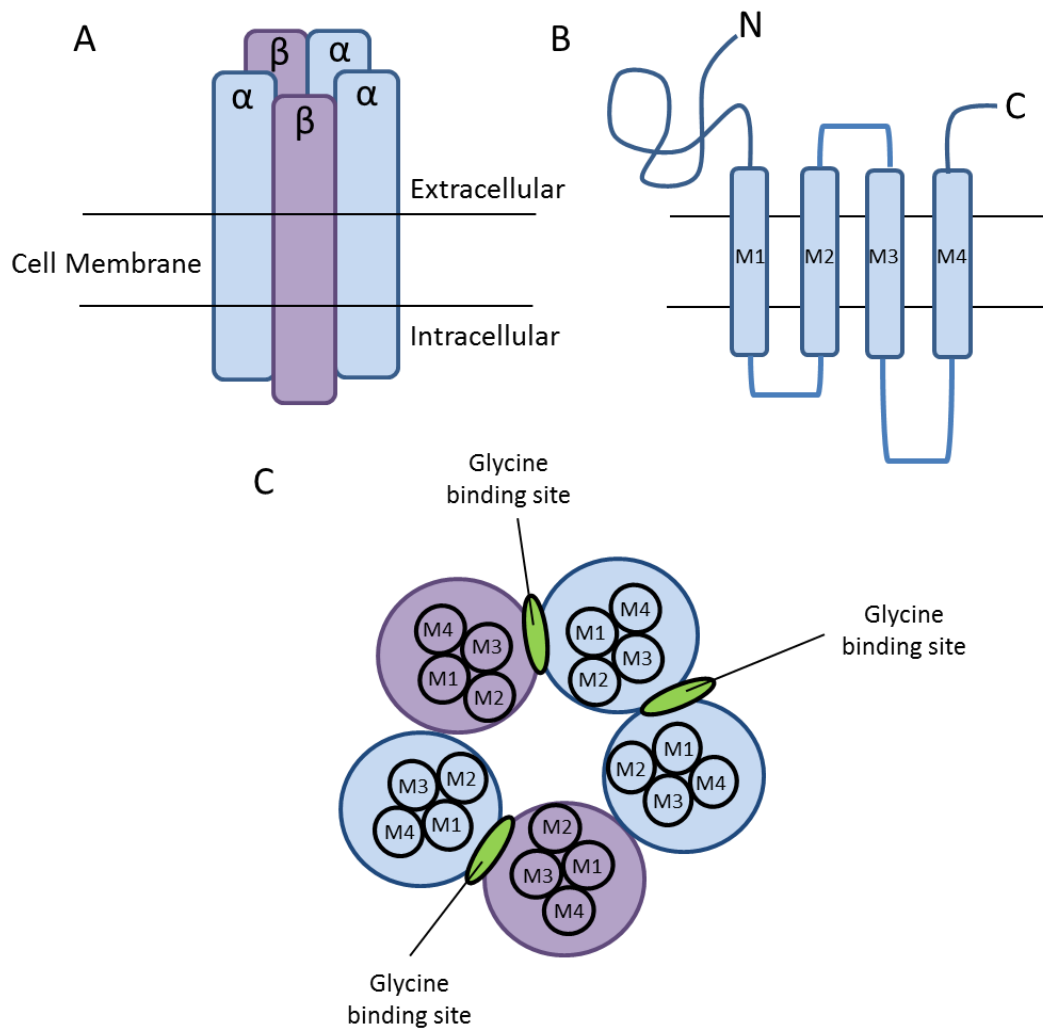


Figure 1.4 The glycine receptor structure. (A) The glycine receptor is comprised of five subunits, which can be composed of only α subunits, or of α and β subunits. (B) Each subunit has four transmembrane spanning domains (M1-M4), with extracellular N- and C-terminal domains. (C) The M2 transmembrane spanning domains of each subunit line the receptor channel pore. The agonist binding site is located at the interface between either two α subunits or an α and a β subunit.

1.4 GABA_A Receptor Pharmacology

The α subunits of the GABA_A receptors are involved in ligand binding and the gating kinetics of the receptor (Gingrich et al., 1995, Labrakakis et al., 2014). The different subtypes of the GABA_A receptor have different receptor gating kinetics and pharmacological profile. For example GABA_A receptors containing the $\alpha 2$ subunit have slower deactivation kinetics, and a higher affinity for GABA compared to $\alpha 1$ -containing GABA_A receptors (Dixon et al., 2014). The agonist GABA binding site is believed to be at the interface between the α and β subunits of the GABA_A receptor (Galzi and Changeux, 1994, Smith and Olsen, 1995, Boileau et al., 1999). Only a small number of compounds bind to the ligand binding site of the GABA_A receptor besides GABA itself. These include muscimol, 4,5,6,7-tetrahydroisoxazolo[5,4-c]pyridine-3-ol (THIP or gaboxadol), taurine, isonipecotic acid and isoguvacine (Krogsgaard-Larsen et al., 2004). THIP has been suggested to bind and have a high potency at extrasynaptic GABA_A receptors, including the $\alpha 4\beta 3\delta$ subtype, while acting as a partial agonist at other GABA_A receptor subtypes (Ebert et al., 2002, Stórustovu and Ebert, 2003, Voss et al., 2003, Drasbek and Jensen, 2006). THIP and morphine have almost equal potency as analgesics (Grognet et al., 1983). THIP also has anxiolytic effects and unlike morphine does not cause respiratory depression, but there are reports of THIP causing sedation and nausea similar to other GABA-mimetics (Hoehn-Saric, 1983, Drasbek and Jensen, 2006).

Benzodiazepines are PAMs enhancing the actions of GABA at GABA_A receptors, and are believed to bind at the interface between the α and γ subunits within a receptor (Duncalfe et al., 1996, Amin et al., 1997). Benzodiazepines have anxiolytic, anticonvulsant, sedative-hypnotic, analgesic and muscle relaxant properties. The sedative effect of benzodiazepines has been demonstrated to be the result of their binding to GABA_A receptors containing the α_1 subunit (McKernan et al., 2000). The analgesic properties of benzodiazepines may be mediated by $\alpha 2$ - and $\alpha 3$ -containing

GABA_A receptors (Knabl et al., 2008). L-838,417 is a compound which binds to the benzodiazepine-site on α 1-, α 2-, α 3- and α 5-containing GABA_A receptors, but selectively exerts its actions through α 2-, α 3- and α 5-containing GABA_A receptors (McKernan et al., 2000). It was shown to exhibit analgesic effects in CCI and spinal nerve ligation (SNL) models primarily through its action at α 2- and α 3-containing GABA_A receptors (Nickolls et al., 2011). GABA_A receptors can also be potentiated by barbiturates, which similarly have sedative-hypnotic effects. Barbiturates bind at another allosteric site separate from the benzodiazepine site (Chiara et al., 2013). Furthermore, a number of anaesthetics also exert their effects through GABA_A receptors including isoflurane, halothane, chloroform and propofol (Jenkins et al., 2001, Richardson et al., 2007).

GABA_A receptor antagonist bicuculline has long been utilised for the characterisation of the GABA_A receptor (Curtis et al., 1970). The poor stability and solubility of bicuculline lead to the development of other GABA_A receptor antagonists. For example, gabazine (SR99531) is a GABA_A receptor antagonist derived from GABA (Heaulme et al., 1986). Gabazine and bicuculline are both selective for GABA_A receptors over GABA_{A-rho} receptors (Zhang et al., 2008a). *In vivo* and *in vitro* studies have shown that administration of bicuculline or gabazine increases excitability in the spinal DH (Green and Dickenson, 1997, Baba et al., 2003, Bremner et al., 2006, Czarnecki et al., 2008, Chapman et al., 2009). Picrotoxin is a non-competitive inhibitor of the GABA_A receptors (Barker et al., 1983), and at higher concentrations also inhibits glycine (Schmieden et al., 1989) and 5-hydroxytryptamine receptor 3 (5-HT₃) receptors (Das et al., 2003). Picrotoxin exerts its inhibitory action on the GABA_A receptor by blocking its channel pore (Gurley et al., 1995). Similarly to the GABA_A receptor antagonists, picrotoxin also increases excitability in the spinal DH (Vikman et al., 2003).

1.5 Glycine Receptor Pharmacology

Glycine receptors can be activated by endogenous amino acids glycine, β -alanine and taurine; glycine is the most potent and β -alanine and taurine are partial agonists (Bormann et al., 1993, Schmieden and Betz, 1995). The ligand binding site on the glycine receptor is at the interface between two subunits, either two α subunits or an α and a β subunit (Brejc et al., 2002). When three glycine molecules are bound to the receptor it is maximally activated (Lewis et al., 2003). The homomeric and heteromeric glycine receptor subtypes have generally similar glycine sensitivities (Yang et al., 2007). Strychnine is a highly selective, potent competitive antagonist of the glycine receptor, frequently used to discriminate GABA_A receptor inhibition from glycine receptor inhibition (Young and Snyder, 1973). There are a limited number of compounds which display some selectivity for the different glycine receptor subtypes. Picrotoxin is an equimolar mixture of picrotin and picrotoxinin, and inhibits both GABA_A and glycine receptors. Picrotoxinin is selective for homomeric α 2 and α 3 glycine receptors over α 1 subtype, and highly selective for homomeric glycine receptors compared to heteromeric glycine receptors containing the β subunit (Pribilla et al., 1992, Yang et al., 2007). Gelsemine is a plant alkaloid that acts primarily at α 3-containing glycine receptors (Zhang et al., 2013, Zhang and Wang, 2015). Gelsemine has displayed analgesic properties in models of neuropathic pain by binding to glycine receptors in the spinal cord (Zhang et al., 2013, Wu et al., 2015b).

1.6 Rhythmic Oscillations in Central Nervous System Networks

Oscillatory activity exists throughout the CNS with a wide range of frequencies, from the slowest delta oscillations of 0.5-3 Hz, to theta oscillations of 3-8 Hz, gamma oscillations at 30-90 Hz and ultrafast 90-200 Hz frequencies (Buzsaki and Draguhn,

2004). These rhythmic oscillations have been linked with a number of functions, including learning and memory, locomotion, behaviour and nociception (Sandkuhler and Eblen-Zajjur, 1994, Bragin et al., 1995, Sejnowski and Destexhe, 2000, Buzsaki et al., 2003, Taccola and Nistri, 2006). Furthermore, during sleep, thalamocortical oscillations can also be observed, where both slow wave sleep (SWS) with a frequency of 1-4 Hz and rapid eye movement (REM) sleep with a frequency between 4 and 9 Hz can be recorded (Sejnowski and Destexhe, 2000). A human study with patients with severe neurogenic pain demonstrated significant differences in their EEG power spectra compared to a healthy control group (Sarnthein et al., 2006). This illustrates that chronic pain is linked to brain oscillations. Furthermore, in a human study brief painful stimuli were applied to the right hand of the subjects while the oscillatory activity and excitability in the sensorimotor cortex were measured (Ploner et al., 2006). A negative linear correlation was found between pain-induced modulations of brain oscillatory activity and pain-induced modulations of cortical excitability in the somatosensory system. This provides evidence for an association between pain and network oscillatory activity and demonstrates that oscillations are related to the functional state of cortical excitability.

The rhythmic oscillations in the brain can be modulated through pharmacologically targeting GABA_A receptors (Sohal et al., 2003, Wafford and Ebert, 2006). There is significant evidence that PV-containing GABAergic interneurons are involved in gamma rhythms in the brain (Lodge et al., 2009, Volman et al., 2011, Kim et al., 2015, Kuki et al., 2015). Furthermore, during an epileptic seizure high frequency oscillations occur in the brain, which can be treated with anticonvulsants that target GABA_A receptors including benzodiazepines and barbiturates (Fisher et al., 1992, Spencer and Lee, 2000, Grenier et al., 2003). Additionally, glycine receptor activity has been implicated in regulating brain oscillations, illustrated through application of glycine receptor agonists and antagonists to an intact corticohippocampal

preparation using field potential recordings (Chen et al., 2014). Many interneurons have been identified as being both GABAergic and glycinergic (Todd and Sullivan, 1990), therefore it is unsurprising they are both involved in the generation of rhythmic oscillations.

GABA_A and glycine receptor neurotransmitters are involved in neuronal network oscillations of the spinal cord ventral horn (VH) (Hinckley et al., 2005, Taccola and Nistri, 2005, 2006) and the spinal DH (Sandkuhler and Eblen-Zajjur, 1994, Eblen-Zajjur and Sandkuhler, 1997, Ruscheweyh and Sandkuhler, 2003, Chapman et al., 2009). The spinal VH network generates locomotion independently of central and peripheral input (Guertin, 2012). It is generally accepted that the left-right alternating motor outputs are synchronised by reciprocal inhibition between the left and right VH networks, which can generate their own rhythmic activity (Butt et al., 2002). There is evidence that GABAergic and glycinergic signalling have distinct roles in the VH network. The GABAergic inhibition modulates the onset and duration of the VH rhythmic activity, while glycinergic inhibition regulates the pattern of the left-right rhythmic alternation (Hinckley et al., 2005).

In vivo and in vitro spinal DH recordings have illustrated that the network can generate and sustain rhythmic oscillatory activity (Sandkuhler and Eblen-Zajjur, 1994, Eblen-Zajjur and Sandkuhler, 1997, Ruscheweyh and Sandkuhler, 2003, Watanabe and Fukuda, 2015), (Loeser and Ward, 1967, Lombard et al., 1979). *In vitro* recordings from spinal cord slices have been used to illustrate that the rhythmic activity in the DH is generated and sustained in isolation by separating one DH quadrant from the remainder of the slice (Asghar et al., 2005, Chapman et al., 2009). In addition, oscillations in the DH interfere with the locomotor activity of the VH (Taccola and Nistri, 2005). The rhythmic oscillations in the spinal DH could be a mechanism by which the afferent input is regulated by permitting signal propagation only at specific time intervals. The spinal DH rhythmic oscillations have been

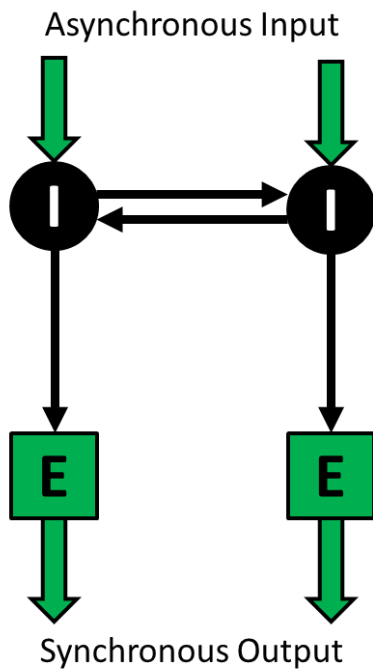
suggested to be involved in synaptic plasticity, causing long-term potentiation (LTP) at synapses which could result in amplification of nociceptive signals before they are propagated to the brain (Ruscheweyh et al., 2011).

The generation of network oscillations requires rhythmic, synchronised activity (Soltesz and Deschenes, 1993). There have been two mechanisms proposed for the generation of brain oscillations that are both dependent on inhibitory interneurons within the network. Firstly, the interneuron gamma (ING) oscillation mechanism could increase synchrony in a network if there is a large number of randomly firing excitatory neurons that synapse with inhibitory interneurons (Tiesinga and Sejnowski, 2009). The convergent inhibitory interneurons generate a summated IPSP from mutually inhibiting each other, and preventing postsynaptic excitatory interneuron activity until the IPSP diminishes. This consequently synchronises action potential firing of all the postsynaptic interneurons across the network (Whittington et al., 2000). Secondly the mechanism of pyramidal interneuron network gamma (PING) oscillations involves excitatory and inhibitory interneurons reciprocally innervating each other (Tiesinga and Sejnowski, 2009). In this case the input to an excitatory interneuron is restrained to the rhythm based on the recovery of the excitatory interneuron from the IPSP (Whittington et al., 2000, Tiesinga and Sejnowski, 2009). A continuous stimulation of an excitatory interneuron stimulates its reciprocal inhibitory interneuron and subsequently is inhibited and unable to stimulate the next postsynaptic excitatory neuron until the IPSP diminishes. Therefore the unsynchronised input to this circuit would become synchronised via the reciprocally inhibiting interneuron. Figure 1.5 illustrates these two proposed mechanisms for the generation of network oscillations. These theories can be extended to spinal DH rhythms where inhibitory to inhibitory interneuron synapses have been identified (Zheng et al., 2010). Furthermore, in the spinal DH PV-containing GABAergic interneurons have also been identified, and have been

linked to modulating DH excitability in a neuropathic pain model (Heinke et al., 2004, Hughes et al., 2012, Polgár et al., 2013).

An additional mechanism for the generation of rhythmic oscillations in neuronal networks involves pacemaker neurons, which are defined by their ability to generate rhythmic bursting activity in the absence of any input (Legendre et al., 1985). Such neurons have been found in the cortex and spinal DH and VH (Silva et al., 1991, Cunningham et al., 2004, Tohidi and Nadim, 2009, Li et al., 2013, Li et al., 2014). In the spinal VH the frequency of pacemaker neuron membrane resonance has been strongly linked with the central pattern generator oscillation frequency (Tohidi and Nadim, 2009). Pacemaker neurons in the superficial spinal DH have been shown to be dependent on inward-rectifying potassium channels (K_{ir}) (Li et al., 2013). Li et al. (2014) demonstrated that there are pacemaker neurons in the spinal DH using patch-clamp recordings from an intact spinal cord preparation. Immunohistochemistry experiments revealed that these pacemaker neurons connect with projection neurons (Li et al., 2014a). This suggests these rhythmically active neurons could be involved in processing and modifying pain signals. However, previous *in vitro* studies using spinal cord slices have shown that the DH rhythm is not dependent on the DH cell holding potential, suggesting that it was not generated from intrinsically active neurons (Ruscheweyh and Sandkuhler, 2003). Ruscheweyh and Sandkuhler (2003) also demonstrated that the rhythmic activity was absent in the presence of the GABA_A receptor antagonist bicuculline. Therefore, given the evidence for the significant role of GABA_A and glycine receptors in rhythmic activity in the brain and spinal cord, these receptors are crucial targets in the development of novel analgesics.

A **ING Oscillation Mechanism**



B **PING Oscillation Mechanism**

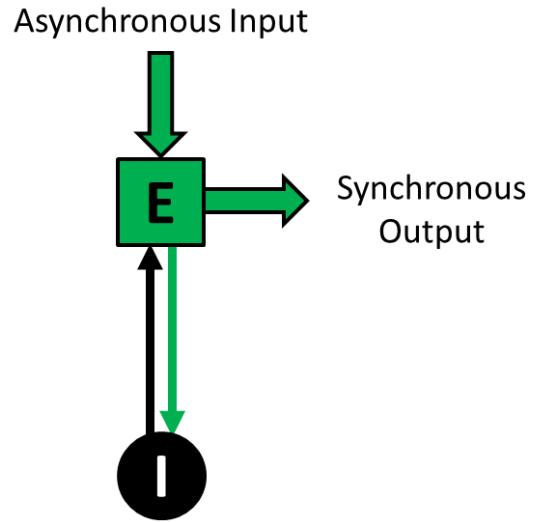


Figure 1.5 Two proposed mechanisms for the generation of neuronal network oscillations. (A) The ING mechanism involves interconnected inhibitory interneurons which mutually inhibit each other and generate a summated IPSP. This synchronises the activity of the postsynaptic excitatory interneurons and subsequently the network. (B) The PING oscillation mechanism requires an excitatory interneuron with a reciprocally inhibiting inhibitory interneuron. This generates rhythmic oscillations from an asynchronous input by restraining the output of the excitatory interneuron to the time in which the excitatory interneuron is recovered from the IPSP generated from the stimulation of the inhibitory interneuron.

1.7 Investigating the Spinal Dorsal Horn Neuronal Network: *In Vitro* Models

1.7.1 *In Vivo* Spinal Cord Recordings

In vivo electrophysiological recordings from the spinal DH allow direct measurement of the activity of individual neurons to the whole network and are useful to investigate the neuronal response to stimulation of the peripheral receptive field. Many early investigations into the spinal cord and pain employed extracellular *in vivo* recordings (Christensen and Perl, 1970, Kumazawa and Perl, 1978). Extracellular recordings from the spinal DH have also been used to measure the oscillatory activity of the network population (Sandkuhler and Eblen-Zajjur, 1994). Extracellular recordings detect the changes in the extracellular field potential caused by the surrounding nearby cell ionic processes; they cannot provide information on individual neurons or ion channel activity (Buzsáki et al., 2012). However, extracellular recordings are ideal for recording the activity of a localised population of cells (Buzsáki et al., 2012). The *in vivo* intracellular recording technique was developed to allow for single cell and ion channel studies where there is control of the cell membrane potential. It is technically difficult to perform intracellular recording from superficial spinal DH neurons *in vivo*. This is due to the poor stability of the recordings and the impalement of the cells with sharp electrodes frequently causing destruction of the cells (Urch and Dickenson, 2003). Furthermore, the neurons of the superficial DH are small and therefore it is more difficult to obtain intracellular recordings. Some additional issues with *in vivo* recordings include maintaining anaesthesia throughout the surgery and recordings, and also the movement of the animal that can affect the recording (Fee, 2000, Cuellar et al., 2004). The surgery and the inaccessibility of the spinal DH have led to the development of *in vitro* models of the spinal DH to further study the network and properties of DH neurons.

1.7.2 *In Vitro Spinal Cord Slices*

Brain and spinal cord slice preparations have been utilized over many decades to study the CNS neurophysiology (Li and Mc, 1957, Yamamoto and McIlwain, 1966). The techniques of both acute and organotypic spinal cord slices have been developed to establish *in vitro* models of the spinal cord network systems. Extracellular and intracellular recording techniques can be more easily performed with *in vitro* slices than *in vivo* preparations. There are a number of advantages of recording from *in vitro* slices compared to *in vivo* preparations (Collingridge, 1995). The preparation of acute spinal cord slices retains the synaptic circuits and cytoarchitecture of the intact spinal cord (Lossi et al., 2009). Preparations with and without dorsal roots attached have been developed (Murase et al., 1982, Marvizon et al., 1997). The absence of any afferent input can be advantageous in allowing the activity of the spinal DH to be studied in isolation. The slices are readily accessible for electrophysiological recordings where the external environment can be controlled and compounds of desired concentrations can be perfused without the influence of anaesthetics and in the absence of a blood-brain barrier or blood-nerve barrier. To study the network of tissue sections the multi-electrode array (MEA) technique has been developed to enable extracellular recordings to be made simultaneously from multiple sites across a tissue slice (Obien et al., 2015). Furthermore, the MEA technique provides information on the synchrony of neurons across a network (Obien et al., 2015).

Organotypic slice cultures are usually obtained from neonatal animals, and cultured *in vitro* for weeks or months (Galimberti et al., 2006, Marksteiner and Humpel, 2007, Humpel, 2015). Therefore they provide a model of the spinal cord that has features of both acute *in vitro* slices and spinal cord cell culture (Pandamooz et al., 2015). Organotypic cultures are frequently used in molecular biology, immunohistochemistry and electrophysiology experiments to investigate molecular

and cellular processes of the spinal cord, its development and cell death (Czarnecki et al., 2008, Ravikumar et al., 2012). Acute spinal cord slices are also typically obtained from neonatal animals and used for electrophysiological experiments where the electrical activity of individual neurons or the network as a whole can be investigated with intracellular or extracellular recordings. The advantages of acute slice experiments are that the slice preparation is relatively quick and therefore the synaptic connections within the slice network is largely unchanged compared to *in vivo* conditions (Lossi et al., 2009). The endogenously released chemicals from the dissecting and slicing procedures are washed out before experimentation begins so as not to affect the activity of the spinal DH networks. Organotypic slices have to be cultured for 10-14 days before it can be ensured the chemicals released from slicing are no longer present (De Simoni and Yu, 2006). In the period of culturing organotypic slices the disruption to the neuronal network that occurred during the slicing procedure is believed to cause re-organization of the synapses between the neurons within the slice, which does not occur in acute slices (Coltman et al., 1995). Furthermore, a major factor to consider with slice cultures is how well the culture conditions enable the survival of the neuronal cells within the slice. Non-neuronal cells typically survive better in culture compared to neuronal cells, which are affected more severely by the preparation speed, culture medium, age of the tissue and sterility (Lossi et al., 2009). Therefore, the proportions of the different cell types within the slice are likely to be altered in the *in vitro* spinal cord slice culture model which could affect the network structure and functionality. This is not an issue with *in vitro* acute slices, which are used for experimentation on the day of dissection (Buskila et al., 2014).

A drawback of utilising acute and organotypic slice models is that the viability of the slices diminishes with increasing age of the animal employed in the study. Consequently, neonatal animals are frequently used (Miletic and Randic, 1981,

Magnuson et al., 1987). However, there can be significant differences in the neurophysiology of neonatal compared to adult animals. An example of age-dependent changes in rodent neurophysiology is the switch of GABA signalling from excitatory in early development to inhibitory in adult animals (Lee et al., 2005). GABA_A receptors switch to become inhibitory as the expression of the KCC2 increases during development (Lee et al., 2005). In this thesis the acute spinal cord slice preparation has been utilised to investigate the activity of the spinal DH network due to its advantages over the slice culture model and its comparability to *in vivo* conditions.

1.7.3 Primary Cell Culture of the Spinal Dorsal Horn

Primary cell culture provides a model system which lends itself to very reproducible and consistent high-throughput screening of compounds. These properties of primary cell culture models have resulted in their extensive use by pharmaceutical companies to screen novel compounds. However, primary cell culture models also provide a highly accessible tool for investigating cell physiology and biochemistry. Neuronal cultures simplify the complex intact CNS, and make it accessible for use in a multitude of assays including electrophysiology, calcium imaging and molecular biology techniques. Recent development of MEA technology has enabled primary cell cultures to be grown on MEAs (Ito et al., 2014). Therefore, the activity across a cultured network can be recorded simultaneously, providing an indication of the synchrony of network's cells.

In neuronal primary cell culture models both individual cells or the whole network of neurons can both be investigated to study the physiology of the system in more detail than is possible with *in vitro* slice or *in vivo* spinal cord recordings. However, the simplification of such a complex system means that caution should be taken

when interpreting results from cell culture models. Typically the tissue dissected for cell culture is completely disrupted dissociating all the cells, therefore in culture the cells re-organise and form synapses, which is largely dependent on the conditions of the culture (Streit et al., 2001, Malin et al., 2007). As previously mentioned in regard to slice cultures, different cell types survive the culture process better than others, which could impact on the reformation of the network of the remaining cells.

Primary cell culture of spinal cord neurons has been widely developed and utilised (Ransom et al., 1977), however, there are far fewer reports using spinal DH culture. Selecting the dorsal region of the spinal cord for primary cell culture isolates those cells specifically involved in processing nociceptive signals. The spinal cord cell culture model exhibits a number of similarities with *in vitro* slice and spinal DH *in vivo* recording data, including rhythmic activity (Keefer et al., 2001, Streit et al., 2001) and the development of central sensitisation (Vikman et al., 2003). However, there is minimal information on the characterisation of spinal cord or spinal DH cultures in terms of the classes of neuronal and non-neuronal cells they contain. In this study a spinal DH primary cell culture model has been established, characterised and utilised to explore the activity of the DH, its responses to pharmacological manipulation and its potential in drug discovery assays.

1.8 Objectives

The overall aim of this project is to investigate the role of GABA_A and glycine receptors in the spinal DH using *in vitro* models as translational platforms for drug discovery. Specific aims of my thesis are as follows:

- 1) Development and characterisation of the rat embryonic spinal DH primary cell culture

- 2) Investigate how targeting GABA_A and glycine receptors modulates calcium release in the rat embryonic spinal DH primary cell culture model.
- 3) Investigate the effect of glycine receptor α subunit short interference RNA (siRNA) gene silencing on calcium response using the rat embryonic spinal DH primary cell culture.
- 4) Investigate how targeting GABA_A and glycine receptors modulates network activity in the rat *substantia gelatinosa* (SG) of the spinal DH using extracellular recordings in the *in vitro* acute spinal cord slice model.
- 5) Investigate how targeting GABA_A and glycine receptors modulates network activity in the rat SG of the spinal DH using MEA methodology in acute spinal cord slices and rat embryonic spinal DH primary cell culture.

2 Characterisation of the Embryonic Spinal Dorsal Horn Cell Culture Model

2.1 Introduction

Primary cell cultures present several advantages for neuronal cell network studies due to their greater similarity with neuronal cells *in vivo* compared to secondary cell lines. However, primary cell cultures are more challenging as the tissue dissection and processing of the cells has to be completed prior to commencing the culturing process (Gordon et al., 2013). Furthermore, primary cultures are not immortal like cell lines, which limits the volume of experimentation with each primary culture (Gordon et al., 2013). Cell culture models provide very versatile platforms, as they can be used with a multitude of techniques including molecular cell biology, immunofluorescence (IF), electrophysiology and calcium imaging. For these reasons pharmaceutical companies have been making use of primary cell cultures to screen novel compounds in various diseases (Eglen and Reisine, 2010, Nickolls et al., 2011, Lovitt et al., 2014).

Typically, for neuronal primary cell cultures the cells of the dissected tissue are completely dissociated before they are cultured (Streit et al., 2001, Malin et al., 2007, Gordon et al., 2013). The primary cell culture models of the spinal cord lack *in vivo* afferent input, which could affect the re-formation of the network in culture and the subsequent activity of the network. However, the more simplistic primary cell culture network makes it easier to decipher the circuitry. Therefore, it is essential to determine and classify the cell types present in the culture and compare to *in vivo* network populations to be able to draw stronger conclusions from the primary cell culture data and determine how transferrable the cell culture data is to the *in vivo* network.

Primary cell culture of spinal cord cells has been developed and utilised to study network activity (Ransom et al., 1977, Keefer et al., 2001, Streit et al., 2001). However, this model system includes both motor neurons of the VH and sensory neurons of the DH mixed together. Therefore, following dissociation these spinal

cord cells are likely to form a very different network in culture compared to what exists *in vivo*. There are fewer reports of spinal DH cultures, which provide a model system to study the spinal DH network without the influence of VH cells (Vikman et al., 2001, Hendrich et al., 2012b).

2.1.1 Aims

In this chapter the techniques of primary cell culture, calcium imaging, IF and quantitative real-time polymerase chain reaction (RT-PCR) have been utilised to develop and characterise the embryonic spinal DH cell culture model. This *in vitro* model has been investigated with the final aim of utilizing it for the screening of novel analgesics and studying the spinal DH network. The aims of this investigation are:

1. To develop the embryonic spinal DH cell culture model
2. To determine the proportion of neuronal and non-neuronal cells in the DH culture.
3. To determine the proportion of inhibitory and excitatory cells in the culture.
4. To define the neurochemical and co-localization profile of cells within the culture
5. To determine which of the GABA_A receptor α subunits are expressed in the DH culture
6. To determine which of the glycine receptor α subunits are expressed in the DH culture.

2.2 Methods

2.2.1 Embryonic Dorsal Horn Primary Cell Culture

The Schedule 1 procedure performed on pregnant female Wistar rats at embryonic day 14 (E14) was either by isoflurane followed by cervical dislocation at the University of Leeds or concussion followed by cervical dislocation when performed at Pfizer Neusentis, Cambridge. This was carried out in accordance with current EU/UK Home Office legislation and University of Leeds or Pfizer Neusentis local legislation. The embryos were removed from the dam and collected in ice-cold Hibernate E medium (Life Technologies, UK). Each embryo was subsequently removed from its embryonic sack and decapitated, then kept in ice-cold Hibernate E medium on ice. The embryonic fluid was collected from each embryonic sac when the sac was opened and added to the Hibernate E medium in which the decapitated embryos were collected in to improve viability of the tissue. The spinal cord was dissected from each embryo and the two thirds of DH of the spinal cords was separated and collected in fresh ice-cold Hibernate E medium immediately post-decapitation. There were typically 11-14 embryos per dam, therefore in each spinal DH cell culture preparation there was tissue from 11-14 embryos which was combined before processing for culturing. Once all the DH tissue had been collected and pooled together the tissue was spun at 1000 rpm for 3 minutes. The supernatant was removed and the tissue was re-suspended in 2 ml of Hibernate E containing trypsin (12.5%) in at 37°C. The tissue was incubated at 37°C for 18-20 minutes, with the tissue being manually mixed by shaking to improve trypsin digestion by separating the tissue sections. Deoxyribonuclease I (DNase I) (0.1%) (Sigma-Aldrich, UK) in 2 ml of culture medium 1 (Table 2.1) was then added to the sample and spun for 3 minutes at 1000 rpm. DNase I treatment is required for the breakdown of extracellular DNA that can arise in the processing of the tissue and cause damage to the cells. The supernatant was removed and 1 ml of culture

medium 1 containing 1% cytosine β -D-arabinofuranoside (Ara-C) (Sigma-Aldrich, UK) at 37°C was added to the tissue. The tissue was manually triturated then pulse centrifuged to 1000 rpm and the supernatant containing the cells was collected. This trituration step was repeated once more, and then a cell count was performed, either using a Countess cell counter (Invitrogen, UK) or manually on a haemocytometer. The cells were plated at 1.7×10^6 cells/100 μ l and then the plates were pulse centrifuged to 1000 rpm to evenly spread the cells across each well. Typically, from a preparation from a single dam with 11-14 embryos, there were 180-220 wells of the spinal DH cells plated normally plated as 36 wells per plate. A flow diagram of the DH tissue processing protocol can be found in Figure 2.1. The BD Falcon cell culture plates (BD Biosciences, UK) were pre-coated with poly-D-lysine (molecular weight: 70,000-150,000; Sigma-Aldrich, UK) and natural mouse laminin protein (Life Technologies, UK) to aid cell attachment to the base of the plate. The poly-D-lysine was dissolved in distilled water and 50 μ l/well was added the day before the cell culture preparation, kept at 4°C overnight. On the day of the cell culture preparation the poly-D-lysine was removed from the plates and 50 μ l/well of laminin diluted in PBS was added. The plates were then kept at 37°C in the incubator until required for plating the cells. After the cells were incubated for 24 hours at 37°C the media was changed to culture medium 2 (Table 2.2), subsequent media changes were done every 2-3 days with culture medium 2. After 12-14 days in culture, the cells were used for experimentation. Spontaneous, synchronous firing of the network was observed in calcium imaging and electrophysiological experimentation after 12-14 days in culture.

Table 2.1 Culture medium 1 components

Component		Company
DMEM/F12	500ml	Invitrogen
Fetal Bovine Serum Gold	50ml	PAA
Glutamax	5ml	Invitrogen
Penicillin/Streptomycin (10,000 U/ml)	5ml	Invitrogen

Table 2.2 Culture medium 2 components

Component		Company
Neurobasal Medium	500ml	Invitrogen
B-27 Supplement	10ml	Invitrogen
Glutamax	5ml	Invitrogen
Penicillin/Streptomycin (10,000 U/ml)	5ml	Invitrogen

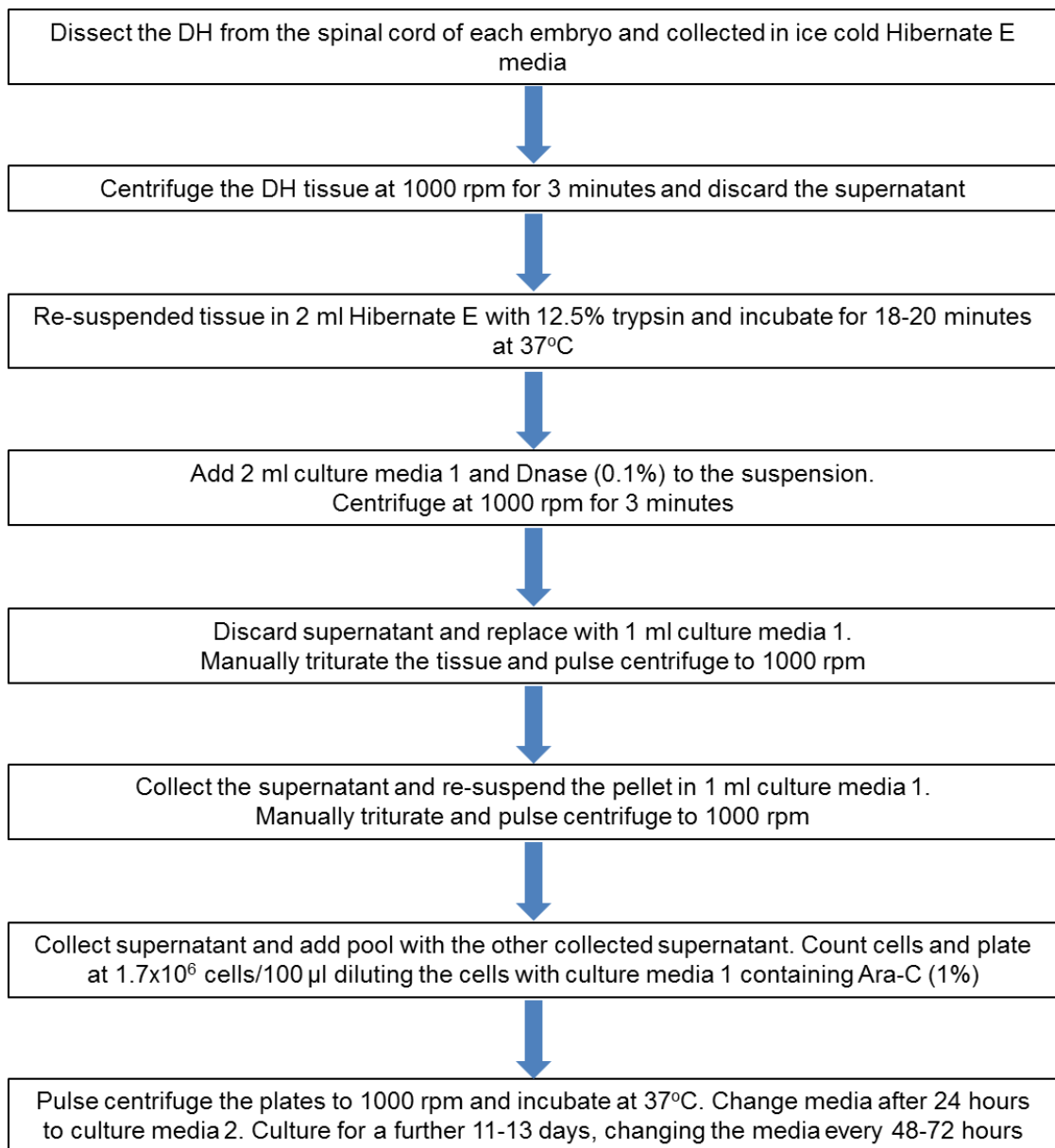


Figure 2.1 A flow diagram of the protocol procedures for the processing and the culturing of the embryonic spinal DH tissue following the removal of the embryos from the dam.

2.2.2 Fluorescent Calcium Imaging with Cultured Dorsal Horn Cells

The culture media was removed from the wells of the plate and replaced with 80 μ l of FLIPR Calcium 5 Dye (Molecular Devices, USA) diluted in Hanks' Balanced Salt Solution (HBSS) (-/-) with calcium chloride (1.8 mM) and 1% HEPES (Sigma-Aldrich, UK), and adjusted to pH 7.4 with sodium hydroxide (Sigma-Aldrich, UK). No magnesium was added to the buffer solution to remove the N-methyl-D-aspartate (NMDA) receptor magnesium block as signalling through this receptor is known to be required for spontaneous activity (Smith et al., 1989, Kilic et al., 1991, Streit et al., 2001). The plate was incubated at 37°C for 30-40 minutes to allow for the cells to take up the dye before calcium imaging was performed. The advantage of the Calcium 5 Dye over other calcium dyes such as Fura 2, is that the cells do not need pre-washing and the Calcium 5 Dye does not need to be washed off prior to running calcium imaging assays. Therefore, there is reduced disruption to the cells before they are used for the assay and there are fewer cells are lost. The fluorescent calcium imaging was done using the live-cell he bioimaging system BD Pathway 855 (BD Biosciences, USA), in combination with the BD Attovision software (BD Biosciences, USA; version 1.6). This system allows for the measurement and recording of fluorescence intensity of live cells in culture. A video is captured of each well as the fluorescence intensity of individual regions of interest (ROI) was recorded. The ROIs were determined using the software with manual adjustment so that only the fluorescence of the cells was captured and any background noise was eliminated. The video recording of the culture enabled visualisation of the culture network within a well, which was vital in the optimisation process of the culture. Identifying which preparation of the cells worked best according to the appearance of the network formation and network firing behaviour enabled the development of the optimal DH cell culture protocol. The baseline activity was recorded for 4 minutes, which was followed by manual addition of a compound diluted to the

required concentration using the HBSS (-/-) buffer. The activity in the presence of the compound was subsequently recorded for another 4 minutes. This data was not quantified or analysed, but used to optimise the spinal DH cell culture protocol through visualising the culture's spontaneous activity and response to compound addition.

2.2.3 Culture Dorsal Horn Cell Immunofluorescence

The cultured DH cells were fixed at 12-14 days *in vitro* (DIV) by removing the media, washing the wells of the plates twice with PBS (0.1 M) and adding 100 μ l paraformaldehyde (4%) per well. After 15-20 minutes the paraformaldehyde was removed and the wells washed three times with PBS (0.1 M). For each wash of the wells 200 μ l of PBS was added to each well and left for 5 minutes before being removed, and the process repeated. After the washes 200 μ l of PBS was added to each well and the cells stored at 4°C until ready to be used for staining. The required volume of blocking buffer was made, which contained PBS (0.1 M) with 3% normal donkey serum and 0.3% triton-X100. When ready to perform the staining the PBS was removed from the wells and 100 μ l of blocking buffer was added per well and incubated at room temperature for 2 hours. The blocking buffer was then removed and replaced with 100 μ l of the required primary antibodies diluted in the same blocking buffer (Table 2.3). A minimum of six wells were tested for each antibody combination. The plates of cells were incubated with the primary antibodies overnight on a rocking platform at 4°C. The primary antibodies were removed and the wells washed with PBS (0.1 M) three times. The secondary antibodies were diluted in the same blocking buffer and 100 μ l of secondary antibody solution was added per well as required (Table 2.4). The plates were wrapped in aluminium foil to protect the antibodies from light damage, and the

samples incubated for 2 hours at room temperature on a rocking platform. The wells were washed 3 times with PBS (0.1 M) and then 200 μ l of PBS was added to each well. The plates were kept wrapped in aluminium foil at 4°C until they were imaged. In parallel negative control experiments were performed for each primary antibody tested omitting the addition of the secondary antibodies. The negative controls demonstrated a lack of positive staining. Examples of some of these negative controls are illustrated in Figure 2.2.

2.2.4 Imaging and Analysis

The cultured cells were imaged using an inverted LSM 700 confocal microscope (Carl Zeiss Microscopy, USA) in conjunction with Zen 2.1 (Black) software (Carl Zeiss Microscopy, USA). The Alexa 488 and Alexa 555 laser filters were selected to image cells. For the cultured DH cells, a minimum of six wells were stained for each antibody combination, and between four and six of the wells were imaged and the cells counted. These six wells utilised for each staining consisted of three wells on one plate and three wells from another plate. The two different plates were from different cell culture preparations, therefore arising from separate sets of embryos. The number of independent culture preparations for each experiment is indicated as N, while the number of individual wells tested is given as n. The number of positively-stained cells in the four to six wells for each antibody staining was counted and the mean calculated. The number of co-localised cells in each staining was also counted and the mean calculated. The percentage of co-localised cells out of the total number of neuronal nuclei (NeuN)-positive cells or the total number of positive cells of that antibody was calculated where required. These values are given with the standard error of the mean (S.E.M).

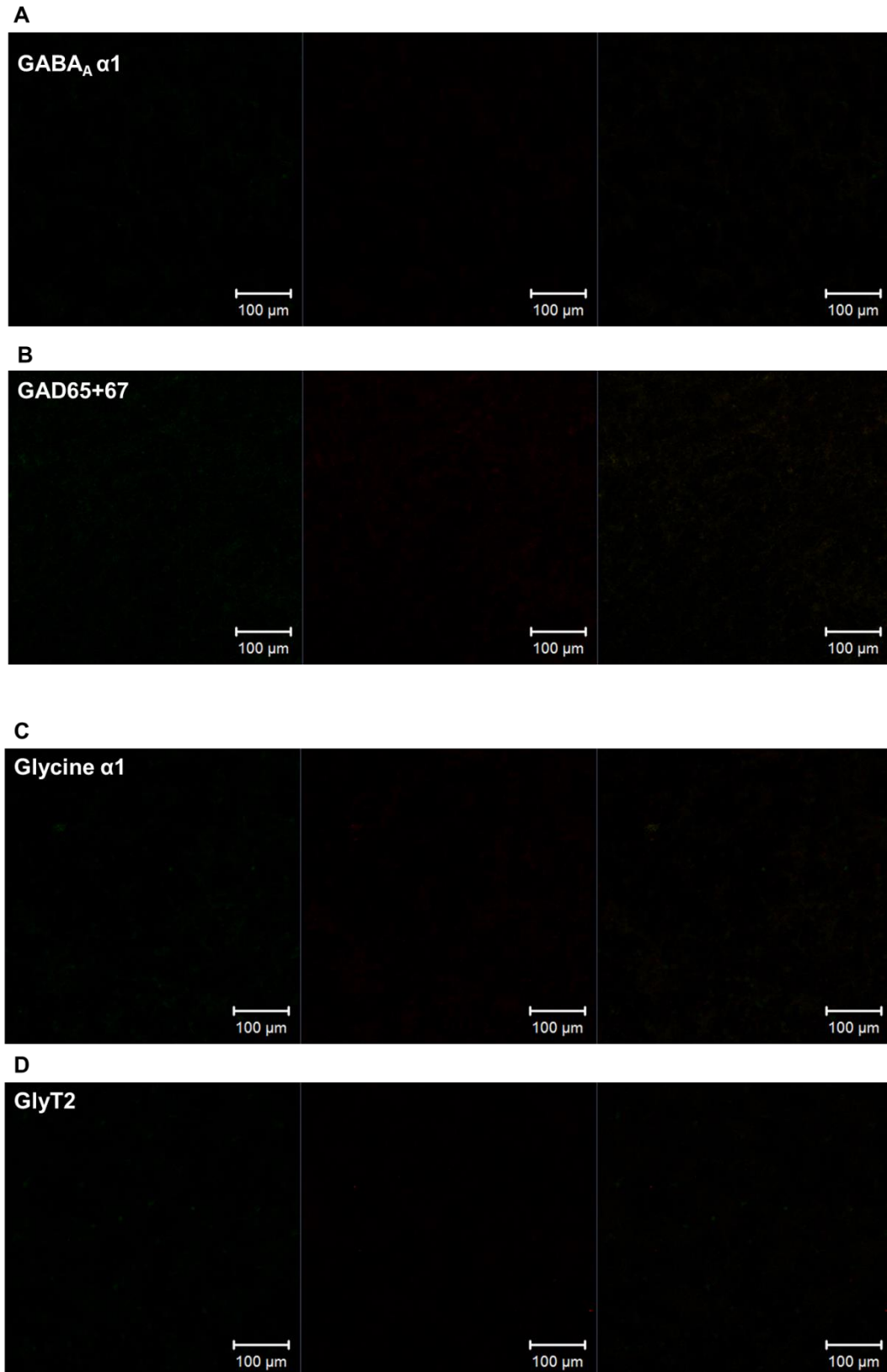


Figure 2.2 IF control experiments in the absence of secondary antibodies, for the primary antibodies for (A) the GABA_A receptor α1 subunit, (B) GAD65+67, (C) the glycine receptor α1 subunit and (D) GlyT2. The left panel for each is taken with Alexa Fluor 488 filter, the middle panel with Alexa Fluor 555 filter and the right panel is the merge.

Primary Antibody	Function	Species	Dilution	Source	Reference
NeuN	Neuronal cell nuclei	Mouse	1:500	Millipore (MAB377)	Seelke et al. (2013)
NeuN	Neuronal cell nuclei	Rabbit	1:500	Cell Signalling (D3S31)	Cell Signalling
GFAP	Astrocytes Glial Cells	Mouse	1:500	Millipore (MAB360)	Kern et al. (2011)
Iba1	Microglia	Rabbit	1:500	Wako Pure Chemical Industries (019-19741)	Le Blon et al. (2014)
GAD 65/67	GABAergic cells	Rabbit	1:500	Abcam (AB1511)	Krosnowski et al. (2012)
GlyT2	Glycinergic cells	Rabbit	1:500	Abcam (AB156022)	Abcam
VGlut2	Glutamatergic cells	Guinea-Pig	1:500	Abcam (AB2251)	Zelano et al. (2009)
Glycine α 1	Receptor subunit	Goat	1:250	Santa Cruz (SC-17278)	Ge et al. (2007)
Glycine α 2	Receptor subunit	Goat	1:200	Santa Cruz (SC-17279)	Majumdar et al. (2008)
Glycine α 3	Receptor subunit	Goat	1:500	Santa Cruz (SC-17282)	Majumdar et al. (2008)
GABA α 1	Receptor subunit	Rabbit	1:150	Abcam (AB33299)	Lindstrom et al. (2010)
GABA α 2	Receptor subunit	Rabbit	1:200	Alomone Labs (AGA-002)	Quadrato et al. (2014)
GABA α 3	Receptor subunit	Rabbit	1:500	Alomone Labs (AGA-003)	Zhou et al. (2013)
GABA α 4	Receptor subunit	Rabbit	1:200	Abcam (AB73874)	Quadrato et al. (2014)
GABA α 5	Receptor subunit	Rabbit	1:200	Abcam (AB10098)	Wu et al. (2014)
GABA α 6	Receptor subunit	Rabbit	1:250	Sigma (G5544)	Sigma-Aldrich
Parvalbumin	Calcium-binding protein	Mouse	1:1000	Sigma (P3088)	Contini and Raviola (2003)
KCC2	Transporter	Rabbit	1:100	Millipore (07-432)	Wang and Sun (2012)
nNOS	Neuronal NOS	Rabbit	1:2000	Abcam (AB5380)	Russo et al. (2013)
Gephyrin	Inhibitory cells	Goat	1:250	Santa Cruz (SC-6411)	Waldvogel et al. (2003)

Table 2.3 List of the primary antibodies used for IF

Secondary Antigen	Species	Fluorophore	Dilution	Source
Mouse	Donkey	Alexa 488	1:500	Invitrogen
Mouse	Donkey	Alexa 555	1:500	Invitrogen
Rabbit	Donkey	Alexa 488	1:500	Invitrogen
Rabbit	Donkey	Alexa 555	1:500	Invitrogen
Rabbit	Goat	Alexa 555	1:500	Invitrogen
Guinea-Pig	Donkey	Alexa 488	1:500	Invitrogen

Table 2.4 List of the secondary antibodies used for IF

2.2.5 Quantitative Real-Time PCR

The total RNA was isolated from the cultured DH cells at 12-14 DIV using RNeasy Mini Kit (Qiagen). Cells cultured from one independent preparation were utilised, with RNA extracted from 30 individual wells. Before commencing all RNA work, surfaces and pipettes were disinfected with RNase Away Reagent (Ambion, Life Technologies) to minimise RNA contamination. The cells were harvested by disrupting the cells with RLT buffer containing β -mercaptoethanol (1%) and triturating with a pipette. The pellet was vortexed and then added to a QIAshredder spin column and centrifuged for 2 minutes at maximum speed. The same volume as lysate of 70% ethanol was added to the homogenised lysate and mixed by pipetting. This sample was then transferred to an RNeasy spin column and centrifuged for 15 seconds at 13,000 rpm. The flow-through was discarded and 700 μ l of RW1 buffer was added to the spin column and spun again for 15 seconds at 13,000 rpm. Again the flow-through was discarded and the step repeated but with RPE buffer. This was repeated with RPE buffer, but spinning for 2 minutes. This ensures no ethanol remains in the spin column as this can effect subsequent reactions in the process. Finally the RNA was eluted by adding 30 μ l of RNase-free water to the spin column and centrifuging for 1 minute at 13,000 rpm. The concentration of RNA was calculated with a NanoDrop 2000c (Thermo Scientific Inc, USA). The human spinal

cord mRNA used in this study was obtained from BioChain (AMS Biotechnology Ltd, UK). The spinal cord mRNA was extracted from the tissue of a healthy male, 59 years old. The RNA was then converted to cDNA with an Omniscript Reverse Transcription Kit (Qiagen, USA). All the reagents for this protocol were thawed and stored on ice throughout the preparation. Two mastermixes were prepared as outlined in Table 2.5, one is the normal mastermix the other was a negative control with no reverse transcriptase added. Once all the reagents were mixed together to make mastermix reactions for each of the RNAs, the samples were incubated for 60 minutes at 37°C. The concentration of cDNA was then determined using the NanoDrop 2000c. The cDNA was stored at -20°C until used for TaqMan PCR experiments.

For the TaqMan relative quantitative RT-PCR the housekeeping gene β -actin (ACTB) was used as a positive control (Thermo Fisher Scientific Inc., USA), either human or rat as required. Including a reference gene in the same well as each of the samples allows for normalisation of each of the target genes. RT-PCR was performed for each of the GABA_A receptor α subunits 1-6, with assay probes GABRA1-6 for human and rat (Applied Biosystems, ThermoScientific), for both the human spinal cord and the rat spinal DH cDNA samples. Similarly, human and rat assay probes for the glycine receptor α subunits 1-4 (Glr1-4) and the β subunit (Glrab) (Applied Biosystems, ThermoScientific) were utilised for RT-PCR with both human spinal cord and rat spinal DH cDNA samples. RT-PCR with the rat spinal DH sample was also performed with the assay probes for the rat glycine transporters 1 and 2 (GlyT1 and GlyT2) (Applied Biosystems, ThermoScientific). All these primers were proprietary of Applied Biosystems, who have not disclosed the sequences but state that all these primers have been verified by the company for their high level of specificity and efficiency. A list of all the assay probes utilised can be found in Table 2.6 and Table 2.7. The Taqman mastermix used for each 20 μ l reaction per well of

the PCR plates is outlined in Table 2.8. A stock mastermix for each assay was made without adding cDNA to minimise pipetting error. The cDNA was added to the plate for the PCR reaction and the mastermix added to it to make 20 μ l total reaction volume per well. Each reaction was done in triplicate, and each of the RT negative cDNA samples for negative controls were done in triplicate. The RNase-free water was also used as a negative control to confirm there was no contamination of the water used in the reactions. The TaqMan RT-PCR amplification reaction and detection was done using a LightCycler 480 II (Roche Diagnostics, Switzerland). This was linked to a computer with the LightCycler 480 II Software (version 1.5.1), where the programme for relative quantification was used with the detection format of dual colour hydrolysis probe. This programme begins with a pre-incubation of 10 minutes at 4.4°C followed by 45 amplification cycles of 10 s at 95°C, 30 s at 60°C then 1 s at 72°C, with an end cooling phase of 30 s at 40°C.

Mastermix Reagents	RT Positive Mastermix (μl)	RT Negative Mastermix (μl)
RT Buffer (x10)	2	2
dNTP mix (5 mM)	2	2
Oligo dT (0.5 μ g/ μ l)	0.2	0.2
Random Nonamers	4	4
RNase Inhibitor (10 U/ml)	1	1
Omniscript RT	1	0
RNA	9.8	9.8
Water	0	1
Total Volume	20	20

Table 2.5 The contents for 20 μ l of mastermix for cDNA production used for all the samples required for the RT-PCR experiments. A negative control mastermix was also prepared for each RNA sample which did not contain reverse transcriptase (Omniscript RT).

Gene	Assay ID
GABRA1	Rn00788315_m1
GABRA2	Rn01413643_m1
GABRA3	Rn00567055_m1
GABRA4	Rn00589846_m1
GABRA5	Rn00568803_m1
GABRA6	Rn00573029_m1
Gira1	Rn00565582_m1
Gira2	Rn00561280_m1
Gira3	Rn00586890_m1
Gira4	Rn01410530_m1
Girb	Rn00583966_m1
GlyT1	Rn01416529_m1
GlyT2	Rn01475607_m1

Table 2.6 A list of the RT-PCR rat assay probes used, with their assay ID number from Applied Biosystems (Thermoscientific, UK).

Gene	Assay ID
GABRA1	Hs00971228_m1
GABRA2	Hs00168069_m1
GABRA3	Hs00968132_m1
GABRA4	Hs00608034_m1
GABRA5	Hs00181291_m1
GABRA6	Hs00181301_m1
Gira1	Hs00609267_m1
Gira2	Hs01033736_m1
Gira3	Hs00197920_m1
Gira4	Hs01595852_m1
Girb	Hs00923871_m1

Table 2.7 A list of the RT-PCR human assay probes used, with their assay ID number from Applied Biosystems (Thermoscientific, UK).

Taqman Mastermix Reagents	Volume (μl)
cDNA	2
Taqman Mastermix	10
Assay (x20)	1
ACTB (x20)	1
Water	6
Total Volume	20

Table 2.8 The TaqMan mastermix reagents for each well of the RT-PCR experiment. The same mastermix was utilised for the negative control sample (RT negative). The Taqman Mastermix, assay probes and ACTB were all sourced from Applied Biosystems.

2.2.6 Analysis of Relative Quantification RT-PCR

After the C_T values were obtained from the RT-PCR experiments an arbitrary copy number was calculated from the C_T values obtained for each repeat performed for all the assay probes. The average of the three housekeeping gene C_T values obtained in the triplicate of repeats for each assay probe was calculated and the arbitrary copy numbers for these average values were then determined. The arbitrary copy number calculation used was $10^{(12-(0.3 \times C_T))}$ (Cox et al., 2008). The scaling factor was determined for each assay probe using the housekeeping gene arbitrary copy number values. The GABA_A receptor subunit arbitrary copy number values were scaled relative to GABRA1 and the glycine receptor subunits and glycine transporters were scaled relative to Glra1. For example, the averaged ACTB arbitrary copy number values for each of the GABA_A receptor subunits was divided by the ACTB arbitrary copy number of GABRA1. The three arbitrary copy number repeats for the GABRA1 were each multiplied by the scaling factor for that receptor subunit. This was repeated for the other GABA_A receptor subunits, each multiplied by their corresponding scaling factor value. Similarly this was done with the glycine

receptor subunit values. The average scaled arbitrary copy number was calculated from the repeats for each receptor subunit and plotted with the S.E.M. The RT-PCR data for the human spinal cord and rat spinal DH samples were analysed separately.

2.2.7 Absolute Quantification of Glycine Receptor Subunits

Plasmid DNA constructs containing the human or rat glycine receptor α subunits were obtained from OriGene Technologies Ltd (USA). Each of the plasmid constructs were transformed into One Shot TOP10 competent *E.coli* cells (Invitrogen, UK). The One Shot TOP10 cells were thawed on ice, and 5 μ l of the plasmid DNA was added to the vial of cells (50 μ l cells/vial) and the solution mixed by swirling or tapping the tube. The cells are then incubated on ice for 30 minutes, then they were heat-shocked for 30 seconds at 42°C. The cells were then returned to ice for 2 minutes then 250 μ l of S.O.C medium was added to each vial. The vials were then incubated on a horizontal shaker at 37°C for one hour. 20 μ l of each of the cell transformations were spread onto pre-warmed LB agar plates, and a repeat of each plate with 100 μ l of each transformation. Two different volumes of cells were plated to ensure maximise the chances of one of them growing colonies. The plates were incubated at 37°C overnight. The colonies were selected from each plate and the DNA purified using a Qiagen Plasmid Plus Maxi Kit (Qiagen, USA), with the concentration of final purified DNA determined using a NanoDrop 2000c. For the absolute quantification RT-PCR experiments 10-fold serial dilutions of the DNA were made in PCR-grade water. These were used in conjunction with the same mastermix described previously with the appropriate TaqMan probe. On the same PCR plate three repeats of the required cDNA of the rat spinal DH culture or human spinal cord were also run. As previously negative control reverse transcription

negative samples and water only samples were also run on the same plate. Similarly the β -actin housekeeping gene was also used in the wells with the rat DH culture cDNA or human spinal cord cDNA. The RT-PCR reaction was done using the LightCycler 480 II as described for the relative quantification RT-PCR experiments.

2.2.8 Analysis of the Absolute Quantification RT-PCR Data

Using the calculated concentrations of each of the serial dilutions of each plasmid DNA and the C_T values, standard curves were plotted for each of the plasmid DNA samples, which were all run as triplicates in the RT-PCR experiment. The mean C_T value of the sample of the human spinal cord or spinal DH culture was calculated from the triplicate repeats of each of these samples. The standard curve was then used to determine the concentration of the cDNA of the sample. From this concentration the number of molecules was calculated for each of the glycine receptor subunits in the two samples using the provided molecular weights of the molecules from Qiagen.

2.3 Results

2.3.1 *Optimisation of the Embryonic Rat Spinal Dorsal Horn Culture*

There was extensive optimisation of the embryonic rat spinal DH cell culture with alterations made to numerous steps of the protocol from the collection of the embryos to the loading of the calcium dye. Initially the viability of the cells harvested from the embryonic spinal cords was low, at around 60%. This was thought to be due to the embryos being kept in Hibernate E media for an extended length of time before their spinal cords were removed and the DH isolated. It was considered that the Hibernate E did not contain sufficient ingredients to prevent degradation of the embryonic tissues. To counteract this amniotic fluid from each embryo's amniotic sac was collected and added to the Hibernate E media in which the decapitated embryos were kept. Furthermore, the length of time for each DH dissection was reduced and consequently the viability of the cells when counted increased to $91.7 \pm 0.38\%$ (S.E.M) (n=17, N=8).

The cells were found to form large clusters with very few projections between cells when cultured at a density of 1×10^6 cells/100 μ l (Figure 2.3 A). When imaged on the BD Pathway system most of these cells did not display any spontaneous activity. The cell density was increased to 1.5×10^6 cells/100 μ l, which improved the culture with fewer clusters forming. However, it was noted that the majority of the cells congregated to the edges of the wells leaving the centre with a much lower density. To resolve this issue the plates of cells were spun in a centrifuge immediately after the cells were plated. This dramatically improved the culture with the cells evenly distributed across the plate, and much less clustering of cells. These cells did spontaneously fire, with a much improved reliability. A further increase in cell density to 1.75×10^6 cells/100 μ l was attempted which further reduced the formation of clusters of cells and thus was the final chosen plating

density (Figure 2.3 B). The progression of the culture through the 12-14 days spent in culture with all optimisation steps in place is depicted in Figure 2.4. The cells were run each day on the BD Pathway from 7 DIV to determine which days displayed the best spontaneous activity. From day 9 the occasional single cell could be seen to fire on their own and by day 10-11 the whole network was observed to display highly synchronously calcium spikes but not rhythmically. Between 12-14 DIV the spinal DH culture had highly synchronous, repetitive calcium spikes with a rhythmic firing pattern. The frequency of this rhythmic calcium activity was 0.082 ± 0.02 Hz (Figure 2.5 and supplementary CD). Beyond 14 DIV the calcium spikes began to diminish, and consequently for subsequent experimentation the spinal DH cultures were used when they reached 12-14 DIV.

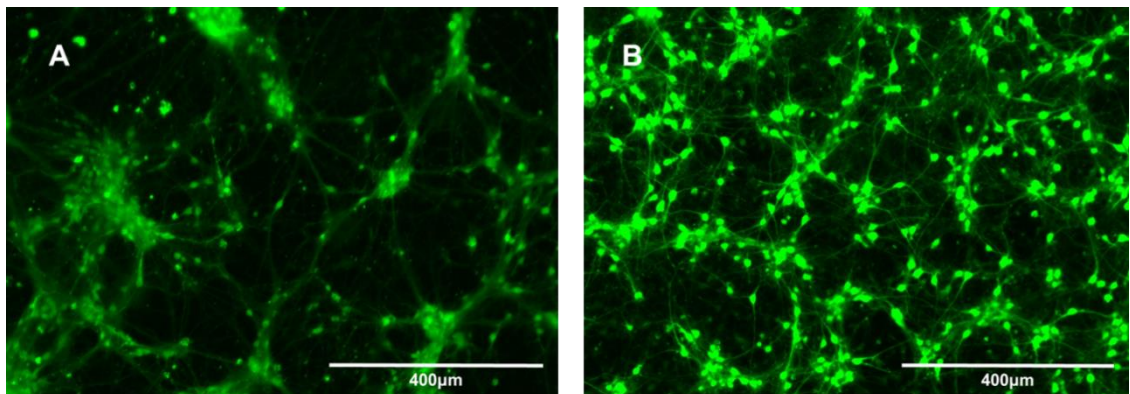


Figure 2.3 Embryonic rat DH cell culture at 14 DIV. In A and B the cells have been dye loaded with Calcium 5 dye. All images were taken using a digital inverted microscope (EVOS, AMG, Life Technologies, UK). (A) An example of the culture when the cell density was 1.5×10^6 cells/100 μ l and without centrifuging the plate. The cells can be seen clustered together, and there were fewer projections between cells. (B) The DH cell culture after application of all optimisation processes at 1.75×10^6 cells/100 μ l. The cells are evenly distributed across the surface with many projections forming the network.

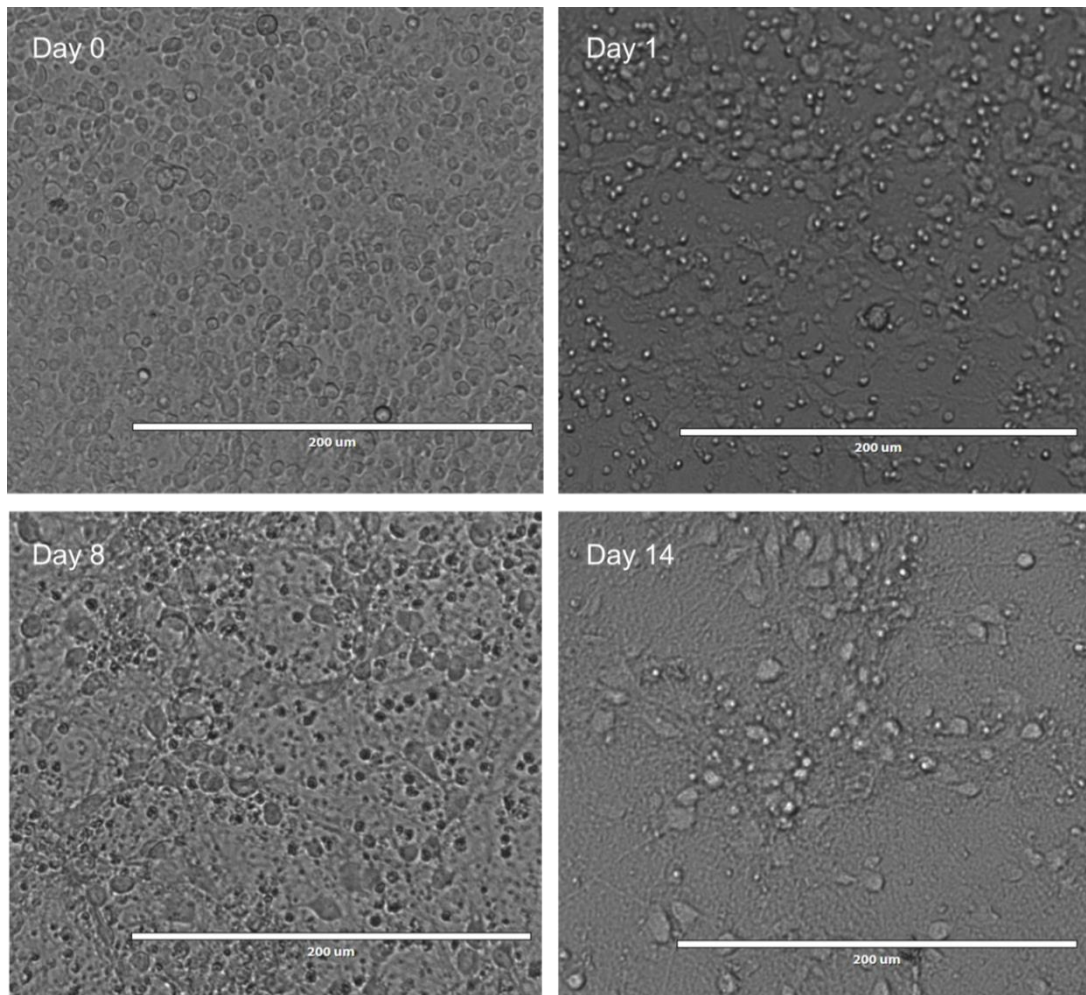


Figure 2.4 Progression of a rat embryonic spinal DH cell culture from day 0, immediately after plating the cells, to 1 DIV, 8 DIV and 14 DIV. At day 0 the cells are completely dissociated and densely packed. After 24 hours in culture, neurite outgrowth from many of the cells can already be seen, and by 8 DIV extensive network connections can be observed. At 14 DIV there is no significant visible change in the network, however, by this stage, the cells are synchronously firing.

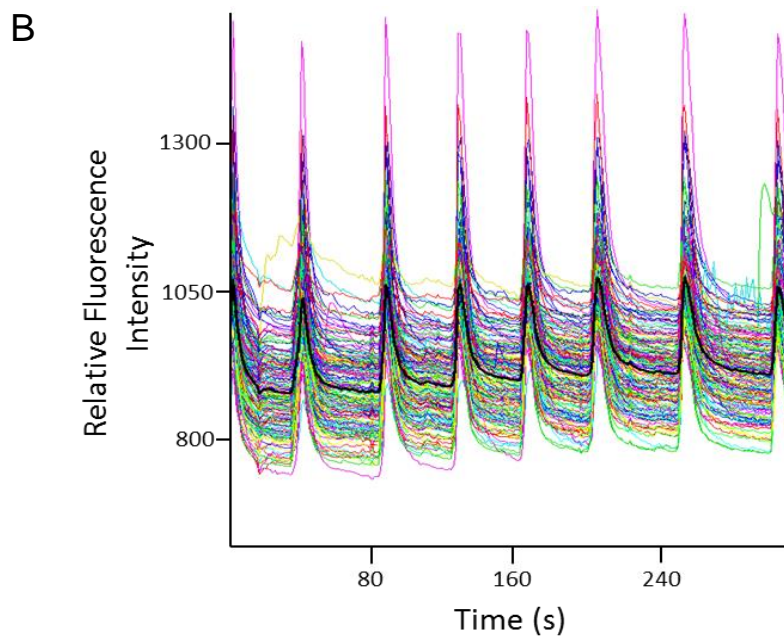
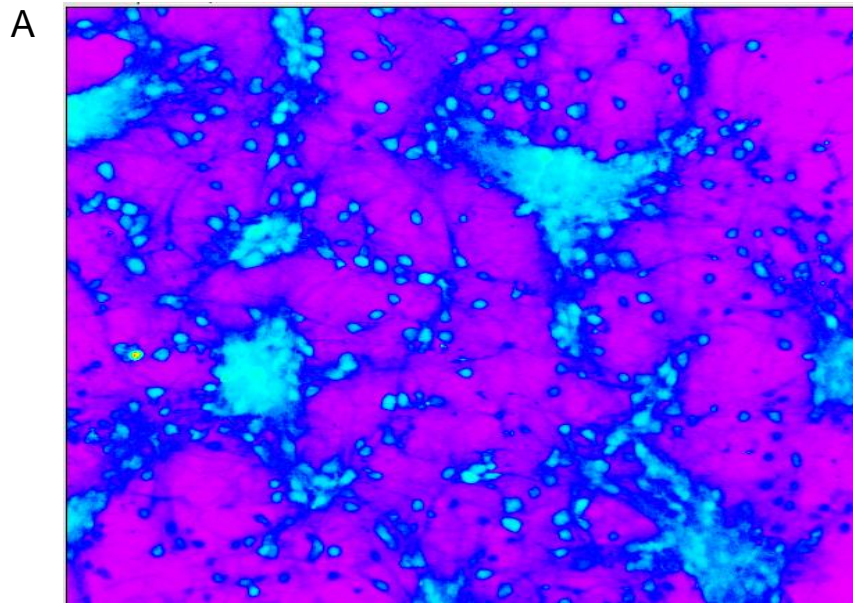


Figure 2.5 An example of the spontaneous, synchronous activity of the embryonic spinal DH cell culture after 13 DIV imaged using the BD Pathway system. (A) A still image of the video recorded using the BD Attovision software of the embryonic DH cell culture. See the supplementary CD for the real-time video. (B) The relative fluorescence intensity plot over time of the spontaneous activity of the culture shown in (A). Each coloured line represents the intensity of a single ROI within the frame of the image. The black line is the average of all the ROI intensities over time. The culture displays highly synchronous, rhythmic activity at all ROIs.

2.3.2 Characterisation of the Spinal Dorsal Horn Cell Culture Model: Neuronal and Non-Neuronal Cells

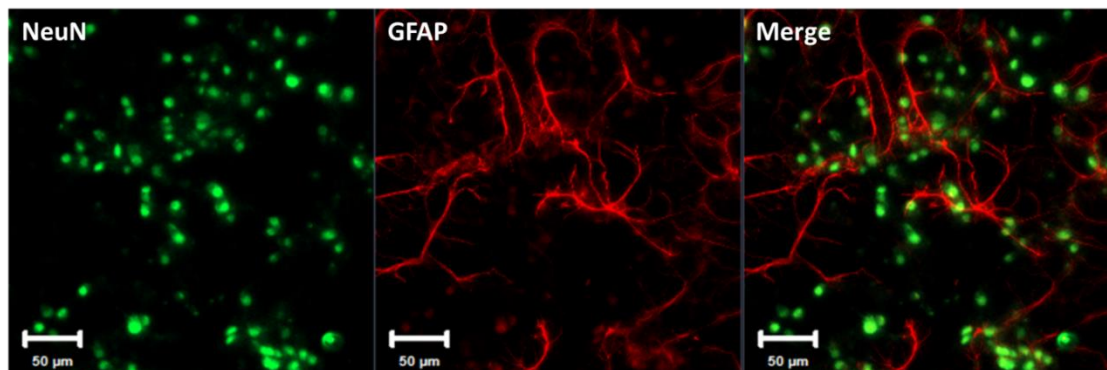
To address the second aim of this study the primary embryonic DH cell cultures were stained with NeuN, glial fibrillary acidic protein (GFAP) and ionized calcium-binding adapter molecule 1 (Iba1) to determine the presence of neuronal, glial and microglial cells, respectively. Positive staining was detected for all three cell types in the DH culture (Figure 2.6). In the NeuN and GFAP double-labelled cultured there were 71.8 ± 5.0 NeuN-positive cells and 19.0 ± 4.2 cells positive for GFAP. Therefore, from the total number of NeuN-positive and GFAP-positive cells in the cultures, there was an average of $79.1 \pm 4.3\%$ of NeuN-positive cells and $20.9 \pm 4.6\%$ GFAP-positive cells (N=2, n=6). In the cultures labelled with NeuN and Iba1, 74 ± 2.7 cells were NeuN-positive and 25.8 ± 3.5 were Iba1-positive. This is an average of $74.2 \pm 1.7\%$ NeuN-positive cells and $25.8 \pm 1.7\%$ Iba1-positive cells (N=2, n=4).

2.3.3 Excitatory and Inhibitory Interneurons in the Spinal Dorsal Horn Cell Culture Model

The second aim of the study was to determine the proportion of excitatory and inhibitory interneurons in the spinal DH cell culture. To investigate this, the excitatory marker vGluT2 was co-stained with NeuN (Figure 2.7). This staining illustrated the presence of glutamatergic interneurons in the DH culture. There were 76 ± 3.7 NeuN-positive cells and 53 ± 4.6 vGluT2-positive cells. An average of $69.8 \pm 5.6\%$ of the NeuN-positive cells were co-localised with the vGluT2-positive cells (N=2, n=4). The inhibitory markers GAD 65 and 67 (Figure 2.8) and glycine transporter 2 (GlyT2) (Figure 2.9), for GABAergic and glycinergic cells, respectively,

were also co-stained with NeuN. In the cultures co-labelled with NeuN and GAD 65 and 67, 97 ± 3.3 cells were NeuN-positive and 53 ± 4.2 cells were GAD 65 and 67-positive. An average of $53.8 \pm 4.9\%$ of the NeuN-positive cells co-stained with GAD65-67-positive cells (N=2, n=4). From the NeuN and GlyT2 co-stained DH cultures 84 ± 5.1 NeuN-positive cells were counted and 24 ± 2.6 GlyT2-positive cells. All the GlyT2-positive cells co-localised with NeuN positive cells. There was an average of $29.0 \pm 8.0\%$ of the NeuN-positive cells which co-localised with GlyT2 (N=2, n=4).

A



B

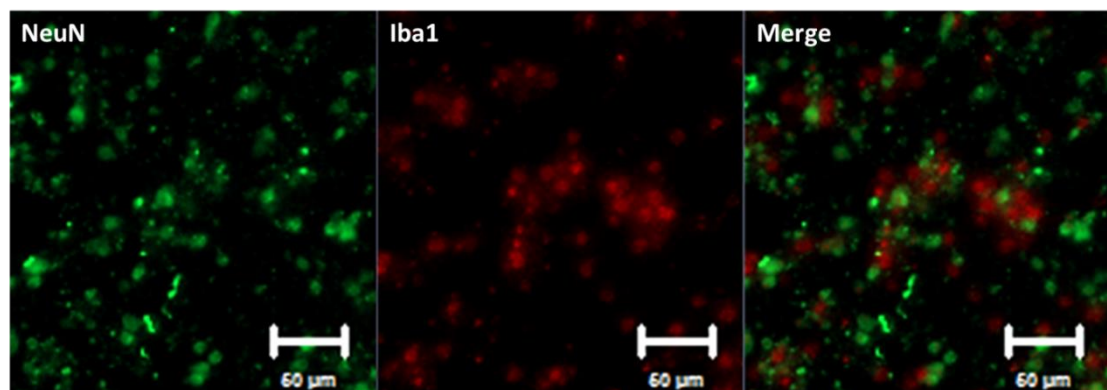


Figure 2.6 NeuN, GFAP and Iba1 staining in the rat embryonic DH cell culture. (A) NeuN (green) and GFAP (red) with the merge image in the right panel. (B) NeuN (green) and Iba1 (red), with the merge on the right. There is no co-localisation of these cell types, and there is a significantly higher proportion of NeuN-positive cells compared to either GFAP- or Iba1-positive cells.

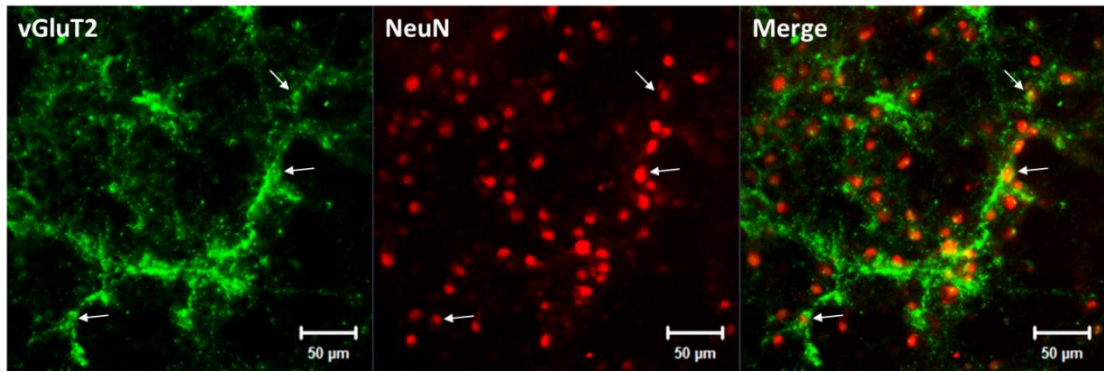


Figure 2.7 Embryonic DH culture stained with NeuN (green) and vGluT2 (red), and the merge image of the two images in the right panel. Examples of those cells co-localised with vGluT2 and NeuN are indicated by arrows.

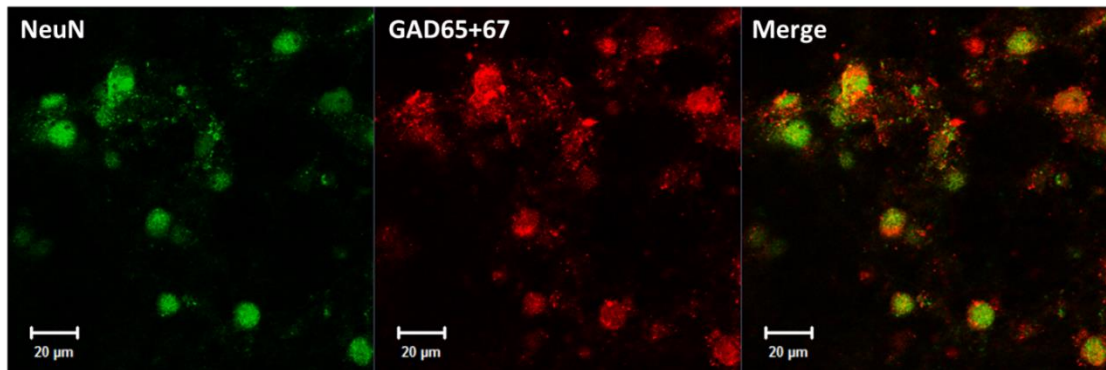
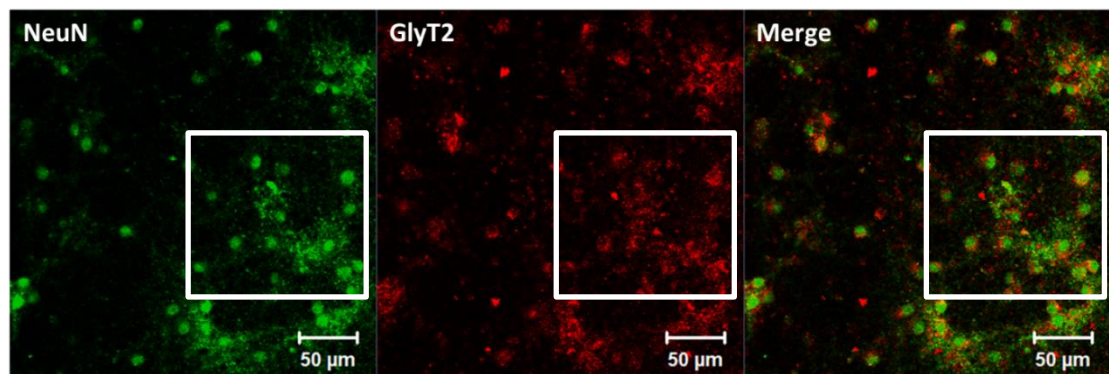


Figure 2.8 The embryonic DH culture stained for NeuN (green) and GAD 65 and 67 (red). The merge image in the right panel shows the co-localisation of GAD 65 and 67 with neuronal cells confirming that there are GABAergic interneurons in the DH culture.

A



B

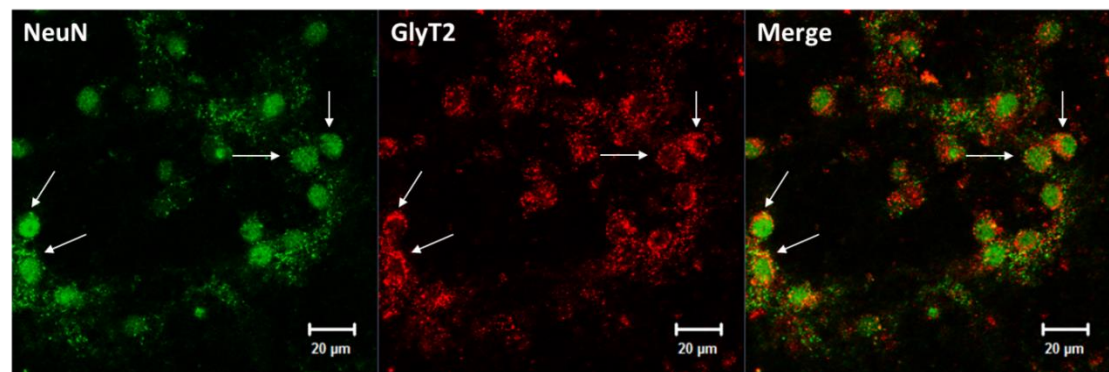
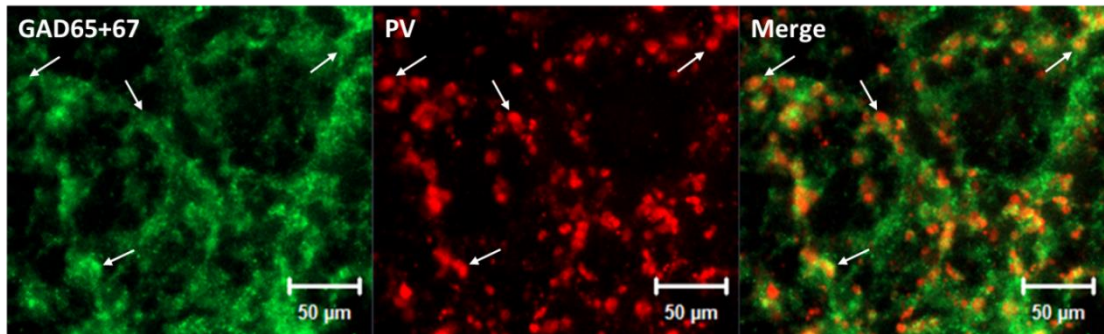


Figure 2.9 Double immunolabelling of the spinal DH culture with NeuN (green) and GlyT2 (red). The white boxes in (A) are the section of the image which is illustrated in (B) in an enlarged view. The enlarged image allows visualisation of the GlyT2 staining surrounding the cell bodies of the neurons. The arrows indicate some of the co-stained cells in the culture for NeuN and GlyT2.

2.3.4 Neurochemically Defining Neuronal Cell Populations in the Dorsal Horn Culture

Neurochemically defined classes of interneurons known to exist *in vivo* in the spinal DH were investigated in the spinal DH culture. PV and nNOS-positive cells were found to exist in the DH culture. PV was co-stained with GlyT2 and GAD65-67 to determine if PV-expressing interneurons are also inhibitory interneurons (Figure 2.10). In the spinal DH cultures co-labelled with PV and GAD 65 and 67, 101 ± 2.2 PV-positive cells and 71 ± 2.7 GAD 65 and 67-positive cells were counted (N=2, n=5). All the GAD 65 and 67 positive cells co-localised with PV-positive cells. Out of the total count of PV-positive cells, $70.7 \pm 3.4\%$ co-localised with GAD65-67-positive cells. In the DH cultures co-labelled for PV and GlyT2 there were 103 ± 2.0 PV-positive cells and 21 ± 3.8 GlyT2 cells. The co-staining of PV with GlyT2 revealed that only $20.9 \pm 4.7\%$ of the PV-positive cells co-localised with the GlyT2-positive cells (N=2, n=5). The nNOS antibody could not be co-stained with the GAD65-67 and GlyT2 antibodies due to the same host species. Therefore nNOS was co-stained with gephyrin which is also a marker for inhibitory interneurons (Figure 2.11). In these cultures 59 ± 5.6 nNOS-positive cells were counted with 23 ± 7.7 gephyrin-positive cells (N=2, n=4). The co-staining of the antibody for the potassium chloride cotransporter 2 (KCC2) with gephyrin was also investigated to indicate if KCC2 is likely to be regulating the chloride ion electrochemical gradient in the DH culture. 75.0 ± 10.1 KCC2-positive cells and 62.8 ± 14.9 gephyrin-positive cells were counted in the DH cultures co-labelled with these antibodies (N=2, n=4). An average of $78.0 \pm 12.0\%$ of the KCC2-positive cells co-localised with gephyrin (Figure 2.12). Out of the total number of gephyrin-positive cells, $95.7 \pm 2.2\%$ co-localised with the KCC2-positive cells.

A



B

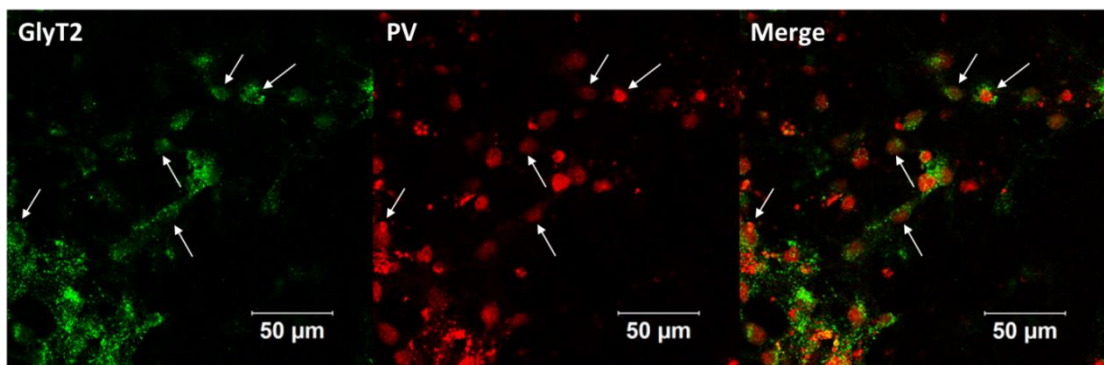


Figure 2.10 The cultured rat embryonic spinal DH cells co-stained with (A) GAD65-67 (green) and PV (red), and (B) GlyT2 (green) and PV (red). The merge of the images are shown on the right. The arrows indicate some of the cells which are positively labelled for both antibodies.

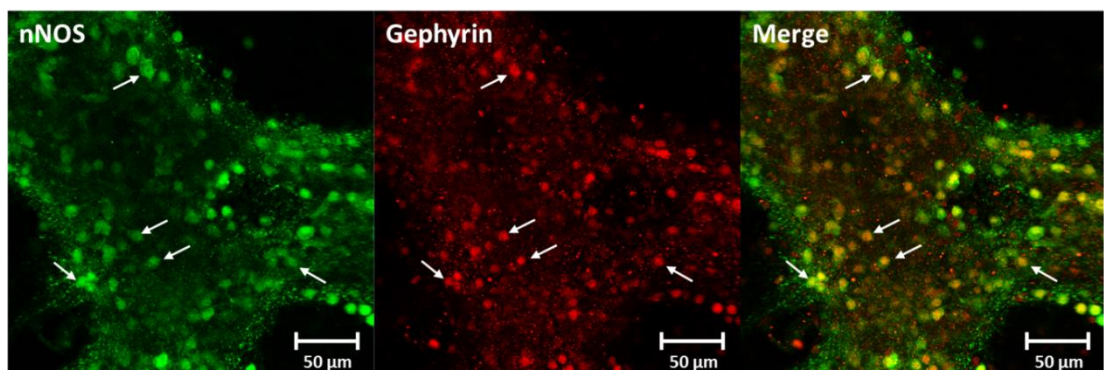


Figure 2.11 The embryonic rat spinal DH culture stained with nNOS (green) and gephyrin (red) with the merge of the images on the right. The arrows indicate some of the cells which co-localized with nNOS and gephyrin.

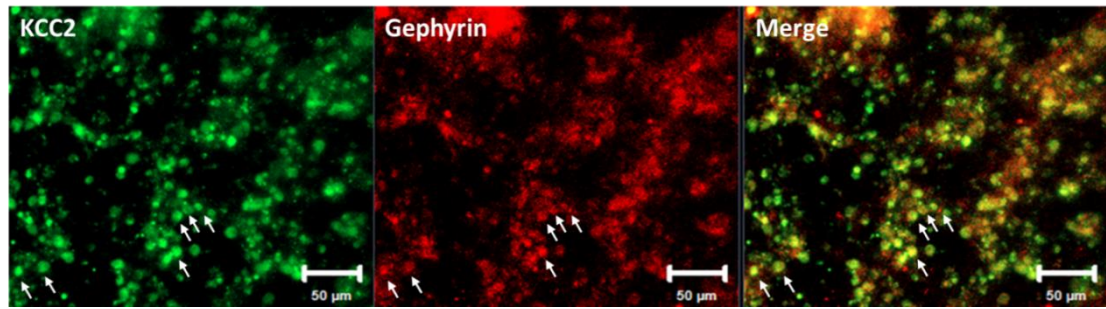


Figure 2.12 The rat embryonic spinal DH culture stained for KCC2 (green) and gephyrin (red) and the merge of the images on the right. The arrows indicate some of the co-stained cells.

2.3.5 *GABA_A Receptor α Subunit Expression in the Embryonic Dorsal Horn Culture*

The GABA_A receptor α subunits 1-6 were each co-stained with NeuN to determine which of the subunits are expressed in the DH culture and whether they co-localise with neurons. The GABA_A receptor α 1 subunit was expressed in 53 ± 6.9 of the 85 ± 4.5 NeuN-positive cells counted, and an average of $97.6 \pm 1.6\%$ of the α 1 subunit-positive cells co-stained with NeuN (N=2, n=6) (Figure 2.13). The GABA_A receptor α 2 subunit was expressed in 55 ± 3.8 of 75 ± 5.2 NeuN-positive cells (N=2, n=6). Out of the α 2 subunit-positive cells, $99.4 \pm 0.6\%$ of them co-stained with NeuN-positive cells (Figure 2.14). The GABA_A receptor α 3 subunit was also detected in the rat embryonic DH cells (Figure 2.15). There were 52 ± 5.7 GABA_A receptor α 3 subunit-positive cells counted, and of the 75 ± 7.9 NeuN-positive cells, $94.2 \pm 1.1\%$ of these co-localised with NeuN (N=2, n=4). In the DH cultures stained with NeuN and the GABA_A receptor α 4 subunit 74 ± 3.6 GABA_A α 4 subunit-positive cells were counted, of these 64 ± 6.1 co-localised with the 108 ± 8.4 NeuN-positive cells (N=2, n=4) (Figure 2.16). The GABA_A receptor α 5 subunit was detected in 102 ± 2.3 of the 110 ± 6.1 NeuN-positive cells, which was the highest proportion of all the GABA_A receptor α subunits (N=2, n=4) (Figure 2.17). There was a mean of $93.0 \pm 6.0\%$ of

the total GABA_A receptor $\alpha 5$ subunit-positive cells which co-localised with NeuN-positive cells. Finally the GABA_A receptor $\alpha 6$ subunit was also present in the DH culture, where 97 ± 7.1 cells were positive for this antibody and 88 ± 4.2 of those co-localised with the 114 ± 3.6 NeuN-positive cells (N=2, n=5) (Figure 2.18).

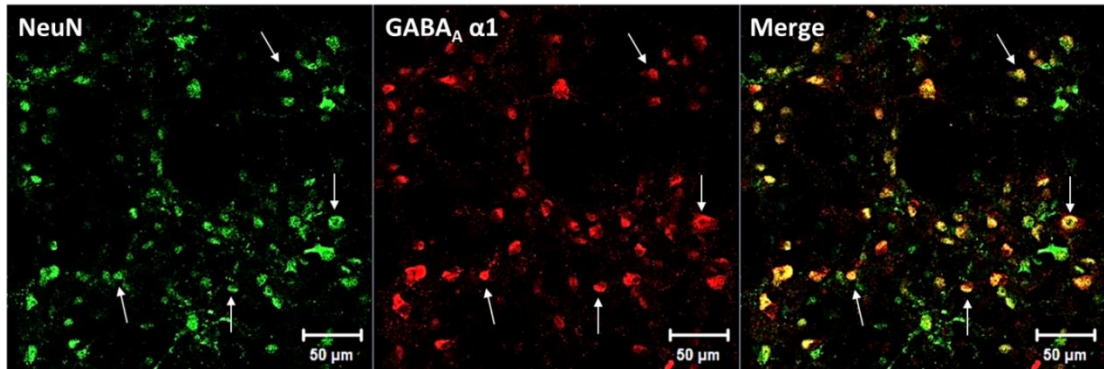


Figure 2.13 The embryonic DH cell culture with double immune-labelling of NeuN (green) and GABA_A receptor $\alpha 1$ subunit (red), with the merge of the images on the right. The arrows indicate some of the cells which were positively stained for both NeuN and the GABA_A receptor $\alpha 1$ subunit.

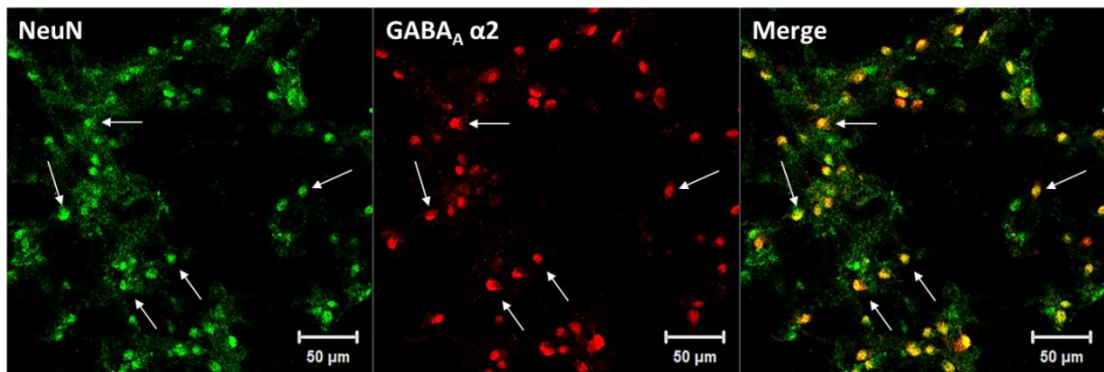


Figure 2.14 The rat embryonic spinal DH cell culture stained with GABA_A receptor $\alpha 2$ subunit antibody (green) and NeuN (red), with the merge image on the right. The arrows indicate some of the cells which were positively stained for both NeuN and the GABA_A receptor $\alpha 2$ subunit.

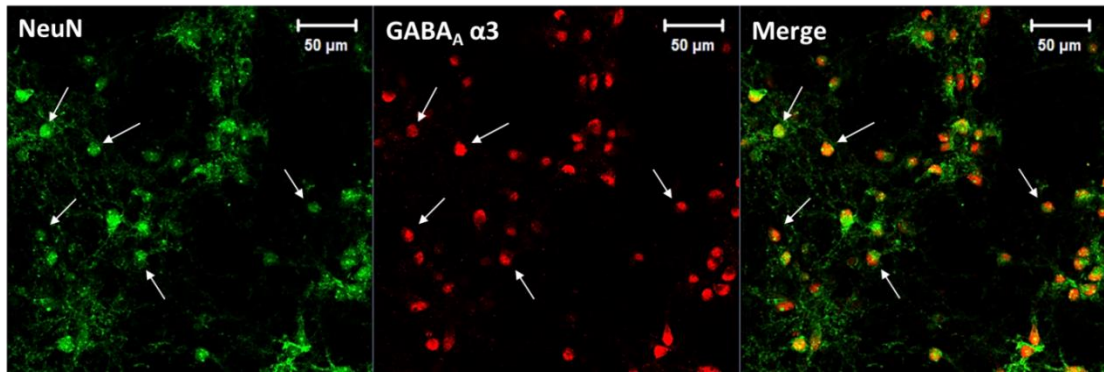


Figure 2.15 Staining of the embryonic DH culture for GABA_A receptor α 3 subunit (green) and NeuN (red) with the merge of the images in the right panel. The arrows indicate some of the cells which were positively stained for both NeuN and the GABA_A receptor α 3 subunit.

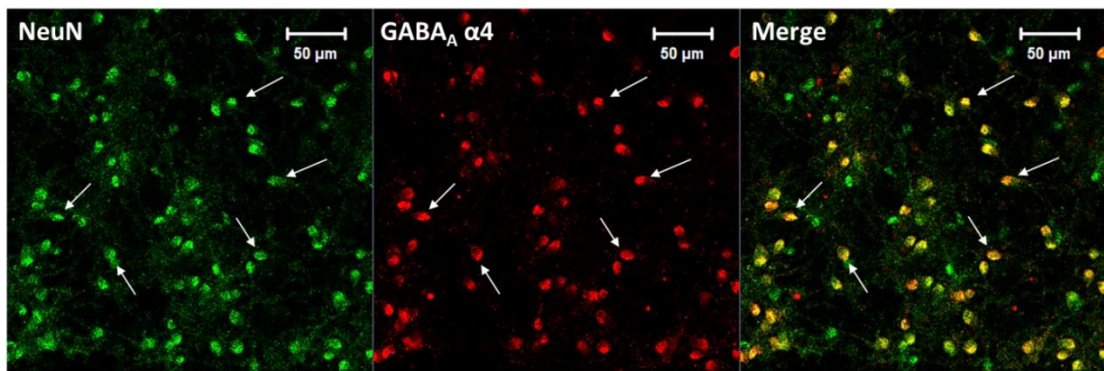


Figure 2.16 The embryonic rat DH culture stained with the antibody for GABA_A receptor α 4 subunit (green) and NeuN (red), and the merge of the two images in the right panel. The arrows indicate some of the cells which were positively stained for both NeuN and the GABA_A receptor α 4 subunit.

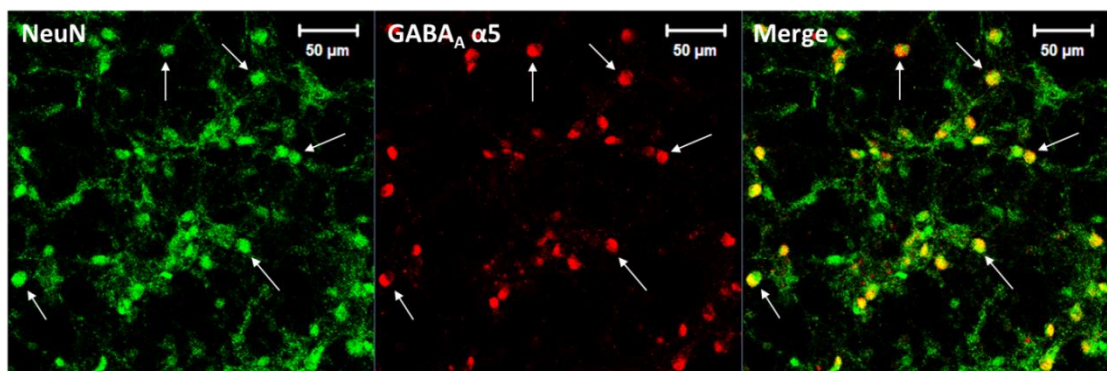


Figure 2.17 Staining of the spinal DH culture for the GABA_A receptor α 5 subunit (green) and NeuN (red), and the merge image in the right panel. The arrows indicate some of the cells which were positively stained for both NeuN and the GABA_A receptor α 5 subunit.

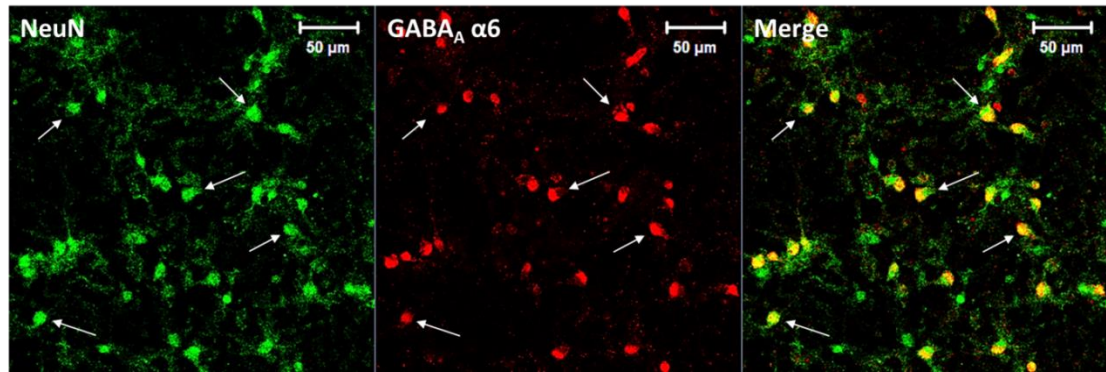


Figure 2.18 The rat embryonic DH culture stained with the GABA_A receptor α6 subunit antibody (green) and NeuN (red), with the merge image in the right panel. The arrows indicate some of the cells which were positively stained for both NeuN and the GABA_A receptor α6 subunit.

2.3.6 Glycine Receptor α Subunit Expression in the Dorsal Horn Culture

The expression of the glycine receptor α subunits 1-3 in the spinal DH culture were each stained separately with NeuN to determine which of the subunits is expressed in the spinal DH culture. In the spinal DH cultures co-stained with the glycine receptor α1 subunit and NeuN there were 126 ± 1.3 NeuN-positive cells and 117 ± 2.4 glycine receptor α1 subunit-positive cells. There was an average of $50.1 \pm 4.5\%$ of the glycine receptor α1 subunit-positive cells that co-stained with NeuN (N=2, n=6) (Figure 2.19). There were only 2 ± 4.6 glycine receptor α2 subunit-positive cells counted in the DH cultures stained with the glycine receptor α2 subunit antibody, of which $71.4 \pm 11.3\%$ co-stained with NeuN. This accounts for only $1.6 \pm 3.4\%$ of the 102 ± 8.5 NeuN-positive cells (N=2, n=3) (Figure 2.20). Finally, the glycine receptor α3 subunit antibody was detected in 29 ± 12.1 cells, in DH cultures co-stained with NeuN which had a total NeuN-positive cell count of 81 ± 6.7 cells in these cultures (N=2, n=4). This is an average of $36.0 \pm 15.4\%$ of the NeuN-positive cells. However, the number of glycine receptor α3 subunit-positive cells varied considerably between the wells (Figure 2.21).

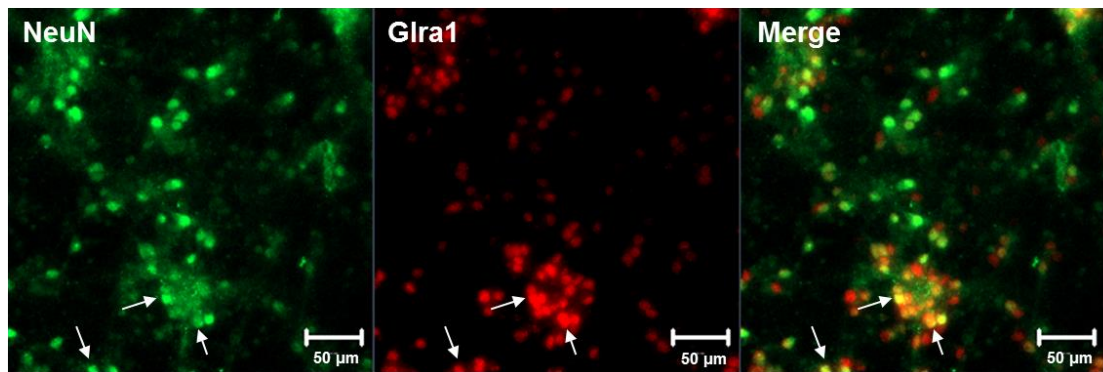


Figure 2.19 The embryonic DH culture stained with NeuN (green) and the glycine receptor $\alpha 1$ subunit (Gla1) (red) with the merge image in the right panel. The arrows indicate some of the cells in the culture which are co-stained with NeuN and the glycine receptor $\alpha 1$ subunit.

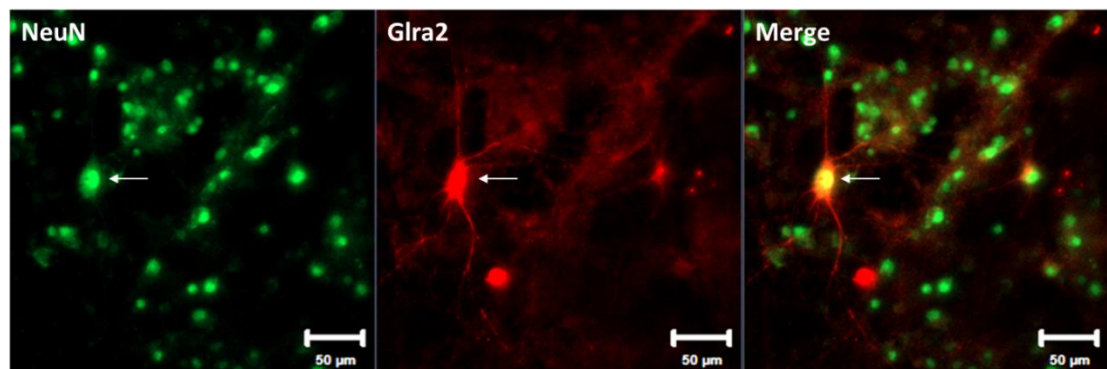


Figure 2.20 The DH culture stained with NeuN (green) and the glycine receptor $\alpha 2$ subunit (red), with the merge image. In this image one of the glycine receptor $\alpha 2$ subunit-positive cells can be seen (indicated by the arrow), which co-localised with NeuN. The neurites of the glycine receptor $\alpha 2$ subunit-positive cells can clearly be observed, furthermore the cell body of these cells is larger than the other.

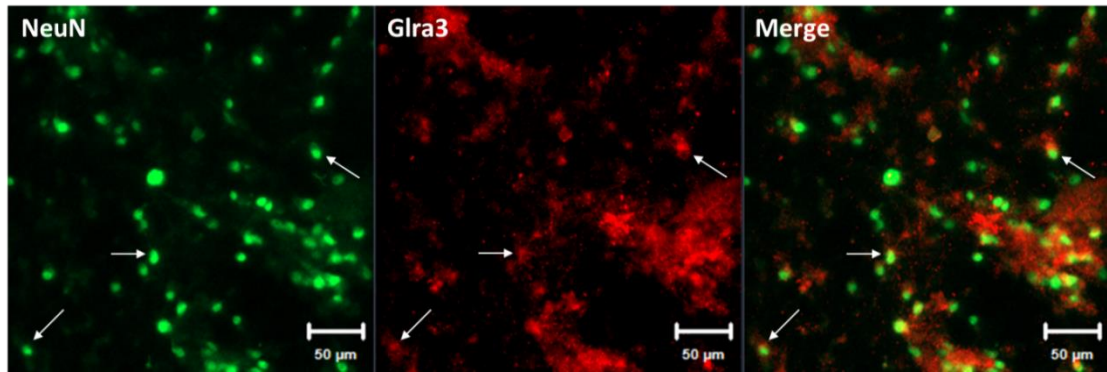


Figure 2.21 The spinal DH culture stained with NeuN (green) and glycine receptor $\alpha 3$ subunit (red), with the merge image on the right. The arrows indicate some of the NeuN- and glycine receptor $\alpha 3$ subunit-positive cells which have co-localised.

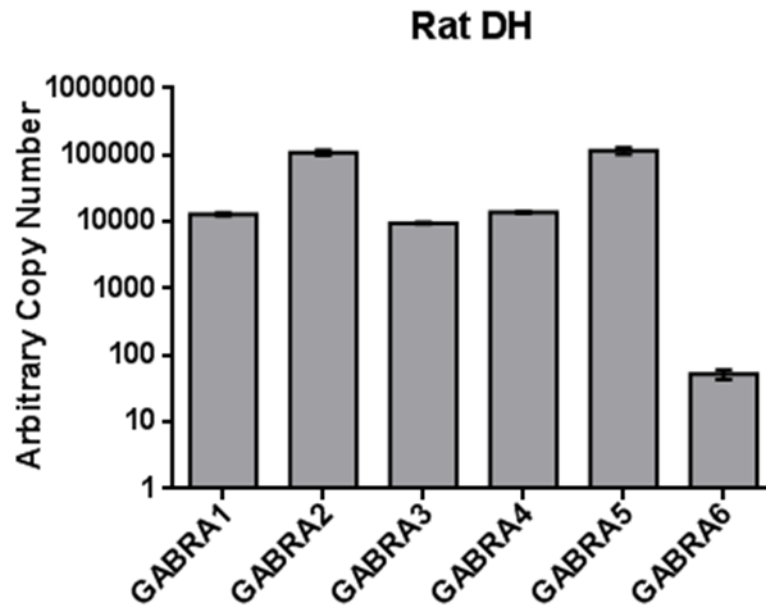
2.3.7 Quantitative Real-Time PCR with Human Spinal Cord and Culture Dorsal Horn Cells

The expression of the GABA_A and glycine receptor subunits in the spinal DH culture were also investigated using RT-PCR. The expression in the adult human spinal cord tissue of these receptor subunits was also determined to verify if there are any differences in the expression of the subunits compared to the rat DH culture. The RT-PCR results show that both the rat spinal DH culture and the adult human spinal cord express all six GABA_A receptor α subunits (Figure 2.22). The glycine receptor subunits were all present except the $\alpha 4$ subunit in both the rat spinal DH culture and in the adult human spinal cord (Figure 2.23). The glycine receptor $\alpha 4$ subunit was not expressed in the human spinal cord, and only detected at a very low level in the rat embryonic spinal DH culture.

Absolute quantification of the human glycine receptor $\alpha 1$ and 3 subunits was performed to determine which of the subunits is more highly expressed in the human spinal cord. The glycine receptor $\alpha 2$ subunit was not investigated as it is known to not be highly expressed in the spinal cord postnatally (Akagi et al., 1991, Watanabe and Akagi, 1995). Plasmid DNA containing the human glycine $\alpha 1$ gene

was used to generate a standard curve (Figure 2.24). Then using the C_T value from the RT-PCR reaction with the glycine $\alpha 1$ subunit assay in the human spinal cord the concentration of RNA could be determined. Subsequently the number of molecules of this subunit in the human spinal cord was calculated. This was repeated for the glycine receptor $\alpha 3$ subunit variants K and L. There were 2.51×10^{11} molecules of the glycine receptor $\alpha 1$ subunit in the human spinal cord. There were 1.02×10^{17} molecules of the $\alpha 3$ subunit K variant, and 1.53×10^{14} molecules of the L variant. These results are listed in Table 2.9. Similarly the number of molecules for each of the glycine receptor α subunits was investigated in the rat spinal DH culture. Here the two variants of the $\alpha 3$ subunit could not be determined due to no TaqMan probe being available for the two variants separately. The standard curves generated for each subunit in the rat DH culture are also shown in Figure 2.24. The number of molecules of the $\alpha 1$ subunit in the DH culture was 1.88×10^{17} molecules. There were 8.39×10^{16} molecules of the glycine receptor $\alpha 2$ subunit, and 1.09×10^{16} molecules of the glycine receptor $\alpha 3$ subunit. These results are listed in Table 2.10.

A



B

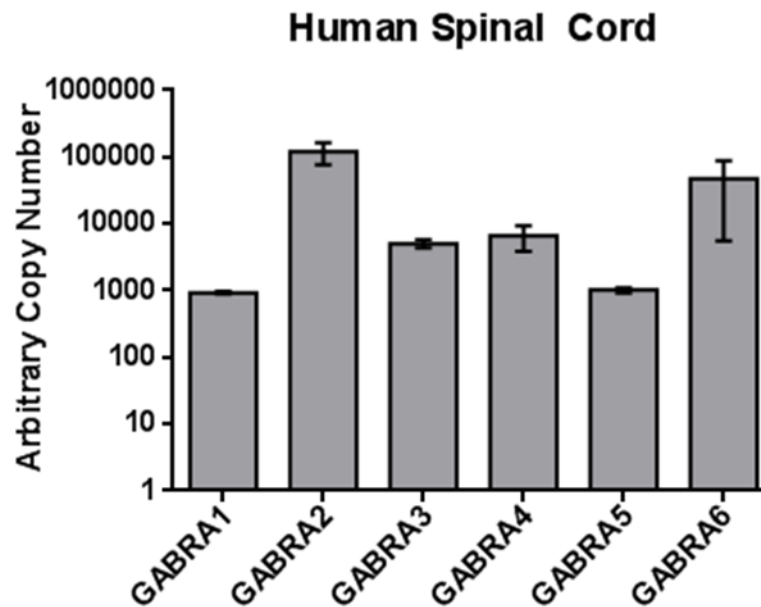
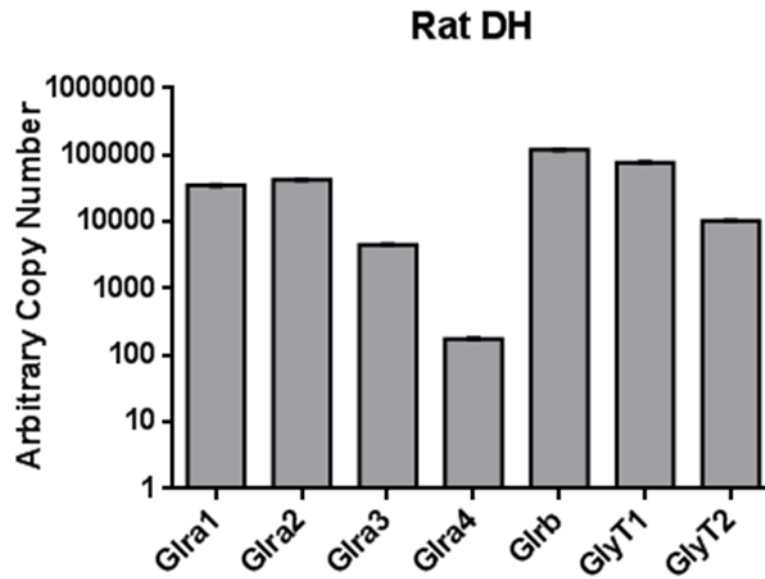


Figure 2.22 The relative expression of each of the GABA_A receptor α subunits (*GABRA1-6*) in the rat spinal DH culture (A) and in the adult human spinal cord (B) determined by relative quantification RT-PCR. The data was scaled relative to the expression of *GABRA1* for each species.

A



B

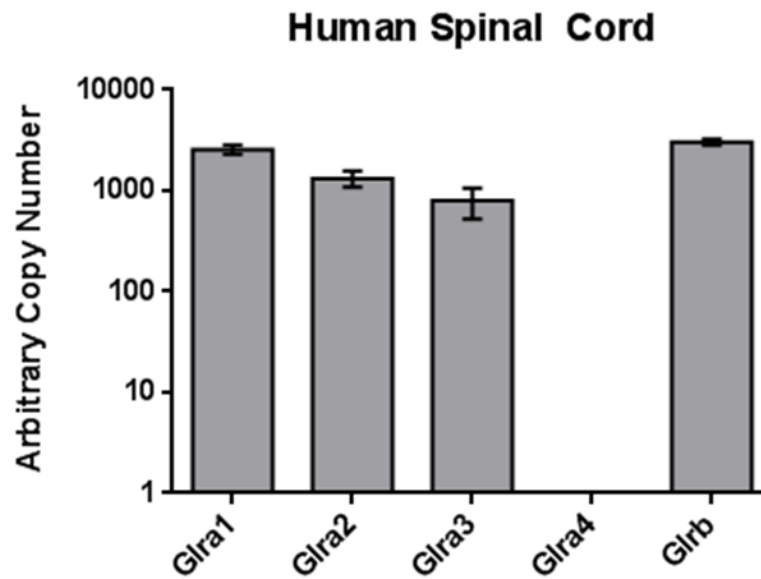


Figure 2.23 The relative expression of each of the glycine receptor α subunits (*Glra1-4*) and β subunit (*Glr**b***) in the rat spinal DH culture (A) and in the human spinal cord (B) determined by relative quantification RT-PCR. In the rat spinal DH culture the expression of the two glycine transporters (GlyT1 and GlyT2) was also investigated. The arbitrary copy numbers were scaled relative to *Glra1* for each species.

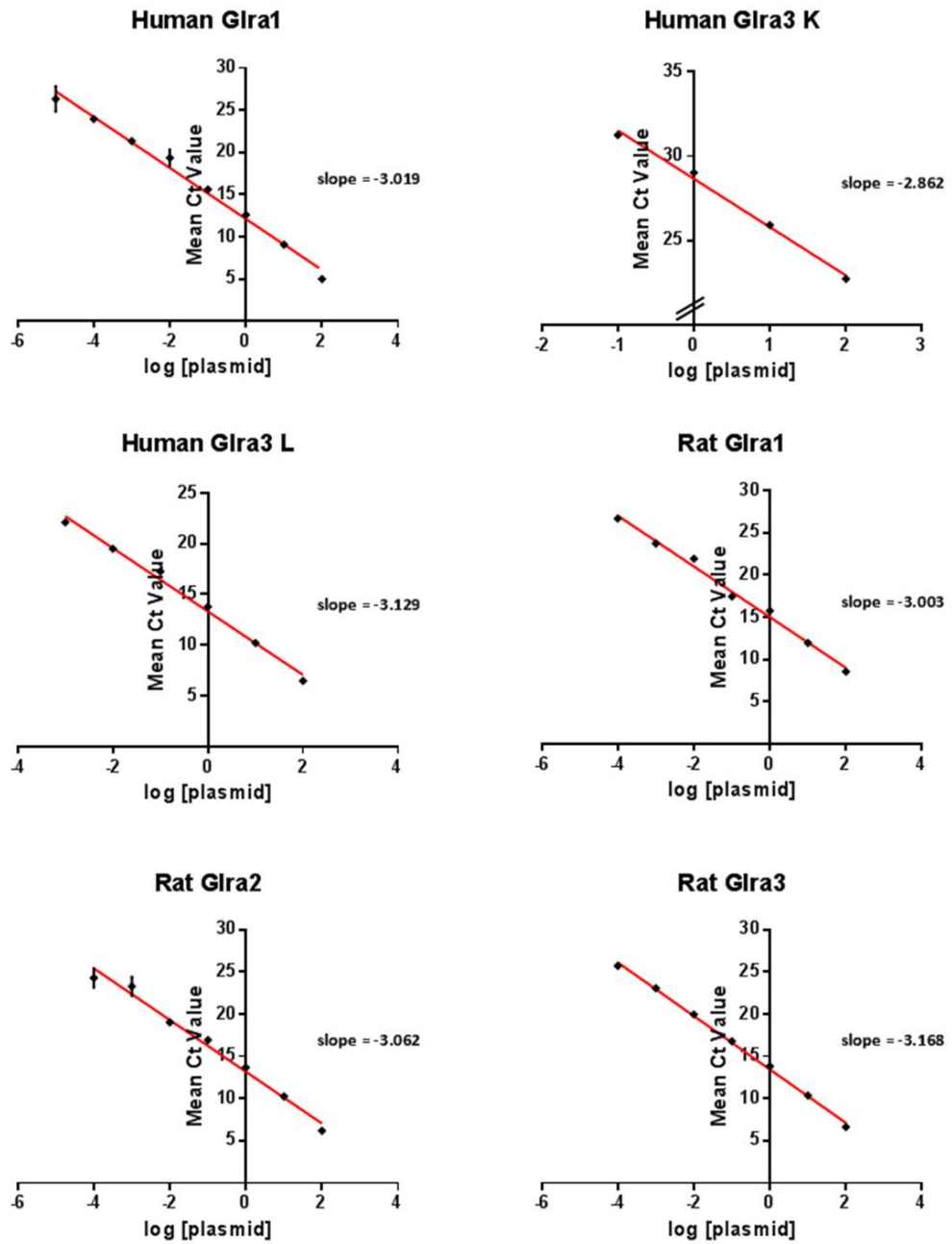


Figure 2.24 The standard curves from each of the absolute quantification RT-PCR experiments to determine the number of molecules of the glycine receptor α subunits in the human spinal cord and in the rat embryonic spinal DH culture.

Glycine Receptor Subunit	Number of Molecules in Human Spinal Cord
$\alpha 1$	2.51×10^{11}
$\alpha 3$ K	1.02×10^{17}
$\alpha 3$ L	1.53×10^{14}

Table 2.9 A summary of the number of molecules of the glycine receptor $\alpha 1$ subunit and $\alpha 3$ subunit variants K and L in the adult human spinal cord as found from absolute quantification RT-PCR.

Glycine Receptor Subunit	Number of Molecules in DH Culture
$\alpha 1$	1.88×10^{17}
$\alpha 2$	8.39×10^{16}
$\alpha 3$	1.09×10^{16}

Table 2.10 A list of the results from the absolute quantification RT-PCR experiment to show the number of molecules of each of the glycine receptor α subunits in the spinal DH culture.

2.4 Discussion

2.4.1 The Spinal Dorsal Horn Culture has a High Proportion of Neuronal Cells

The aim of this study was to develop and characterise the rat embryonic spinal DH cell culture model and to assess its potential to be an assay for screening novel analgesics. Once the DH culture was optimised, the culture was characterised with IF and RT-PCR. Firstly, the presence of neurons, glia and microglia was determined. Secondly, the proportion of neuronal cells to glial cells within the culture was calculated. The dissection and processing of the spinal DH tissue and the cell culture conditions can result in cell death of neuronal cells, leaving primarily non-neuronal populations (Gordon et al., 2013). This study is focused on the neuronal network of the spinal DH, and therefore it is important to determine a high proportion of neuronal cells in the culture. There were almost four times as many neurons as glia found in the culture, and three times as many neuronal cells as microglia. The higher proportion of neuronal cells supports this model for study of the spinal DH neuronal network.

2.4.2 Excitatory and Inhibitory Interneurons in the Spinal Dorsal Horn Culture

The classic excitatory cell marker for the spinal cord, vGluT2, was co-stained with NeuN to determine the proportion of excitatory interneurons in the spinal DH culture to address the second aim of this study. Approximately 70% of the labelled neuronal cells in the culture were excitatory. This is consistent with rat spinal cord slice IF studies which identify between 60 and 70% of interneurons in the superficial DH being excitatory (Todd et al., 2003, Maxwell et al., 2007, Yasaka et al., 2010, Polgar

et al., 2013). Labelling the GABAergic interneurons with GAD65-67 and glycinergic interneurons with GlyT2 revealed a larger population of inhibitory interneurons than anticipated based on the theory that the proportion of non-excitatory interneurons are inhibitory and vice versa. Just over 50% of the neuronal cell population detected were co-labelled with GAD65-67. This is a slightly larger proportion of inhibitory interneurons than has been reported in superficial spinal DH of spinal cord slices. In rats, 28% of neurons in lamina I up to 46% in lamina III of the superficial spinal DH have been reported to be GABAergic (Todd and Spike, 1993, Polgar et al., 2003, Polgar et al., 2013). The glycinergic labelled cells co-localised with just less than 30% of the neuronal cell population. Similarly this is fairly consistent with previous reports of glycinergic interneurons ranging from 9% of lamina I neurons to 30% in lamina III (Todd and Spike, 1993). The proportions of excitatory and inhibitory cells in the DH culture therefore do correlate well with published spinal cord slice IF studies focusing on the superficial laminae. This could imply that this ratio of inhibitory to excitatory interneuron populations is a requirement of the rhythmic activity which has been recorded in the spinal DH *in vivo* and in *in vitro* studies, and was reported in this spinal DH culture with calcium imaging recordings. The generation of rhythmic activity in neuronal networks has been suggested to involve a cycling interaction between inhibitory and excitatory interneurons (Tiesinga and Sejnowski, 2009).

2.4.3 The Spinal Dorsal Horn Culture Contains Parvalbumin and nNOS Neuronal Cells

Neuropeptides PV and nNOS were both detected in the spinal DH culture, and were identified to co-localise with inhibitory interneurons. nNOS is expressed primarily in lamina II of the spinal DH, with very few nNOS-positive cells also found in lamina I

and III (Sardella et al., 2011). In the rat spinal cord it has also been shown that a small population of 2-6% of nNOS-expressing interneurons in the superficial DH is GABAergic (Sardella et al., 2011, Polgar et al., 2013, Polgár et al., 2013). In this study around 2% of the nNOS-positive cells co-stained with gephyrin, which therefore concurs with the reports in the superficial DH of spinal cord slices. It has been implied that the remaining nNOS-expressing cells in the spinal DH which don't co-express gephyrin must therefore be glutamatergic interneurons. The NO produced by nNOS in the spinal cord has been demonstrated to have a role in developing and maintaining hyperalgesia in inflammatory and neuropathic pain (Guan et al., 2007, Schmidtko et al., 2009). Furthermore, there is evidence of NO causing prolonged changes in synaptic strength and the development of LTP in the superficial DH (Zhang et al., 2005, Ikeda et al., 2006). It has been demonstrated that the activation of NMDA receptors in the spinal DH is linked to increased production of nNOS, which consequently increases synthesis of NO (Lange et al., 2012). Intracellular signalling of NO can lead to modulation of neurotransmitter release at the pre-synaptic terminal, which has been associated with the development of LTP (Infante et al., 2007, Lange et al., 2012). Moreover, antagonists of the NMDA receptor have an analgesic effect (Tong and MacDermott, 2014). This could result from a decrease in nNOS expression, NO synthesis and LTD which therefore would decrease spinal DH network excitability and prevent development of central sensitisation and the manifestation of pain.

PV-expressing interneurons are present in the superficial spinal DH (Polgár et al., 2013), and a number of GABAergic interneurons express PV in the spinal DH (Labrakakis et al., 2009, Hughes et al., 2012). The results of this study show that the spinal DH culture does express a large proportion of GABAergic interneurons which are PV-positive, and furthermore a number of glycinergic interneurons are also PV-positive. Since not all of the PV-expressing interneurons in the culture or in

spinal cord slices are GABAergic interneurons, it has been suggested that a population of these PV-positive neurons are glutamatergic (Grudt and Perl, 2002). PV is a calcium binding protein and transports intracellular calcium to the calcium stores in the cell. Through controlling the calcium ion concentration in the presynaptic terminal, PV impacts on the release of neurotransmitter from the cell and consequently the activity of the network of interneurons. Stimulation of PV-expressing neurons in the brain has been illustrated to affect the cortical gamma rhythm (Kim et al., 2015). It is therefore possible that PV-positive interneurons in the spinal DH are required for the generation and maintenance of the rhythmic activity of the spinal DH network.

2.4.4 Inhibitory Interneurons in the Spinal Dorsal Horn Culture Express KCC2

The results of this IF study have identified that almost all of the inhibitory interneurons in the spinal DH culture express KCC2. However, not all the KCC2-positive cells co-localised with gephyrin, suggesting that some glutamatergic interneurons also express KCC2. This resembles the spinal cord slices, where KCC2 is expressed throughout the grey matter, with much stronger expression in the superficial laminae (Javdani et al., 2015). KCC2 exports chloride ions from the cell to maintain a low intracellular chloride ion concentration (Rivera et al., 1999). Confirming the expression of KCC2-positive interneurons in the DH culture demonstrates that the action of GABA and glycine at their respective receptors will likely produce an inhibitory effect due to an influx of chloride ions. Furthermore, KCC2 expression increases quickly in early postnatal days (Ben-Ari et al., 2007). Therefore, as this culture was from embryonic rat spinal DH this finding suggests that the culture has reached a more mature state following 12-14 DIV.

2.4.5 All GABA_A Receptor α Subunits are Expressed in the Spinal Dorsal Horn Culture

The IF performed in this study shows that each of the GABA_A receptor α subunits is expressed in the spinal DH culture. This was confirmed with the relative quantification RT-PCR results showing mRNA expression. This largely concurs with IF studies for these subunits in spinal cord slices. In adult rat spinal cord, GABA_A receptor α 1 and α 5 subunits are expressed throughout the grey matter of the spinal cord, with particularly high expression in lamina III (Bohlhalter et al., 1996). The α 2 and α 3 subunits also have a much stronger expression in laminae I and II, with α 3 strongly detected in lamina III (Bohlhalter et al., 1996). However, the GABA_A receptor α 6 subunit has not been detected in the adult rat spinal cord, but low levels have been detected in embryonic spinal cord (Poulter et al., 1992). Additionally, Poulter et al. (1992) did not detect the GABA_A receptor α 1 or 2 subunits in the embryonic spinal cord. The RT-PCR results show that the adult human spinal cord expresses all the GABA_A receptor α subunits as found in the culture. These results demonstrate strong similarities between the cultured spinal DH cells, rat spinal cord and the adult human spinal cord in terms of the expression of the GABA_A receptor α subunits. This is beneficial for drug screening, as it could provide an early indication of the clinical potential of a drug. Therefore, this data supports the use of this spinal DH culture as a model to investigate the roles of the GABA_A receptor subtypes in this network, and furthermore to screen for compounds acting at GABA_A receptors.

2.4.6 Differences in Glycine Receptor α Subunit Expression in the Spinal Dorsal Horn Culture Compared to Human Spinal Cord

The IF staining for the glycine receptor α 1-3 subunits demonstrated the expression of each of these subunits in the spinal DH culture. The glycine receptor α 2 subunit expression was very low, and although the α 1 and α 3 subunit staining was not of good quality there was a higher expression of each of these subunits compared to the α 2 subunit. The relative quantification RT-PCR results also demonstrated expression of each of the α subunits 1-3 in both the spinal DH culture and in adult human spinal cord. Expression of the α 4 subunit was very low or absent in the DH culture and human spinal cord, which agrees with this subunit being found in mice but not human or rat (Matzenbach et al., 1994). The expression of the glycine receptor β subunit was confirmed with the RT-PCR results in both the DH culture and human spinal cord, which is known to be expressed throughout the CNS (Jonsson et al., 2012). The expression of the α 1 and α 3 glycine receptor subunits has previously been shown to increase postnatally, while the expression of the α 2 subunit is higher during development and decreases postnatally (Watanabe and Akagi, 1995, Jonsson et al., 2012). As the relative quantification RT-PCR data does not provide an indication of the levels of expression of the subunits, the actual number of molecules of each of the glycine receptor α subunits was determined from absolute quantification RT-PCR. These results revealed that there is more glycine receptor α 3 subunit than α 1 in the human spinal cord, and more of the α 3 K variant than the L variant. However, in the spinal DH culture the expression of these subunits was not comparable. In the DH culture the expression of the glycine receptor α 1 subunit was far greater than the α 3 subunit expression, which is consistent with the IF cell count data for the α 1 and α 3 subunits in the spinal DH culture. The absolute RT-PCR quantification also demonstrated there was a higher expression of the α 2 subunit than the α 3 subunit in the spinal DH culture, which was

not found in the IF experiments where the expression of the glycine receptor $\alpha 2$ subunit was much lower than $\alpha 1$ and $\alpha 3$ subunit expression. This could result from differences in the PCR assay probe for the glycine receptor $\alpha 2$ subunit compared to the antibody for this protein. As the expression of these glycine receptor subunits does not correlate between the culture and the human spinal cord, it is likely that the glycine receptor pharmacology will be different. It is known that the different glycine receptor subunits display slightly different pharmacology and receptor kinetics, which could affect the network activity (Kuhse et al., 1993, Maksay et al., 2001).

2.4.7 Conclusions

The first aim of this chapter was to develop an *in vitro* rat embryonic spinal DH cell culture model, which was successfully achieved following extensive optimisation including the use of calcium imaging. The characterisation of this spinal DH culture suggests there is a strong uniformity between the types of cell classes that have been described in the *ex vivo* spinal cord to those found in the spinal DH culture. This includes the proportions of inhibitory to excitatory interneurons and the expression of PV, nNOS and KCC2 positive cells. A summary of these comparisons can be found in Table 2.11. The expression of the GABA_A receptor α subunits detected by IF and RT-PCR, at the protein and mRNA, respectively, correlate well with the human adult spinal cord and also the rat spinal DH slices. However, there were some discrepancies discovered between the expression of the glycine receptor α subunits in the spinal DH culture compared with the human spinal cord. However, this is only concerning the different proportions of expression of the subunits. Overall the characterisation of the spinal DH culture illustrates that this model could be a useful platform for development of drug discovery assays. Caution should be taken when interpreting the results of drug testing using this

model, due to the absence of afferent input and the potential differences in the network due to the complete tissue dissociation and culturing processes. However, the versatility of cell culture models makes them ideal for the initial screening process of novel compounds prior to *in vivo* studies in animal models.

Antibodies	Spinal DH Culture (%)	<i>Ex vivo</i> Spinal Cord (%)
vGlut2/NeuN	70	60-70 (Polgár et al., 2013)
GAD65-67/NeuN	50	≤46 (Polgár et al., 2013)
GlyT2/NeuN	30	9-30 (Todd and Spike, 1993)
nNOS/Gephyrin	2	2-6 (Sardella et al., 2011)
GAD65-67/PV	70	25 (Labrakakis et al., 2009)
GAD65-67/KCC2	78	n.d

Table 2.11 A summary of the comparisons in expression of the antibodies utilised for characterisation of the spinal DH culture, between the spinal DH culture and the *ex vivo* spinal cord from published sources. The percentage values indicate the expression of the first antibody staining out of the total number of positive cells counted for the second antibody. Quantification of the expression of KCC2 and GAD65-67 has not been defined in the *ex vivo* spinal cord.

3 Calcium Response as a Measure of the Embryonic Spinal Dorsal Horn Network

3.1 Introduction

3.1.1 *Neuronal Primary Cell Culture*

In this chapter a calcium imaging assay has been used with the embryonic spinal DH cell culture developed and characterised in Chapter 2 to investigate the activity of the DH network. Primary cell culture provides the format by which the cells can be studied under controlled conditions and are versatile due to their adaptability and easy access for use with different assays and techniques. For example, primary cell cultures can be used for electrophysiological techniques (Massobrio et al., 2015), calcium imaging (Tibau et al., 2013) and molecular biology techniques (Emamghoreishi et al., 2015). Cultured cells can be used to investigate normal physiology of cells of a particular tissue and their biochemistry. Furthermore, drug efficacy and toxicity can also be assessed (Pratten et al., 2012). A major advantage of using cultured cells is the reproducibility of the results given the ability to maintain consistent conditions. In primary cell culture models, the advantages of high-throughput assays mean that the number of animals required for an assay is reduced. There are a number of limitations of primary cultures; firstly it is likely that the different populations of cells in the spinal DH require different culture conditions therefore some populations of cells might not survive in the culture (Gordon et al., 2013). This could affect the growth and activity of the remaining populations (Mergenthaler et al., 2014). Furthermore, neuronal cultures are typically from embryonic or early post-natal animals. Therefore, the developmental stage of maturation of the cells in the culture is unknown. Finally the presence of non-neuronal cells within the culture should be considered in terms of their contribution to the responses observed in assays (Gordon et al., 2013).

The primary cultures of embryonic DH cells were demonstrated in Chapter 2 to be spontaneously active after 12-14 days in culture using calcium imaging.

Spontaneous activity has been recorded *in vitro* in dissociated spinal cord cultures previously (Streit, 1993, Li and Baccei, 2011, Hendrich et al., 2012a). Li and Baccei (2011) demonstrated the existence of ‘pacemaker’ neurons within the superficial spinal DH which drive the spontaneous firing. These pacemaker neurons were later shown to be glutamatergic cells, which connect with ascending projection neurons transmitting their signals to supraspinal areas involved in nociception including the parabrachial nucleus (Li et al., 2014). Therefore, the inhibitory and excitatory interneurons within the DH network could be involved in generating and/or modifying this rhythmic activity and provide a mechanism for regulating nociceptive signals. Consequently, pharmacologically targeting the receptors whose signalling influences the spinal DH network rhythmic activity could have an analgesic effect.

3.1.2 Calcium Imaging Techniques to Measure Neuronal Network Activity

Calcium ions have a variety of intracellular functions in virtually all types of mammalian cells, including muscle contraction, cell proliferation and cell death (Berridge et al., 2000). In neurons, intracellular calcium release initiates exocytosis of synaptic vesicles in the pre-synaptic terminals which contain neurotransmitter molecules (Neher and Sakaba, 2008). Postsynaptically, the influx of calcium ions through NMDA receptors produces activity-dependent synaptic plasticity (Lu et al., 2001). Calcium dyes, can be used to detect changes in the intracellular calcium ion concentration, which occur in neuronal cells during neurotransmitter release (Grienberger and Konnerth, 2012). Typically neurons at rest have an intracellular calcium ion concentration of 50-100 nM, which can increase by over ten-fold during action potential stimulation (Berridge et al., 2000). Therefore, the detection of a large transient increase in intracellular calcium ion concentration is an indicator of neuronal excitability.

Calcium ions enter neuronal cells via a number of mechanisms including voltage-gated calcium channels, NMDA receptors and nicotinic acetylcholine receptors (Kovalchuk et al., 2000, Fucile, 2004). Release of calcium ions from intracellular stores also contributes to the signalling for the release of neurotransmitters from presynaptic terminals (Neher and Sakaba, 2008). Voltage-gate calcium channels are expressed in the spinal DH, where they influence DH neuron excitability (Diaz and Dickenson, 1997, Matthews and Dickenson, 2001a, Matthews and Dickenson, 2001b, Zhang et al., 2008b, Youn et al., 2013, Xia et al., 2014). Calcium imaging techniques have been used with developing neuronal cell cultures to investigate network activity (Albantakis and Lohmann, 2009, Grienberger and Konnerth, 2012). Therefore, this technique has been employed in this study to investigate the embryonic spinal DH culture network activity.

3.1.3 Aims

In this chapter a calcium imaging assay is used to investigate the embryonic spinal DH culture network activity. The aims of this investigation are to use calcium imaging techniques:

1. To determine whether GABA_A receptor pharmacological tools can modulate the spontaneous activity of the spinal DH cell culture model
2. To determine whether glycine receptor pharmacological tools can modulate the spontaneous activity of the spinal DH culture model
3. To determine the effects of blocking the KCC2 co-transporter on the spinal DH culture activity
4. To determine if activating or inhibiting the NMDA receptors in the spinal DH culture effects the network activity

3.2 Methods

3.2.1 *Embryonic Dorsal Horn Primary Cell Culture*

The spinal DH cell culture was performed as described in Chapter 2 (section 2.2.1).

The cultures were used for the calcium imaging experiments between 12-14 DIV.

3.2.2 *Flexstation Calcium Imaging with Cultured Dorsal Horn Cells*

As described in Chapter 2 (section 2.2.2), the media was removed from the cultured DH cells and replaced with 80 μ l of FLIPR Calcium 5 Dye (Molecular Devices, USA) diluted 1 ml of Calcium 5 Dye in 9 ml HBSS (-/-), with calcium chloride (1.8 mM) and 1% HEPES (Sigma-Aldrich, UK), and adjusted to pH 7.4 with sodium hydroxide (Sigma-Aldrich, UK). After 30 minutes incubation at 37°C the DH cell cultures were transferred to the Flexstation II 384 (Molecular Devices, USA). The Flexstation is a scanning fluorometer with an integrated fluid transfer system to allow for addition of compounds to a multi-well plate. SoftMax Pro software (version 5.4) (Molecular devices, USA) was used in conjunction with the Flexstation for data acquisition and analysis. The Flexstation is able to simultaneously measure the fluorescence intensity from a column of wells of a 96-well plate, and is therefore higher-throughput than the previously utilised BD Pathway system which can only measure one well at a time. However, unlike the BD Pathway the Flexstation does not capture a video of each well so there is no record of which cells display spontaneous activity and/or respond to compound addition. An image of each well was captured separately after dye loading using an AMG digital inverted microscope (EVOS Thermofisher Scientific, UK). Those wells where the cells were seen not to form networks or did not display spontaneous firing were not included in the analysed data.

The Flexstation assay involved measuring the baseline activity of each well for 4 minutes, at which point the compound was applied. The response of the cultured cells to the compound was recorded for the following 4 minutes. Depending on the experiment, a second compound could be added and the response to the second addition was recorded for a further 4 minutes. A recording duration of 4 minutes for each section of the assay was determined to be sufficiently long enough to capture the change in fluorescence of the culture in response to a compound without sacrificing the health of the dye loaded cells. The cells stop firing and start to die when they are exposed to the dye for over 90 minutes. The compounds could not be washed off; therefore it cannot be shown if the firing frequency would return to normal baseline firing after removal the compounds. Consequently, each well of the plate could only be used for one concentration of one compound. A list of the compounds and their concentrations investigated in this assay with the spinal DH culture model can be found in Table 3.1. The response to the vehicle DMSO was tested on the spinal DH culture to determine the maximum final percentage of DMSO that can be utilised if required as a solvent for a compound. The SoftMax Pro software was used to control the excitation and emission wavelengths of the Flexstation, the excitation wavelength was set to 485 nm and the emission wavelength was 525 nm. The sensitivity reading was set to 12 with a high photomultiplier tube (PMT) sensitivity, and the fluorescence intensity was set to be measured every 2 seconds. Compound addition of 20 µl was set to be added at a rate of 75 µl/second. The Flexstation II has a temperature control system, which maintained the plate at 37°C throughout the experiments.

3.2.3 *Flexstation Data Analysis*

From the graph of relative fluorescence against time for each well, the area under the curve was determined for each section of the recording. The area under the curve was calculated from the baseline value for each well using the SoftMax Pro software. Due to the occurrence of artefacts with the addition of many compounds, the area under the curve for the section with compound present was calculated with the area under curve of the artefact duration subtracted. The same time period was compared for each section, therefore if 10 seconds of the area under the curve of the section where compound was present was removed for the artefact then 10 seconds was also removed from the baseline section when calculating the area under the curve. The percentage change in the fluorescence was calculated as the difference between the area under the curve of the section of the trace with compound present minus that of the baseline section divided by the area under the curve of the baseline section. Concentration-response curves were generated with normalised percentage change values. GraphPad Prism 6 (GraphPad Software, La Jolla California USA; version 6.00) was used to obtain a concentration-response curve for the data using a non-linear fit model. Data points are plotted with error bars of S.E.M. The n values stated are the number of wells tested with each concentration of the compound. Each compound concentration was tested on a minimum of 6 different wells denoted as n, which were from at least two different cell culture preparations, denoted as N.

Compound	Concentration Range (μM)	Supplier	Solvent
GABA	1 - 10	Sigma	dH ₂ O
Muscimol	0.3 - 100	Sigma	dH ₂ O
Diazepam	0.1 - 30	Sigma	DMSO
Bicuculline methiodide	1 - 300	Sigma	dH ₂ O
Gabazine (SR-95531)	1 - 300	Sigma	dH ₂ O
Baclofen hydrochloride	0.1 - 1000	Sigma	dH ₂ O
2-Hydroxysaclofen	0.3 - 100	Alfa Aesar	DMSO
Glycine	1 - 1000	Sigma	dH ₂ O
Taurine	30 - 10000	Sigma	dH ₂ O
CP-802079 hydrochloride	1 - 1000	Sigma	DMSO
Strychnine	0.1 - 30	Sigma	DMSO
Gelsemine hydrochloride	0.1 - 300	Extrasynthese	DMSO
VU0240551	0.1 - 300	Sigma	DMSO

Table 3.1 A list of the compounds and their range of concentrations applied to the spinal DH culture in the Flexstation calcium imaging assay. Supplier information and solvent utilised for each compound is also provided.

3.3 Results

3.3.1 *Optimisation of the Flexstation Calcium Imaging with the Cultured Embryonic Spinal Dorsal Horn Cells*

The BD Pathway system was utilized to optimise the culture and its spontaneous activity in Chapter 2. During the initial optimisation of the calcium imaging assay it was found that the spinal DH culture is highly sensitive to dimethyl sulfoxide (DMSO). When DMSO is applied at a concentration as low as 0.006%, the baseline fluorescence increases to a level where the spontaneous rhythmic peaks of the cell network can only just be deciphered from the background level of fluorescence (Figure 3.1). Consequently any compounds which were required to be dissolved in DMSO were diluted so that the final concentration of DMSO was 0.001% or less to prevent a significant effect on the baseline calcium fluorescence. Due to the higher throughput of the Flexstation fluorometer, all pharmacological studies with the DH culture were performed using the Flexstation. The spontaneous firing of the DH culture was the same when observed with both systems (Figure 3.2). Therefore once the culture protocol had been optimised, the same DH cell culture protocol could be performed for the Flexstation assays. The Flexstation does not provide a video of each well on the DH culture plate and thus the synchrony of the individual cells could not be visualised. However, the high similarity between the two calcium imaging system traces with the DH culture suggested that the cultures could be considered to be synchronously firing when run on the Flexstation from the fluorescence intensity graph.

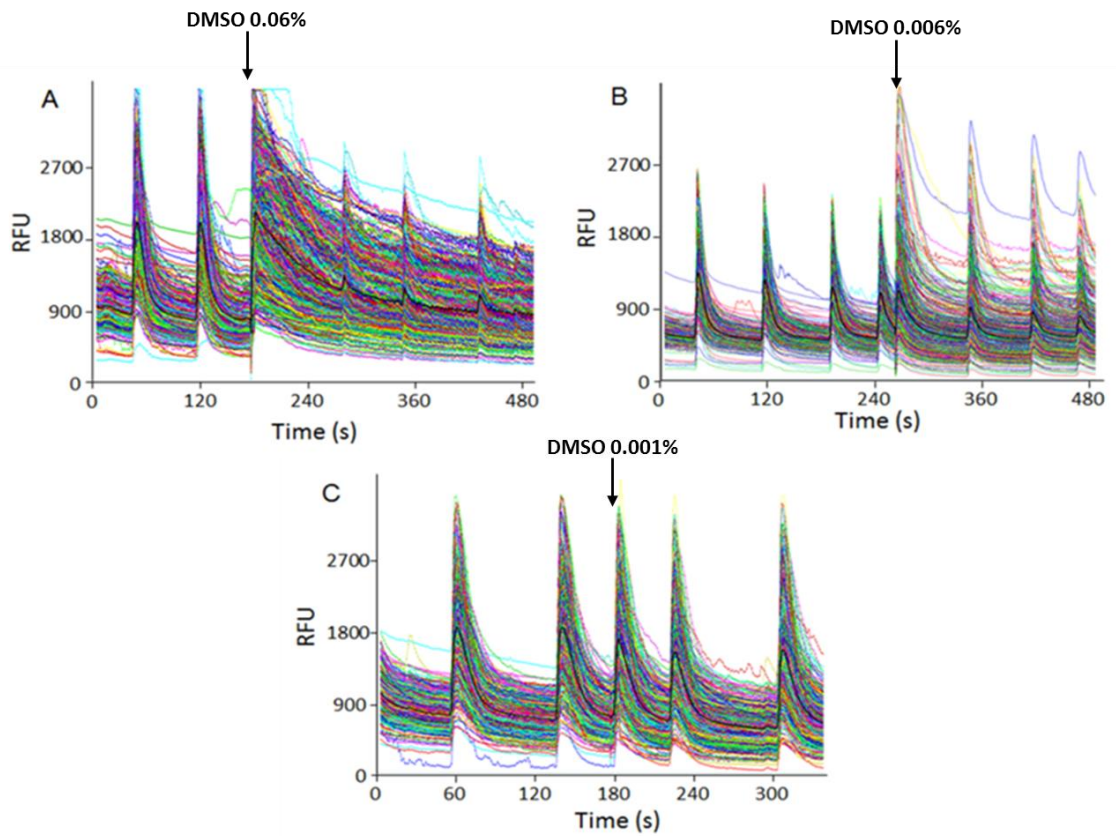


Figure 3.1 The effect of DMSO on the embryonic spinal DH culture baseline spontaneous activity. (A) DMSO at a concentration of 0.06% was applied to the DH culture at 180 s and caused a long-lasting increase in the baseline fluorescence. (B) 0.006% DMSO was applied to the spinal DH culture at 260 s into the recording. At this concentration, DMSO also increased the baseline fluorescence of the DH culture. (C) 0.001% DMSO was applied to the DH culture at 180 s, which did not have any effect on the baseline spontaneous activity of the culture.

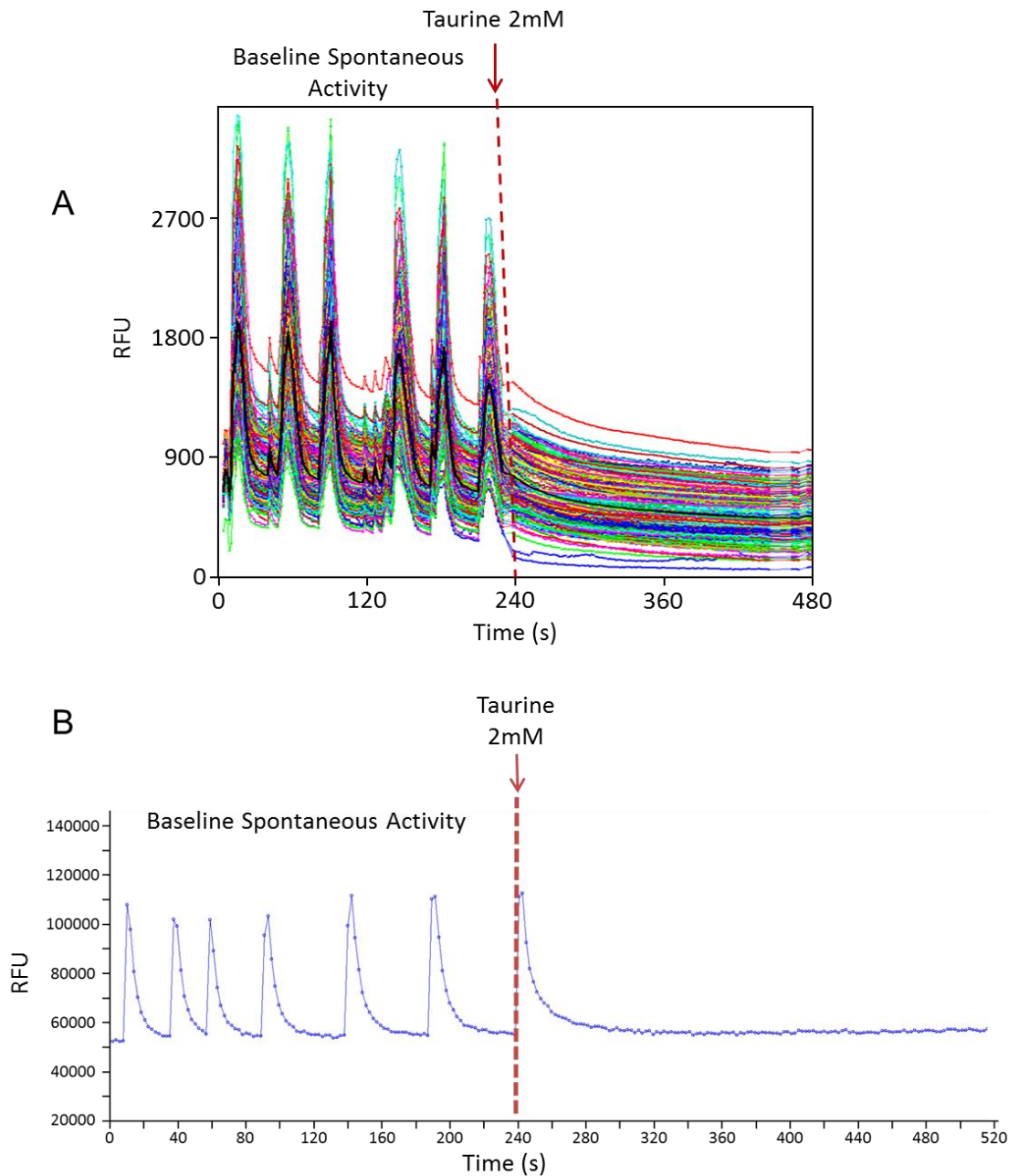


Figure 3.2 Spontaneous firing of the DH culture observed by calcium imaging using two different fluorometer systems. (A) A recording from the BD Pathway system with the cultured DH cells. The first section shows the baseline spontaneous activity followed by addition of taurine to the well as shown, which completely removed all firing. (B) A recording from the Flexstation, demonstrating similar spontaneous activity followed by addition of taurine which also prevented any subsequent firing of the DH culture.

3.3.2 The Role of GABA_A Receptor Signalling in Dorsal Horn Activity

Agonists of the GABA_A receptor, GABA and muscimol, both dose-dependently decreased the spontaneous activity of the DH culture (Figure 3.3). Furthermore, the GABA_A receptor PAM, diazepam, also dose-dependently reduced the spontaneous activity (Figure 3.4). Incidentally, the GABA_A receptor antagonists bicuculline and gabazine increased the spontaneous activity in a dose-dependent manner, increasing the rate of peaks in fluorescence and fluorescence intensity (Figure 3.5). Additionally baclofen, a GABA_B receptor agonist, dose-dependently decreased the DH culture activity (Figure 3.6). The GABA_B receptor antagonist 2-hydroxysaclofen dose-dependently increased the spinal DH culture activity (Figure 3.6).

3.3.3 The Role of the Glycine Receptor in the Dorsal Horn Activity

Application of each of the glycine receptor agonists, glycine and taurine, both produced a decrease in the spontaneous activity of the DH culture in a dose-dependent manner (Figure 3.7). The potent and selective glycine transporter type 1 (GlyT1) antagonist CP-802079 also dose-dependently decreased the spontaneous activity (Figure 3.8). The two glycine receptor antagonists, strychnine and gelsemine, each dose-dependently increased the activity of the DH culture (Figure 3.9). Conversely, the antagonist of the KCC2 co-transporter, VU 0240551, dose-dependently increased the spinal DH culture spontaneous activity (Figure 3.10).

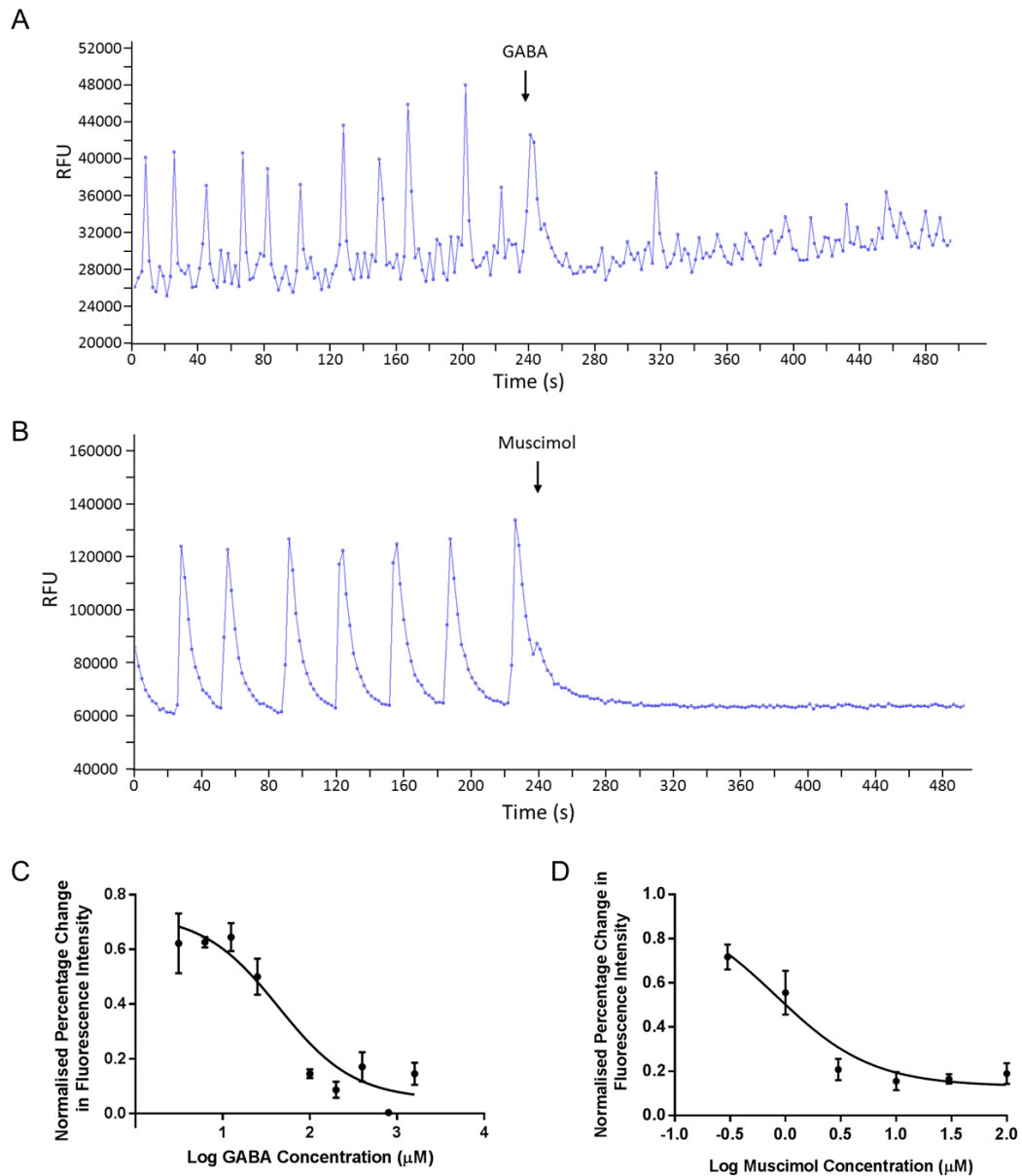


Figure 3.3 Inhibition of the DH culture spontaneous activity by GABA_A receptor agonists. (A) A Flexstation relative fluorescence trace against time with the DH cultured cells. GABA (100 μM) was added to the well at 240 seconds into the recording which completely inhibited the spontaneous activity. (B) A Flexstation trace of a recording with muscimol (10 μM) applied at 240 seconds into the recording, which similarly prevented the spontaneous firing. (C) The concentration response curve generated from the Flexstation data with GABA, where the EC_{50} is $43.5 \pm 0.1 \mu\text{M}$ ($n=3-5$). (D) The concentration response curve for muscimol, where the EC_{50} is $6.7 \pm 0.2 \mu\text{M}$ ($n=4-6$).

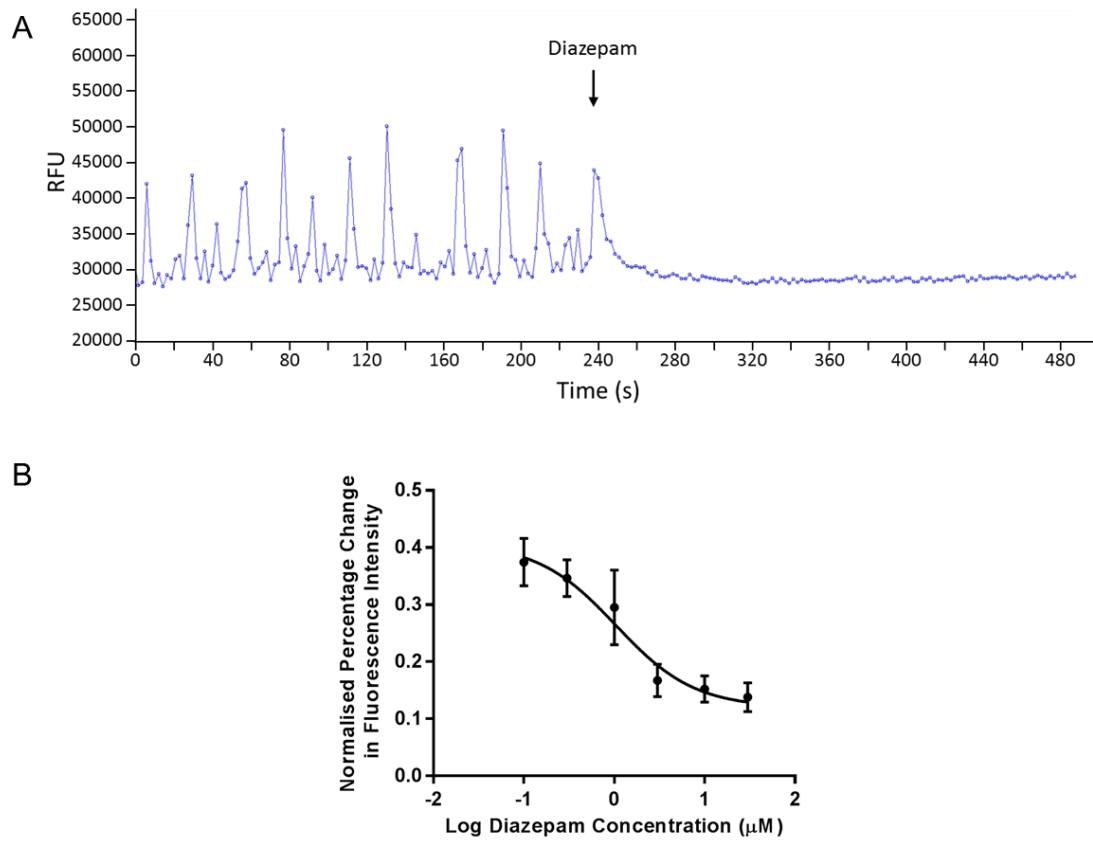


Figure 3.4 GABA_A receptor PAM, diazepam decreases the spontaneous activity of the spinal DH culture. (A) An example Flexstation trace with the cultured DH cells illustrating the effect of application of diazepam (10 μM) on the spontaneous activity. (B) The concentration-response curve generated from the DH culture Flexstation recordings with diazepam application. The EC₅₀ for diazepam is $1.0 \pm 0.3 \mu\text{M}$ (n=14-22).

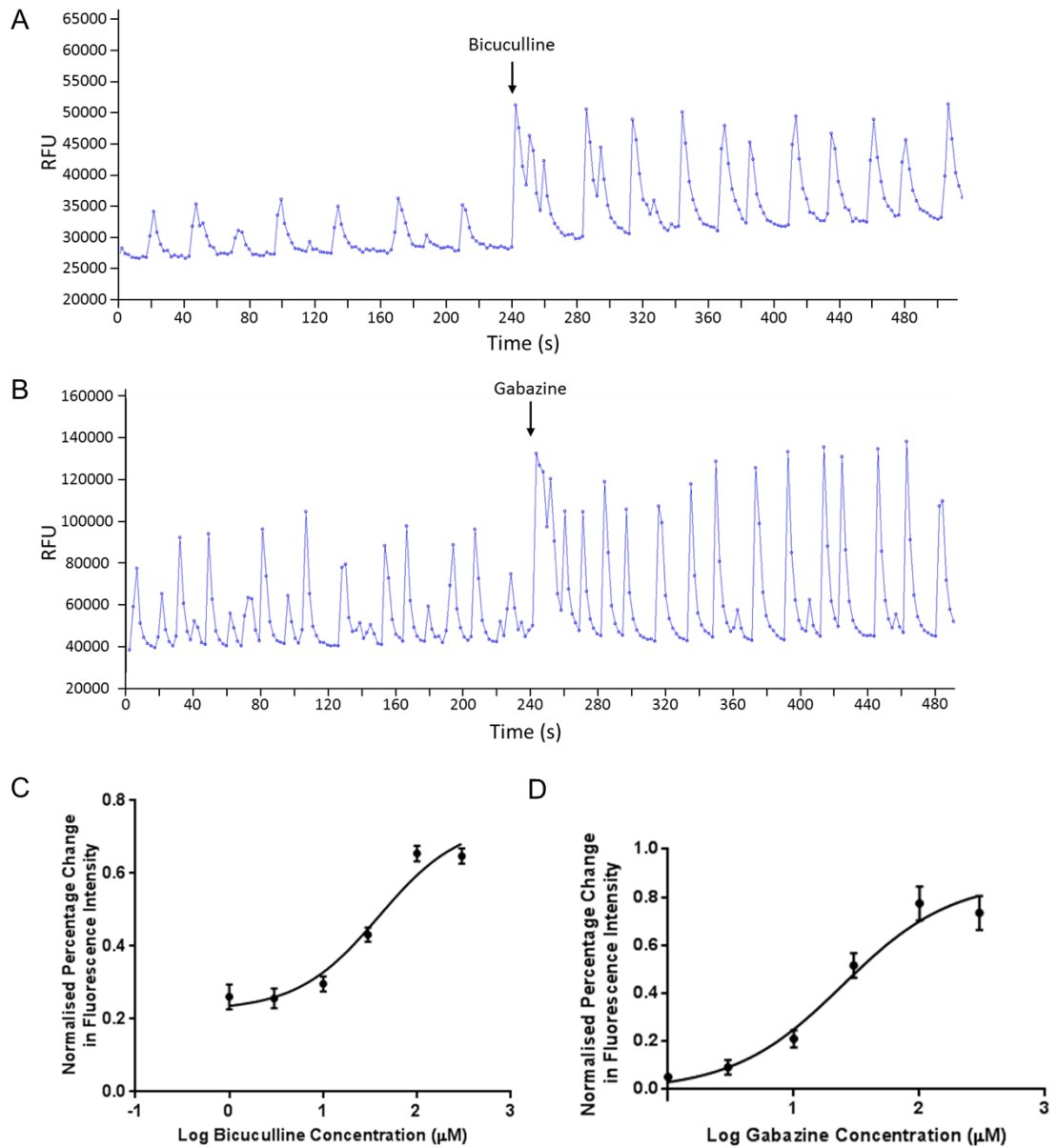


Figure 3.5 The effects of GABA_A receptor antagonists' bicuculline and gabazine on the DH culture activity. (A) A Flexstation trace to show the effect of bicuculline (10 µM) on the DH spontaneous activity. (B) A Flexstation trace to demonstrate the effect of gabazine (30 µM) on the DH culture spontaneous activity. Bicuculline was added at 240 s into the experiment. (C) The concentration-response curve generated from the bicuculline data obtained from the Flexstation, where the IC₅₀ is 39.3 ± 0.04 µM (n=4). (D) The concentration-response curve for gabazine, where the IC₅₀ is 18.2 ± 0.8 µM (n=6-9).

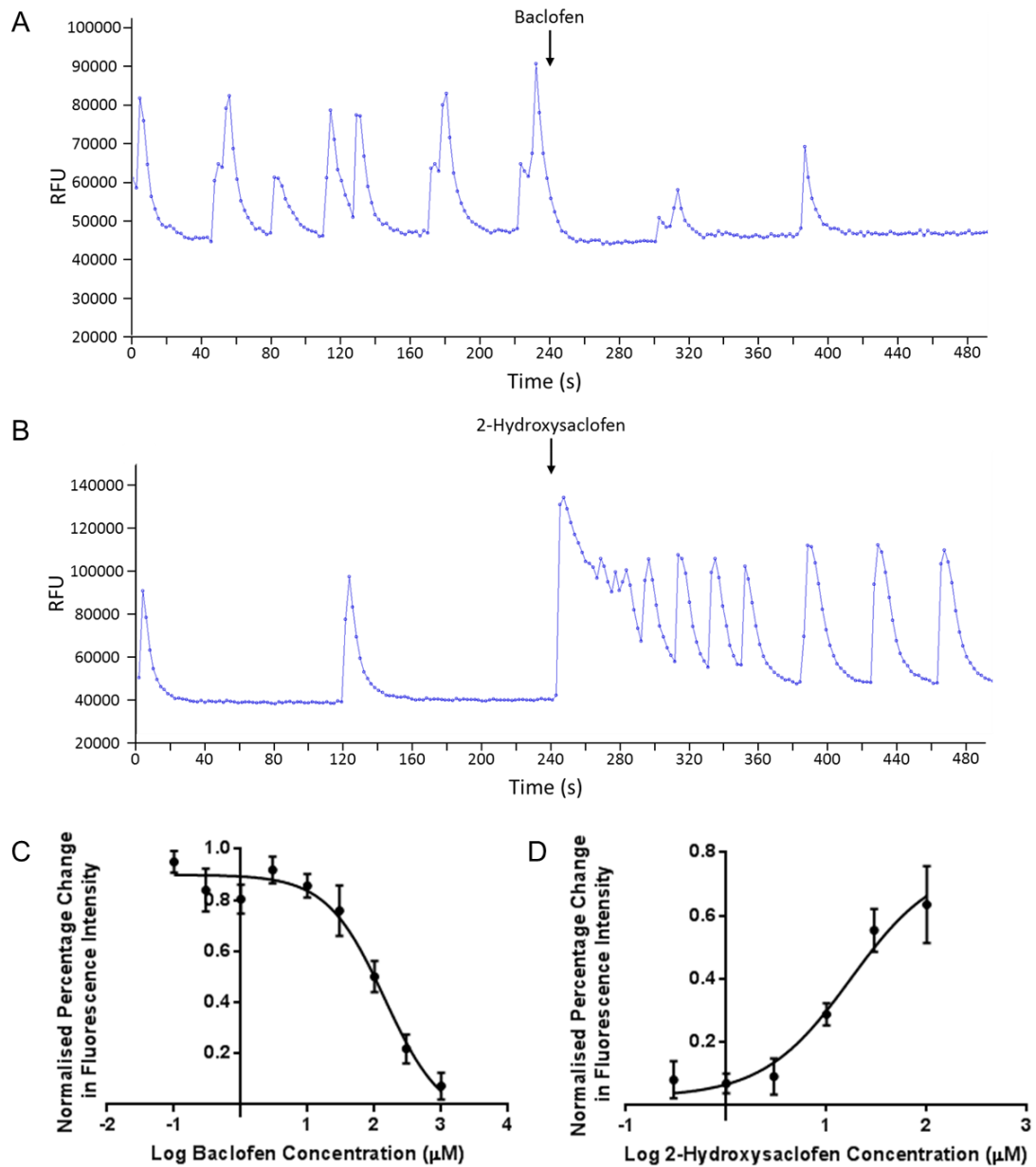


Figure 3.6 The actions of GABA_B receptor agonist and antagonist on the DH cell culture spontaneous activity. (A) An example of a Flexstation trace using the DH culture where GABA_B receptor agonist baclofen (100 µM) was applied at 240 s. (B) An example trace from a Flexstation recording with the DH culture where GABA_B antagonist 2-hydroxysaclofen was applied at 240 s. (C) The concentration-response curve for baclofen generated from the FLExstation data, where the EC₅₀ is 118.2 ± 0.9 µM (n=3-6). (D) The concentration-response curve for 2-hydroxysaclofen, with an IC₅₀ of 17.3 ± 0.11 µM (D) (n=3-6).

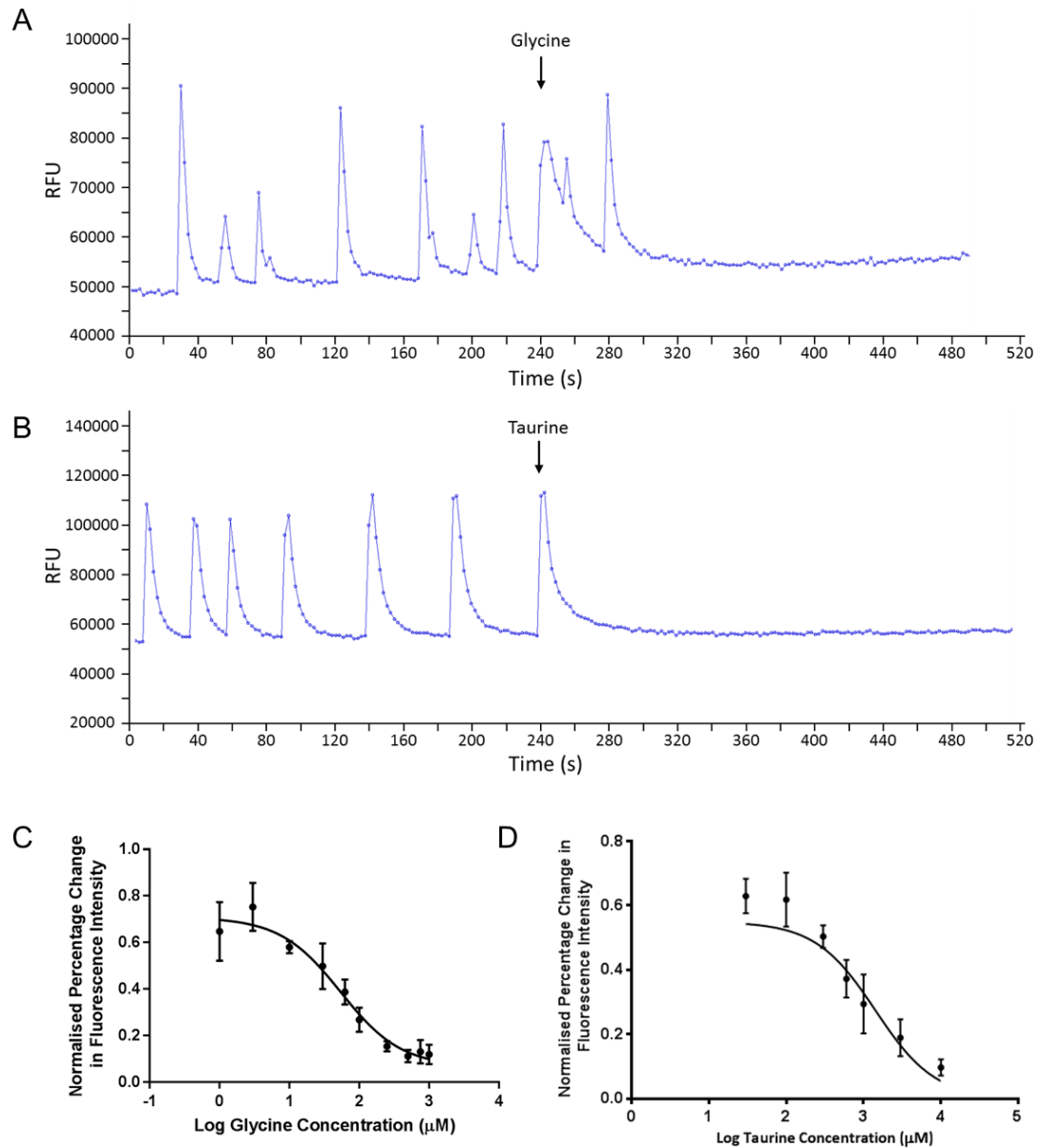


Figure 3.7 Glycine receptor agonist effects on the DH cultured cells. (A) A graph of the relative fluorescence over time from a single well of DH cells cultured to day 12. The baseline spontaneous activity was measured for 240s, at which point 1 mM glycine was added to the well. This resulted in a loss of firing. (B) An example of the effects of 2 mM taurine on the DH cultured cells. Taurine was added at 240s, which similarly removed all spontaneous firing. (C) and (D) show the concentration-response curves for glycine (n=3-8) and taurine (n=4-6), respectively. The EC_{50} for glycine is $74.34 \pm 0.64 \mu\text{M}$ and the EC_{50} for taurine is $1.4 \pm 0.55 \text{ mM}$.

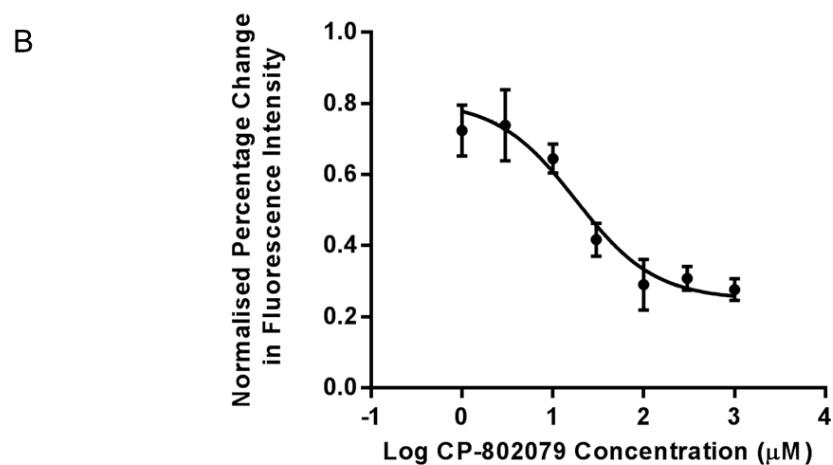
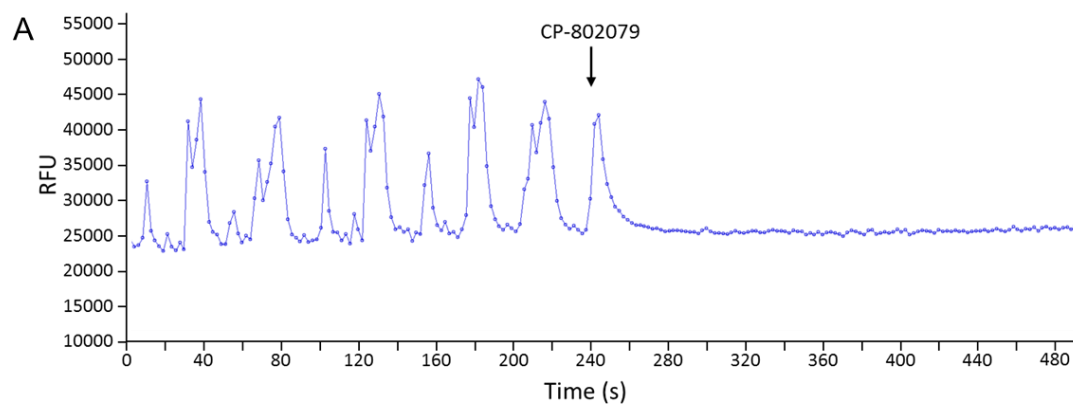


Figure 3.8 The effect of the GlyT1 antagonist CP-802079 addition on the DH culture spontaneous activity. (A) A trace from a Flexstation recording with CP-802079 (100 µM) added at 240 seconds. (B) The concentration-response curve generated for CP-802079 from the Flexstation data with the DH cultured cells, with an IC_{50} value of 18.0 ± 0.6 µM ($n=4-12$).

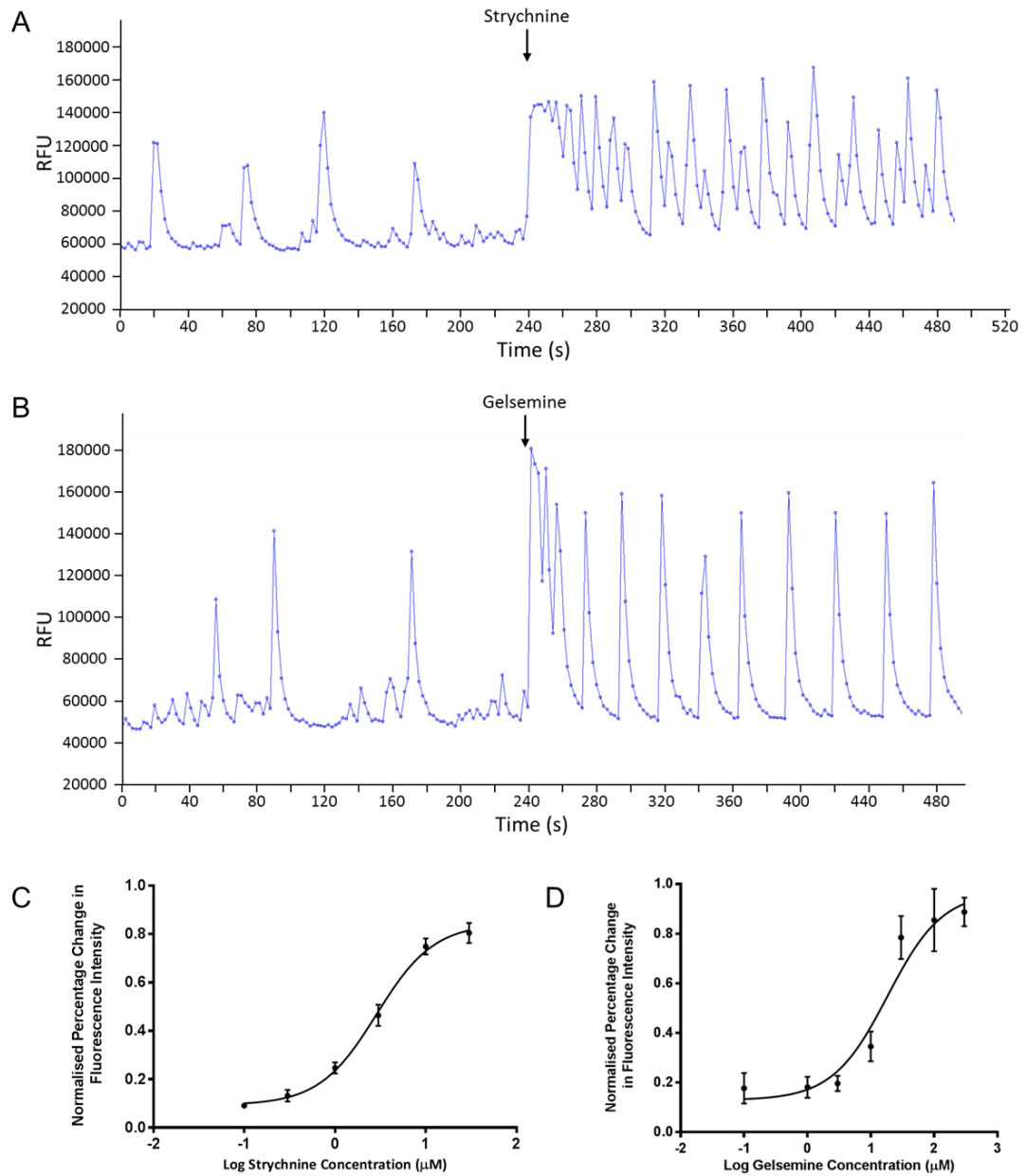


Figure 3.9 The effect of strychnine and gelsemine on the spontaneous activity of the spinal DH culture. (A) An example trace from the Flexstation with strychnine (3 μM) added to the DH cells at 240 seconds. (B) An example trace with gelsemine (30 μM) added to the culture at 240 seconds. Concentration-response curves were generated for both strychnine (C) ($n=4-5$) and gelsemine (D) ($n=3-7$) from the Flexstation data with these glycine receptor antagonists. The IC_{50} value for strychnine was $2.9 \pm 0.07 \mu\text{M}$, and for gelsemine $18.4 \pm 0.8 \mu\text{M}$.

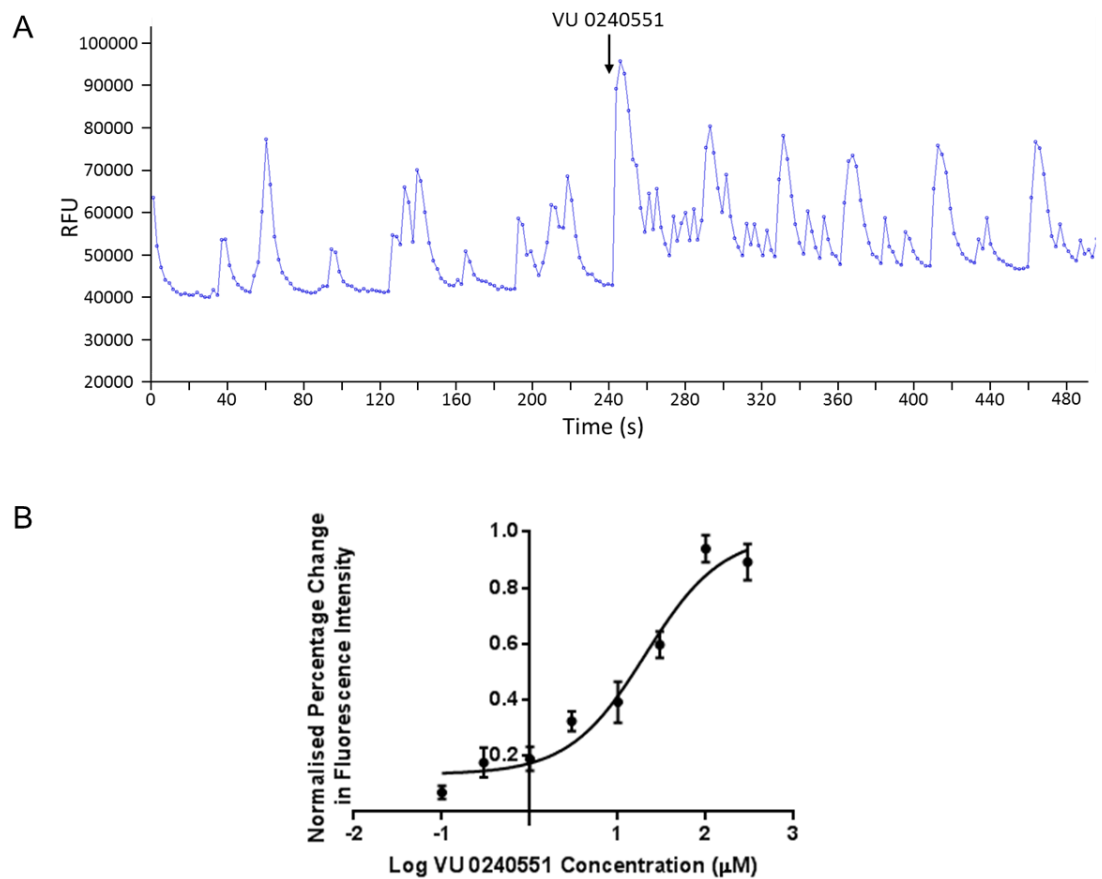


Figure 3.10 The effect of blocking the KCC2 co-transporter in the spinal DH culture. (A) An example recording from the DH cultured cells on the Flexstation, with KCC2 antagonist VU 0240551 applied at 240 s. (B) The concentration-response curve of the VU 0240551 data from the DH culture Flexstation recordings, with an IC_{50} of $23.3 \pm 0.6 \mu\text{M}$ ($n=4-6$).

3.4 Discussion

The embryonic spinal DH culture developed in Chapter 2 was used to investigate calcium responses, an indicator of the DH culture network activity. A series of well-characterised pharmacological tools of the GABA_A and glycine receptors were applied to the DH culture to investigate the role of these receptors in the spontaneous, rhythmic network activity. Consequently, the validity and potential utility of this *in vitro* model with the Flexstation calcium imaging assay to screen novel compounds can be evaluated. In Chapter 2 the rhythmic activity of the cultured spinal DH was shown to have a frequency of 0.082 ± 0.02 Hz. The results obtained with the calcium imaging assay illustrate that the rhythmic activity of the DH culture can be modulated by GABA_A, GABA_B and glycine receptor signalling. Furthermore, KCC2 was also shown to be critical for the generation of the rhythmic activity.

Spontaneous activity has been previously reported in cortical and spinal cord cultures, as well as organotypic spinal cord slices (Legendre et al., 1985, Streit et al., 2001, Czarnecki et al., 2008, Hendrich et al., 2012a). Spinal spontaneous activity *in vitro* is believed to originate at least in part in the spinal cord itself. Pacemaker neurons within the superficial DH exist and synapse with both other interneurons within the DH and with projection neurons, as observed in *ex vivo* preparations of neonatal spinal cords (Li et al., 2014). Evidence that these pacemaker neurons project to the nociceptive processing supraspinal regions, including the periaqueductal grey and parabrachial nucleus, suggests a role for this spontaneous activity in modulating nociceptive signals (Li et al., 2014). The proposed ING and PING circuitry mechanisms for the generation of rhythmic oscillations in brain networks could apply to the spinal DH network.

3.4.1 *GABA_A and Glycine Receptor Agonists and Antagonists Modulate the Spinal Dorsal Horn Culture Activity*

GABA_A, GABA_B and glycine receptor agonists both dose-dependently decreased the spontaneous activity. Antagonists of the GABA_A, GABA_B and glycine receptors both dose-dependently increased the spontaneous activity of the DH culture. These results indicate that GABA_A, GABA_B and glycine receptor signalling is inhibitory in this DH culture. During embryonic development GABA has an excitatory action which is essential for the development and maturation of the CNS (Owens et al., 1996, Cancedda et al., 2007). The excitatory action of GABA has also been linked to the generation of oscillations in the cortex (Ben-Ari et al., 2007). It is possible that during the 12-14 DIV, the DH culture has matured to a state in which GABA_A and glycine receptor signalling is inhibitory. This is supported by the expression of KCC2 detected in the IF study in Chapter 2, since the expression of KCC2 is believed to be low in early postnatal life (from P10), dramatically increases at P17, and then increases gradually peaking at the onset of adulthood (Zhang et al., 2006). This is thought to correspond with the switch in GABA from being excitatory to inhibitory around P17. This suggests that if both GABA and glycine are inhibitory in the DH cell culture model, then the expression of KCC2 in this culture has increased to the stage at which the E_{Cl} is similar to that of adult spinal DH cells. This could be linked to the onset of the spontaneous activity that occurs within the culture, indicating that the inhibitory signalling in the DH network is required for the spontaneous rhythmic activity. This is further supported by the data with the KCC2 blocker, VU0240551, dose-dependently increasing calcium response in the DH culture.

The results presented in this chapter clearly identify the vital role of GABA_A and glycine receptors in the modulation of the rhythmic activity in DH culture. GABAergic PV-expressing interneurons in the brain regulate cortical oscillations (Lodge et al., 2009, Kim et al., 2015, Kuki et al., 2015). In Chapter 2, GABAergic PV-positive cells

were detected in the DH culture, therefore these cells are potentially involved in the regulation of the rhythmic activity of the DH culture network. Glycine receptor signalling in the brain is also important in regulating brain oscillations, where glycine receptor agonists suppress epileptiform activity (Chen et al., 2014). In the spinal DH there are neurons releasing both GABA and glycine (Todd and Sullivan, 1990). Therefore, it is highly probable that glycine receptor signalling is also involved in the generation and regulation of the spinal DH network rhythmicity.

The KCC2 antagonist, VU 0240551, dose-dependently increased the DH culture activity. The KCC2 co-transporter exports chloride and potassium ions, therefore blocking the export of chloride ions increases the intracellular chloride ion concentration (DeFazio et al., 2000). This can cause the equilibrium potential for chloride ions to become more positive than the cell resting membrane potential, which leads to GABA_A and glycine receptor signalling to be excitatory (Rivera et al., 2002, Watanabe and Fukuda, 2015). In the brain a down-regulation of the KCC2 transporter increases seizure susceptibility (MacKenzie and Maguire, 2015). Therefore, the increase in the activity of the DH culture in the presence of the KCC2 antagonist is likely to be the result of a shift in the chloride equilibrium potential causing GABA_A and glycine receptors to have a depolarising effect. Furthermore, in the embryonic spinal cord a chronic block of glycine receptors with strychnine down-regulates KCC2 expression, while glycine up-regulates it through non-synaptic mechanisms (Allain et al., 2015). Therefore, in the spinal DH culture the application of strychnine could increase the DH activity through two mechanisms. Firstly, strychnine blocks the glycine receptors and prevents glycinergic inhibition resulting in unregulated excitation. Secondly, the blocking of glycine receptors with strychnine could also cause downregulation of KCC2 expression and a shift in the chloride equilibrium potential. This could result in the signalling of GABA_A and any glycine receptors, which are not blocked by strychnine, to produce depolarisation of the

network's interneurons. A downregulation of KCC2 has been identified in *in vivo* models of inflammatory and neuropathic pain (Zhang et al., 2008c, Lu et al., 2009, Hasbargen et al., 2010, Kahle et al., 2014). Furthermore, the change in intracellular chloride concentration has been linked to a change in expression of GABA_A receptor subtype, which is believed to influence the tonic and phasic firing patterns of GABAergic signalling (Succol et al., 2012). Therefore, to restore the KCC2 expression and consequently the chloride electrochemical gradient in the spinal DH, could restore GABAergic signalling and provide a mechanism for analgesia. KCC2 has been investigated as a potential target in the development of novel analgesics (Kahle et al., 2014). Upregulation of KCC2 in the spinal DH by increasing glycinergic signalling suggests the glycine receptor as an ideal target for the development of novel analgesics.

Gelsemine has been shown to have analgesic properties, and be selective for glycine receptors containing the $\alpha 3$ subunit (Zhang et al., 2013, Zhang and Wang, 2015). Interestingly, in this study gelsemine addition increased DH activity similarly to the other glycine receptor antagonist strychnine. Strychnine and also bicuculline exacerbate pain, therefore it is unexpected that gelsemine has anti-nociceptive effects *in vivo*, despite also being a glycine receptor antagonist and increasing the DH culture activity like strychnine (Yamamoto and Yaksh, 1993). This could be due to differences in the spinal DH network of the culture compared to *in vivo* conditions, which could result in differing effects of gelsemine. However, gelsemine is an antagonist of the glycine receptor, like strychnine, therefore the response of the DH culture to gelsemine is consistent in the effects of a glycine receptor antagonist. Therefore, gelsemine could have alternative actions to strychnine other than simply inhibition of glycine receptors which produce an anti-nociceptive response. Gelsemine has been linked with upregulating allopregnanolone synthesis in the spinal cord (Venard et al., 2011). In the spinal cord, allopregnanolone has an

analgesic effect (Candeletti et al., 2006), therefore its upregulation by gelsemine could provide the mechanism underlying the analgesic effect of gelsemine.

3.4.2 Conclusions

In conclusion, the Flexstation calcium imaging assay with the *in vitro* spinal DH cell culture model provides a platform in which the culture can be utilized for drug screening. Through the application of well characterised GABA_A, GABA_B and glycine receptor compounds it has been demonstrated that this assay can effectively detect calcium responses to compound addition. Therefore, this platform can be used to provide an indication of the effect of a compound on the DH network activity. The higher-throughput of this platform is also advantageous for fast screening of multiple compounds.

4 siRNA Knockdown of Glycine Receptor α Subunits in the Dorsal Horn Cell Culture Model

4.1 Introduction

4.1.1 RNA Interference Mechanism

RNA interference (RNAi) is the mechanism by which siRNA or short hairpin RNA (shRNA) target and cleave their complementary mRNA in eukaryotic cells. shRNA and siRNA have emerged as powerful tools in the study of gene function in mammalian cells since the discovery of their ability to achieve knockdown of a specific target gene in mammalian cell lines and *in vivo* (Elbashir et al., 2001a, McCaffrey et al., 2002). These molecules are typically 19-23 nucleotides long, double-stranded RNAs with one strand being the anti-sense active strand that is complementary to a specific target mRNA sequence (Elbashir et al., 2001b). One of the principal problems with RNAi technology is to achieve high transfection efficiency (Whitehead et al., 2009). Incomplete transfection is unlikely to completely silence the target gene, therefore not causing a significant change in the downstream effects. The delivery of siRNA into the cytoplasm has proved problematic in many cell types, where additional delivery systems are required to facilitate the transfection (Kim and Eberwine, 2010). This is because RNA molecules are relatively large and they have a negative charge which prevents them from easily crossing the cell membrane. Furthermore, RNA molecules are quickly degraded by endogenous enzymes, therefore ineffective delivery of siRNA has prevented its utilisation in scientific experimentation and its therapeutic potential (Whitehead et al., 2009).

This study has utilised two delivery systems, lentivirus delivery of shRNA and Accell siRNA (GE Healthcare Dharmacon Inc., USA). The lentivirus delivery of shRNA has been well documented and utilised both experimentally and clinically. Viruses are able to inject their RNA directly into a cell where it is converted to DNA and transported to the nucleus where it is integrated into the cell's own DNA (Matrai et

al., 2010). The viral DNA is then transcribed into the shRNA along with the cell's own DNA and is then exported to the cytosol (Figure 4.1). Accell siRNA (GE Healthcare Dharmacon Inc., USA) is delivered directly to the cytosol of a cell as it is able to cross the cell membrane unaided, however, the exact mechanism has not yet been disclosed. Accell siRNA needs to be lipophilic to cross the cell membrane, this is possible if the Accell siRNA is cholesterol-conjugated siRNA (Wolfrum et al., 2007).

Once the shRNA or siRNA are in the cytosol of the cell it uses the cell's enzymatic pathway to degrade the complementary endogenous mRNA (Elbashir et al., 2001b, Maniataki and Mourelatos, 2005). The double stranded molecule is loaded into the endogenous RNA-induced silencing complex (RISC), where the two strands are separated and the sense-strand, or passenger strand, is cleaved by the argonaute 2 protein contained within the RISC complex (Rand et al., 2004, Matranga et al., 2005). The anti-sense strand of the siRNA remains attached to the activated RISC, which then locates and degrades the complementary target mRNA (Ameres et al., 2007). The cleaved mRNA is further degraded by other nucleases within the cytoplasm, and the activated RISC complex can then go on to find other target mRNA molecules and repeat the process thereby silencing the gene's expression (Hutvagner and Zamore, 2002).

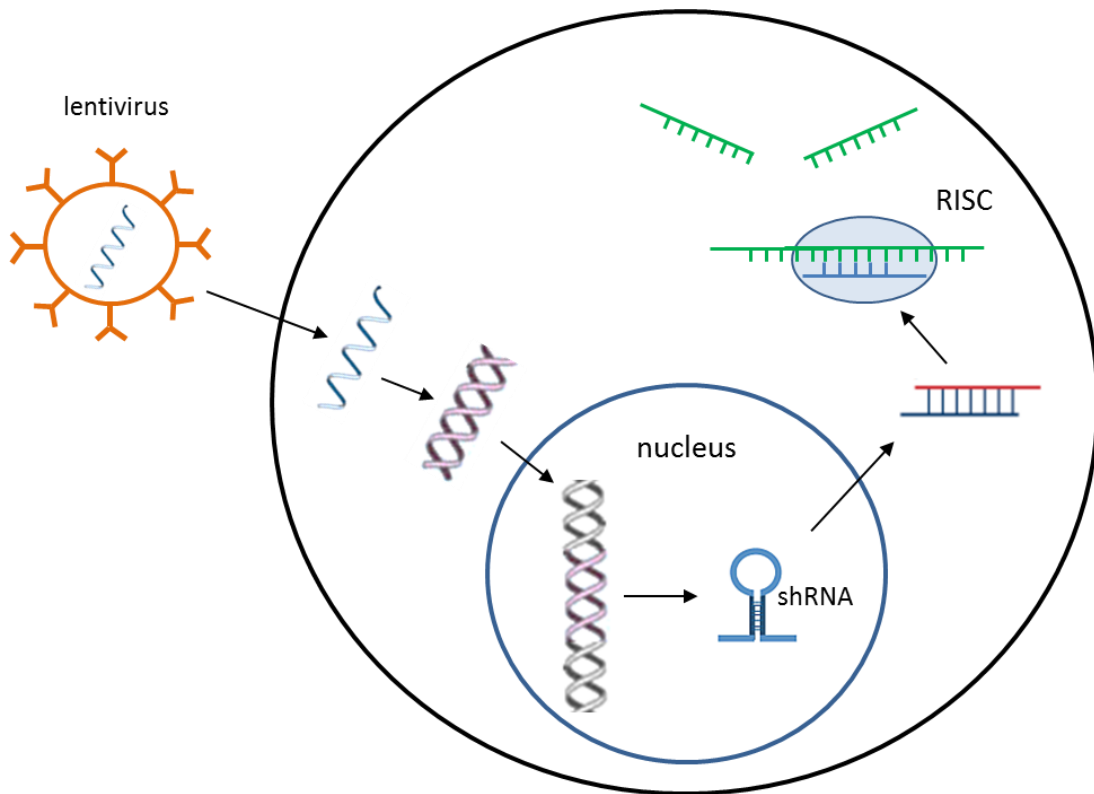


Figure 4.1 Gene silencing by transfection of shRNA using a lentiviral vector. The viral RNA is injected into the cell's cytosol using a lentiviral vector which is then reverse transcribed into DNA that is then transported into the nucleus and integrated into the cell's own DNA. The DNA is then transcribed, generating the shRNA. The shRNA is transported into the cytosol and loaded into the RISC complex which separates the strands of the shRNA and degrades the sense strand (red) and uses the anti-sense strand (blue) to locate the complementary target gene's mRNA (green). The argonaute 2 protein within the RISC complex then cleaves the target gene's mRNA silencing the gene.

4.1.2 Glycine Receptor Subunit Gene Silencing

There are a limited number of drugs known to selectively bind the glycine receptor. This has prevented the clinical utility of this receptor and the progress in further investigating its physiology (Lynch and Callister, 2006). As an alternative to pharmacological assays, the present study has utilised RNAi technology to investigate the effects of silencing the glycine receptor α subunits on the activity of the cultured DH cells. Only the α subunits were silenced in this study as functional

homomeric glycine receptors form only from α subunits (Griffon et al., 1999), while β subunits cannot form functional glycine receptors alone (Bormann et al., 1993, Kuhse et al., 1993). Furthermore, the α subunits form at least part of the ligand binding domain of the glycine receptors, therefore they influence the pharmacology of the glycine receptor (Schmieden et al., 1993, Meier et al., 2005). The β subunit requires α subunits to form functional heteromeric glycine receptors, with 2 α :3 β subunit stoichiometry being the most prevalent *in vivo* (Grudzinska et al., 2005). Homopentamers have been found extrasynaptically and in early development (Malosio et al., 1991b, Harvey et al., 2004). The primary role of the β subunit is to anchor the glycine receptor at synapses as it interacts with gephyrin, a cytoskeleton-associated protein, which is known for synaptic clustering of receptors (Meyer et al., 1995a, Kneussel and Betz, 2000).

In humans deficiencies in glycinergic inhibition causes hyperekplexia, which is characterised by an exaggerated startle reflex and muscular rigidity (hypertonia) (Bakker et al., 2006). It is predominantly point mutations in the glycine receptor $\alpha 1$ gene (*Glr1*) which result in hyperekplexia in humans (Bakker et al., 2006). A small population of people with hyperekplexia can alternatively have mutations in the glycine receptor β subunit (Rees et al., 2002). Interestingly, mouse models with mutations in the glycine receptor $\alpha 1$ gene have much more severe phenotype than humans, with many of the mutations being lethal in mice (Buckwalter et al., 1994, Kling et al., 1997). This suggests that there could be different compensatory mechanisms in mice compared to humans (Becker et al., 1986). This has been shown pharmacologically where administration of the benzodiazepine clonazepam, which increases GABAergic neurotransmission and decreases startle attacks in humans but is ineffective in mouse models (Buckwalter et al., 1994, Bakker et al., 2006). Glycine receptor $\alpha 2$ knockout mice do not display any significant morphological or molecular alterations in the nervous system; furthermore, brain

development as not affected (Young-Pearse et al., 2006). This could be the result of other glycine receptor subunits compensating for the loss of the $\alpha 2$ subunit. The glycine receptor $\alpha 3$ knockout mice do not display a typical overt behavioural phenotype but do have a reduced pain sensitisation following application of prostaglandin E₂ (PGE₂) or peripheral inflammation (Harvey et al., 2004, Harvey et al., 2009). This is in line with the findings that the glycine receptor $\alpha 3$ subunit is predominantly expressed in the superficial spinal DH (Harvey et al., 2004).

4.1.3 Aims

The aims of this study using siRNA gene silencing technique in the DH cell culture model were:

1. To investigate the effect of glycine receptor α subunit siRNA gene silencing on the DH culture calcium response.
2. To determine if glycine receptor α subunit gene silencing affects the response of the DH culture activity to glycine receptor antagonist strychnine and agonist glycine.

4.2 Methods

4.2.1 Lentiviral shRNA Preparation

SMARTvector 2.0 Lentiviral shRNAs (GE Healthcare Dharmacon Inc., USA) were used in this study to silence the expression of three rat glycine receptor α subunits: *Glr1*, *Glr2* and *Glr3*. Each of the glycine receptor α subunits were silenced in the spinal DH culture separately to decipher if any of these subunits has a significant role in the spinal DH network activity. Three different SMARTvector shRNAs were obtained for each of these three genes to test their efficacy in knocking down at least one of the sequences below. The sequences of the shRNAs of the *Glr1* lentivirus were 5'-GTCCGTGGTGATCTCGTGG-3', 5'-GATGTCAATAGCTTTCACG-3' and 5'-TATAACCAAAGCTTTCAG-3'. The three *Glr2* lentivirus shRNA sequences were 5'-ACGAGTAACATCTTCTTCC-3', 5'-AAAATGTTCACTCGGTAGT-3' and 5'-CGAGATATGGTGTGCGATTC-3'. The three *Glr3* lentivirus shRNA sequences were 5'-TTCTTAGCCCTGTCGATGA-3', 5'-GAAACGGTAAACTTCTCC-3' and 5'-GATACCCAACGCTACCCGA-3'. These shRNAs all had a TurboGFP fluorescent reporter within the sequence to enable visualisation of cells which had been transfected with the lentivirus allowing determination of the percentage of cells within the culture that had been transfected with the lentivirus. A control lentivirus with scrambled shRNA, also containing a green fluorescent protein (GFP) reporter tag was used to illustrate that the effects on the culture was the result of the shRNA knockdown of the subunits and not solely due to the presence of the lentivirus. All lentivirus work was done in a Class 2 safety cabinet to minimise the risk of direct contact with lentiviruses which can have harmful properties. The lentiviruses exist as viral particles, stored at -80°C, which were freeze-thawed on ice when ready to use. Following a quick-spin in a table-top centrifuge each of the lentiviruses were suspended in serum-free culture media 2, pre-heated to 37°C. The culture media 2 was the same as used in the cell culture

described in the methods section of Chapter 2. The media is required to be serum-free as the transduction of the lentivirus into the cells is affected by serum. The culture media 2 has a B-27 supplement replacement for serum and therefore could still be used to culture the DH cells transfected with lentivirus. By using the same media in which the cells are cultured prevents an additional variable on changing the health and activity of the cultured network. Three different multiplicity of infection concentrations (MOIs) of 10, 5 and 2.5 were tested for each of the lentiviruses. The MOI is the number of viral particles per cell and testing three different MOIs allows determination of the optimal MOI. The volume of viral particle required for the highest MOI was determined from the following calculation:

$$MOI = \frac{Volume\ of\ Virus \times Viral\ Titer}{Number\ of\ Cells}$$

The viral titer for each of the lentiviruses was provided by Dharmacon (USA). The cells were plated with a density of 1.7×10^6 cells/well and the volume of the lentivirus particles required could be calculated for a MOI of 10. The suspended lentiviruses were then further diluted in the culture media to obtain solutions with an MOI of 5 and 2.5.

4.2.2 Lentiviral Transfection

The embryonic rat DH cells were extracted and cultured as described previously in Chapter 2. After 7-8 DIV the media was removed from the cells and replaced with 50 μ l of the culture media 2 containing lentivirus. A minimum of six wells were transfected for each of the different lentiviruses and for each MOI. These six repeats were done in wells from minimum of 2 different culture preparations. All tips used for pipetting the lentiviruses were changed for each transfer and deactivated in Virkon solution (DuPont, USA) before disposal. The plates of cells were then incubated at

37°C overnight. After this incubation period an additional 100 µl of pre-heated culture media 2 was added to each well of cells with the lentivirus. The cells were incubated at 37°C for a further 24 hours with the lentivirus. The lentivirus-containing media was then removed and replaced with the culture media 2, and placed back in the incubator. This was repeated the following day, and from this point the cells were considered safe to be removed from the class 2 safety laboratory and could be used for experimentation. At this point the cells have been in culture for 11-12 days, which is the same time point at which the DH culture was previously identified to display spontaneous activity.

Images of the cultured cells previously incubated with the lentivirus were taken using the EVOS digital inverted microscope (AMG, Fisher Scientific, UK) using the GFP filter. The overlay feature of this microscope was used to determine the proportion of GFP-positive cells that had been infected by the lentivirus in the whole population (Figure 4.2). This feature overlays the GFP fluorescent image with the transmitted light image. The number of GFP-positive cells and the total number of cells could then be counted and the percentage transfected cells determined from at least 3 wells per glycine receptor α subunit lentivirus knockdown.

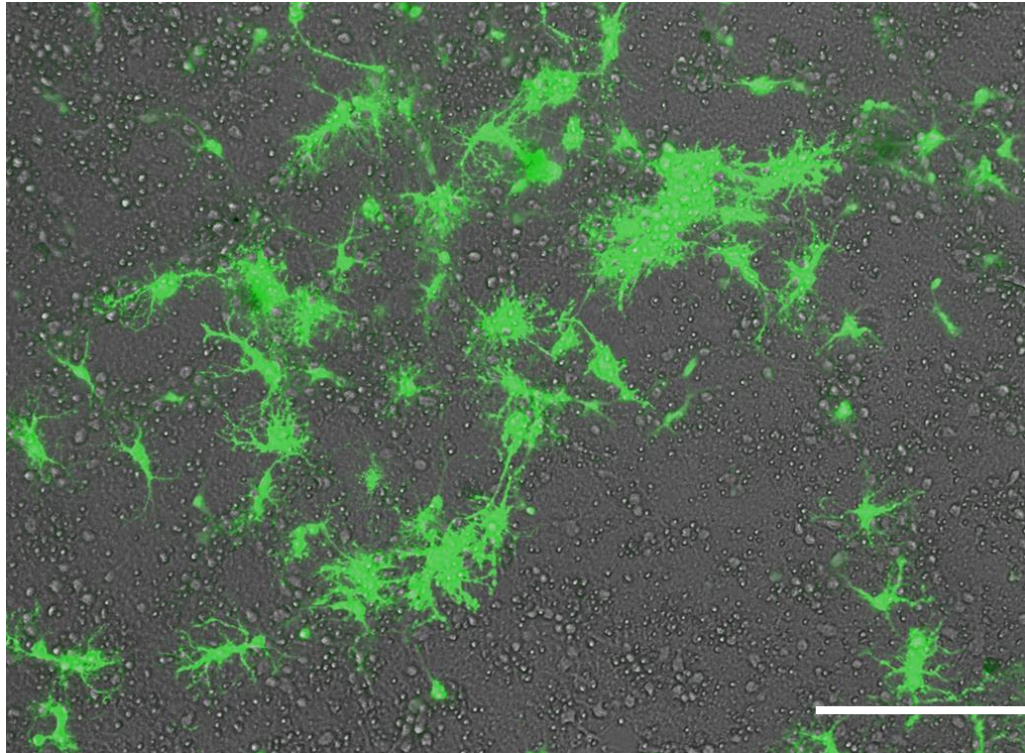


Figure 4.2 Image of the DH culture infected with the glycine receptor $\alpha 3$ lentivirus shRNA with TurboGFP tag. The image is an overlay of the images taken with transmitted light and with GFP fluorescence using an EVOS digital inverted microscope (AMG, Fisher Scientific, UK). The number of GFP positive cells and the number of cells which are not GFP-labelled were counted manually allowing the proportion of transfected cells to be determined. Scale bar is 200 μm .

4.2.3 *Accell siRNA Preparation and Transfection*

The embryonic primary cell culture was performed as previously described in section 2.2 of Chapter 2, with the cells plated at a density of 1.7×10^6 cells/well. At 9 or 10 days in culture the media was removed from the wells and replaced with the culture media 2 containing Accell siRNA (GE Healthcare Dharmacon Inc., USA). Three target-specific SMARTpool siRNA's for the three glycine receptor α subunits were used to silence their expression in the DH culture. Each of the SMARTpool siRNAs contains a mixture of siRNAs with four different sequences to improve gene silencing potency. The Accell rat *Gira1* (glycine receptor $\alpha 1$ gene) target sequences

were 5'-GUCUCGCCUACAAUGAAUA-3', 5'-CUGGAAAGCUUUGGUUAUA-3', 5'-GGAUCAGACCCAACUUUAA-3' and 5'-CCAGGGUGUUACAAUAUCC-3'. The four Accell rat *Gira2* target sequences were 5'-GAAUCAGGCCAAAUUUUAA-3', 5'-CUACUAGUCCUAAUGUUGA-3', 5'-GUGUAUUGCGUAAUUGAUU-3' and 5'-GCUACAUGUUUUAAGUAAG-3'. The target sequences for the Accell rat *Gira3* were 5'-CCAAUGGAUCUCAAGAAUU-3', 5'-GCUUAAGCAAUCAUGUUUA-3', 5'-CGAUGAAGUAACAAGAUCA-3' and 5'-CUACAAUACAGGAAAGUUU-3'. A negative control, non-targeting siRNA, was utilised to discriminate any off-target effects of the Accell siRNA from that of the sequence-specific gene silencing. Cyclophilin B siRNA and Glyceraldehyde-3-Phosphate Dehydrogenase (GAPDH) siRNA were utilised as a positive control for the gene silencing. Additionally a red fluorescent protein (RFP) non-targeting siRNA was used to assess the uptake of the siRNA by the cells when used in conjunction with fluorescent microscopy. As an additional control, 3 wells per plate of cells used in the siRNA experiments were cultured without siRNA in the normal culture media 2. All the siRNAs were initially re-suspended in 1x siRNA buffer, made by mixing one volume of 5x siRNA buffer (GE Healthcare Dharmacon Inc., USA) in 4 volumes of RNase-free water. The buffer has been developed by Dharmacon for the re-suspension and long-term storage of short double- or single-stranded synthetic RNA molecules (GE Healthcare Dharmacon Inc., USA). A 100 μ M solution of each of the siRNAs was made using the 1X siRNA buffer, which was mixed the solution by pipetting the solution 3-5 times avoiding the introduction of bubbles and then placing in an orbital mixer for 30 minutes at room temperature. Each of the siRNAs was added to the culture media 2 to obtain a final siRNA concentration of 1 μ M. 100 μ M of siRNA-containing media was added per well of the cultured DH cells. As described for the lentivirus transfection, 6 wells from at least two different culture preparations were transfected per siRNA. The cells were incubated at 37°C for 72 hours, with 100 μ l of culture media 2 added after 36 hours to maintain the health of the culture. The

Dharmacon protocol for using their siRNAs suggests using their Accell Delivery Media (GE Healthcare Dharmacon Inc., USA) as it is enriched for culturing in serum-free conditions. This Accell Delivery Media with added B-27 supplement (2%) and Glutamax (1%), as are included in the culture media 2, was tested on 12 wells of the DH culture used in the normal DH cell culture. After 24 hours in this media all the cells in the culture had died, therefore the siRNAs were all suspended in the normal culture media 2, as it is also serum-free. After the 72 hours incubation of the culture with the siRNAs the cells could then be assayed. An AMG EVOS digital microscope was used to assess the uptake of the siRNA by the culture by viewing the RFP control siRNA wells, as done with the lentivirus experiments.

4.2.4 Calcium Imaging Assay of the Dorsal Horn Culture Transduced with Lentivirus or Accell siRNA

Once the cultures transduced with the lentivirus or Accell siRNA were ready for assaying, the media was removed and replaced with 80 μ l FLIPR Calcium 5 dye (Molecular Devices, USA). As outlined in Chapter 3, after 30 minutes of incubation at 37°C with the calcium dye the DH cell culture plates were transferred to the Flexstation calcium imaging system (Molecular Devices, USA). The baseline relative fluorescence units (RFU) were recorded for 4 minutes, followed by addition of strychnine (10 μ M). The activity in the presence of strychnine was measured for a following 4 minutes, then glycine (2 mM) was added and the activity recorded for a final 4 minutes.

4.1.1.1 Flexstation Data Analysis

A graph of the RFU against time was generated during the experiments for each well of the plate with the cultured DH cells using the Softmax Pro software. The area under the curve was determined for each of the three sections of the recordings using the Softmax Pro software. There did not appear to be any difference between the three different shRNAs sequences for each of the glycine receptor α subunit lentiviruses. Therefore, for the analysis for the three shRNAs for *Glar1* were combined, similarly for *Glar2* and *Glar3* shRNA data. The first section was the baseline activity, followed by activity in the presence of strychnine and thirdly with the addition of glycine. A one-way ANOVA test was used to compare the mean area under the curve of the baseline data for each of the cultures transduced with the different lentiviruses, and also from the control group of cultures with no lentivirus. Similarly the baseline data of the cultures transduced with each of the Accell siRNAs were also compared with a one-way ANOVA. To determine if the cultures transduced with the various lentiviruses or Accell siRNAs responded differently to strychnine and glycine, repeated measures one-way ANOVA was performed comparing baseline area data to strychnine and strychnine area data with the glycine data. The same process was repeated for the spike frequency data for all the lentivirus and Accell siRNA data. GraphPad Prism 6 (GraphPad Software, La Jolla California USA; version 6.00) was used to perform the statistical tests and draw the graphs. In the results where $P \leq 0.05$ this is indicated by *, a $P \leq 0.01$ value is indicated by **, $P \leq 0.001$ by *** and $P \leq 0.0001$ indicated by ****, with S.E.M error bars.

4.2.5 Real-Time PCR with Accell siRNA Transfected Dorsal Horn Cells

Immediately following the experiments on the Flexstation with the DH cell culture the dye was removed and the cells washed twice with PBS (0.1 M). RNA extraction and purification from the cultures transfected with each of the glycine receptor α subunit siRNAs and the untreated DH cultures was completed as described in Chapter 2 (section 2.2.5). Relative quantitative TaqMan RT-PCR was also similarly performed as previously described in Chapter 2, section 2.2.5. Three mastermixes were made, one for each of the glycine receptor α subunit assays. The housekeeping gene ACTB was used as a positive control (Thermo Fisher Scientific). The RT-PCR reactions for each glycine receptor α subunit were done in triplicate, as were each of the RT negative cDNA samples as negative controls. RNase-free water was also used as a negative control to confirm there was no contamination of the water used in the reactions. The TaqMan RT-PCR amplification reaction and detection was done using the LightCycler 480 II (Roche Diagnostics, Switzerland) with the LightCycler 480 II Software (version 1.5.1) as previously described in section 2.2.5.

4.2.6 Real-Time PCR Analysis

The RT-PCR data with the Accell siRNA transfected cultures was analysed using the same method described in Chapter 2, section 2.2.6, where the copy numbers were scaled relative to the untreated culture expression. GraphPad Prism 6 (GraphPad Software, La Jolla California USA; version 6.00) was used to perform one-way ANOVA with Tukey's multiple comparisons statistical tests and to generate the graphs, which are plotted with S.E.M error bars.

4.3 Results

4.3.1 *Lentivirus Transfection*

Initially transfection with the lentiviruses resulted in extensive cell death (Figure 4.3). Optimisation of a number of steps in the transfection process improved the health of the culture. The incubation time of the cells with the lentivirus was reduced from 72 hours to 48 hours, which greatly improved the health of the cells without changing the transfection efficiency. Adding the lentiviruses earlier in the culturing process, at 7-8 DIV compared to 9-10 DIV, and allowing an extra 24 hours before experimentation also enhanced the health of the culture and enhanced transfection. However, even with the optimised conditions the transfection of the control scrambled shRNA lentivirus was very low, on average transfecting $22.1 \pm 6.4\%$ of the cells in the cultures (Figure 4.4). The *Gira1* shRNA lentiviruses had a higher transfection rate and were counted in an average of $53.2 \pm 5.2\%$ of the DH culture cells (Figure 4.5), while the *Gira2* lentiviruses were taken up by $50.2 \pm 5.8\%$ of the total number of cells (Figure 4.6). Finally the *Gira3* lentiviruses were counted in an average of $68.6 \pm 4.1\%$ of the DH cells (Figure 4.7).

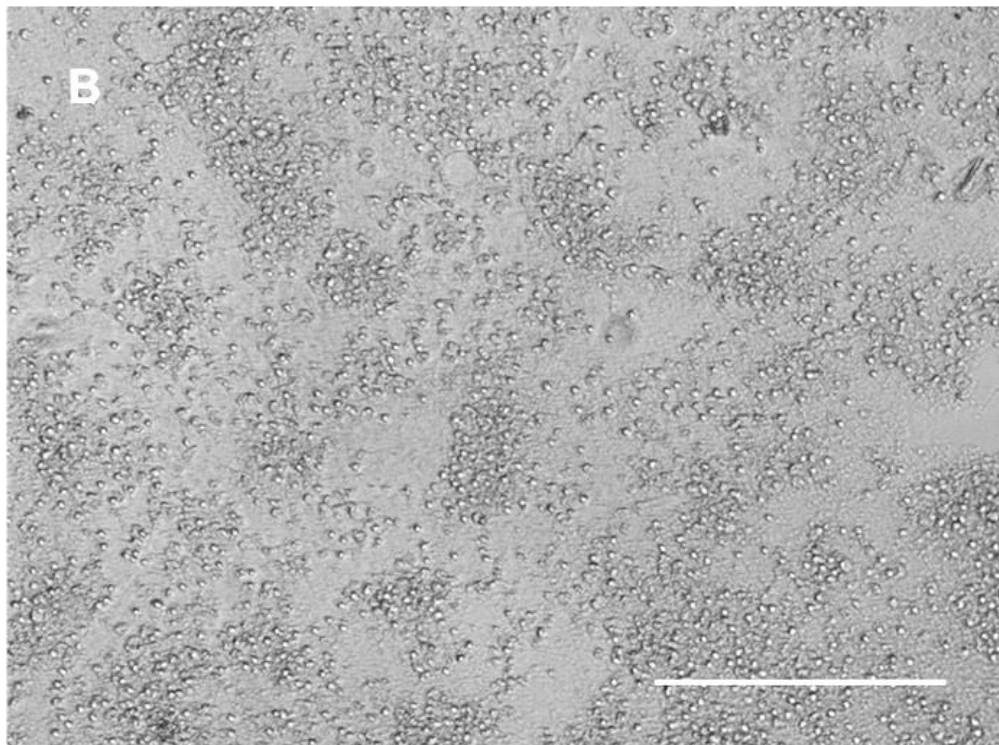
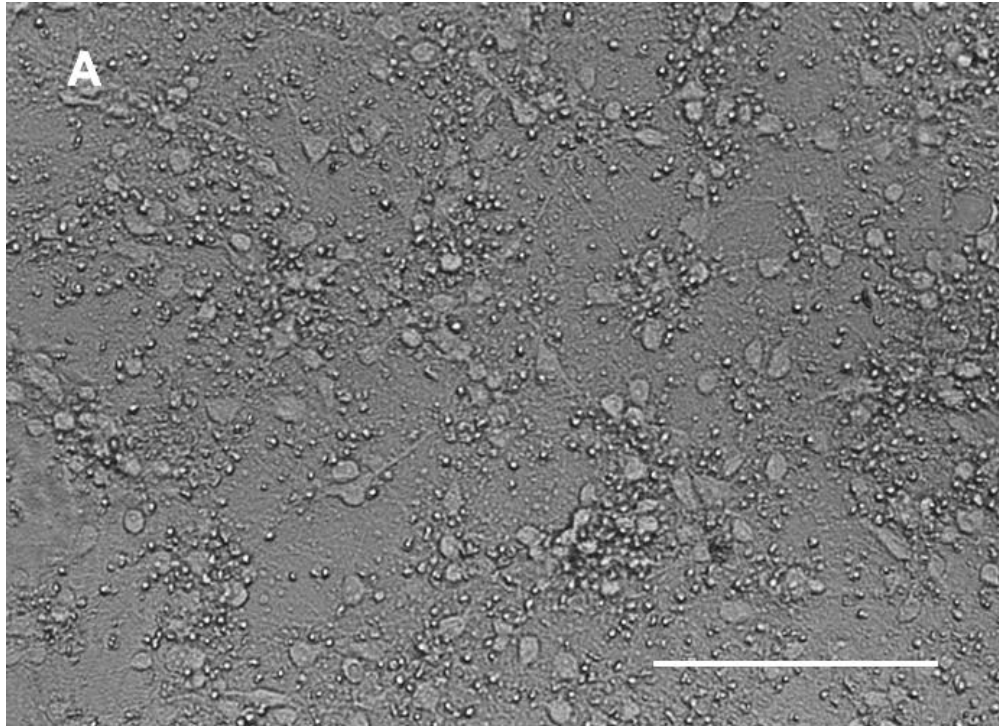


Figure 4.3 Images taken of a DH culture at 13 DIV. (A) An image of an untreated DH culture at 13 DIV which has not been transfected with lentivirus, illustrating the network of neuronal DH cells. (B) A DH culture from the same cohort of cells as shown in (A) also at 13 DIV which was transfected with the control lentivirus of scrambled shRNA. The lentivirus was added to the culture at 10 DIV and incubated for 72 hours, which has resulted in cell death and the loss of the network. Scale bars are 200 μm .

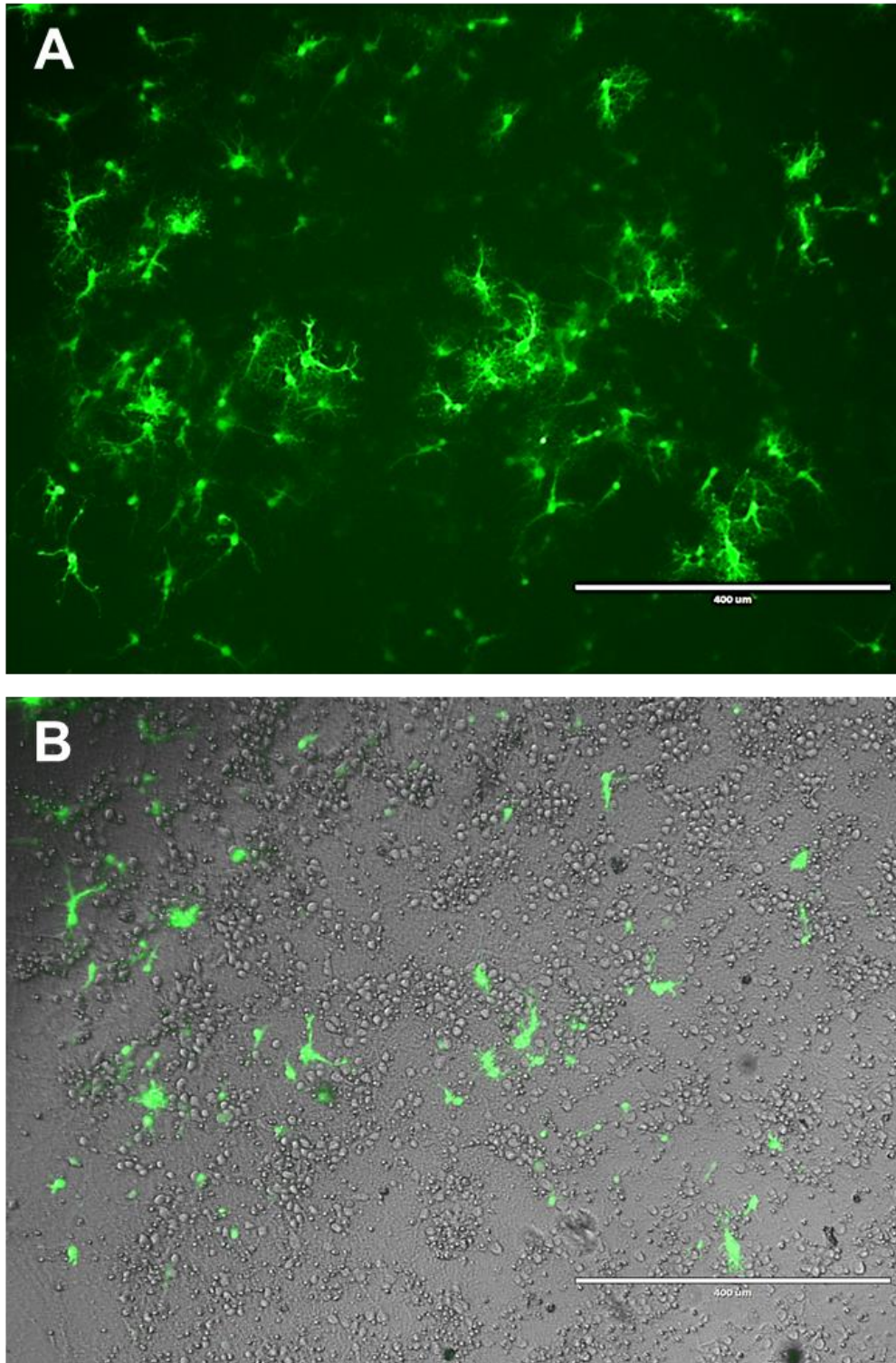


Figure 4.4 Images of a DH culture transfected with the control lentivirus with scrambled shRNA. (A) Image of GFP- positive cells showing successful transfection with scrambled lentivirus. (B) An overlay image of the same culture showing both transmitted light image and the GFP fluorescence image combined. This overlay image shows that the transfection efficiency of this control lentivirus is low, on average this control lentivirus only transfected 22.1% of the cells in the culture. Scale bars are 400 μm .

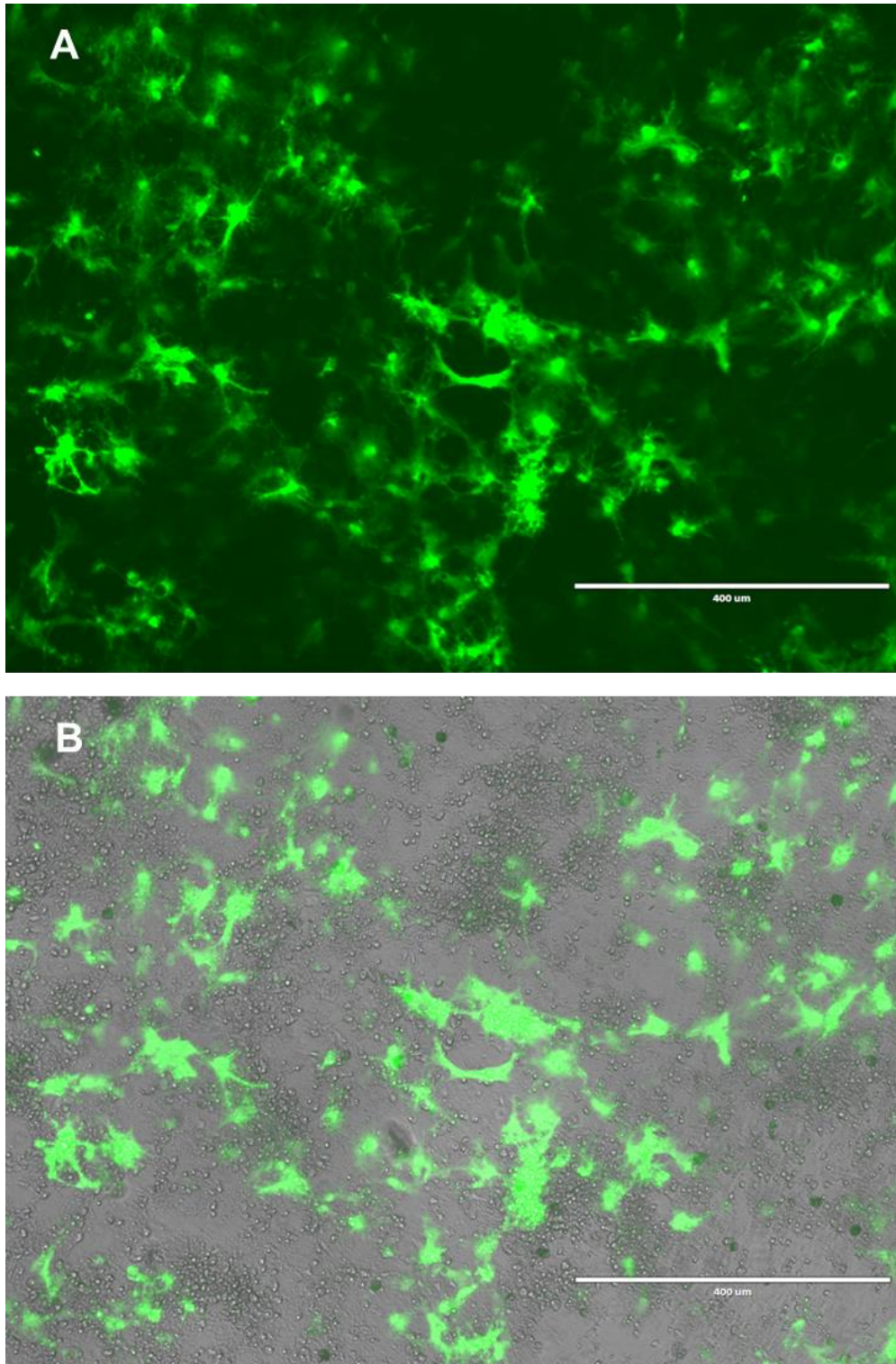


Figure 4.5 Images of a DH culture transfected with the lentivirus with *Gira1* shRNA. (A) The DH culture imaged under GFP fluorescence, where those cells containing the virus are visible. (B) An overlay image of the same culture showing both transmitted light image and the GFP fluorescence image combined. On average 53.2% of the cells in the culture were transfected with the *Gira1* lentiviruses. Scale bars are 400 μm .

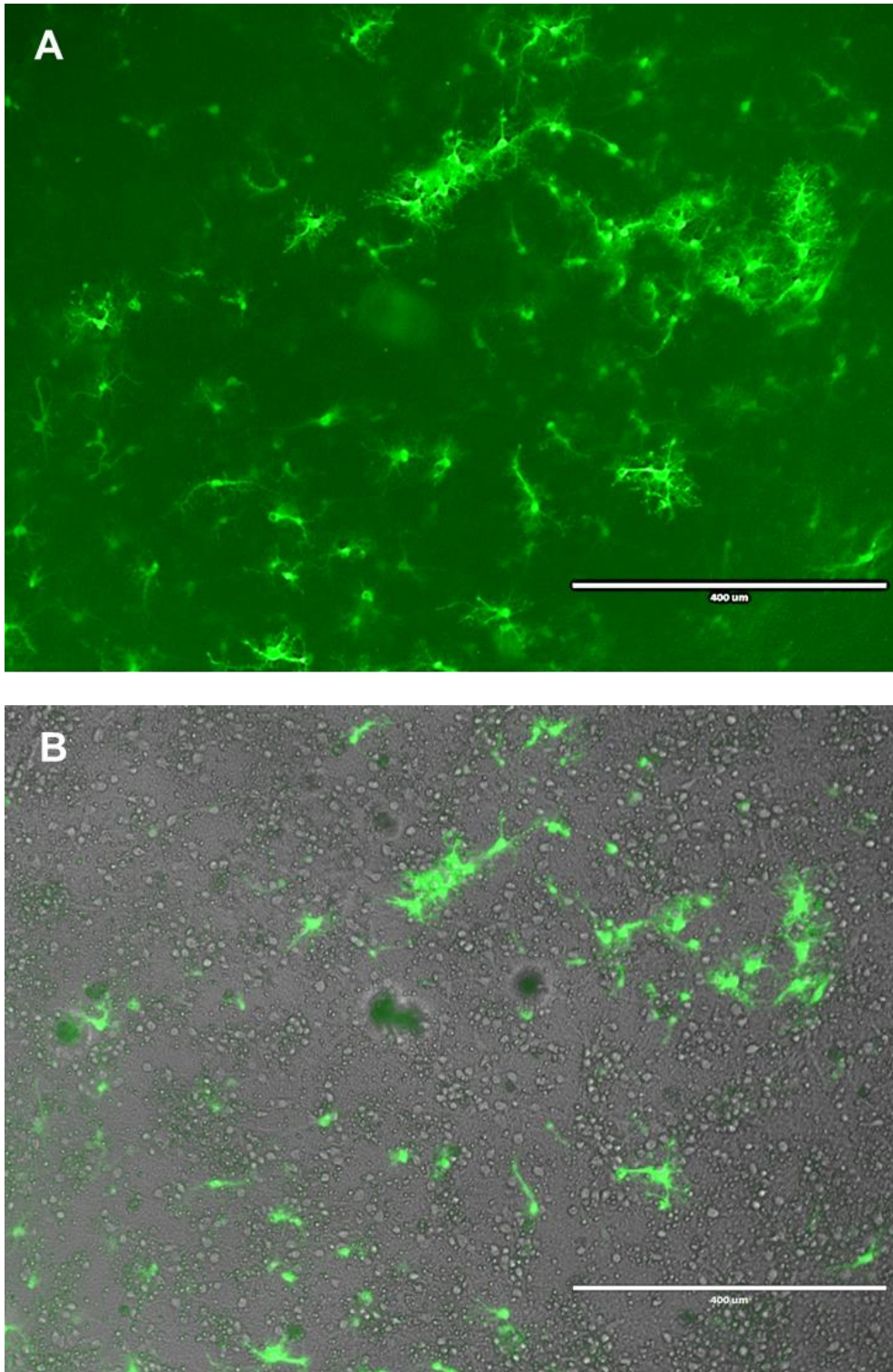


Figure 4.6 Images of a DH culture transfected with the lentivirus with *Gira2* shRNA. (A) The DH culture imaged under GFP fluorescence to determine if this lentivirus can transfected any of the cells in the culture. (B) An overlay of the GFP fluorescence image and a transmitted light image of the same region of the culture to determine the proportion of cells transfected by this virus. The *Gira2* lentiviruses transfected 50.2% cells on average. Scale bars are 400 μm .

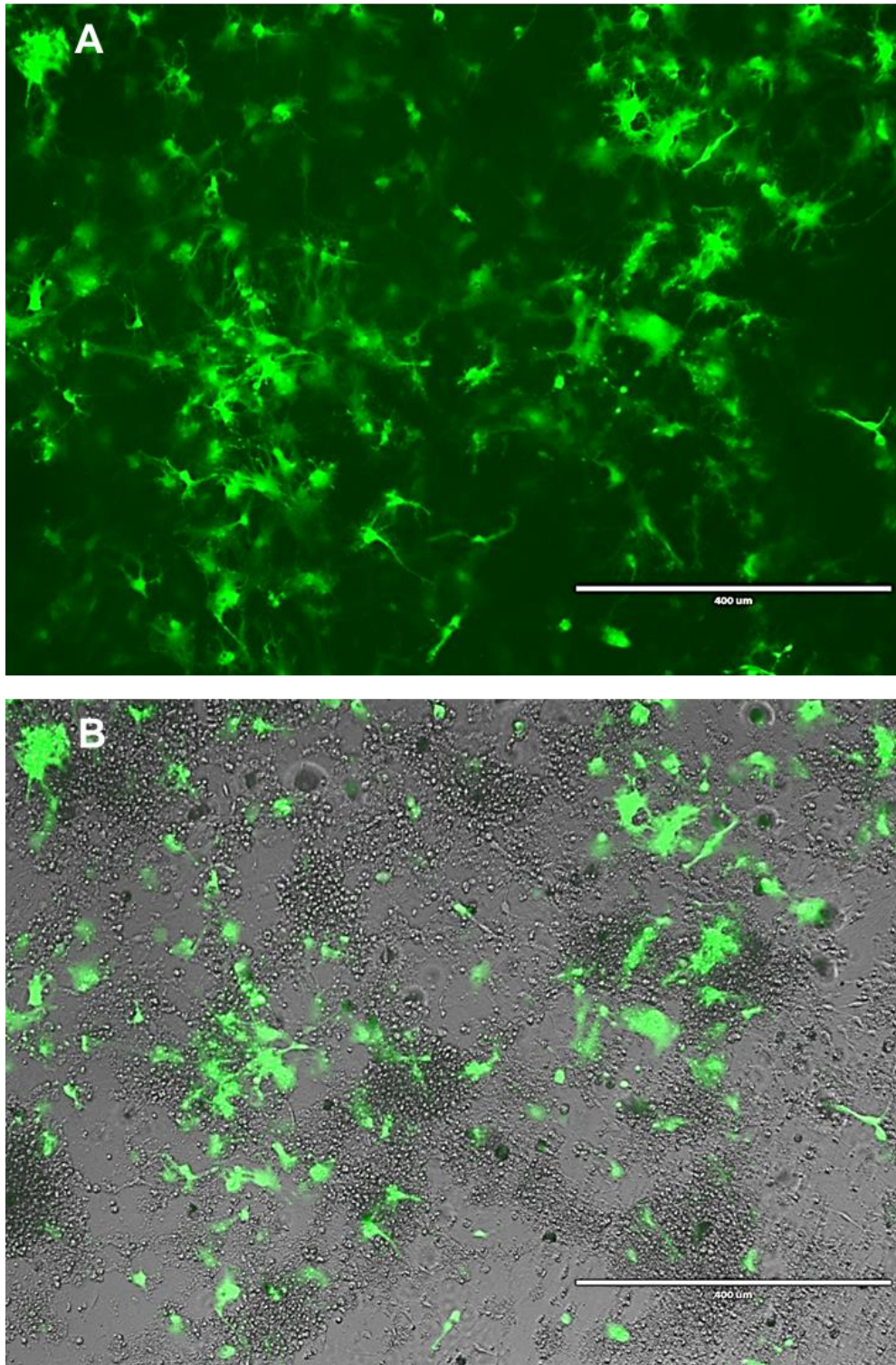


Figure 4.7 Images of a DH culture transfected with the *Glra3* lentivirus shRNA. (A) The DH culture imaged under GFP fluorescence to determine if this lentivirus can transfect any of the cells in the culture. (B) An overlay of the GFP fluorescence image and a transmitted light image of the same region of the culture to determine the proportion of cells transfected by this virus. The *Glra3* lentiviruses had the highest transfection efficiency of all the lentiviruses, transfecting 68.6% of cells. Scale bars are 400 μm .

4.3.2 Activity of the Dorsal Horn Cultures Transfected with Lentivirus

Despite the relatively low transfection efficiency of these lentiviruses in the DH culture, the effect on the spontaneous activity was dramatic when compared to untreated DH cultures which were from the same DH preparation. Comparing the baseline spontaneous activity of the DH cultures, all those cultures treated with lentivirus significantly reduced the area under the curve and the frequency of spontaneous spikes ($P < 0.0001$) (Figure 4.8). However, the effect of the scrambled control lentivirus was the same, implying that the changes in the baseline activity in the cultures transfected with the lentiviruses was not exclusively or at all the result of gene silencing of the glycine receptor α subunits.

The baseline activity of the untreated DH culture had a mean area under the curve of $2.281 \times 10^6 \pm 121761$ RFU.s, and a mean spike frequency of 0.074 ± 0.007 Hz. On average, strychnine (10 μ M) doubled the area under the curve to $4.543 \times 10^6 \pm 181524$ RFU.s compared to baseline ($P < 0.0001$). The subsequent addition of glycine almost halved the area under the curve compared to that with strychnine, to an average of $2.925 \times 10^6 \pm 539550$ RFU.s, similar to the baseline level ($P < 0.05$) (Figure 4.9B). Likewise the spike frequency was increased with the addition of strychnine to 0.107 ± 0.004 Hz ($P < 0.05$) compared to baseline, and the following addition of glycine reduced the spike frequency to 0.072 ± 0.010 Hz ($P < 0.05$) compared to in the presence of strychnine. The spike frequency in the presence of glycine is comparable to the baseline frequency (Figure 4.9C). The scramble control lentivirus had a mean baseline area under the curve of 682418 ± 78049 RFU.s. Strychnine addition increased this to $1.522 \times 10^6 \pm 212066$ RFU.s ($P < 0.001$), which was decreased to 803461 ± 331830 RFU.s by glycine ($P < 0.05$). The spike frequency of the DH cultures transfected with the scrambled control lentivirus was not affected by the application of strychnine. The baseline spike frequency was 0.003 ± 0.0008 Hz, in the presence of strychnine the frequency was 0.004 ± 0.001

Hz ($P>0.05$). However, glycine significantly decreased the spike frequency to 0.0009 ± 0.0003 Hz ($P<0.0001$) (Figure 4.10).

The DH cells transfected with the *Gira1* lentiviruses had a baseline area under the curve mean value of 664150 ± 76315 RFU.s. Neither the addition of strychnine or glycine had any effect on the area under the curve ($P>0.05$). However, the spike frequency of the *Gira1* lentivirus transfected cultures was increased with strychnine and decreased with the addition of glycine. The baseline spike frequency was 0.0043 ± 0.0014 Hz, in the presence of strychnine the frequency was increased to 0.0071 ± 0.0017 Hz ($P<0.001$) compared to baseline. Glycine then decreased the frequency to 0.0051 ± 0.0018 Hz ($P<0.05$) compared to in the presence of strychnine (Figure 4.11).

The *Gira2* lentivirus transfected DH cultures were also not influenced by strychnine or glycine application, with no effect to either the area under the curve or the spike frequency ($P>0.05$) (Figure 4.12). The baseline area under the curve was 749541 ± 116496 RFU.s, with strychnine added the area was 944714 ± 138984 RFU.s and in the presence of glycine the mean area under the curve was 778313 ± 173143 RFU.s. The spike frequencies were 0.11 ± 0.002 , 0.014 ± 0.003 and 0.011 ± 0.002 Hz for baseline, with strychnine and with glycine respectively. The activity of the *Gira3* lentivirus transfected DH cells was increased with the addition of strychnine, however the addition of glycine had no effect. The baseline area under the curve was 816633 ± 68419 RFU.s, which increased to $1.78 \times 10^6 \pm 165957$ RFU.s following strychnine addition. In the presence of glycine the mean area under the curve was $1.68 \times 10^6 \pm 233882$. The same pattern was observed in the spike frequency data, the baseline spike frequency was 0.0081 ± 0.0013 Hz, which increased to 0.017 ± 0.0021 Hz with strychnine ($P<0.0001$). However, again glycine had no significant effect, as the spike frequency remained similar with a mean of 0.014 ± 0.002 Hz

(Figure 4.13). A summary of the lentivirus area data is shown in Table 4.1 and the spike frequency data in Table 4.2.

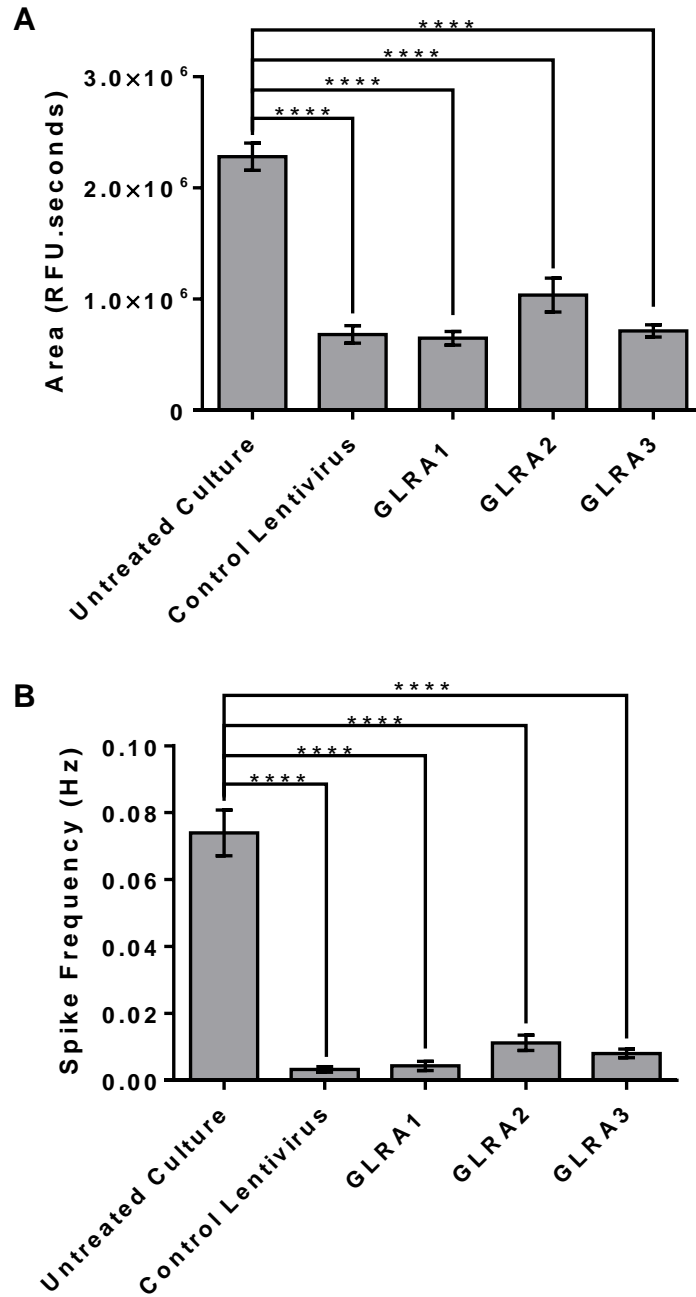


Figure 4.8 Comparison of the baseline activity of the cultures transfected with each of the lentiviruses to the untreated DH culture. The activity was measured using calcium fluorometry with the Flexstation microplate reader. (A) The area under the curve of relative fluorescence against time for the baseline section of the recordings from the DH cultures transfected with each of the lentiviruses. (B) The spike frequency during the baseline section of the recordings for each of the same cultures. The number of wells with the spinal DH culture utilised to generate these graphs for each group are as follows: untreated culture n=7, control lentivirus n=40, Glra1 n=68, Glra2 n=25 and Glra3 n=91.

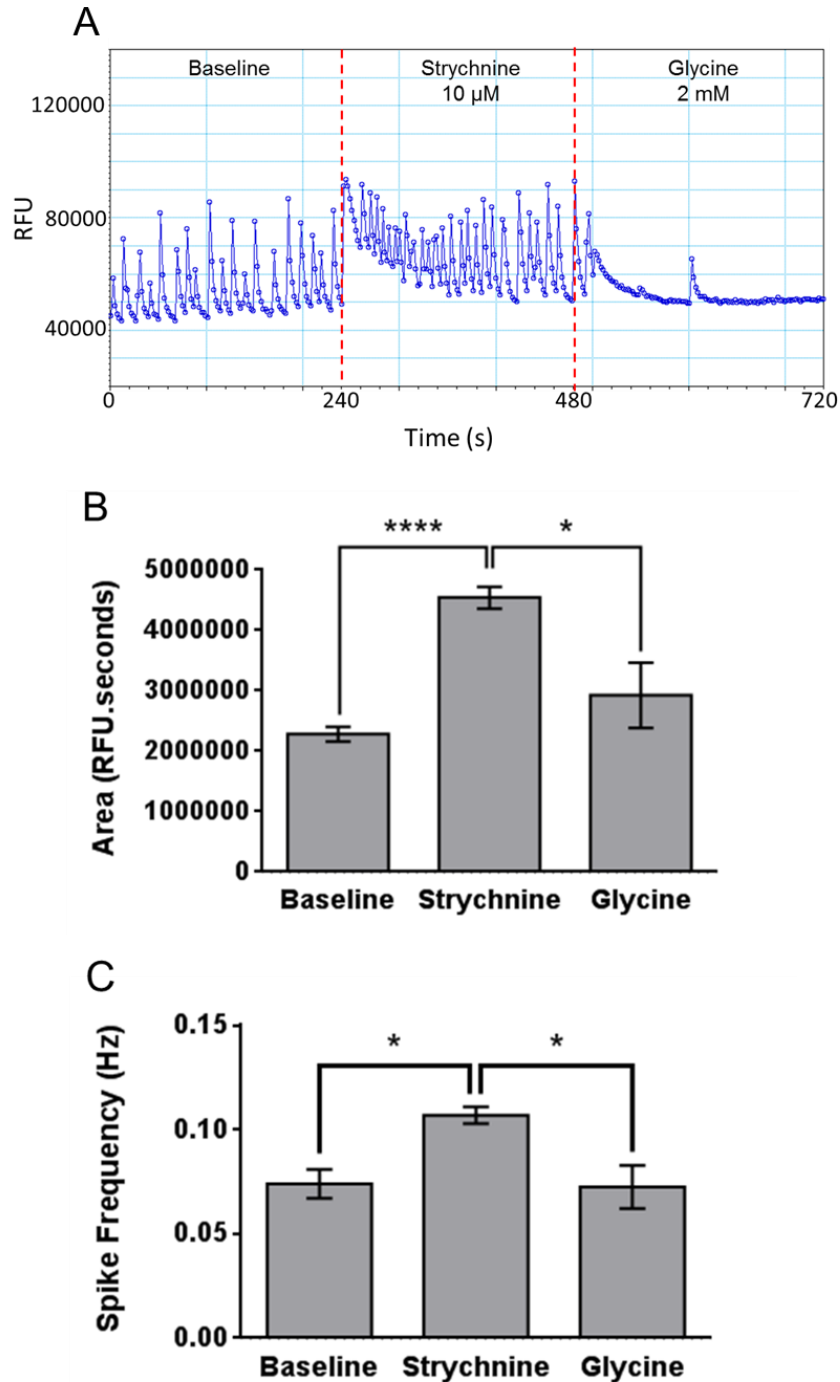


Figure 4.9 The activity of the DH culture not transfected with lentivirus, analysing both the area under the curve and the spike frequency of the baseline activity, the activity in presence of strychnine and glycine. (A) An example recording from an untreated DH culture, illustrating the normal baseline activity and responses to strychnine and glycine. The vertical red dashed lines separate the different sections of the recording. (B) The average area under the curve for the baseline 4 minutes of the recordings, the 4 minutes with strychnine (10 μ M) present and the 4 minutes with glycine (2 mM) present. (C) The spike frequencies for each of these same sections of the recordings with the standard non-transfected DH cultured cells (N=3, n=7).

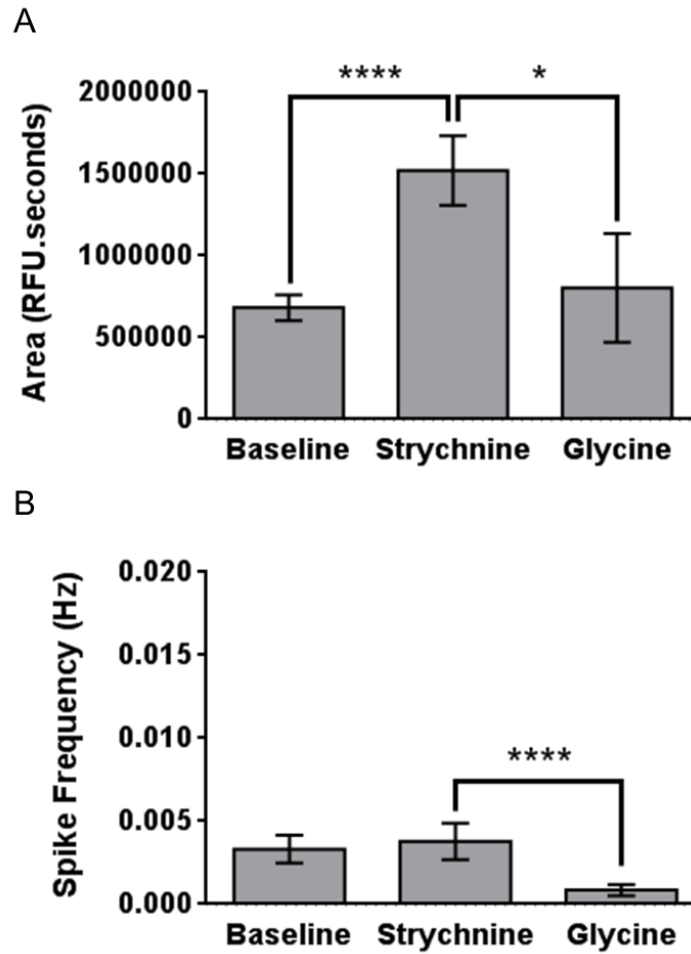


Figure 4.10 The activity of the DH cultures transfected with the control scrambled lentivirus at baseline and in the presence of strychnine (10 μ M) and glycine (2 mM). Two parameters of the activity analysed were the area under the curve of the RFU against time recordings for each section of the recordings shown in (A), and the spike frequency for each of those sections (B) (N=6, n=40).

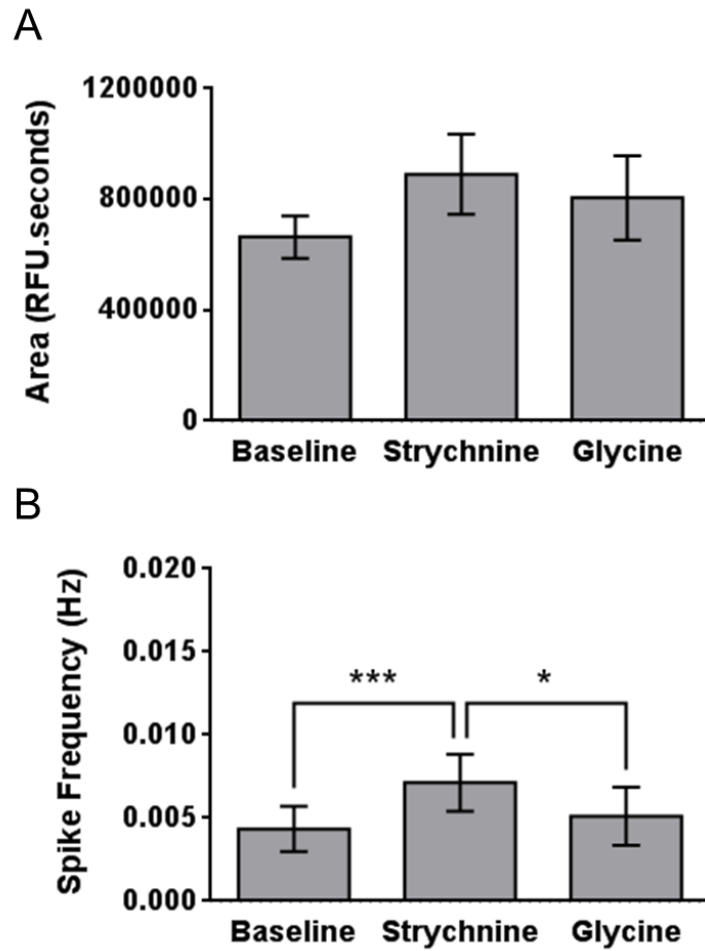


Figure 4.11 The activity of the DH cultures transfected with the *Gira1* lentivirus, and their responses to strychnine (10 μ M) and glycine (2 mM). (A) The area under the curve for each section of the recordings, the baseline, with strychnine and with glycine. (B) The spike frequencies for each of the same sections of the recordings as in (A) (N=9, n=53).

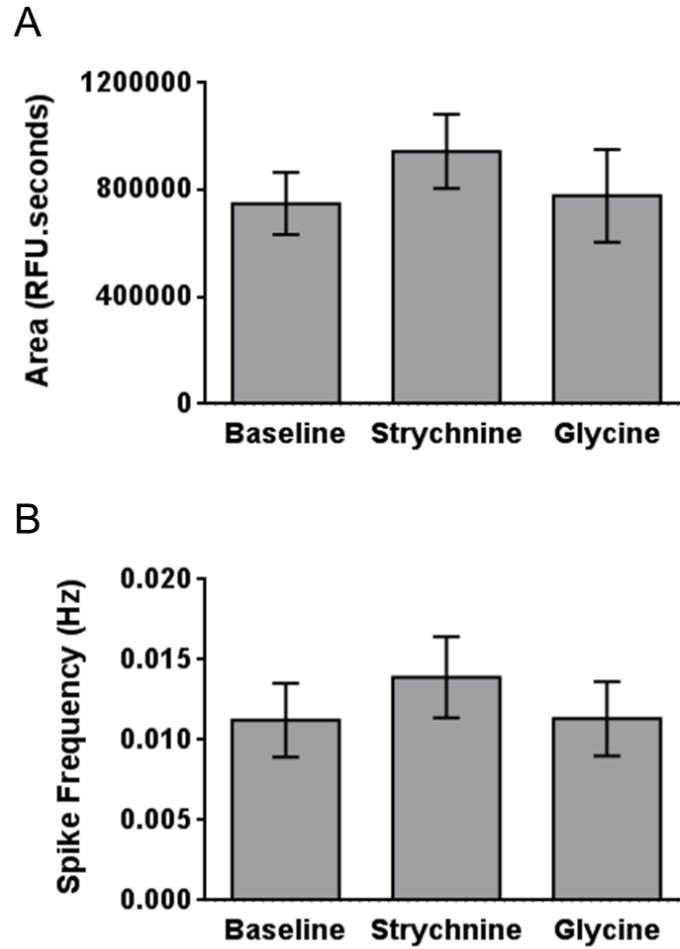


Figure 4.12 The activity of *Glra2* lentivirus transfected DH cultures and their responses to strychnine (10 μ M) and glycine (2 mM). (A) The area under the curve for the three sections of the recordings: baseline, with strychnine and with glycine. (B) The spike frequencies for each of the same three sections of these recordings. No significant difference was detected with the addition of strychnine or glycine in these *Glra2* lentivirus transfected cells (N=8, n=38)

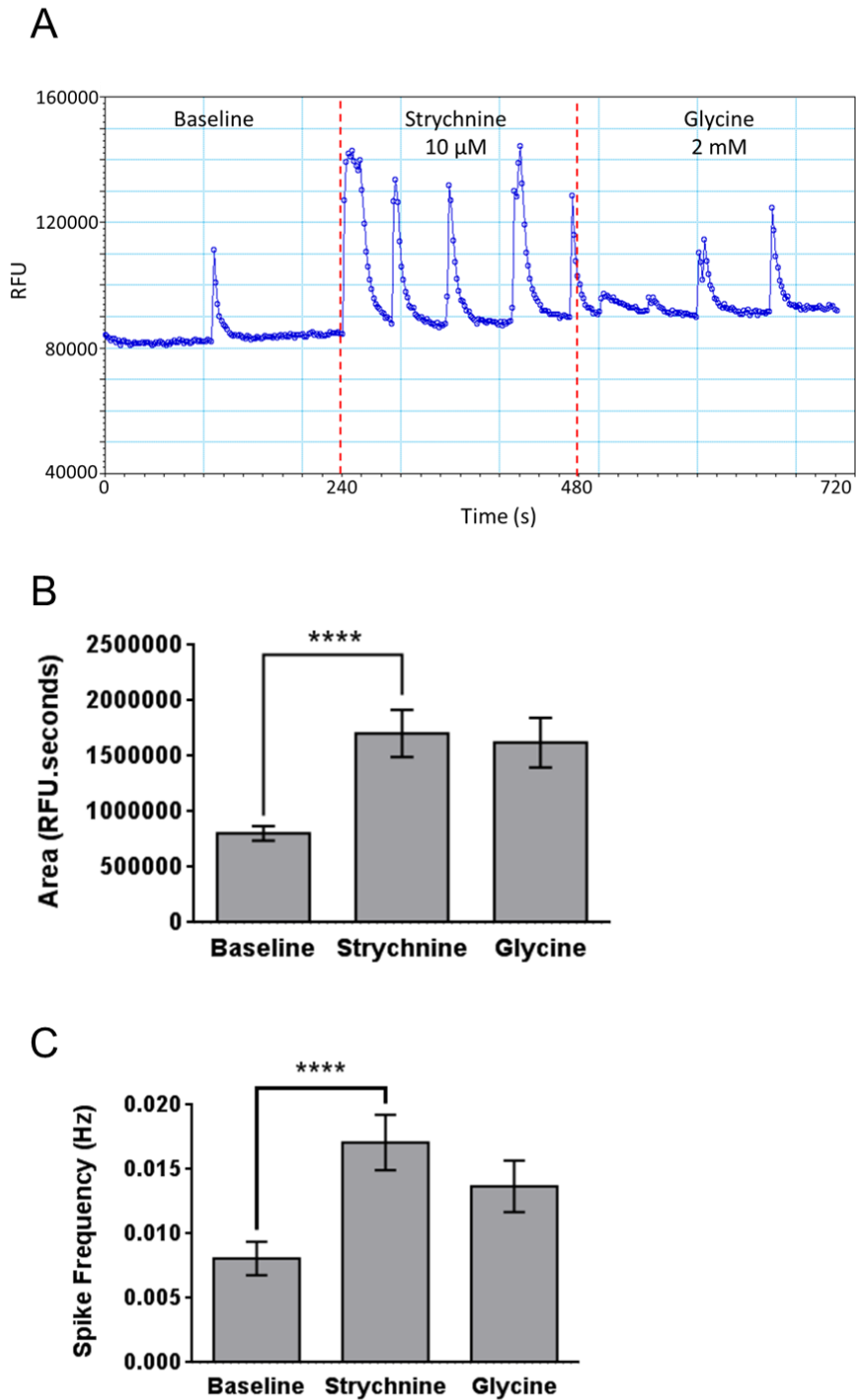


Figure 4.13 The activity of *Gla3* lentivirus transfected DH cultures and their responses to addition of strychnine (10 μ M) and glycine (2 mM). (A) An example trace of the relative fluorescence units against time, illustrating the baseline activity and effects of the addition of strychnine and glycine. The vertical red lines separate the sections of the recordings based on the addition of the compounds. (B) The mean area under the curve for each four minute section as indicated in (A). (C) The spike frequency of the cultures for each of the three sections. (N=12, n=74)

Lentivirus	Strychnine	Glycine
Untreated	↑	↓
Control Lentivirus	↑	↓
<i>Gla1</i>	n.s.	n.s.
<i>Gla2</i>	n.s.	n.s.
<i>Gla3</i>	↑	n.s.

Table 4.1 A summary of the effects on the area under the curve following application of strychnine (10 μ M) and glycine (2 mM) on each of the DH cultures transfected with lentivirus and the untreated DH culture. n.s. indicates no significant effect, \uparrow indicates a significant increase and \downarrow indicates a significant decrease.

Lentivirus	Strychnine	Glycine
Untreated	↑	↓
Control Lentivirus	n.s.	↓
<i>Gla1</i>	↑	↓
<i>Gla2</i>	n.s.	n.s.
<i>Gla3</i>	↑	n.s.

Table 4.2 A summary of the effects on the spike frequency with the addition of strychnine (10 μ M) and glycine (2 mM) on each of the DH cultures transfected with lentivirus and the untreated DH culture. n.s. indicates no significant effect, \uparrow indicates a significant increase and \downarrow indicates a significant decrease.

4.3.3 Accell siRNA Transfection

As the control lentivirus also produced an effect on the DH cell culture an alternative gene silencing technique was investigated. Accell siRNA does not require a virus for delivery of the siRNA molecules into cells. Therefore glycine receptor α subunit Accell siRNAs were employed in this study to determine if silencing of these genes can affect the DH culture activity. Two negative control siRNAs and two positive control siRNAs were utilized to validate if any changes in the activity profile of the DH cultures transfected with the siRNAs are the result of the knockdown of the glycine receptor α subunits. The imaging of RFP Accell siRNA transfected DH cultures show that the transfection efficiency was much higher than the lentiviruses, with on average $97 \pm 4.8\%$ of the cells infected with the siRNA (Figure 4.14).

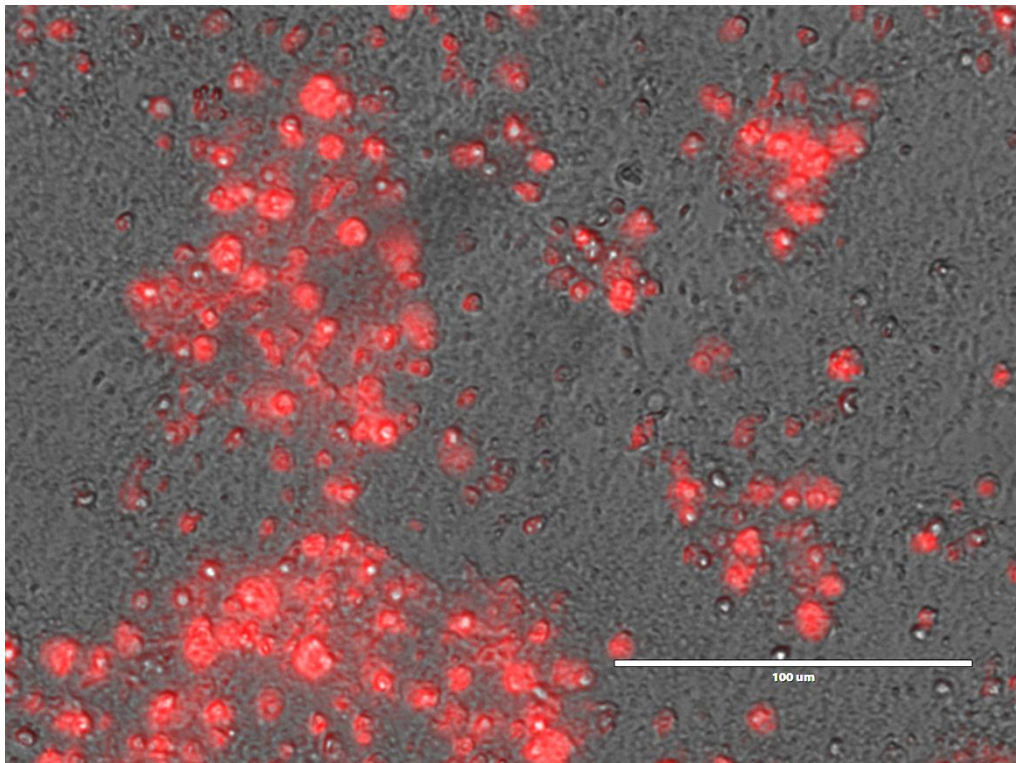


Figure 4.14 The primary DH culture transfected with the control Accell siRNA with encoded RFP at 12 DIV. This is an overlay of two images, one taken with RFP fluorescence and another with transmitted light using an AMG EVOS digital microscope. This image shows the Accell siRNA was taken up by almost 100% of the cells in the DH culture. Scale bar is 100 μm .

4.3.3.1 Real Time-PCR of Dorsal Horn Cultures Transfected with Accell siRNA

TaqMan quantitative RT-PCR was used to determine the extent of the silencing of the glycine receptor α subunits by their Accell siRNAs in the DH cultures. The mRNA expression of each of the glycine receptor α subunits was determined in each of the cDNA samples from the cultures transfected with each of the Accell siRNAs encoding the three subunits, and also for the untreated culture with no siRNA transfection. Firstly, analysing the *Glr1* TaqMan assay in each of the samples revealed that the DH cultures transfected with the *Glr1* Accell siRNA had a reduced expression of *Glr1* compared to the untreated DH culture and compared to the cultures transfected with the Accell siRNAs encoding the other glycine receptor α subunits ($P < 0.05$) (Figure 4.15). Similarly investigating the expression of *Glr2* gene in each of the samples it was found that the DH cultures transfected with the *Glr2* Accell siRNA also had reduced expression of this mRNA compared to the other DH cultures ($P < 0.05$) (Figure 4.16). The levels of expression of the *Glr3* mRNA were significantly reduced in each of the transfected cultures compared to the untreated culture ($P < 0.001$) (Figure 4.17).

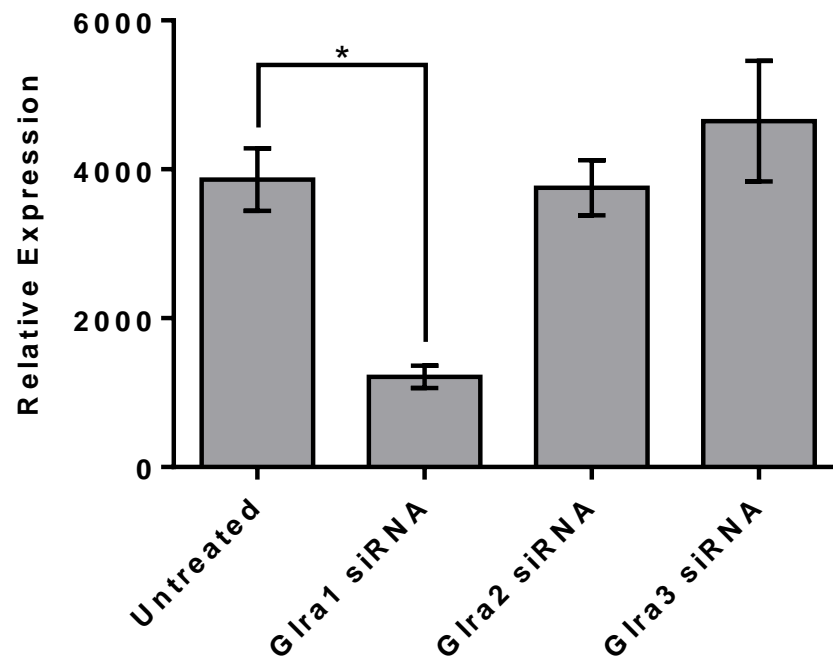


Figure 4.15 The expression of *Glra1* mRNA in each of the four DH cultures relative to the untreated DH culture (n=3). The expression of the *Glra1* mRNA was significantly less in the *Glra1* siRNA transfected DH culture compared to the untreated DH culture. The other two cultures transfected with *Glra2* and *Glra3* siRNA displayed equivalent expression of the *Glra1* mRNA to the untreated DH culture.

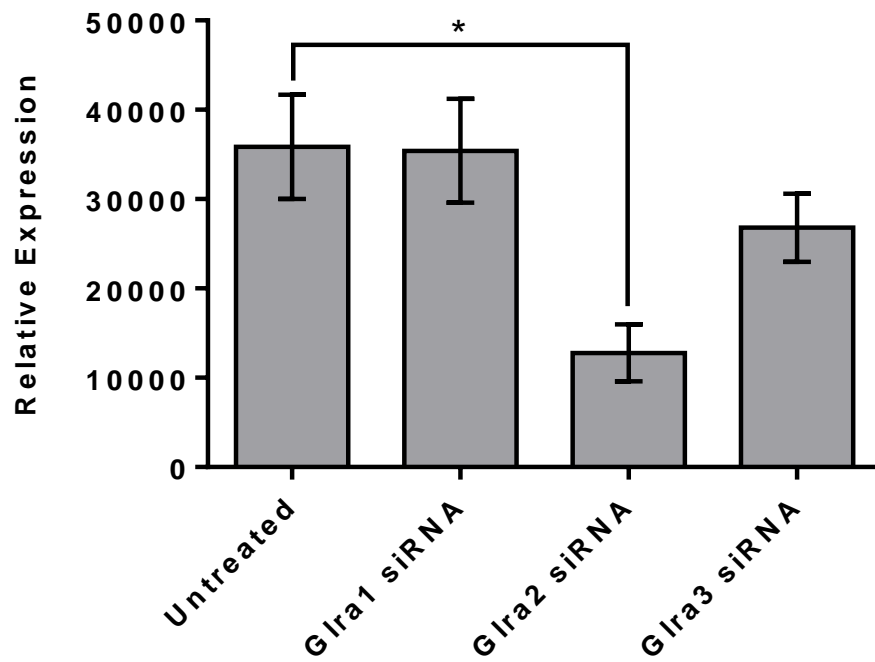


Figure 4.16 The relative expression of *Glra2* mRNA in each of the four different DH cultures relative to the untreated DH culture (n=3). The *Glra2* mRNA expression was significantly reduced in the DH culture transfected with the *Glra2* Accell siRNA compared to the untreated DH culture. The *Glra1* and *Glra3* siRNA transfected cultures had equivalent expression of *Glra2* mRNA as the untreated DH culture.

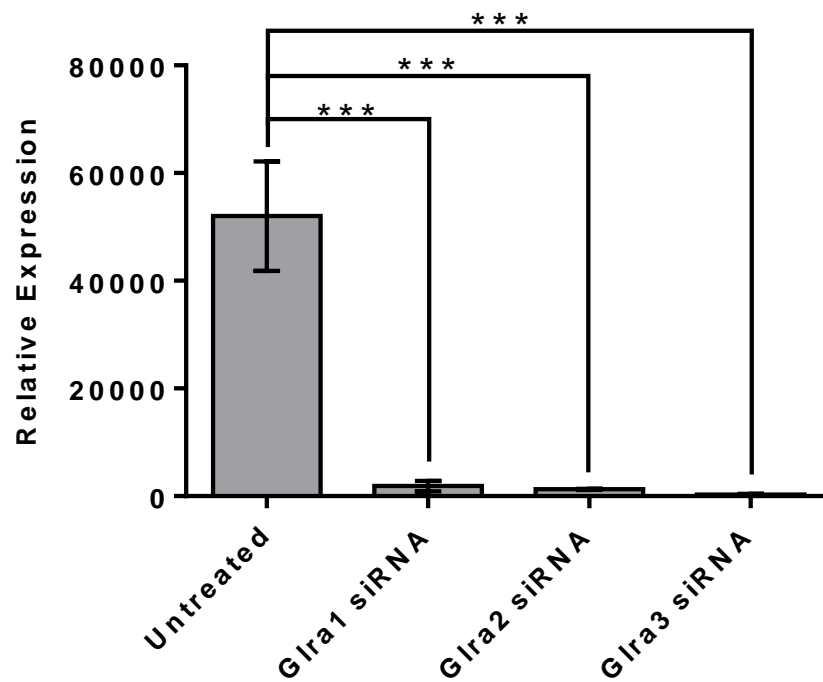


Figure 4.17 The relative expression of the *Glra3* mRNA in each of the DH cultures relative to the untreated DH culture (n=3). The *Glra3* mRNA expression was significantly reduced in all three of the DH cultures transfected with the Accell siRNAs encoding each of the glycine receptor α subunits compared to the untreated culture.

4.3.4 Activity of the Dorsal Horn Cultures Transfected with Accell siRNA

The baseline activity of the DH cultures transfected with the Accell siRNAs was analysed in terms of the area under the curve of the RFU against time graph of the calcium imaging recordings and the spike frequency. Comparing the area under the curve of the baseline data for the siRNA transfected cultures with that of the cultures without siRNA transfection the activity was significantly reduced by all the Accell siRNAs (Figure 4.18A). The baseline spike frequency of the cultures with the Accell siRNAs were also significantly reduced, except the two negative controls (Figure 4.18B).

As done previously with the lentivirus transfected cultures, the activity of the cultures transfected with the Accell siRNAs were also recorded following the addition of strychnine and glycine. The cultures not transfected with Accell siRNAs, displayed the characteristic spontaneous firing at the 12-14 DIV, the area under the curve increased from the baseline level of $1.46 \times 10^6 \pm 245151$ RFU.s to $4.18 \times 10^6 \pm 417376$ RFU.s in the presence of strychnine (10 μ M) ($P < 0.0001$). The subsequent addition of glycine (2 mM) significantly reduced the activity to $2.92 \times 10^6 \pm 247494$ RFU.s ($P < 0.001$) compared to that in the presence of strychnine (Figure 4.19). The same effect was observed with the spike frequency of these cultures. The baseline spike frequency was 0.018 ± 0.0029 Hz, which significantly increased to 0.050 ± 0.0054 Hz with addition of strychnine. The spike frequency then significantly decreased with application of glycine to 0.040 ± 0.0057 Hz ($P < 0.001$) compared to the frequency in the presence of strychnine (Figure 4.19).

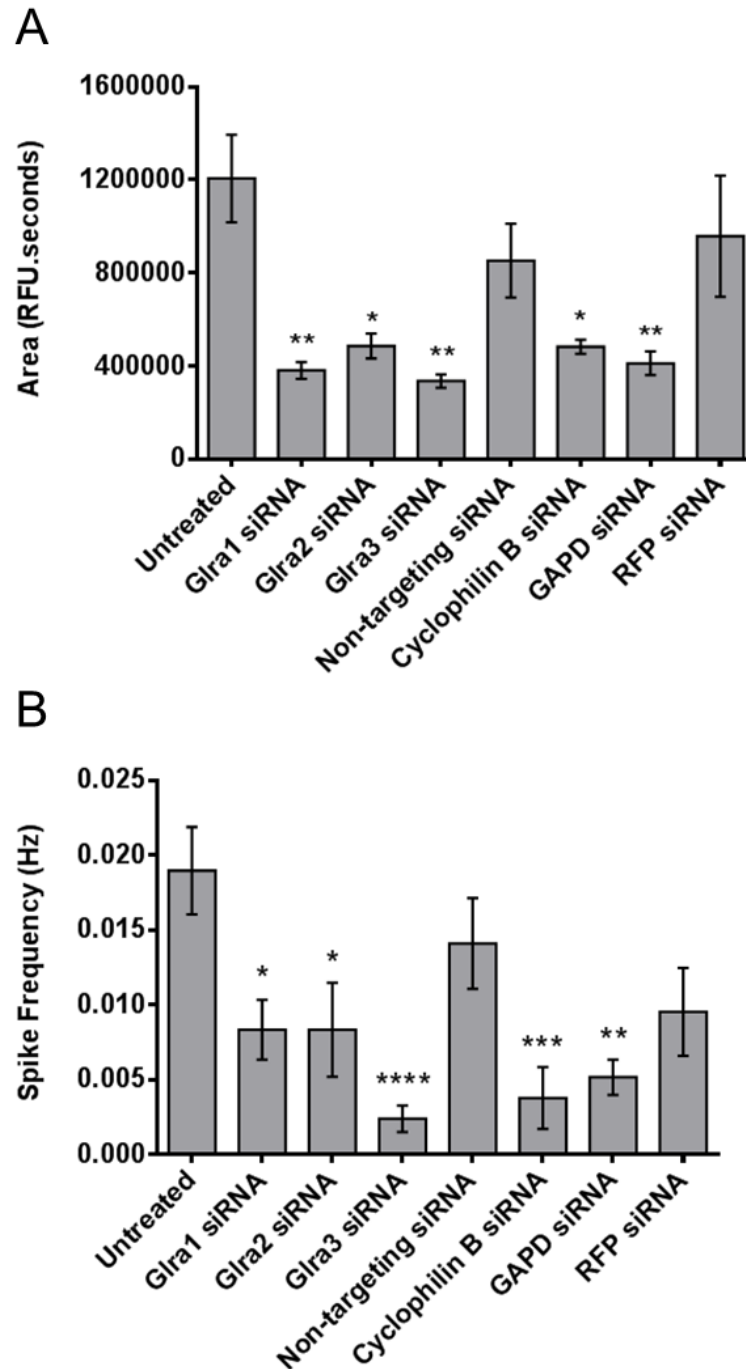


Figure 4.18 The baseline activity of the DH cultures transfected with the Accell siRNAs, each compared to the baseline activity of the untreated cultures (N=6, n=18). The negative controls are the non-targeting siRNA and RFP siRNA. The positive controls are cyclophilin B and GAPD siRNAs. (A) The baseline activity determined by measuring the area under the curve of the baseline section of the calcium imaging recordings. (B) The mean baseline spike frequency for each of the DH cultures determined from the same calcium imaging recordings as for (A). Asterisks show statistical significance when compared to untreated.

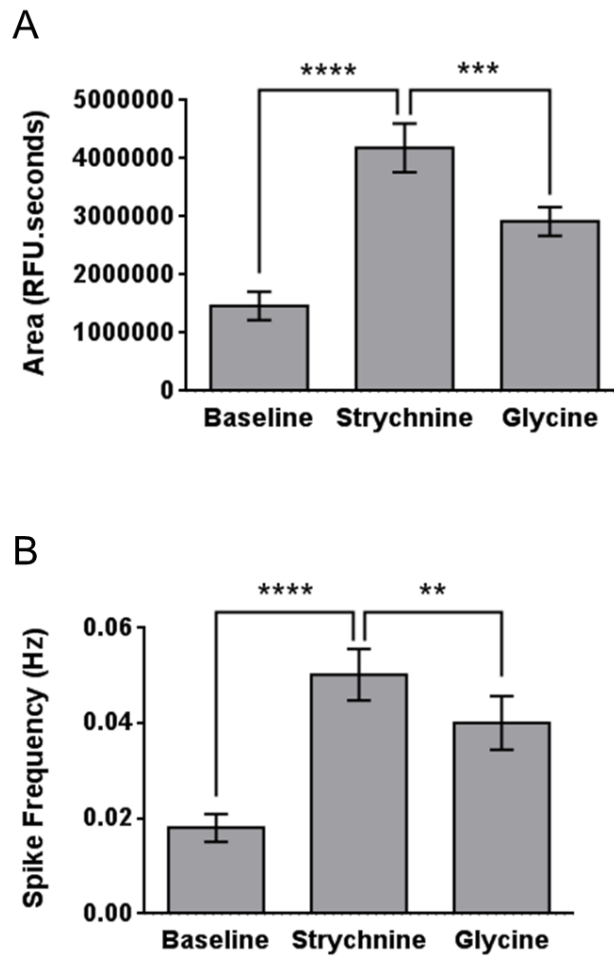


Figure 4.19 The activity of the DH cultures without siRNA to illustrate the normal activity of the cultures and their responses to the addition of strychnine (10 μ M) and glycine (2 mM). These cultures were on the same plates as those transfected with the Accell siRNAs, from the same DH cell dissections (N=5, n=21). (A) The activity of the cultures as measured from the area under the curve for each of the three sections of the recordings: baseline, strychnine (10 μ M) and glycine (2 mM). The compounds could not be washed out therefore glycine was applied following strychnine addition and therefore is also in the presence of strychnine. (B) The baseline spike frequency of these cultures, and the spike frequency in the presence of strychnine then glycine for the same cultures as in (A).

4.3.4.1 Negative Control Accell siRNAs

The non-targeting negative control Accell siRNA transfected DH cultures had the same responses to strychnine and glycine as the non-transfected cultures (Figure 4.20). The baseline mean area under the curve increased with application of strychnine, from 852624 ± 158693 RFU.s to $2.22 \times 10^6 \pm 306007$ RFU.s ($P < 0.0001$). Glycine subsequently decreased this to $1.58 \times 10^6 \pm 195324$ RFU.s ($P < 0.05$). The mean spike frequency of the baseline activity was 0.014 ± 0.003 Hz which was increased to 0.024 ± 0.004 Hz by strychnine ($P < 0.05$) and then decreased by application of glycine to 0.017 ± 0.004 Hz ($P < 0.05$). The responses of the DH cultures transfected with the other negative control Accell siRNA with the added RFP tag were the same as the first negative control siRNA (Figure 4.21). The area under the curve increased from the baseline of 423987 ± 40751 RFU.s to $1.22 \times 10^6 \pm 113747$ RFU.s with strychnine added to the culture ($P < 0.0001$). Glycine decreased this activity to 980754 ± 155046 RFU.s ($P < 0.05$). The spike frequency of the baseline data from these DH cultures was 0.012 ± 0.0029 Hz, strychnine increased this to 0.027 ± 0.0073 Hz ($P < 0.05$) and glycine decreased it to 0.013 ± 0.0045 Hz ($P < 0.05$).

4.3.4.2 Positive Control Accell siRNAs

The cultures transfected with the two positive control Accell siRNAs both responded to the addition of strychnine which increased the area under the curve from 483189 ± 30070 RFU.s to $1.21 \times 10^6 \pm 137240$ RFU.s in the cyclophilin siRNA transfected cells ($P < 0.001$). Glycine did not significantly decrease the area under the curve ($P > 0.05$) (Figure 4.22). The GAPD positive control siRNA had a baseline area under the curve of 394732 ± 42636 RFU.s which increased to $1.08 \times 10^6 \pm 150909$ RFU.s following the addition of strychnine ($P < 0.0001$). The application of glycine had no

significant effect on the area under the curve which was $1.06 \times 10^6 \pm 195143$ RFU.s in presence of glycine ($P > 0.05$) (Figure 4.23).

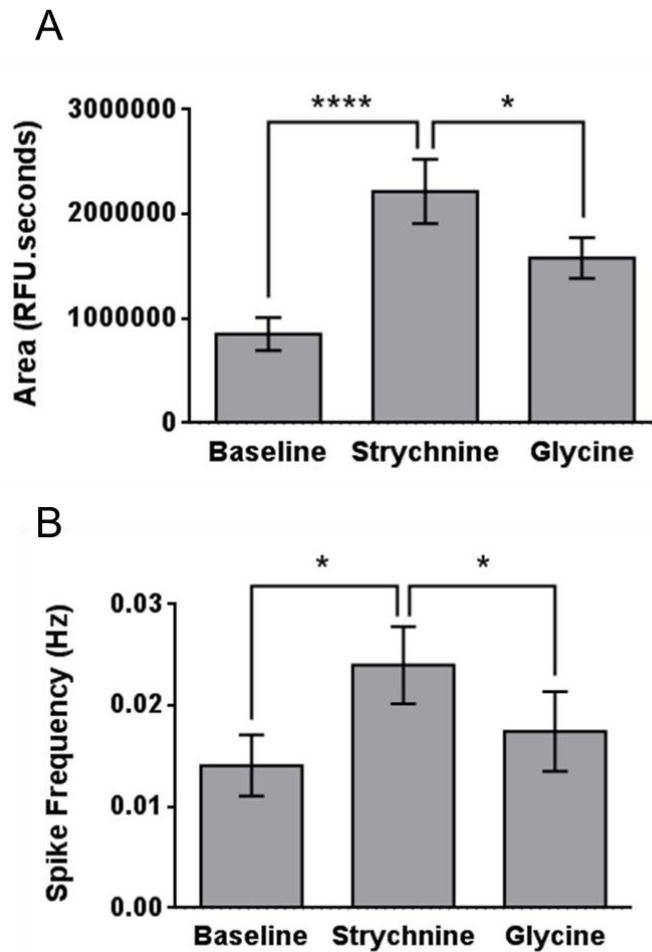


Figure 4.20 The activity of the DH cultures transfected with the non-targeting negative control siRNA, and their responses to the application of strychnine (10 μ M) and glycine (2 mM) (N=7, n=21). (A) The area under the curve of the recording during the baseline section, with strychnine and with glycine. (B) The spike frequency of the cultured DH cells for the same recordings as analysed for (A) during each of the sections of the recordings.

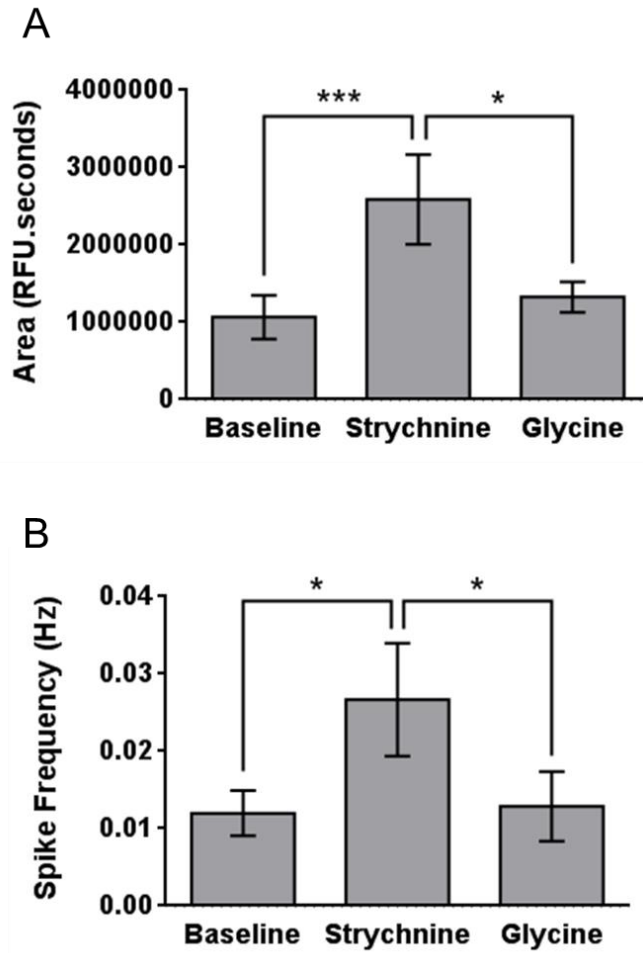


Figure 4.21 The activity of the DH cultures transfected with the non-targeting negative control Accell siRNA with an RFP tag, and their responses to the application of strychnine (10 μ M) and glycine (2 mM) (N=7, n=21). (A) The area under the curve of the calcium imaging recordings for the baseline section, with strychnine and with glycine. (B) The spike frequency for each of the same sections of the recordings.

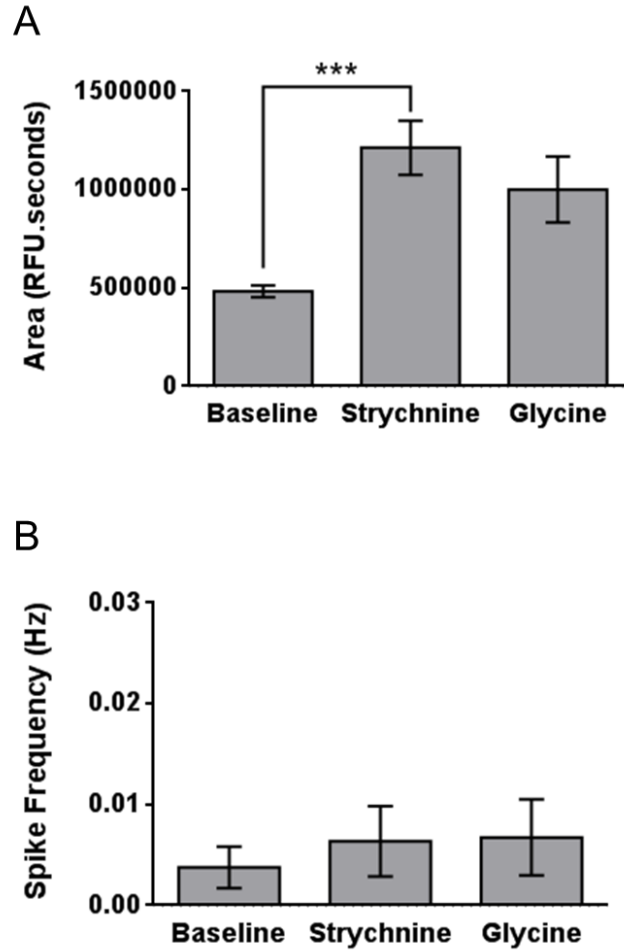


Figure 4.22 The activity of the cultured DH cells transfected with the positive control Accell siRNA encoding cyclophilin B, and their responses to the application of strychnine (10 μ M) and glycine (2 mM) (N=7, n=21). (A) The area under the curve of the baseline sections of the recordings from these cultures and the area under the curves following addition of strychnine and glycine. (B) The spike frequency during each of the same sections of the recordings with these DH cultures.

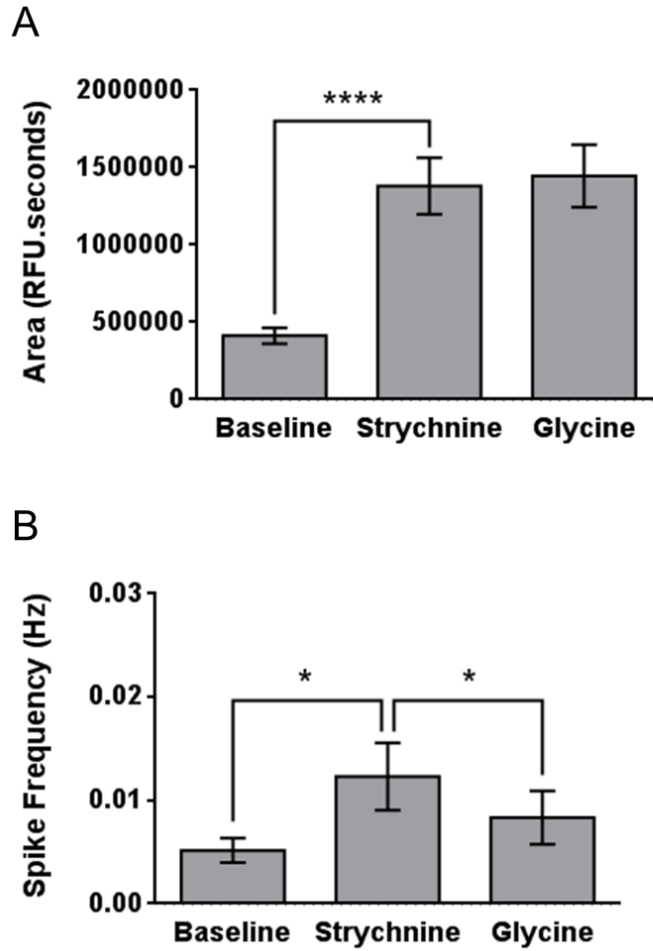


Figure 4.23 The activity of the cultured DH cells transfected with the positive control Accell siRNA encoding GAPD, and their responses to the application of strychnine (10 μ M) and glycine (2 mM) (N=8, n=24). (A) The area under the curve of the baseline sections of the recordings from these cultures and the area under the curves following addition of strychnine and glycine. (B) The spike frequency during each of the same sections of the recording as shown in (A).

4.3.4.3 Accell siRNA Knockdown of the Glycine Receptor A Subunits

The DH cultures transfected with the *Glr1* Accell siRNA responded normally to the addition of strychnine and glycine (Figure 4.24). The baseline area under the curve of these cultures was 381082 ± 35980 RFU.s, which increased to $1.51 \times 10^6 \pm 245161$ RFU.s following the addition of strychnine ($P < 0.01$). Glycine significantly decreased this to $1.16 \times 10^6 \pm 144549$ RFU.s ($P < 0.05$). The spike frequency of these same cultures had a baseline frequency of 0.008 ± 0.002 Hz, which in the presence of strychnine increased to 0.017 ± 0.004 Hz ($P < 0.01$). Following glycine addition the spike frequency decreased to 0.001 ± 0.003 Hz ($P < 0.05$).

The transfection of the DH cultures with the *Glr2* Accell siRNA did affect the response of these cultures to glycine (Figure 4.25). The mean baseline area of these DH cultures was 485864 ± 53852 RFU.s, which did significantly increase with the addition of strychnine to $1.04 \times 10^6 \pm 139600$ RFU.s ($P < 0.001$). Glycine did not decrease this activity, the area under the curve following the addition of glycine was $1.22 \times 10^6 \pm 205798$ RFU.s ($P > 0.05$). The baseline spike frequency of the DH cultures transfected with the *Glr2* Accell siRNA was 0.008 ± 0.003 Hz, which increased to 0.015 ± 0.006 Hz following the addition of strychnine. Glycine did significantly decrease the spike frequency to 0.012 ± 0.005 Hz ($P < 0.05$).

In the *Glr3* Accell siRNA transfected cultures the addition of glycine had no effect on the area or the spike frequency of the cultures (Figure 4.26). The baseline area was 202582 ± 29431 RFU.s, which was increased by addition of strychnine to 996683 ± 81664 RFU.s ($P < 0.0001$). The addition of glycine did not significantly change the area which was $1.10 \times 10^6 \pm 155150$ RFU.s ($P > 0.05$). The baseline spike frequency was 0.002 ± 0.001 Hz. In the presence of strychnine the frequency was increased to 0.008 ± 0.002 Hz ($P < 0.05$). In the presence of glycine the spike frequency was 0.007 ± 0.002 Hz, which is not significantly different to the frequency with strychnine present ($P > 0.05$).

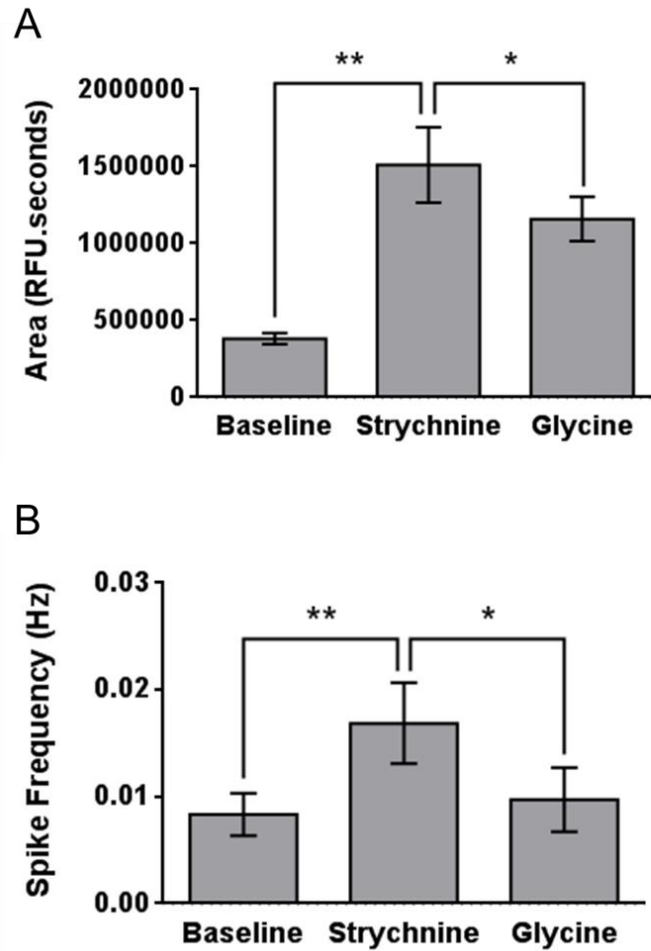


Figure 4.24 The activity of the DH cultures transfected with the Accell siRNA encoding the *Glra1* gene for the knockdown of the glycine receptor α 1 subunit (N=7, n=21). The effects of the addition of strychnine (10 μ M) and glycine (2 mM) to these DH cultures is also illustrated. (A) The area under the curve of the recordings with these cultures for the baseline section, the section with the addition of strychnine and the section with glycine added. (B) The spike frequency of these DH cultures for each of the same sections described for (A).

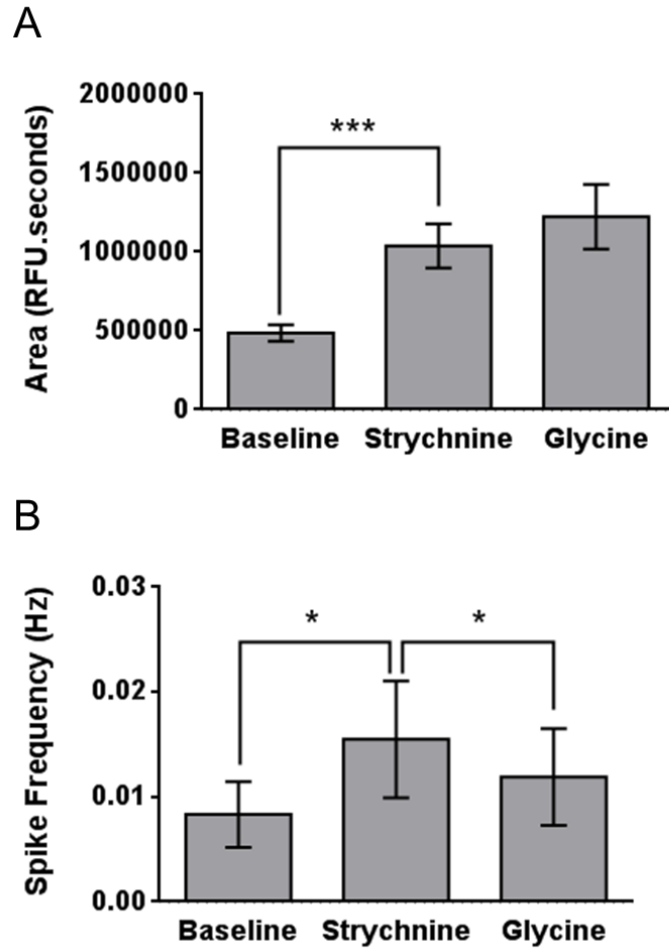


Figure 4.25 The activity of the DH cultures transfected with the Accell siRNA encoding the *Glra2* gene for the knockdown of the glycine receptor $\alpha 2$ subunit (N=7, n=21). The effects of the addition of strychnine (10 μ M) and glycine (2 mM) to these DH cultures is also illustrated. (A) The area under the curve of the recordings with these cultures for the baseline section, the section with the addition of strychnine and the section with glycine added. (B) The spike frequency of these DH cultures for each of the same sections described for (A).

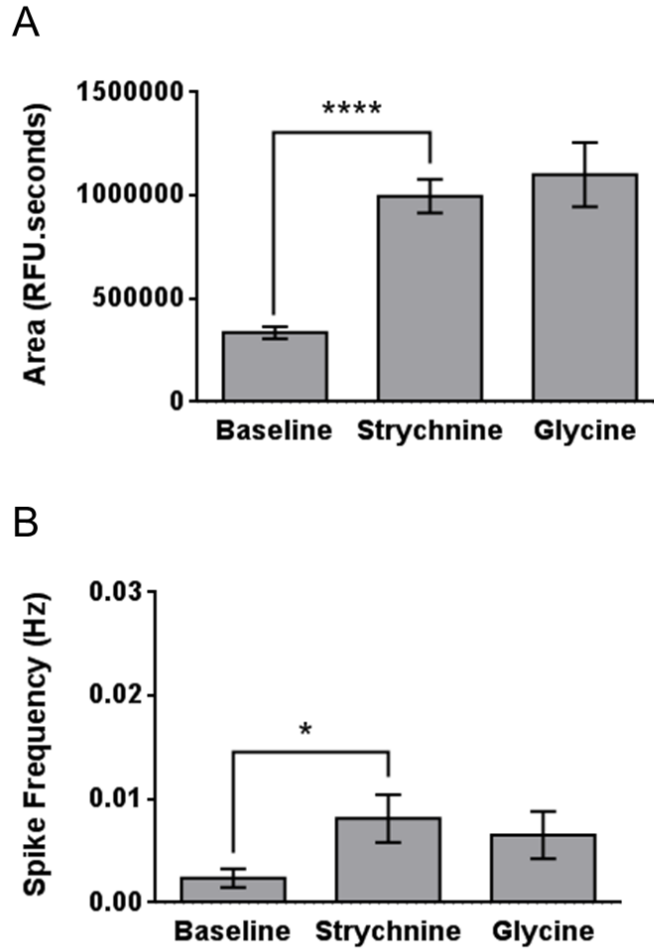


Figure 4.26 The activity of the DH cultures transfected with the Accell siRNA encoding the *Glra3* gene for the knockdown of the glycine receptor $\alpha 3$ subunit (N=7, n=21). The effects of the addition of strychnine (10 μ M) and glycine (2 mM) to these DH cultures is also illustrated. (A) The area under the curve of the recordings with these cultures for the baseline section, the section with the addition of strychnine and the section with glycine added. (B) The spike frequency of these DH cultures for each of the same sections described for (A).

DH Culture	Baseline	Strychnine (10 μ M)	Glycine (2 mM)
Untreated		↑	↓
Non-targeting siRNA	n.s.	↑	↓
Cyclophilin B siRNA	↓	↑	n.s.
GAPD siRNA	↓	↑	n.s.
RFP siRNA	n.s.	↑	↓
Gla1 siRNA	↓	↑	↓
Gla2 siRNA	↓	↑	n.s.
Gla3 siRNA	↓	↑	n.s.

Table 4.3 A summary of the area under the curve data illustrating the effects of each of the Accell siRNAs on the DH culture baseline activity compared to the untreated DH culture and the responses of the cultures to strychnine and glycine. The n.s. indicates no significant difference, ↑ indicates an increase in activity and ↓ indicates a decrease in activity. The symbols in black are where the comparison was made to the untreated culture. The blue symbols are comparing the effect of strychnine on the baseline activity of the culture. The symbols in red are comparing the effect of glycine on the strychnine activity.

DH Culture	Baseline	Strychnine (10 μ M)	Glycine (2 mM)
Untreated		↑	↓
Non-targeting siRNA	n.s.	↑	↓
Cyclophilin B siRNA	↓	n.s.	n.s.
GAPD siRNA	↓	↑	↓
RFP siRNA	n.s.	↑	↓
Gla1 siRNA	↓	↑	↓
Gla2 siRNA	↓	↑	↓
Gla3 siRNA	↓	↑	n.s.

Table 4.4 A summary of the spike frequency data illustrating the effects of each of the Accell siRNAs on the DH culture activity and its responses to strychnine and glycine compared to the untreated DH culture. The n.s. indicates no significant difference, ↑ indicates an increase in activity and ↓ indicates a decrease in activity. The symbols in black are where the comparison was made to the untreated culture. The blue symbols are comparing the effect of strychnine on the baseline activity of the culture. The symbols in red are comparing the effect of glycine to the strychnine activity of that culture.

4.4 Discussion

The experiments of this study set out to determine how glycine receptor α subunit gene silencing affects primary spinal DH cell culture calcium activity. Consequently, the role of the glycine receptor in controlling the spinal DH network activity can be assessed, and it can be determined whether any of the glycine receptor subtypes are more or less influential. Thus, the results of this chapter can help to focus the development of novel analgesics to a selective glycine receptor subtype, which would likely aid in reducing adverse side-effects of the drug. It is not possible to assess the extent of individual glycine receptor subtypes pharmacologically as compounds which selectively target each subtype are lacking. This is not necessary for GABA_A receptors, as there are numerous compounds which selectively target GABA_A receptor subtypes.

Lentivirus transfection of the DH culture produced a significant loss of the DH culture characteristic spontaneous firing at 12-14 DIV. However, the control lentivirus produced similar effects in the DH culture calcium activity, suggesting an effect of the virus itself. Lentiviruses are toxic at high titres for some neuronal cell types (Yee et al., 1994, Chen et al., 1996). All the DH cultures transfected with lentivirus did display noticeable cell death in this study, even following optimisation. Therefore, it is likely that the lentiviruses utilized in this study were toxic to the cultured DH cells. Furthermore, the lentivirus transfection efficiency varied from 22 to 68%, which implies insufficient gene silencing and consequently definitive conclusions cannot be made from the calcium imaging data with these cultures. For these reasons an alternative technology for glycine receptor α subunit gene silencing was subsequently assayed.

Accell siRNA had improved transfection efficiency within the primary DH cell culture that reached almost 100%. The siRNA transduction did not have the complications

of toxicity that occurred with lentivirus transduction of the DH cultures, therefore there was a low incidence of cell death following the Accell siRNA transduction. Performing the RT-PCR with the transfected cultures demonstrated significant decreases in gene expression of each of the glycine receptor α subunits compared to the untreated DH cultures for each of the siRNAs. However, the *Glr1* and *Glr2* siRNAs also caused a significant knockdown in the expression of *Glr3*. Therefore, the effects observed in the cultures transfected by *Glr1* can be considered to include silencing of both *Glr1* and *Glr3*. Similarly the effects recorded in the *Glr2* siRNA transfected cultures can be considered to be the effect of *Glr2* and *Glr3* silencing. Furthermore, from the RT-PCR results there was no compensatory increase in the expression of the other α subunits when any one of the Accell siRNAs was transfected. This implies that in the Accell siRNA transfected cultures there were fewer glycine receptors compared to the untreated culture.

4.4.1 *Glycine Receptor α Subunit Gene Silencing Reduces Dorsal Horn Network Activity*

All three of the Accell siRNAs encoding for the three glycine receptor α subunits significantly decreased the baseline spontaneous activity compared to the untreated DH cultures. However, since the RT-PCR results show that only the *Glr3* Accell siRNA selectively silences the expression of this subunit, with the other two siRNAs silencing the *Glr3* gene as well as their own target gene, the reduction in the baseline activity in all the cultures could primarily be the result of a loss of the glycine receptor $\alpha 3$ subunit. This is consistent with a previous *in vivo* study that used siRNA to silence *Glr1* and *Glr3* showing that silencing only *Glr3* prevented the analgesic action of gelsemine (Zhang et al., 2013). Furthermore, findings from the present study are also in agreement with previous reports of glycine $\alpha 3$

knockout mice displaying reduced behavioural manifestations of pain in response to PGE₂ injection, peripheral inflammation and acetic acid-induced visceral pain (Harvey et al., 2004, Racz et al., 2005). Thus, these published findings indicate that the α 3-containing glycine receptors have a more significant role in the processing of nociceptive signals in the superficial DH compared to the α 1- or α 2- containing glycine receptors. Interestingly, the RT-PCR data from chapter 2 illustrated a higher expression of the α 1 subunit in the DH culture, and relatively similar expressions of the α 2 and α 3 subunits. This ratio of expression of the glycine receptor α subunits is not the same as that found in the *in vivo* spinal DH, where there is a higher α 3 expression relative to the α 1 subunit expression illustrated in chapter 2 with RT-PCR with a human adult spinal cord sample and by Harvey et al. (2004) in mice. Therefore, despite the less dominant expression of the α 3 subunit in the DH culture compared to *in vivo* conditions, the silencing of its expression alone was sufficient to prevent the generation of the spontaneous activity in the culture. This is possibly because the generation of the rhythmic, synchronous activity of the DH cultured cells requires inhibitory interneurons, as discussed previously in describing the mechanisms of ING and PING (Tiesinga and Sejnowski, 2009).

Inhibiting glycine receptors with the antagonist strychnine, as reported in chapter 3, caused an increase in firing of the DH cultures, while the agonist glycine decreased activity. Strychnine similarly increased activity in the spinal DH cultures transfected with the glycine receptor α subunit siRNA. This is presumably through the action of strychnine at the glycine receptors in the DH culture which have formed from the subunits that do not include the silenced α subunit. However, the response of the DH cultures transfected with the *Glr3* siRNA displayed a lack of response to glycine addition. The *Glr2* siRNA transfected DH cultures also did not display a decrease in activity in terms of area under the curve with the addition of glycine, however the spike frequency of these cultures was significantly reduced. Since the

Gira2 siRNA also silenced the glycine receptor $\alpha 3$ subunit in the culture this loss of effect with glycine could be primarily through the loss of the $\alpha 3$ subunit, and the $\alpha 1$ subunit not being able to compensate for the silencing of the other two α subunits.

4.4.2 Conclusions

The Accell siRNA results presented in this chapter confirm previous findings that the $\alpha 3$ -containing glycine receptors are potentially more selective targets for the design and development of novel analgesics. Gelsemine has analgesic properties *in vivo* and bind selectively to $\alpha 3$ -containing glycine receptors (Zhang et al., 2013, Wu et al., 2015b, Zhang and Wang, 2015). Interestingly, in this spinal DH culture the application of gelsemine increased firing frequency, similarly to the antagonist strychnine. Many previous studies have implicated that inhibition in the spinal DH needs to be re-instated in neuropathic and inflammatory pain models following the loss of GABAergic and glycinergic inhibition (Ibuki et al., 1996, Meisner et al., 2010, Berrocal et al., 2014). However, gelsemine action implies that its mechanism of action through $\alpha 3$ -containing glycine receptors is contrary to this hypothesis. The analgesic action of gelsemine could be to prevent the rhythmic oscillations in the spinal DH by inhibiting the inhibition through $\alpha 3$ -containing glycine receptors. Consequently, development of other compounds which can modulate the spinal DH rhythmic activity could prove potentially beneficial analgesics.

5 Extracellular Single Electrode Spinal Cord Slice Recordings

5.1 Introduction

5.1.1 4-Aminopyridine-Induced Rhythmic Activity in the Central Nervous System

4-aminopyridine (4-AP) is a non-selective potassium channel blocker (Smith et al., 2009), which causes depolarisation in cells as a result of preventing the repolarisation by efflux of potassium ions following an action potential. 4-AP has been shown to increase neurotransmitter release from both inhibitory and excitatory interneurons (Perreault and Avoli, 1991). Application of 4-AP to brain slices is commonly used as a model of epilepsy. Extracellular recordings of 4-AP-induced epileptic-like activity in hippocampal slices have shown that the 4-AP-induced rhythmic activity can be modulated by GABA_A and GABA_B receptor compounds (Watts and Jefferys, 1993). 4-AP has also been used as a model of pain in spinal cord slices, where 4-AP-induced activity in the spinal DH is akin to that observed in pain states, including neuropathic pain (Ruscheweyh and Sandkuhler, 2003, Asghar et al., 2005, Chapman et al., 2009). Sandkuhler and Eblen-Zajjur (1994) detected rhythmic activity with a frequency of 0.5-13 Hz in their *in vivo* spinal DH recordings. In *in vitro* recordings from the spinal DH the frequency of the 4-AP-induced rhythmic activity detected was similar to the *in vivo* rhythm, between 4 and 12 Hz (Chapman et al., 2009, Visockis and King, 2013). Ruscheweyh and Sandkuhler (2003) also investigated the effects of anticonvulsants on the 4-AP activity in the spinal DH and revealed that the anticonvulsants also caused an attenuation of the 4-AP-induced hyperactivity. This concurs with the anti-nociceptive actions of these anticonvulsants *in vivo* (Swerdlow, 1984) and the role of inhibitory signalling in processing nociceptive inputs from the periphery. It has therefore been proposed that the spinal DH rhythmic activity is involved in regulating the propagation of nociceptive signals from the periphery before they are transmitted to the brain (Ruscheweyh and Sandkuhler, 2005, Zeilhofer et al., 2012). Developing novel analgesics which target

the GABA_A and glycine receptors in the spinal DH could produce their actions by modulating the rhythmic activity of this network, which may in turn be linked with the excitability of the network. The correlation between rhythmic oscillations and excitability of a network has previously been identified in the brain (Ploner et al., 2006) and therefore could be extrapolated to spinal DH network oscillations. In this chapter 4-AP has been utilised to induced rhythmic oscillations in the spinal DH of acute rat spinal cord slices. The potential utility of this *in vitro* model system with 4-AP-induced oscillations will be assessed by recording the effects of classic GABA_A and glycine receptor compounds.

5.1.2 Aims

In this chapter 4-AP-induced rhythmic activity has been measured in the spinal DH of acute rat spinal cord slices using extracellular recordings. The aim of this chapter is to demonstrate whether or not enhancing or blocking GABA_A and glycine receptors affects the 4-AP-induced rhythmic activity and population spikes in the SG region of the spinal DH in the acute rat spinal cord slices. Pharmacologically targeting these receptors with well characterised compounds will help elucidate the effects these receptors have on the rhythmic activity and population spikes. Consequently, the potential of this *in vitro* model system for screen novel GABA_A and glycine receptor analgesics can be assessed. In addition GABA_B receptors were also investigated into their effects on the 4-AP-induced rhythmic activity in the SG of acute spinal cord slices. In this chapter the following aims are investigated:

1. Obtain extracellular recordings of 4-AP-induced hyperexcitability in the SG of acute spinal cord slices
2. Determine the effects of GABA_A, GABA_B and glycine receptor compounds on the 4-AP-induced rhythmic oscillatory activity with power spectral analysis.

3. Determine the effects of GABA_A, GABA_B and glycine receptor compounds on the 4-AP-induced population spikes in the SG of the acute spinal cord slices

5.2 Methods

The focus of this study is on the superficial spinal DH where the primary nociceptive neurons innervate the spinal cord, are processed and then transmitted to higher brain centres. To investigate the activity of this network, extracellular recordings were made from the SG laminae of acute transverse spinal cord slices. The SG lamina II region of the spinal DH can be easily identified by its more translucent appearance compared to the other laminae in a transverse section of a spinal cord making it easy to position a recording electrode into this region. The translucent appearance of this lamina region exists because of the lower concentration of myelinated fibres. Extracellular field recordings have been used in this study to investigate the rhythmic oscillations of the superficial spinal DH as well as the population spikes generated by this network within the spinal cord slices. This method of recording allows for the activity of a small group of synchronously firing neurons to be measured simultaneously within a network. The more stable nature of extracellular recording compared to intracellular recording, means the activity of a network within a slice can be recorded for hours, allowing for the effects of a series of perfused compounds to establish and stabilise.

5.2.1 Spinal Cord Slices

Wistar rats aged 12-16 days (27-35 g) were anaesthetised with an intraperitoneal injection of pentobarbital 40-50 mg/kg (Henry Schein Medical). A trans-cardiac perfusion was performed with sucrose-containing artificial cerebrospinal fluid (aCSF), which was made using distilled water and contained 126 mM sucrose, 2.5 mM KCl, 1.4 mM NaH₂PO₄, 1.2 mM MgCl₂, 2.4 mM CaCl₂, 25 mM NaHCO₃ and 11 mM glucose. The sucrose aCSF was made in advance and kept at 4°C, using chilled solutions throughout the preparation slows the deterioration of the tissue and

improves the quality of the slices (Lein et al., 2011). Trans-cardiac perfusion with sucrose aCSF slows neuronal and metabolic activity to provide more time for the dissection and slicing, and consequently improves tissue viability. To perform the trans-cardiac perfusion the rat was pinned to a dissection board placed inside a plastic container, positioned on its back. The chest cavity was opened to expose the heart, and held open using clamping scissors. An incision was made into the right atria of the heart using small spring scissors, and then the 23-gauge needle containing the sucrose-aCSF was inserted into the base of the left ventricle. 20 ml of the sucrose-aCSF was then perfused throughout the body from the left ventricle around the body and out of the through the incision that was made in the right atria thereby removing the blood from body. Following the trans-cardiac perfusion a dorsal laminectomy was performed. The rat was turned over and the neck was cut to confirm death. The skin from the back of the animal was removed, and then small spring scissors were used to open the spinal column. The vertebrae were cut either side of the spinal cord from the incision made at the cervical region down to the sacral vertebrae. The dorsal side of the cut vertebrae was held and peeled away with forceps as the vertebrae were cut. The spinal cord could then be removed, picking it up with forceps and cutting the connecting spinal nerves to separate the cord. The spinal cord was placed in oxygenated (95% oxygen, 5% carbon dioxide), ice-cold standard aCSF, without sucrose. The standard aCSF contained 126 mM NaCl, 2.5 mM KCl, 1.4 mM NaH_2PO_4 , 1.2 mM MgCl_2 , 2.4 mM CaCl_2 , 25 mM NaHCO_3 and 11 mM glucose,. While in the ice cold aCSF, the meninges surrounding the spinal cord were removed under a dissection microscope (Nikon, Japan). Using two pairs of fine forceps the meninges could be separated from the spinal cord which also removed any remaining dorsal and ventral roots that were attached to the cord. The meninges were removed prior to slicing as the vibratome is unable to cut through them. The spinal cord was cut to separate the lumbar region. 3% agar solution (Alfa Aesar, UK) made in distilled water was microwaved

for 40-50 seconds, and poured into a small weigh boat surrounded by ice. Once cooled slightly the lumbar section of the spinal cord was embedded into the agar. When the agar had set around the spinal cord, the spinal cord section encased within a rectangular agar block was cut out with a scalpel and super glued onto the base plate of the vibratome (Leica VT1000S, Leica Microsystems, Germany). This was then placed into the vibratome bath which contained oxygenated, ice-cold, standard aCSF. Transverse slices were cut to a thickness of 350 μm with a stainless steel blade (Campden Instruments Limited, UK) and transferred to a holding chamber (Figure 5.1), where they were submerged in oxygenated aCSF, maintained at 32°C using a waterbath. Typically 10-12 slices were obtained from one spinal cord preparation. The slices were transferred using a dropper pasture pipette with the tip cut off to minimise physical contact with the slice and therefore reduce damage to the tissue. All the slices were then incubated for one hour before commencing the electrophysiological recordings. This incubation time allows for the slice to recover from the cutting of the tissue which causes the release of enzymes and ions that can alter the metabolic state of the tissue and will remove some of the dead cells from the surface of the slices caused by the slicing (Lein et al., 2011). An hour incubation time is widely considered sufficient for the slices to equilibrate to the solution and conditions and consequently regain their electrophysiological and biochemical activity (Teyler, 1980).

5.2.2 Single-Electrode Extracellular Slice Recordings

To record from a slice, one spinal cord slice was transferred onto a custom built Perspex interface recording chamber, where a humidified atmosphere (95% oxygen-5% carbon dioxide) could be maintained (Figure 5.2). The slices were bathed in oxygenated aCSF (36°C), which flowed at 2 ml/min using a gravity

perfusion system. The slices were positioned on filter paper, which improves the flow of solution around the slice.

Extracellular field recordings were made using borosilicate glass microelectrodes (Harvard Apparatus, Kent, UK) (10-15 M Ω) filled with standard aCSF. The electrodes were pulled from 1.2 mm OD x 0.94 mm ID glass capillaries using a vertical PP830 electrode puller (Narishiges, Japan). The electrode is placed into an electrode holder which goes onto a HS-2A headstage (Axon Instruments) that is attached to a micromanipulator. Using the manipulator, the electrode was guided into place into the SG region of a slice, identifiable due to its translucent appearance under the microscope, and inserted to a depth of 150 μ m. The headstage connects to an Axoclamp 2A system (Molecular Devices, CA, USA) which was used to record and amplify (x10) the voltage waveforms. A Neurolog NL106 module (Digitimer, Welwyn Garden City, UK) was used for further amplification (x1000). The low pass band filter of the Neurolog NL106 set at 120 Hz was used for initial filtering of the voltage signals. An additional low pass band filter setting of 40 Hz (Neurolog NL106, Digitimer) was also used for all recordings. To minimise electrical disturbance, a Humbug noise eliminator was included in the circuit. The signals recorded were translated into digital values using the CED 1401 acquisition interface which in turn fed into the computer with Spike 2 software (Cambridge Electronic Design, UK) for recording and analysis. Figure 5.3 shows a diagram of this complete circuit.

Spike 2 software was used to capture the voltage waveforms at a sampling rate of 10,000 Hz. The sampling rate is required to be at least twice that of the highest possible frequency of the analogue signal (5000 Hz determined by the CED 1401) to avoid losing any of the recording's signal information, according to the Nyquist-Shannon sampling theorem. A 60 second baseline recording was made during perfusion of standard aCSF for each spinal cord slice from the SG. The slice was then perfused with 25 μ M 4-AP (Sigma, UK) in standard aCSF for 45 minutes, to

allow for the response to stabilise (Figure 5.4). Previous studies using 4-AP to induce epileptiform activity in spinal cord slices have used either 50 or 100 μ M 4-AP (Ruscheweyh and Sandkuhler, 2003, Chapman et al., 2009). However, while this induced highly reliable activity it would be difficult to determine if addition of other compounds could enhance this activity further as it appears to be almost maximal firing of the SG network. Therefore a lower concentration was used which was able to reliably produce activity, but allowed scope for further increases in activity with the addition of other compounds (Visockis and King, 2013). The Spike 2 configuration used for recordings was set to record one minute every 3 minutes as usually approximately 30 minutes was required for an effect of the compound perfused to materialise and reach a stable level, so not all the data was required for analysis. Population spikes and rhythmic oscillations were induced by application of 4-AP. The effects of GABA and glycine receptor compounds were then tested against this 4-AP induced activity. Each GABA and glycine receptor compound was co-applied with the 4-AP diluted in standard aCSF for 45 minutes similarly with one minute recorded every three minutes. This was then followed by perfusions with 4-AP-containing aCSF (4-AP wash) to show if the activity could be recovered. An aCSF alone wash was then done to show if the 4-AP-induced activity could reversed to normal baseline levels.



Figure 5.1 Photograph of the spinal cord slice holder. The glass beaker is filled with standard aCSF and the slice holder placed inside it. The slice holder is made from a plastic beaker with the base removed and replaced with a nylon netting. The nylon net allows the oxygenated aCSF to pass through it and is soft so that it does not damage the slices.

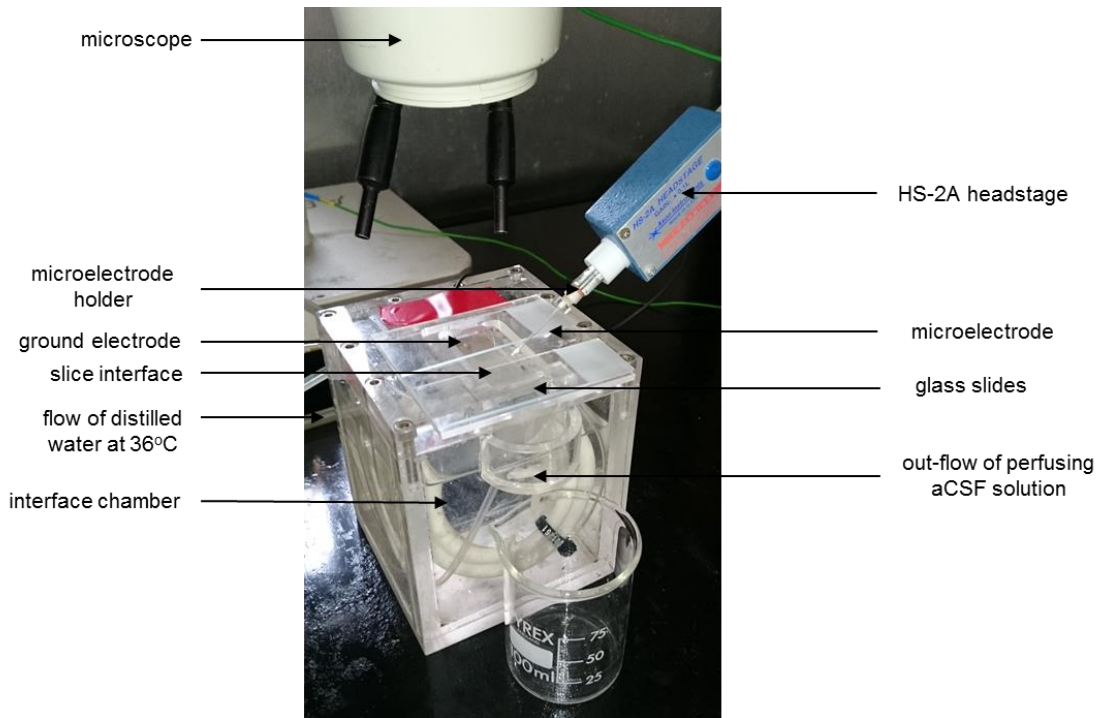


Figure 5.2 Photograph of the interface chamber used for the single electrode slice recordings. The flow of heated distilled water into the chamber warms the slice interface. The warm air from the chamber passes into the slice interface through holes either side of the interface. The slice interface is kept humid by placing glass slides on top of the interface to retain the heat and humidity, leaving a gap for the microelectrode to enter the slice. The tubing containing the perfusion solution is passed through the chamber so that it is also heated before it enters the slice interface.

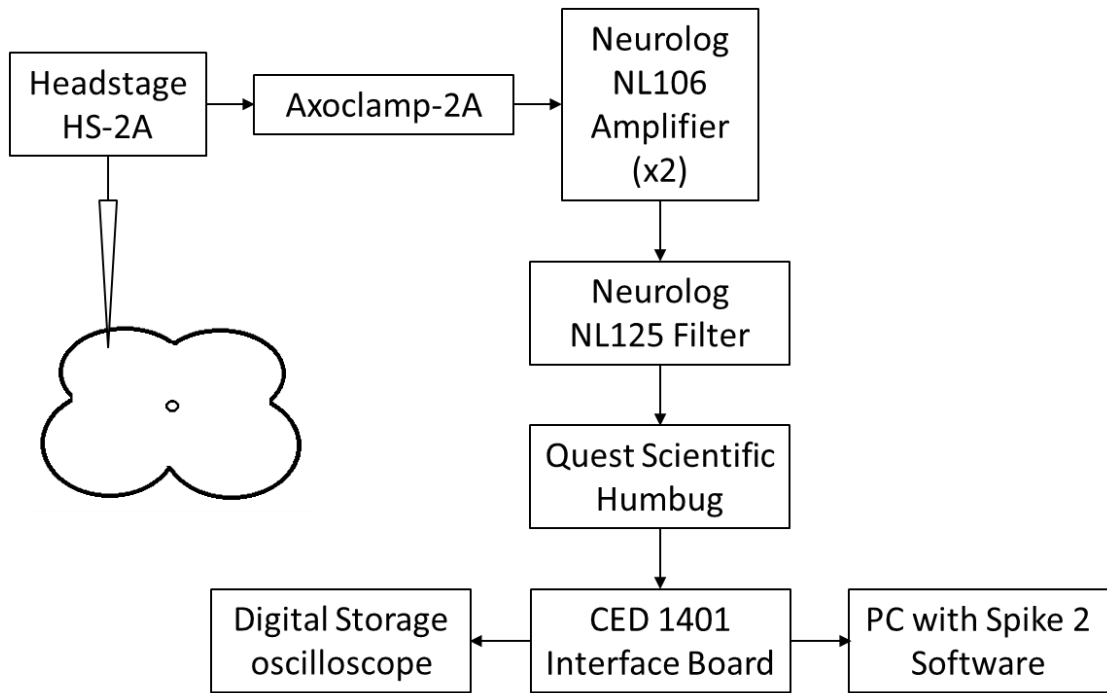


Figure 5.3 A schematic diagram of the circuit used for the single electrode recordings from the spinal cord slices.

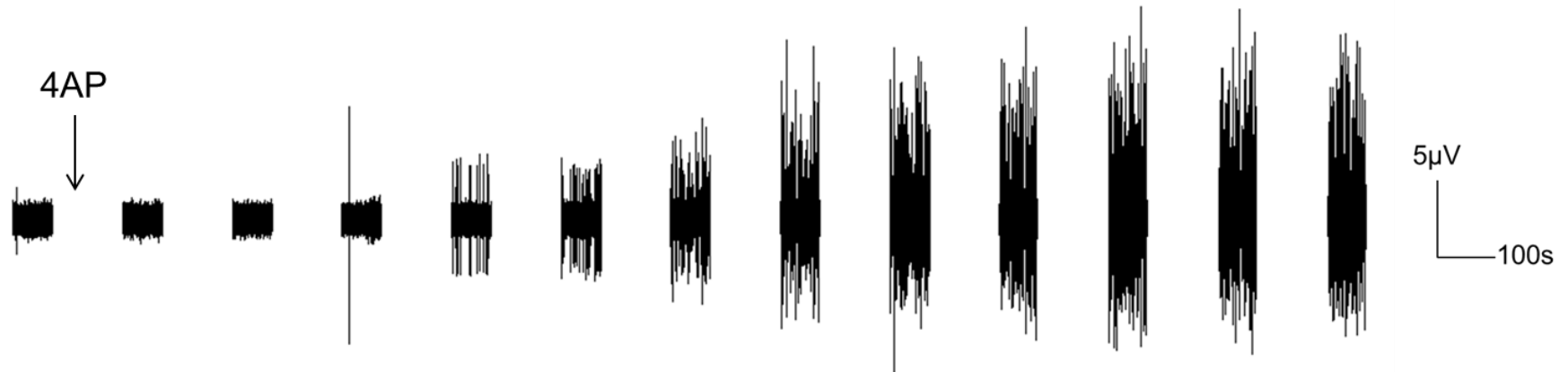


Figure 5.4 An example of a recording from the SG of a spinal cord slice using the single electrode extracellular recording technique. Illustrated here are one minute sections of a recording from left to right with only the first of every three minutes recorded. The first minute section is the baseline with standard aCSF perfusion. Following this aCSF containing 4-AP (25 μM) was then perfused from the time point indicated by the arrow. After 15 minutes (the 5th section) population spikes can be observed, which further increase in amplitude and frequency until after approximately 30 minutes of perfusion of 4-AP where the activity stabilises.

5.2.3 Spike 2 Data Analysis

The first minute of baseline and the final minute recorded in the presence of each compound were used for analysis. The recordings were analysed in two ways, firstly the underlying inter-spike interval oscillatory rhythmic activity of the superficial dorsal horn network was studied. Fast Fourier Transform (FFT) Power Spectral analysis was performed to quantify any changes in the inter-spike interval oscillatory activity. The FFT analysis determines all the different amplitudes, frequencies and phases which are the components of the oscillating activity of the slice recordings and converts them to cosine waves. The power value is generated from the amplitudes of each cosine waves for each frequency, with units of μV^2 (10^{-6}V^2). The output of this analysis is a Power Spectra displaying the power at each frequency. Therefore, the strongest frequency and how strong this frequency is can be determined for a chosen time period of the recording and compared with different sections of the recording where a compound was present.

The data were initially processed using the DC remove process in Spike 2, with a time constant of 0.1 s. A low pass digital FIR (Finite Impulse Response) filter was then applied to the recording, which reduces the noise of the recording and enhances the remaining frequencies. A script was specially designed by C.E.D. which removed the population spikes with amplitudes above a chosen threshold of 15 μV . The script detects the rising phase of a spike as it crosses the 15 μV threshold and removes the data 0.5 s before and after the spike leaving the inter-spike interval regions of the recording (Figure 5.5). A minimum amplitude of 15 μV was chosen because the baseline voltage was typically between ± 10 μV , therefore to distinguish between the baseline and a spike 15 μV was selected. Power spectra could then be created from the inter-spike interval data for the 60 second epochs. The Power Spectra had an FFT size of 8192 with a Hanning window function. From the FFT analysis the peak power amplitude, area and frequency were determined

within the 4-12 Hz frequency range (Figure 5.6B). This frequency range was selected because the power spectra show that this frequency was the most dominant frequency range observed to occur with no other strong frequency range detected, which has also been demonstrated previously (Chapman et al., 2009, Visockis and King, 2013) (Figure 5.6A). *In vivo* recordings from the spinal SG region have also detected similar frequency range, 6-13 Hz (Sandkuhler and Eblen-Zajjur, 1994). The second aspect of the analysis of the recorded data involved characterising the changes in the population spikes. Spike amplitude and frequency were characterised for large amplitude population spikes over 15 μ V using Spike 2 for the same 60 second sections of the recordings.

5.2.4 Statistics

The percent change in each of the parameters from the power spectrum analysis and the population spike analysis of the single electrode recordings was calculated for each slice as paired data. The mean percent change in power area was then determined from all the recordings with 4-AP and GABA, and displayed as a histogram with the S.E.M. A minimum of 6 slices were recorded from for each compound, with slices from at least 2 different rats. The data was analysed using GraphPad Prism software. Two-tailed, paired T-tests or a repeated measure one-way ANOVA, where values for each parameter were compared with the value of 4-AP with a Dunnett's multiple comparisons test. A $P < 0.05$ significance level was used for t-test or one-way ANOVA analysis. On the graphs a $P < 0.05$ is indicated by *, $P < 0.01$ by ** and $P < 0.001$ by *** when comparing the values with 4-AP.

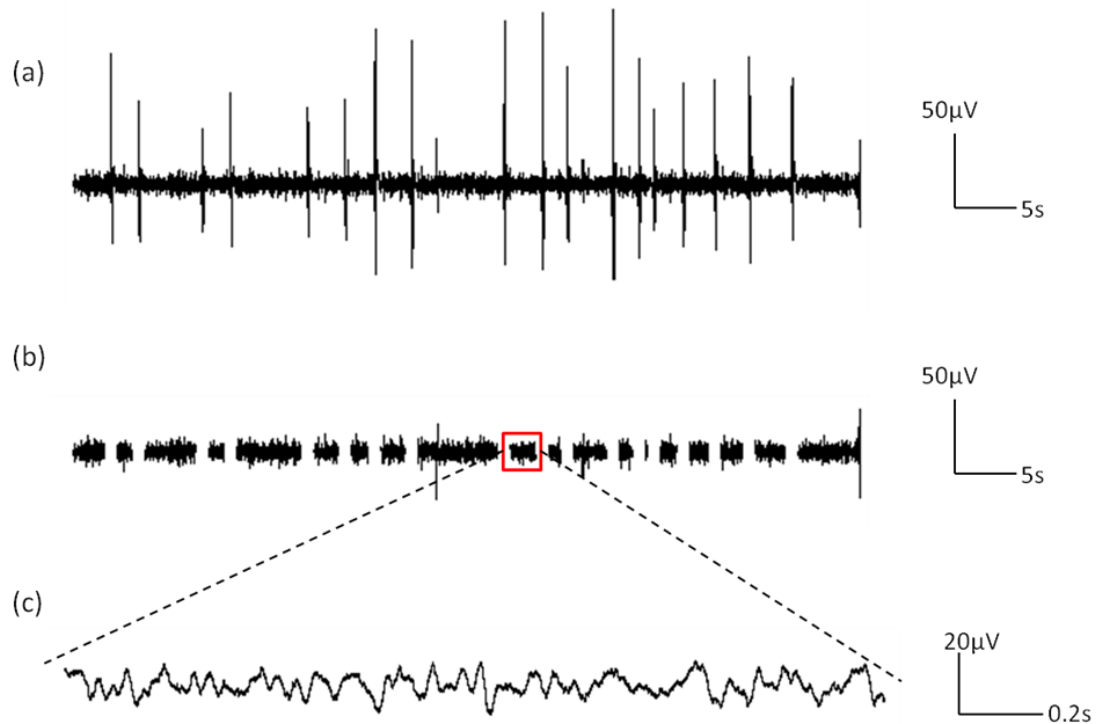


Figure 5.5 Processing of extracellular recordings from the SG region of a rat spinal cord slice for analysis of the rhythmic oscillations. (a) A 60 s section of a single electrode extracellular recording from the SG region of a transverse lumbar spinal cord slice during perfusion of 4-AP (25 μM). This display shows the large population spikes induced by 4-AP of variable amplitudes, and the inter-spike interval regions of variable durations. (b) The same section of the recording as shown in (a) following the removal of all population spikes over 15 μV. This is the result of running the script written in Spike 2 software used to analyse the data. The script was coded to remove the section of recording where the voltage crosses the 15 μV threshold and removes 0.5 s either side of the spike. (c) An inter-spike interval region of the recording in (b) magnified to illustrate the underlying oscillating activity of the network within the superficial DH.

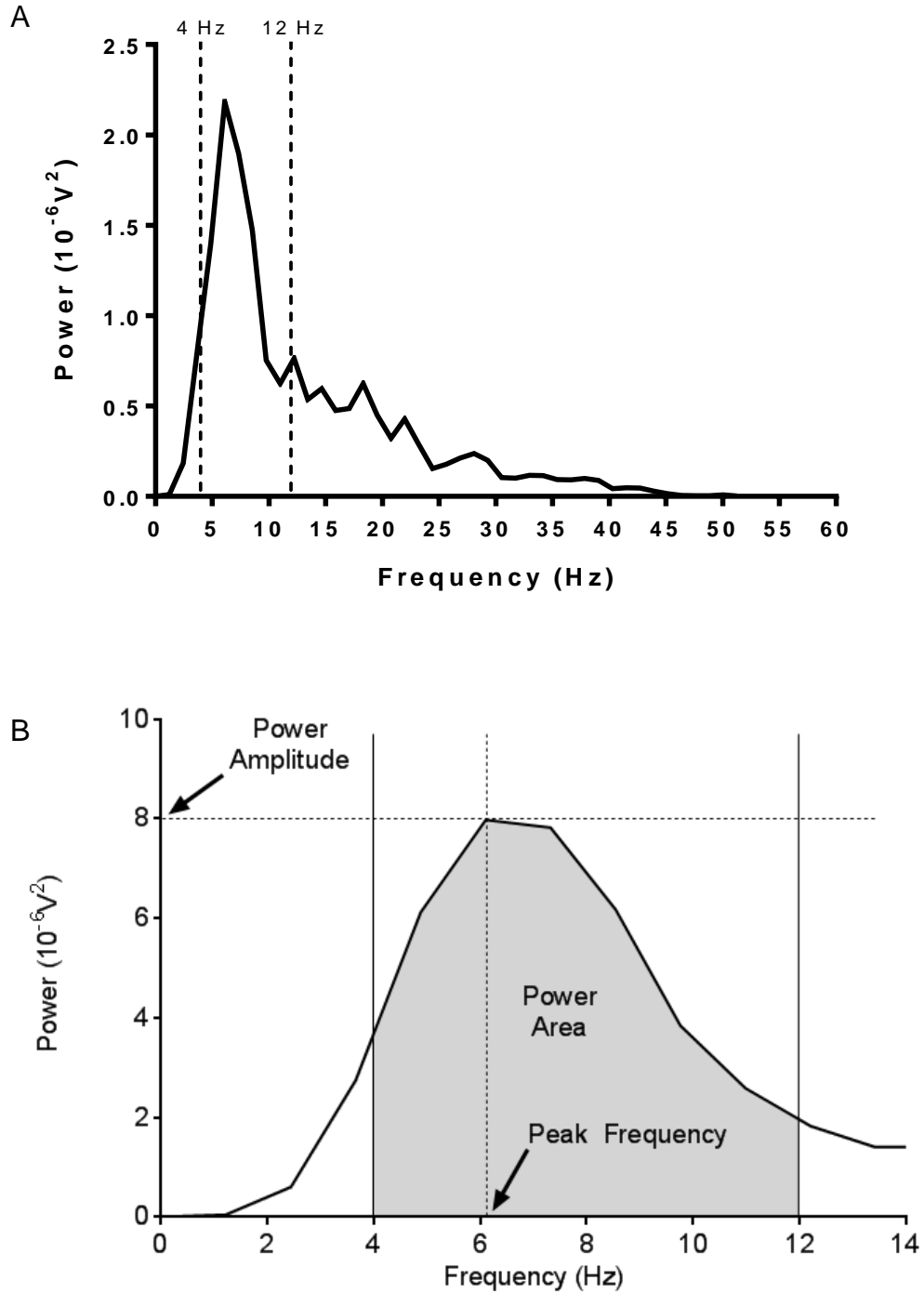


Figure 5.6 A Power Spectra generated from FFT Power Spectrum analysis of the rhythmic oscillations recorded from the SG region of the spinal cord slices. (A) An example Power Spectra showing the frequency range from 0 to 60 Hz. The only dominant frequency range is between 4-12 Hz. (B) An example Power Spectra showing the 4-12Hz frequency range and illustrating how the three parameters, power amplitude, power area and peak frequency, are measured.

5.2.5 Materials

A full list of the compounds used in this study is shown in **Error! Not a valid bookmark self-reference.**, along with their details of concentrations and suppliers.

Table 5.1 List of compounds used in the single electrode extracellular acute spinal cord slice recordings

Compound	Action	Working Concentration	Supplier	References
4-Aminopyridine	K ⁺ channel blocker	25 µM	Sigma	Chapman et al. (2009), Ruscheweyh and Sandkuhler (2003), Visockis and King (2013)
GABA	GABA _A and GABA _B agonist	200 µM	Sigma	Andersen et al. (1980)
Muscimol	GABA _A agonist	10 µM	Sigma	Neal and Shah (1989)
THIP	GABA _A agonist	10 µM	Sigma	Drasbek and Jensen (2006)
L-838,417	GABA _A PAM	10 µM	Sigma	(Mirza and Nielsen, 2006), (Nickolls et al., 2011)
Bicuculline Methiodide	GABA _A antagonist	50 µM	Sigma	Chapman et al. (2009)
Gabazine	GABA _A antagonist	10 µM	Sigma	Drasbek and Jensen (2006)
Baclofen	GABA _B agonist	10 µM	Sigma	Ault and Nadler (1983), (Neal and Shah, 1989)
2-Hydroxysaclofen	GABA _B antagonist	10 µM	Alfa Aesar	Chub and O'Donovan (1998)
Glycine	Glycine agonist	2 mM	Sigma	(Kullmann et al., 2002)
Strychnine	Glycine antagonist	10 µM	Sigma	Chub and O'Donovan (1998), Ruscheweyh and Sandkuhler (2003)

5.3 Results

5.3.1 *GABA_A Receptor Agonist and Antagonist Effects on Spinal Dorsal Horn Activity*

5.3.1.1 *Rhythmic Oscillatory Activity*

GABA_A receptor agonist GABA (200 μ M) did not significantly affect any of the three parameters measured from the power spectral analysis (Figure 5.7). However, muscimol (10 μ M) decreased power amplitude from 9.24 to 4.2 μ V² ($P < 0.05$) and power area from 36.01 to 28.92 μ V².Hz ($P < 0.05$) (Figure 5.8). Although, the power spectra peak frequency was unchanged by muscimol ($P > 0.05$). THIP (10 μ M) significantly decreased power amplitude from 10.76 μ V² with 4-AP to 2.93 μ V² with 4-AP and THIP perfusion ($P < 0.05$). THIP also significantly reduced power area from 41.91 to 15.17 μ V².Hz ($P < 0.05$), but had no effect on the peak frequency ($P > 0.05$) (Figure 5.9). Furthermore, L-838,417 (10 μ M), the positive allosteric modulator (PAM) of GABA_A receptors, significantly reduced power amplitude by 38.5% from 8.32 to 5.28 μ V² ($P < 0.01$). Power area was reduced by 34.1% on average from 39.09 to 27.5 μ V².Hz ($P < 0.05$). Peak frequency was unaffected by this GABA_A receptor PAM ($P > 0.05$) (Figure 5.10).

GABA_A receptor antagonist bicuculline (50 μ M) significantly decreased power amplitude and power area and significantly increased the peak frequency of the Power Spectra analysis. The mean power amplitude was decreased from 6.74 to 2.22 μ V² ($P < 0.001$), power amplitude was reduced from 29.1 to 11.95 μ V².Hz ($P < 0.001$) and peak frequency was increased from 6.19 to 7.06 Hz ($P < 0.01$) (Figure 5.11). Gabazine (50 μ V), the second GABA_A receptor antagonist investigated, similarly decreased power amplitude and power area, and increased peak frequency of the rhythmic activity in the SG of the spinal cord slices (Figure 5.12). The power amplitude mean was decreased from 6.76 μ V² with 4-AP to 4.59 μ V² with

4-AP and gabazine ($P<0.05$). The mean power area was decreased from 29.70 to 17.09 $\mu\text{V}^2\cdot\text{Hz}$ by gabazine ($P<0.01$), while the peak frequency was significantly increased from 7.06 to 7.71 Hz ($P<0.05$). The GABA_A receptor antagonists were the only compounds to significantly affect the peak frequency of the rhythmic activity in the spinal DH recordings. A summary of all the effects of the GABA_A receptor compounds is listed in Table 5.2.

Table 5.2 A summary of the effects of the GABA_A receptor compounds on the 4-AP-induced rhythmic activity parameters investigated. The symbols \uparrow and \downarrow indicated a significant increase or decrease respectively in the parameter, n.s. indicates no significant change in the parameter.

Compound	Effect on 4-AP-Induced Rhythmic Activity		
	Power Amplitude	Power Area	Peak Frequency
GABA	n.s	n.s	n.s
Muscimol	\downarrow	n.s	n.s
THIP	\downarrow	\downarrow	n.s
L-838417	\downarrow	\downarrow	n.s
Bicuculline	\downarrow	\downarrow	\uparrow
Gabazine	\downarrow	\downarrow	\uparrow

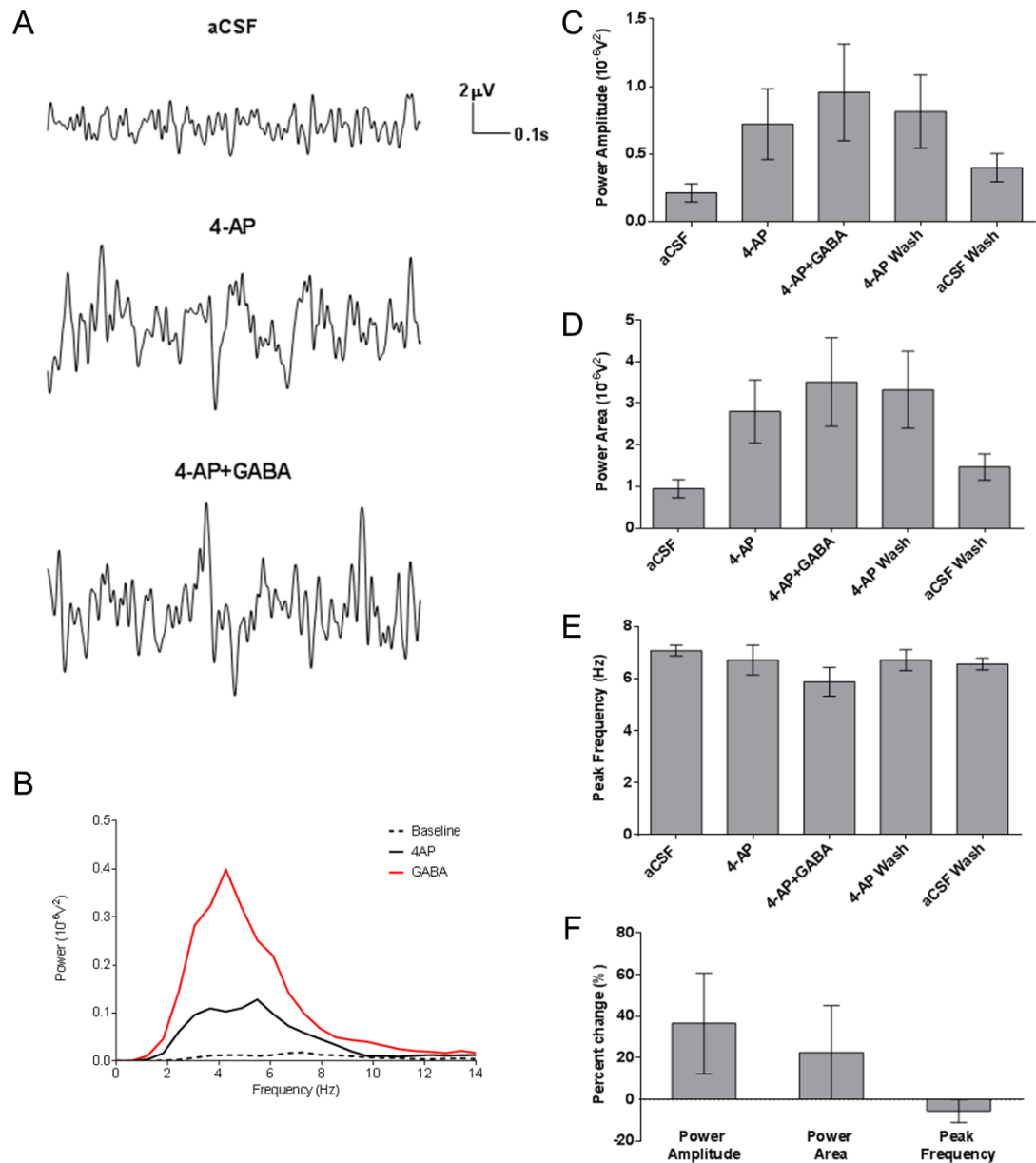


Figure 5.7 The effects of GABA (200 μ M) on the 4AP-induced rhythmic activity in the SG region of rat spinal DH. (A) Sections from the recording of a slice during perfusion of standard aCSF, followed by aCSF containing 25 μ M 4-AP and then aCSF with 4-AP and GABA. (B) The power spectra generated from the recording in (A) for each condition. (C) The mean power amplitude values during perfusion of standard aCSF, aCSF with 4-AP and aCSF with 4-AP and GABA. (D) The mean power area values for each condition. (E) The mean peak frequency values for each condition. (F) The overall percent change in each of the rhythmic activity parameters comparing activity during perfusion of 4-AP to that with 4-AP and GABA. (N=3, n=6)

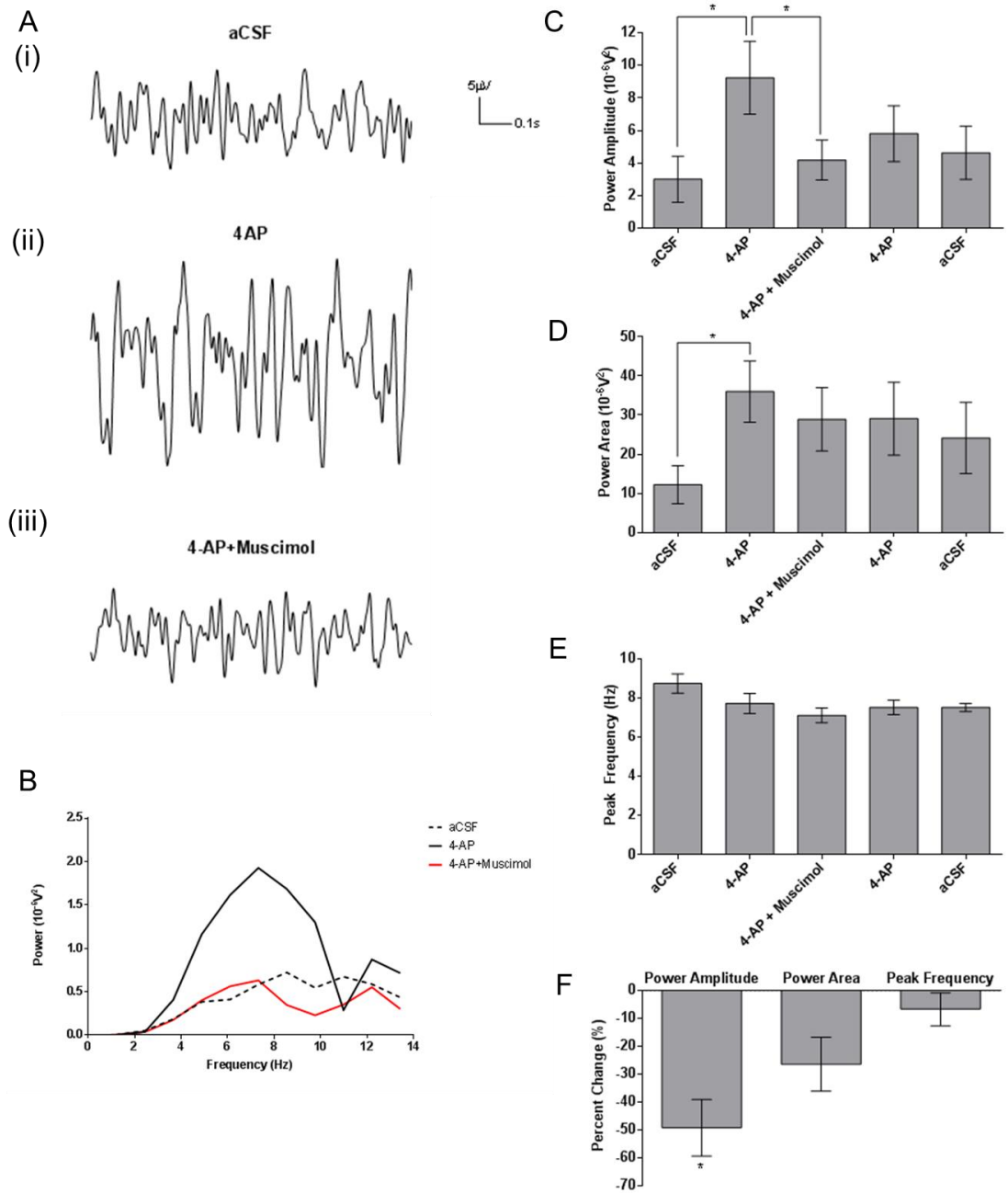


Figure 5.8 GABA_A receptor agonist muscimol effects on the 4-AP-induced activity in the SG of rat spinal cord slices. (A) One second sections of a recording during the perfusion of (i) aCSF, (ii) aCSF with 4-AP and (iii) aCSF with 4-AP and muscimol. (B) The power spectra of the data from the recording in (A) for each of the three conditions. The mean power amplitude values (C), power area (D) and peak frequency (E) of the recordings during perfusion of aCSF alone and with 4-AP and muscimol as indicated. (F) The percent change in power amplitude power area and peak frequency from 4-AP to 4-AP with muscimol. (N=4, n=8)

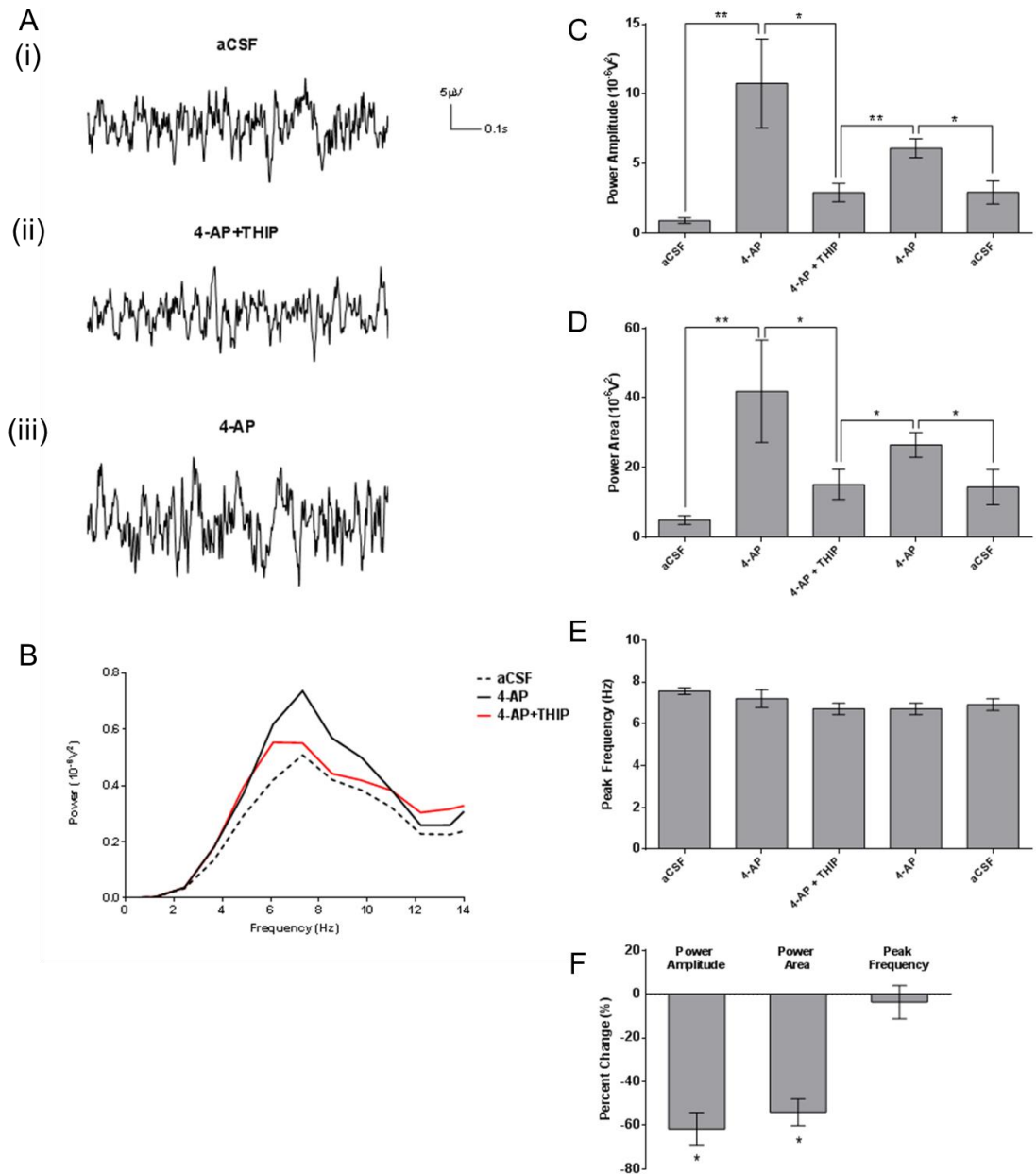


Figure 5.9 The effects of GABA_A agonist THIP on the 4-AP-induced rhythmic activity in the spinal DH SG. (A) One second sections from a slice recording during perfusion of aCSF alone (i), aCSF with 4-AP (ii) and aCSF with 4-AP and THIP. (B) The power spectra for the recording shown in part (A). The power amplitudes (C), power area values (D) and peak frequency values (E) for each section of the recording. (F) The percent change values for power amplitude, area and peak frequency, comparing 4-AP induced activity with 4-AP with THIP activity. (N=4, n=9)

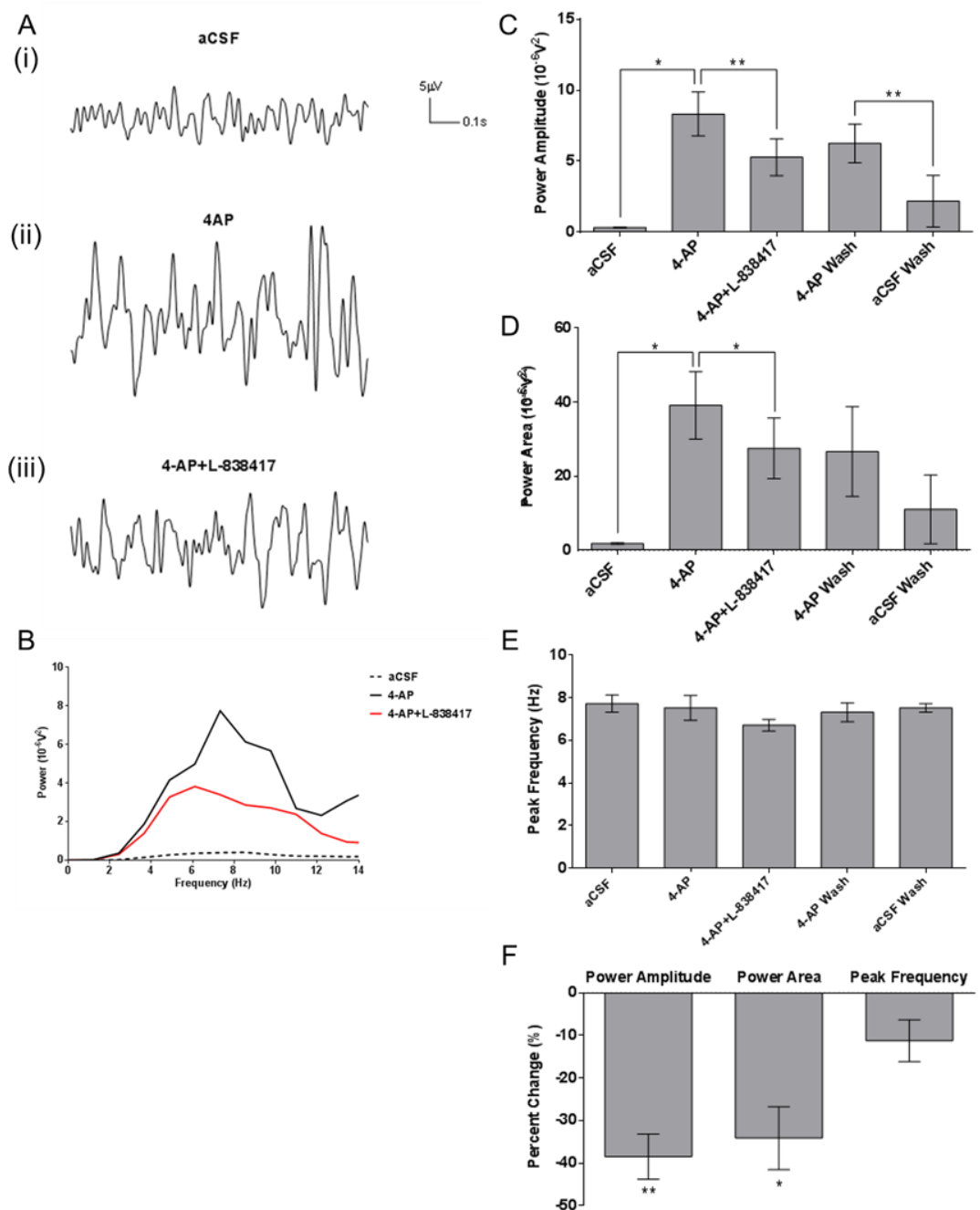


Figure 5.10 The effects of the GABA_A receptor positive allosteric modulator L-838,417 on the 4-AP-induced rhythmic activity. (A) Three one second sections of a recording to show the rhythmic activity during perfusion of aCSF alone, with 4-AP and with 4-AP and L-838,417. (B) The power spectra for the recording in (A). The mean power amplitudes (C), power areas (D) and peak frequencies (E) for the recordings with L-838,417 for each of the sections in the recordings as indicated. (F) The percent change in the three parameters to describe the rhythmic activity comparing the 4-AP activity to that with 4-AP and L-838,417 (N=2, n=6).

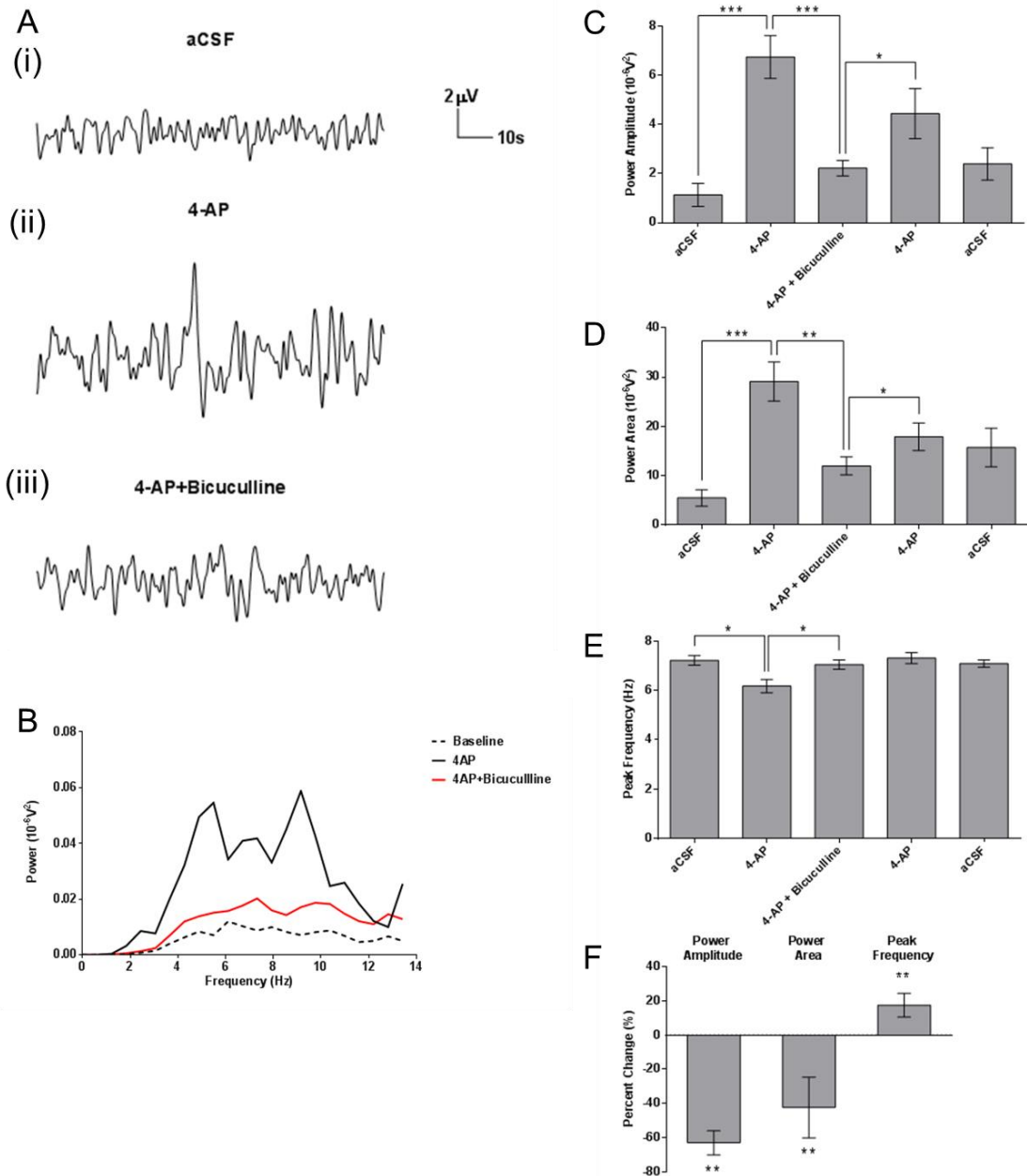


Figure 5.11 GABA_A receptor antagonist bicuculline effects on 4AP-induced rhythmic activity in the SG laminae of a lumbar spinal cord slice recorded using single electrode extracellular recording technique. (A) Inter-spike interval sections of a slice recording during perfusion of (i) aCSF, (ii) aCSF with 4-AP and (iii) aCSF with 4-AP and bicuculline (50 μ M). (B) The power spectra for each section of the recording in part (A). (C) The mean power amplitudes of each section of the slice recordings. (D) The power area values for each section of the recordings. (E) The peak frequency values for each section of the recordings. (F) The percentage change in each of the rhythmic activity parameters comparing 4-AP activity to the activity with 4-AP and bicuculline. (N=4, n=11)

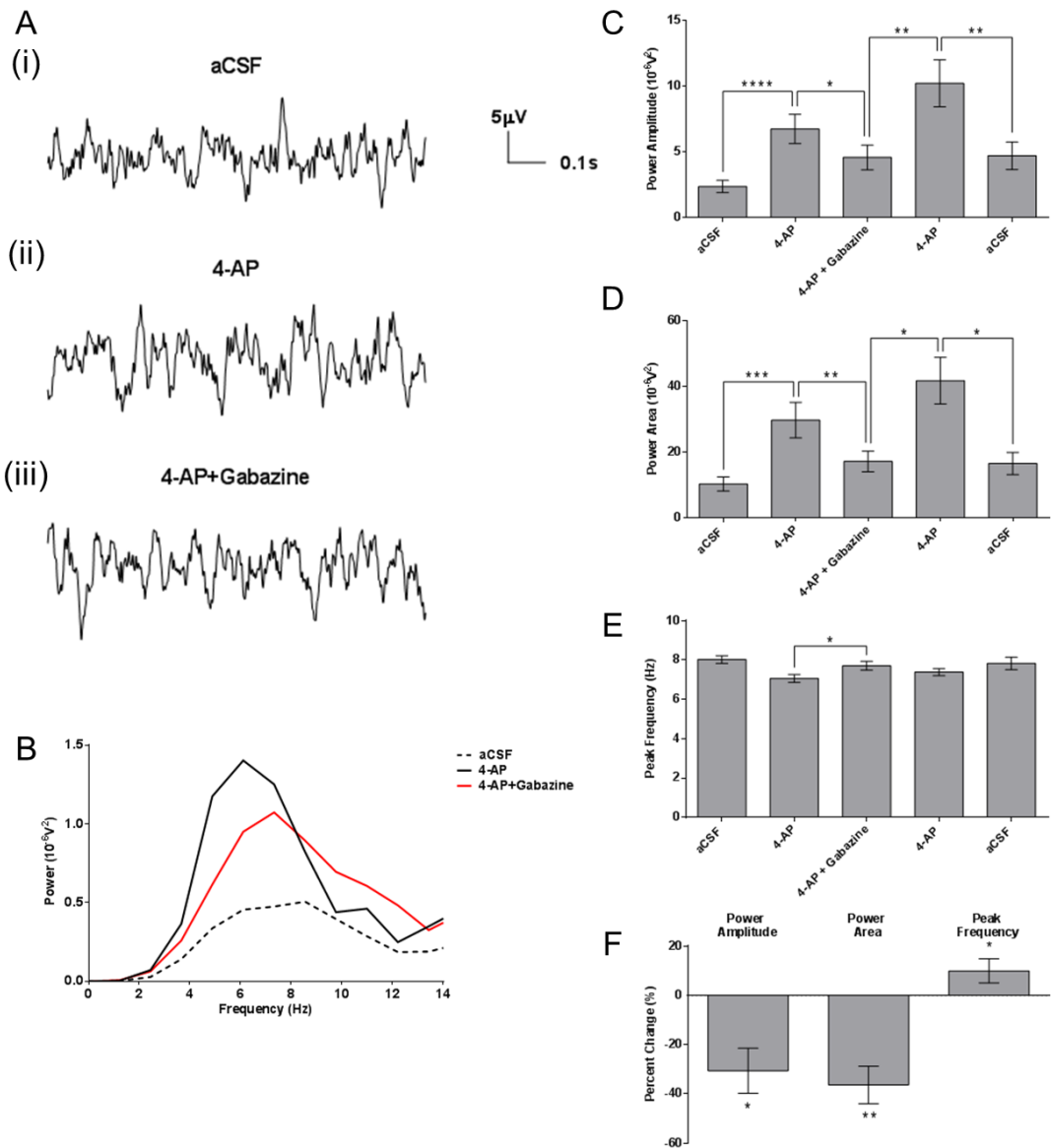


Figure 5.12 The effects of gabazine on the 4-AP-induced rhythmic activity in the SG of spinal cord slices recorded from using single electrode extracellular recording technique. (A) Sections of a recording during perfusion of (i) aCSF alone, (ii) aCSF with 4-AP and (iii) aCSF with 4-AP and gabazine (50 μ M). (B) The power spectra generated for each of the sections of the recording described in part (A). (C) The mean power amplitude values for each section of these slice recordings as indicated. (D) The power area values for each section of the recordings. (E) The peak frequency values for each section of these slice recordings. (F) The percent change in each of the rhythmic activity parameters, comparing the 4-AP activity to that with 4-AP and gabazine (N=5, n=16).

5.3.1.2 Population Spikes

GABA had a more profound effect on the population spikes, significantly increasing spike frequency from 0.67 to 0.97 Hz ($P < 0.01$) and spike amplitude from 22.29 to 40.06 μV ($P < 0.05$) (Figure 5.13). Muscimol significantly decreased population spike frequency from 0.70 Hz to 0.01 Hz ($P < 0.01$). The mean population spike amplitude decreased from 123.1 μV with 4-AP to 5.42 μV with the perfusion of 4-AP and muscimol ($P < 0.001$) (Figure 5.14). In all but one of the recordings with muscimol the population spikes were completely inhibited. THIP similarly decreased spike frequency from a mean of 0.76 to 0.36 Hz ($P < 0.05$). However, spike amplitude was unaffected, with a mean of 136.4 μV during 4-AP perfusion to 133.6 μV during perfusion with 4-AP and THIP ($P > 0.05$) (Figure 5.15). The GABA_A receptor PAM, L-838,417, did not affect population spike amplitude or frequency. The 4-AP mean population spike frequency was 0.91 Hz, and with the addition of L-838,417 the frequency was 1.06 Hz ($P > 0.05$). The mean spike amplitude with 4-AP was 126.0 μV , and with 4-AP and L-838,417 it was 125.5 μV ($P > 0.05$) (Figure 5.16).

Both GABA_A receptor antagonists significantly decreased 4-AP-induced population spike amplitude and frequency. In many of the slices the spikes were completely abolished or had very few spikes remaining following perfusion of gabazine or bicuculline. Bicuculline (50 μM) decreased spike frequency on average by $97 \pm 0.73\%$, from a mean of 0.59 to 0.02 Hz ($P < 0.0001$). Spike amplitude was significantly decreased by bicuculline on average by $73 \pm 5.93\%$ from 115.80 to 35.58 μV ($P < 0.0001$) (Figure 5.17). Gabazine (10 μM) decreased population spike frequency on average by $93 \pm 2.51\%$ from a mean of 0.75 to 0.03 Hz ($P < 0.0001$). Spike amplitude was reduced by $73 \pm 9.26\%$ on average by gabazine, from a mean of 113.7 to 23.9 μV ($P < 0.001$) (Figure 5.18). A summary of the effects of the GABA_A receptor compounds on the 4-AP-induced population spikes in the SG of the spinal cord slices are listed in Table 5.3.

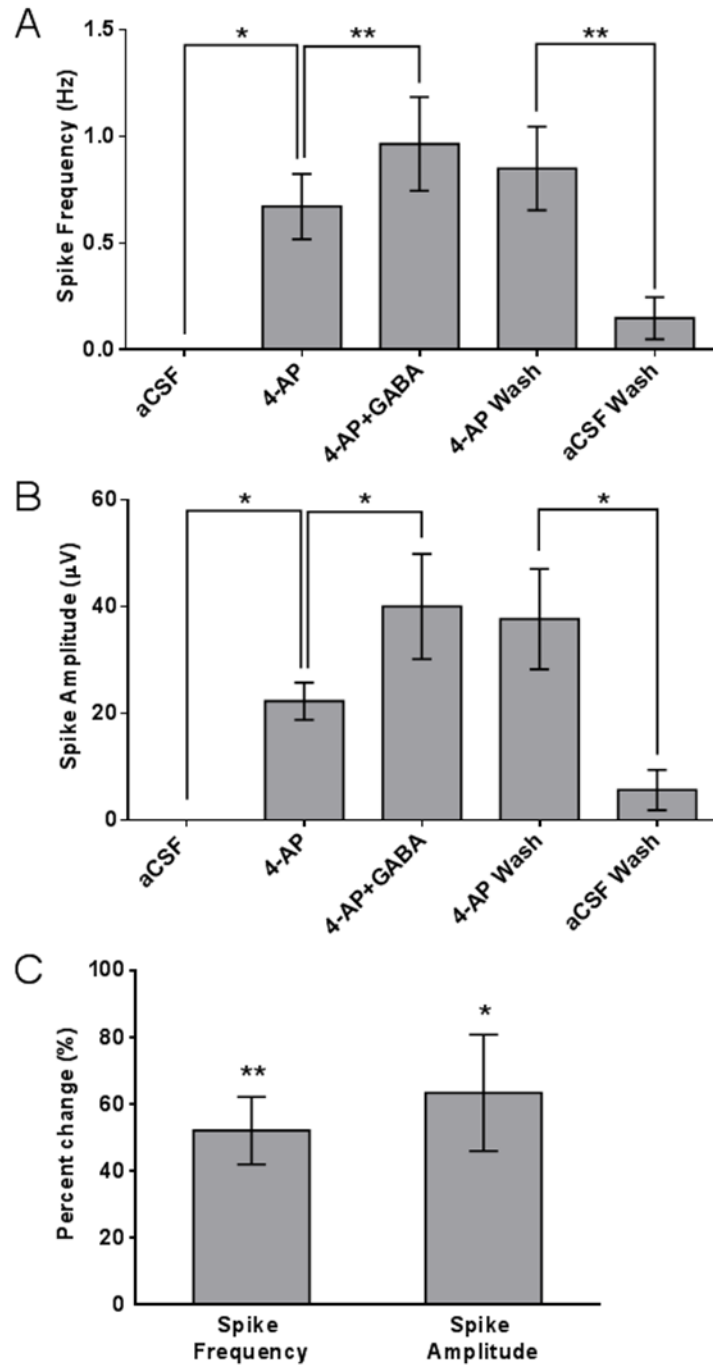


Figure 5.13 The changes in population spike frequency and amplitude by GABA (200 μ M) recorded in the SG of the spinal cord slices using single electrode extracellular recordings. (A) The mean spike frequencies measured during perfusion of standard aCSF, aCSF with 4-AP and aCSF with 4-AP and GABA, followed by a wash with 4-AP then a wash with aCSF to show recovery of activity. (B) The mean spike amplitudes measured during each of the same sections of the recording as indicated. (C) The percent change in spike frequency and amplitude from those recorded during 4-AP perfusion and 4-AP with GABA perfusion. (N=3, n=10)

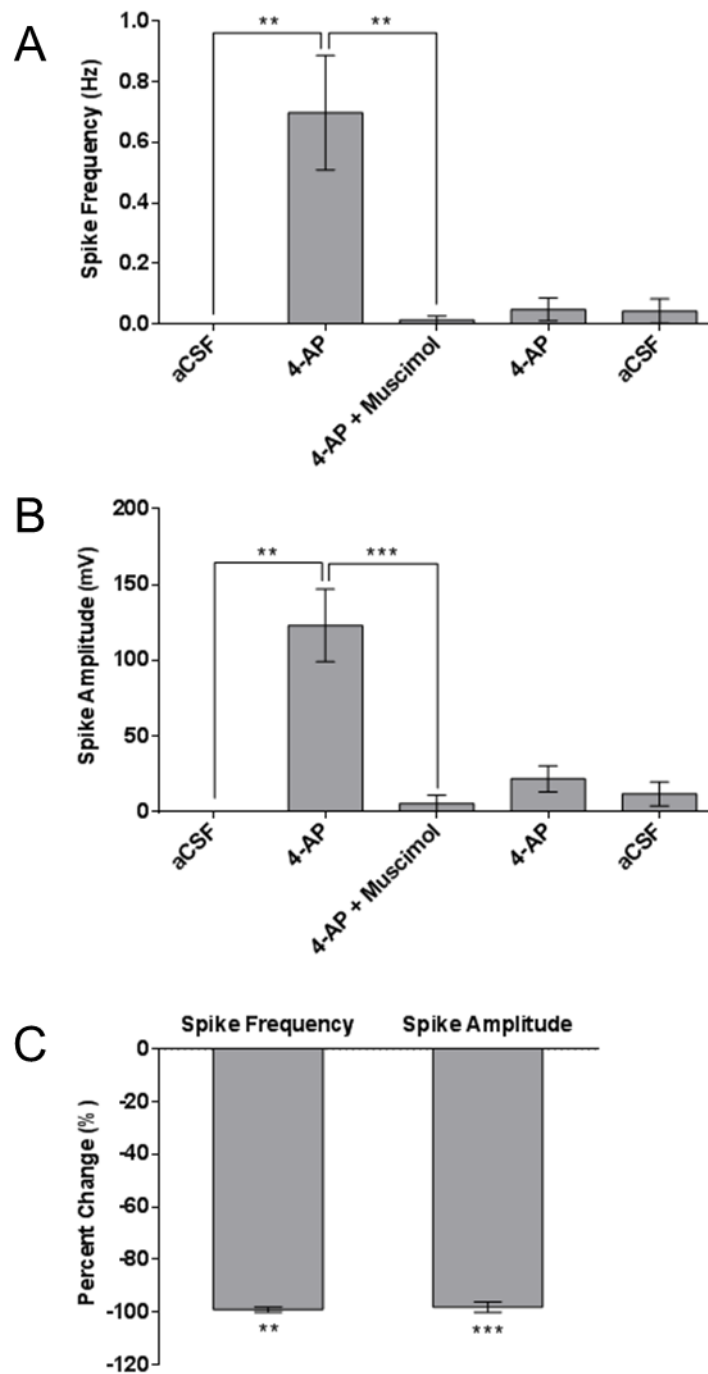


Figure 5.14 The changes in population spike frequency and amplitude in the SG of spinal cord slices by GABA_A receptor agonist muscimol (10 μ M). (A) The mean spike frequencies measured during perfusion of standard aCSF, aCSF with 4-AP and aCSF with 4-AP and muscimol, followed by a wash with 4-AP then a wash with aCSF to show recovery of activity. (B) The mean spike amplitudes measured during each of the same sections of the recording as indicated. (C) The percent change in spike frequency and amplitude from those recorded during 4-AP perfusion and 4-AP with muscimol perfusion. (N=4, n=8)

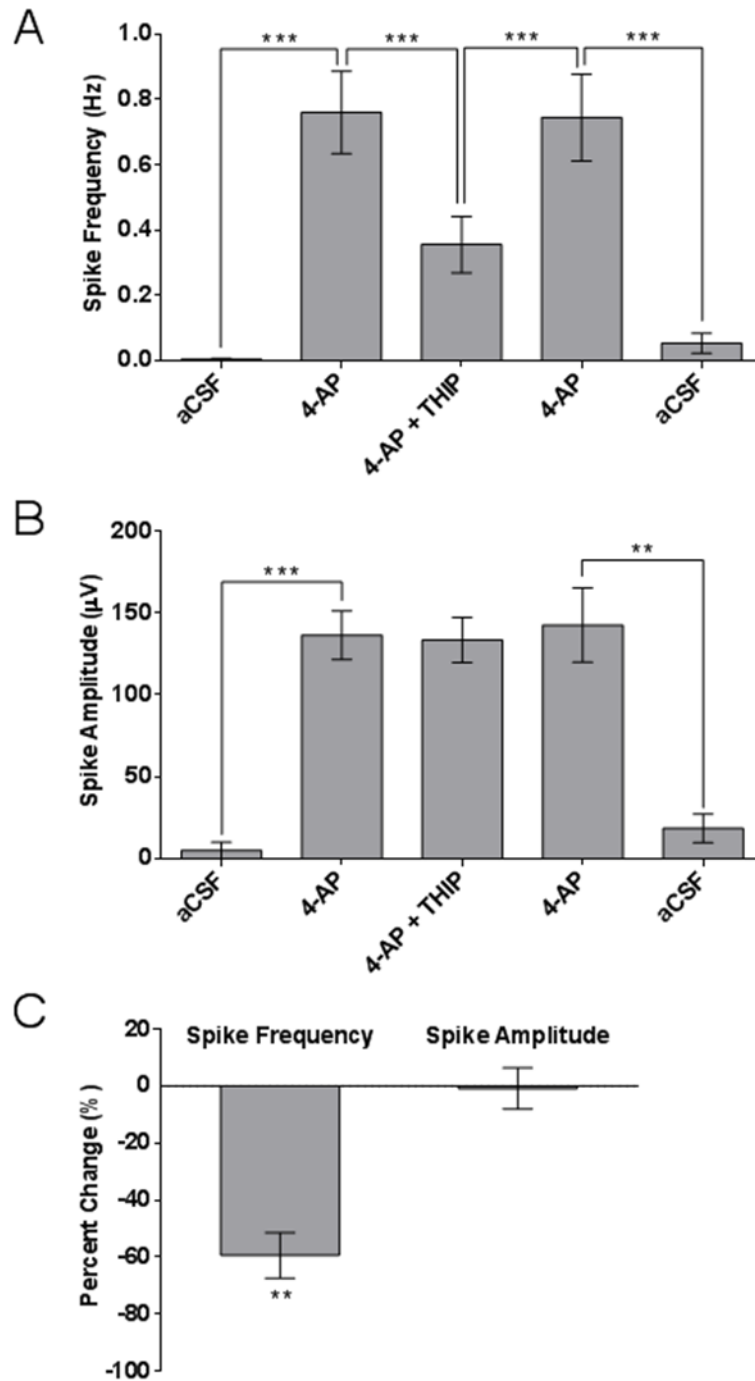


Figure 5.15 The changes in population spike frequency and amplitude in the SG of spinal cord slices by GABA_A receptor agonist THIP (10 μM). (A) The mean spike frequencies measured during perfusion of standard aCSF, aCSF with 4-AP and aCSF with 4-AP and THIP, followed by a wash with 4-AP then a wash with aCSF to show recovery of activity. (B) The mean spike amplitudes measured during each of the same sections of the recording as indicated. (C) The percent change in spike frequency and amplitude from those recorded during 4-AP perfusion and 4-AP with THIP perfusion. (N=4, n=9)

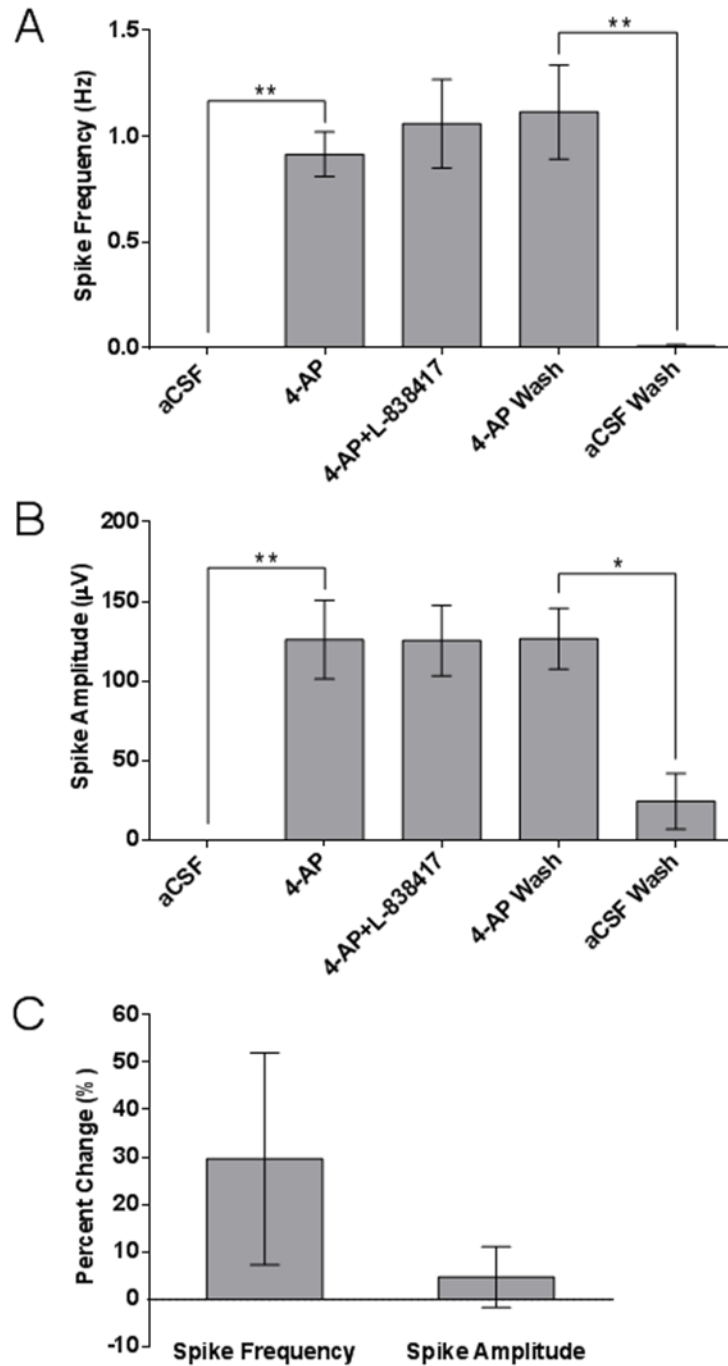


Figure 5.16 The changes in population spike frequency and amplitude in the SG of spinal cord slices by GABA_A receptor PAM L-838,417 (10 µM). (A) The mean spike frequencies measured during perfusion of standard aCSF, aCSF with 4-AP and aCSF with 4-AP and L-838,417, followed by a wash with 4-AP then a wash with aCSF to show recovery of activity. (B) The mean spike amplitudes measured during each of the same sections of the recording as indicated. (C) The percent change in spike frequency and amplitude from those recorded during 4-AP perfusion and 4-AP with L-838,417 perfusion. (N=2, n=6)

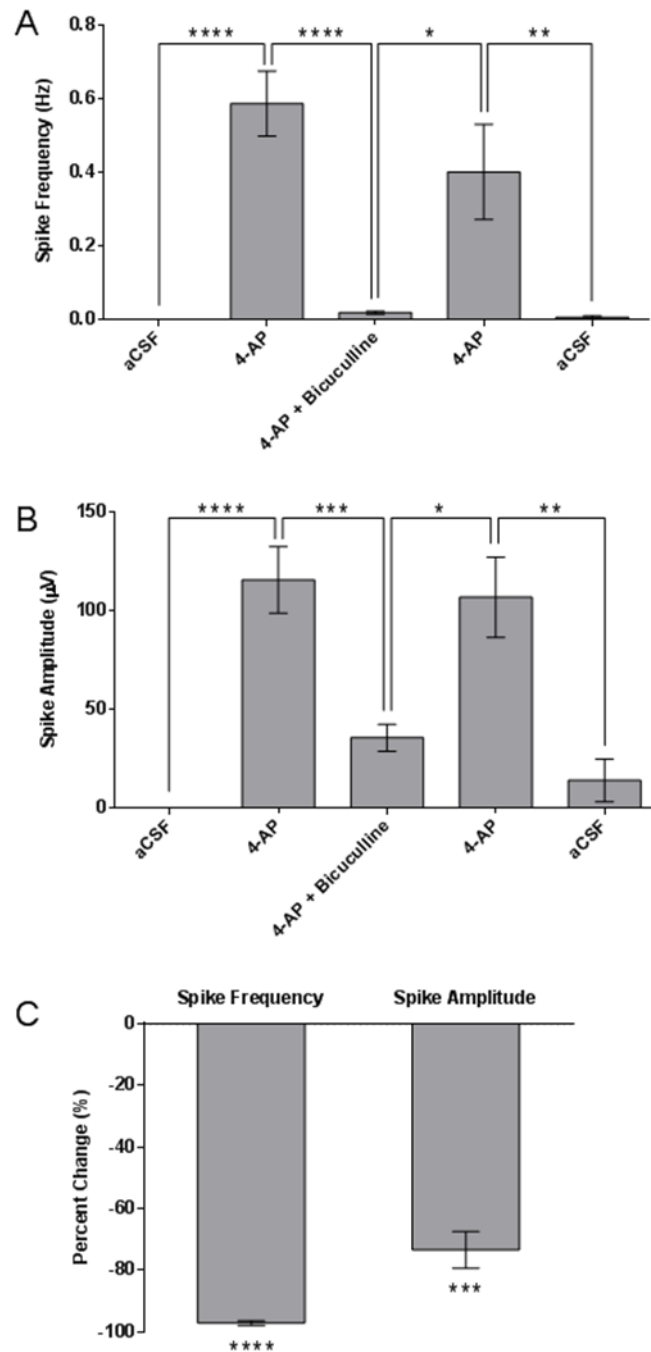


Figure 5.17 The changes in 4-AP-induced population spike frequency and amplitude in the SG of spinal cord slices by GABA_A receptor antagonist bicuculline (50 µM). (A) The mean population spike frequencies measured during perfusion of standard aCSF, aCSF with 4-AP and aCSF with 4-AP and bicuculline, followed by a wash with 4-AP then a wash with aCSF to show recovery of activity. (B) The mean spike amplitudes measured during each of the same sections of the recording as indicated. (C) The percent change in spike frequency and amplitude from those recorded during 4-AP perfusion and 4-AP with bicuculline. (N=4, n=14)

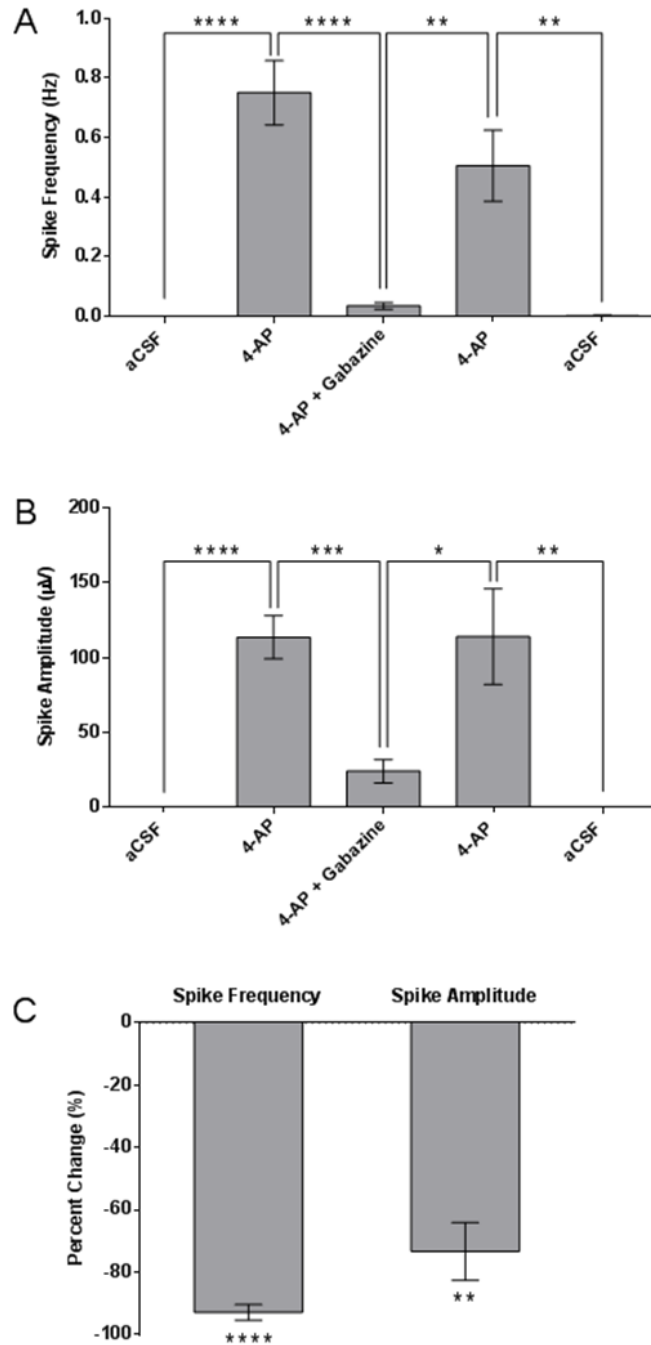


Figure 5.18 The changes in 4-AP-induced population spike frequency and amplitude in the SG of spinal cord slices by GABA_A receptor antagonist gabazine (10 μM). (A) The mean population spike frequencies measured during perfusion of standard aCSF, aCSF with 4-AP and aCSF with 4-AP and gabazine, followed by a wash with 4-AP then a wash with aCSF to show recovery of activity. (B) The mean spike amplitudes measured during each of the same sections of the recording as indicated. (C) The percent change in spike frequency and amplitude from those recorded during 4-AP perfusion and 4-AP with gabazine. (N=5, n=16)

Table 5.3 A summary of the effects of the GABA_A receptor compounds on the 4-AP-induced population spikes in the SG of the spinal cord slices recorded using single electrode extracellular recordings. The symbols ↑ and ↓ indicated a significant increase or decrease respectively in the parameter, and n.s. indicates no significant change.

Compound	Effect on 4-AP-Induced Population Spikes	
	Spike Frequency	Spike Amplitude
GABA	↑	↑
Muscimol	↓	↓
THIP	↓	n.s
L-838417	n.s	n.s
Bicuculline	↓	↓
Gabazine	↓	↓

5.3.2 GABA_B Receptor Compound Effects on Spinal Dorsal Horn Activity

5.3.2.1 Effects on the 4-AP-Induced Rhythmic Activity

The GABA_B receptor agonist baclofen (10 μM) significantly decreased power amplitude and area by an average of $82 \pm 3.7\%$ and $81 \pm 3.4\%$ respectively, but had no effect on the peak frequency of the rhythmic activity (Figure 5.19). Baclofen decreased power amplitude from a mean of 3.80 to 0.73 μV² ($P < 0.05$), and power area from a mean of 17.92 to 3.71 μV².Hz ($P < 0.01$). GABA_B receptor antagonist 2-hydroxysaclofen (10 μM) increased power amplitude and power area of the rhythmic activity, while peak frequency was again unaffected (Figure 5.20). 2-Hydroxysaclofen increased power amplitude on average by $121 \pm 57.7\%$ from a mean of 5.87 μV² to a mean of 10.27 μV² ($P < 0.05$). Power area was increased on average by $127 \pm 66\%$, from a mean of 29.69 to 52.39 μV².Hz ($P < 0.05$). A summary of the effects of GABA_B receptor agonist and antagonists on the 4-AP-induced rhythmic activity in the spinal SG region is shown in Table 5.4.

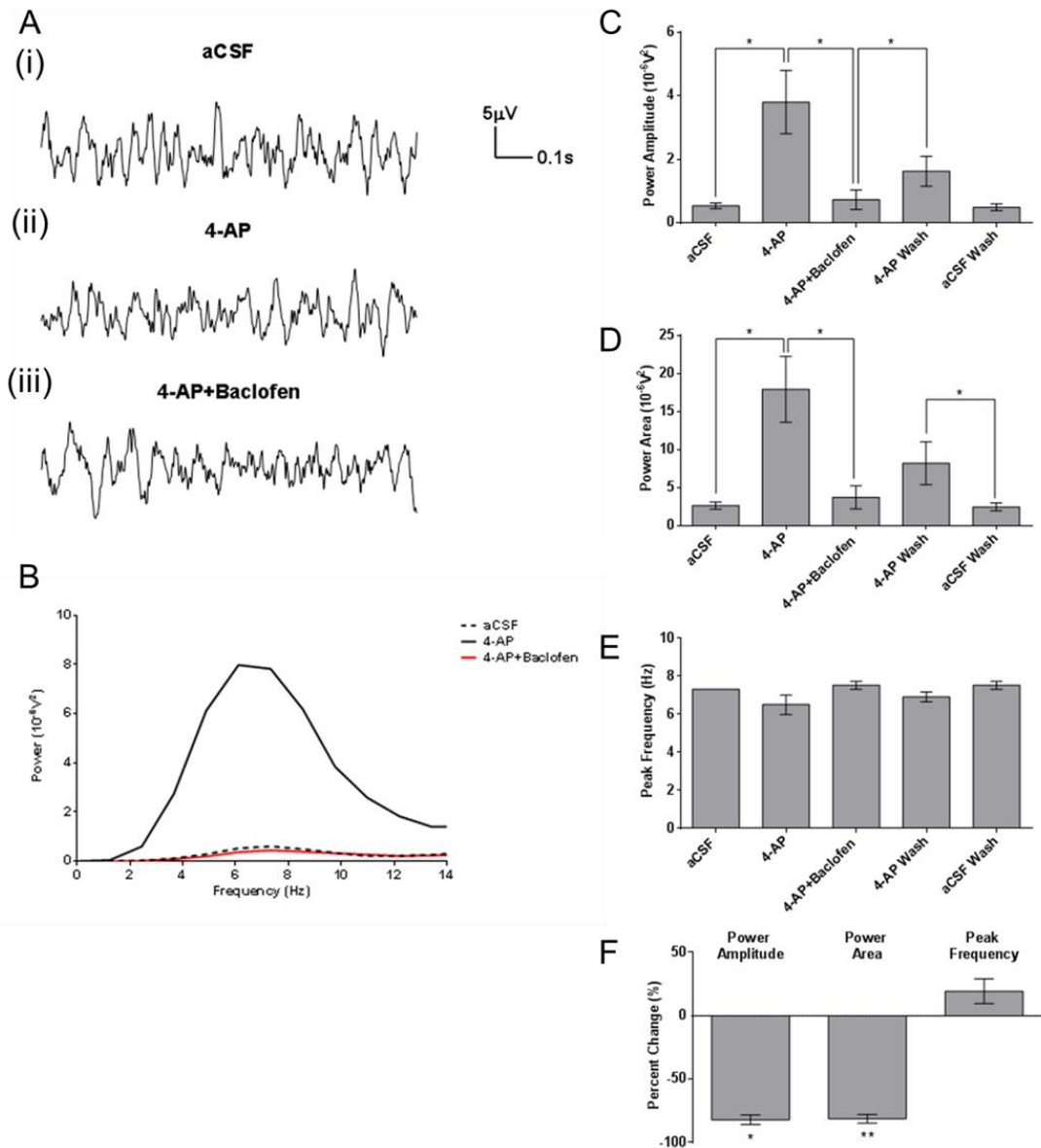


Figure 5.19 The effects of GABA_B receptor agonist baclofen on the 4-AP-induced rhythmic activity in the SG of spinal cord slices recorded from using single electrode extracellular recording technique. (A) Sections of a recording during perfusion of (i) aCSF alone, (ii) aCSF with 4-AP and (iii) aCSF with 4-AP and baclofen (10 μ M). (B) The power spectra generated for each of the sections of the recording described in part (A). (C) The mean power amplitude values for each section of the slice recordings as indicated. (D) The power area values for each section of the slice recordings. (E) The peak frequency values for each section of these slice recordings. (F) The percent change in each of the rhythmic activity parameters, comparing the 4-AP activity to that with 4-AP and baclofen. (N=2, n=6)

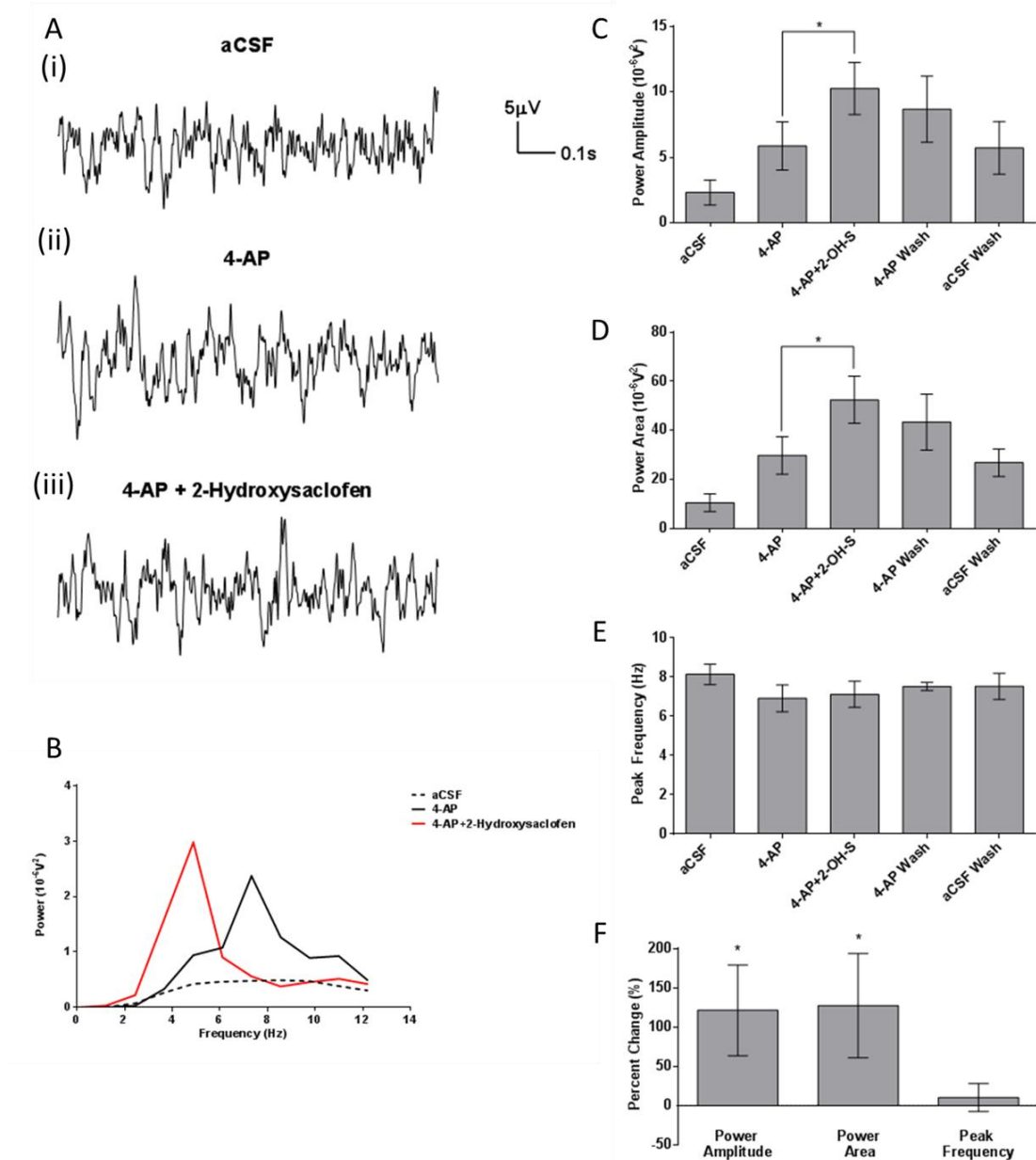


Figure 5.20 The effects of GABA_B receptor antagonist 2-hydroxysaclofen on 4-AP-induced activity in the SG of spinal cord slices recorded from using single electrode extracellular recording technique. (A) Sections of a recording during perfusion of (i) aCSF alone, (ii) aCSF with 4-AP and (iii) aCSF with 4-AP and 2-hydroxysaclofen (2-OH-S) (10 μ M). (B) The power spectra generated for each of the sections of the recording described in part (A). (C) The mean power amplitude values for each section of the slice recordings as indicated. (D) The power area values for each section of the slice recordings. (E) The peak frequency values for each section of these slice recordings. (F) The percent change in each of the rhythmic activity parameters, comparing the 4-AP activity to that with 4-AP and 2-hydroxysaclofen. (N=2, n=6)

Table 5.4 A summary of the effects of the GABA_B receptor agonist baclofen, and antagonist 2-hydroxysaclofen (2-OH-S) on the 4-AP-induced rhythmic activity. The symbols ↑ and ↓ indicated a significant increase or decrease respectively, n.s. indicates no significant change in the parameter.

Compound	Effect on 4-AP-Induced Rhythmic Activity		
	Power Amplitude	Power Area	Peak Frequency
Baclofen	↓	↓	n.s
2-HO-S	↑	↑	n.s

5.3.2.2 GABA_B Receptor Signalling Effects on 4-AP-Induced Population Spikes

Baclofen significantly decreased population spike amplitude and frequency, with almost all spikes being completely eradicated (Figure 5.21). The population spike frequency was reduced by $99 \pm 0.21\%$ on average from 0.52 to 0.003 Hz ($P < 0.05$). Spike amplitude was reduced from a mean of 120.8 to 9.5 μV , an average of $94 \pm 5.6\%$ ($P < 0.05$). Antagonist 2-hydroxysaclofen significantly increased spike frequency but although increases in spike amplitude could be seen the effect was not significant due to large variation (Figure 5.22). On average the population spike frequency increased by $81 \pm 38\%$ from 0.67 to 1.11 Hz ($P < 0.05$). Spike amplitude on average increased by $33 \pm 27\%$ from a mean of 76.84 μV to 106.80 μV ($P > 0.05$). A summary of these effects are displayed in Table 5.5.

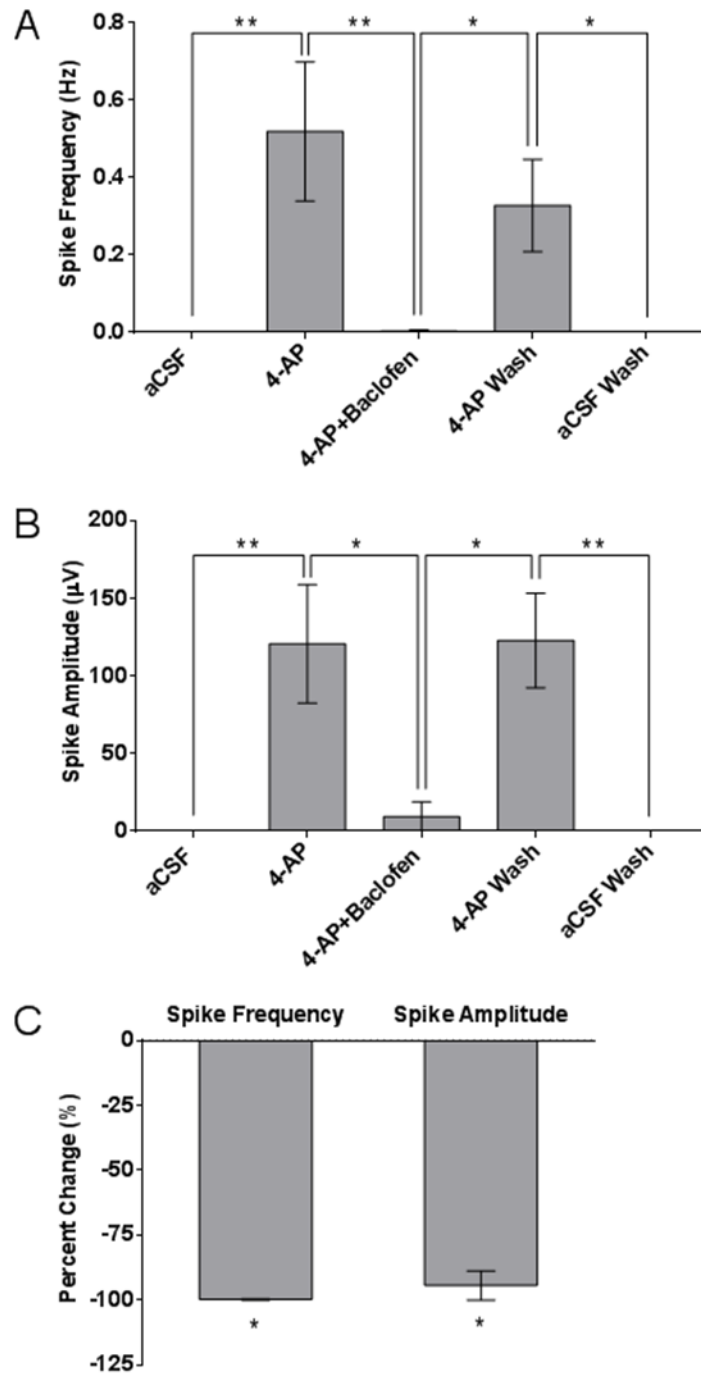


Figure 5.21 The changes in 4-AP-induced population spike frequency and amplitude in the SG of spinal cord slices by GABA_B receptor agonist baclofen (10 µM). (A) The mean population spike frequencies measured during perfusion of standard aCSF, aCSF with 4-AP and aCSF with 4-AP and baclofen, followed by a wash with 4-AP then a wash with aCSF to show recovery of activity. (B) The mean spike amplitudes measured during each of the same sections of the recording as indicated. (C) The percent change in spike frequency and amplitude from those recorded during 4-AP perfusion and 4-AP with baclofen. (N=2, n=6)

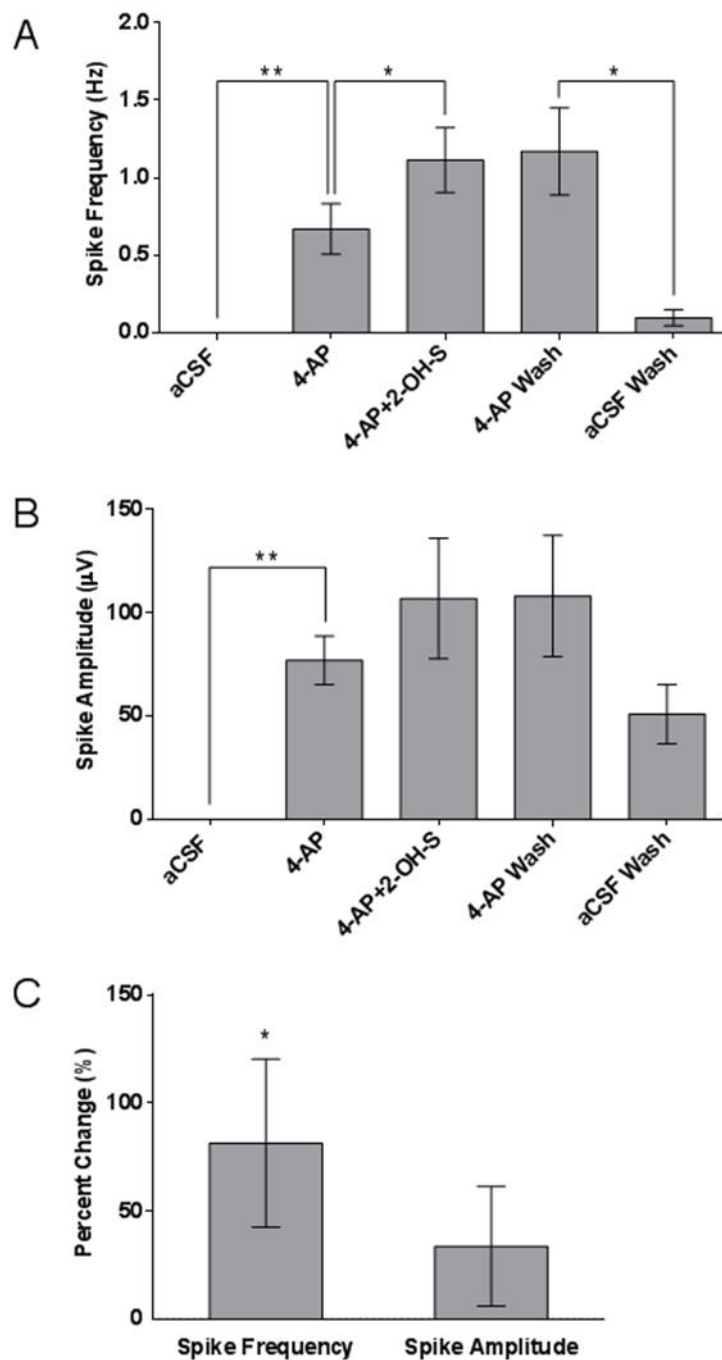


Figure 5.22 The changes in 4-AP-induced population spike frequency and amplitude in the SG of spinal cord slices by GABA_B receptor antagonist 2-hydroxysaclofen (10 μM) (n=6). (A) The mean population spike frequencies measured during perfusion of standard aCSF, aCSF with 4-AP and aCSF with 4-AP and 2-hydroxysaclofen, followed by a wash with 4-AP then a wash with aCSF to show recovery of activity. (B) The mean spike amplitudes measured during each of the same sections of the recording as indicated. (C) The percent change in spike frequency and amplitude from those recorded during 4-AP perfusion and 4-AP with 2-hydroxysaclofen.

Table 5.5 A summary of the effects of the GABA_B receptor agonist baclofen, and antagonist 2-hydroxysaclofen (2-OH-S) on the 4-AP-induced population spikes. The symbols ↑ and ↓ indicated a significant increase or decrease respectively.

Compound	Effect on 4-AP-Induced Population Spikes	
	Spike Frequency	Spike Amplitude
Baclofen	↓	↓
2-HO-S	↑	↑

5.3.3 Glycine Receptor Agonist and Antagonist Effects on Spinal Dorsal Horn Activity

5.3.3.1 Rhythmic Activity

The glycine (2 mM) was perfused on to the spinal cord slices and significantly increased the 4-AP-induced power amplitude by $96.2 \pm 35.1\%$ ($P < 0.05$) from $0.062 \mu\text{V}^2$ with 4-AP perfusion to $0.14 \mu\text{V}^2$ with 4-AP and glycine perfusion. Power area was increased on average by $74.3 \pm 28.2\%$ from a mean of 0.23 to $0.320 \mu\text{V}^2 \cdot \text{Hz}$ ($P < 0.01$) (Figure 5.23). The peak frequency of the oscillations was not affected by glycine ($P > 0.05$). Strychnine (10 μM), the potent and selective glycine receptor antagonist, decreased the power amplitude and power area of the DH rhythm by 43.2 and 54.6% respectively, but did not affect the peak frequency ($P > 0.05$) (Figure 5.24). Power amplitudes were decreased from a mean of 8.21 to $2.34 \mu\text{V}^2$ ($P < 0.001$), and power area was decreased from 15.67 to $5.41 \mu\text{V}^2 \cdot \text{Hz}$ ($P < 0.05$). Table 5.6 summarises the effects of glycine and strychnine on the 4-AP-induced rhythmic activity in the spinal DH.

5.3.3.2 Population Spikes

Glycine did not affect population spike frequency, the mean spike frequency with 4-AP perfusing the slices was 6.98 Hz, and with glycine the frequency was 6.64 Hz ($P>0.05$). However, the population spike amplitude was significantly increased by $197.2 \pm 52.9\%$ on average, from 70.3 to 139.7 μV ($P<0.05$) (Figure 5.25). Strychnine reduced the population spike frequency by $83 \pm 7.4\%$ from a mean of 0.70 to 0.12 Hz with strychnine ($P<0.01$). Strychnine's effects on spike amplitude were extremely variable, with an overall decrease of $40 \pm 36.2\%$, consequently no significant effect was determined ($P>0.05$) (Figure 5.26).

Table 5.7 summarises the effects of glycine and strychnine on the 4-AP-induced population spike amplitude and frequency in the DH of the spinal cord slices.

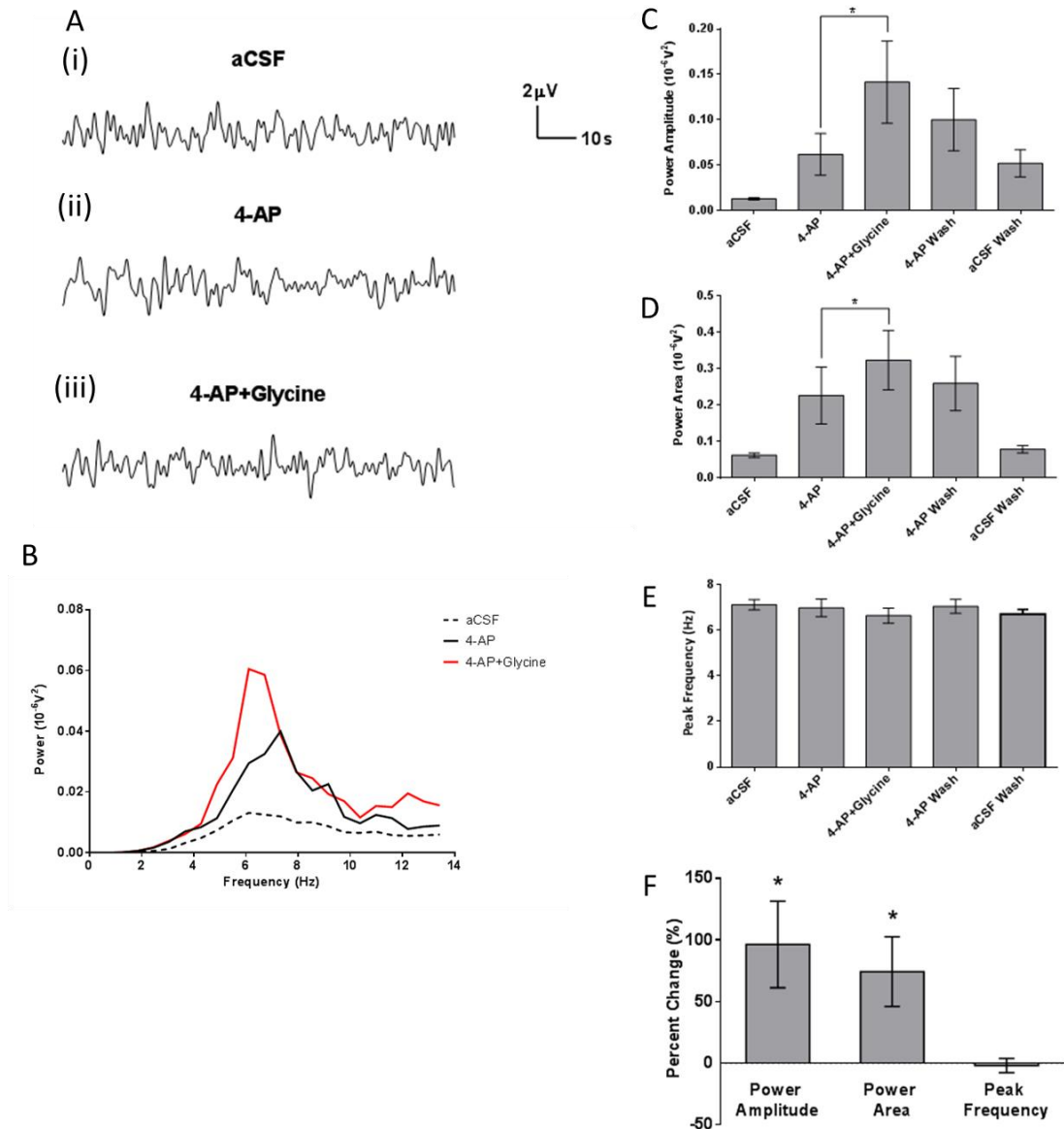


Figure 5.23 The effects of glycine on 4-AP-induced activity in the SG of spinal cord slices recorded from using single electrode extracellular recording technique. (A) Sections of a recording during perfusion of (i) aCSF alone, (ii) aCSF with 4-AP and (iii) aCSF with 4-AP and glycine (2 mM). (B) The power spectra generated for each of the sections of the recording described in part (A). (C) The mean power amplitude values for each section of the slice recordings as indicated. (D) The power area values for each section of the slice recordings. (E) The peak frequency values for each section of these slice recordings. (F) The percent change in each of the rhythmic activity parameters, comparing the 4-AP activity to that with 4-AP and glycine. (N=3, n=7)

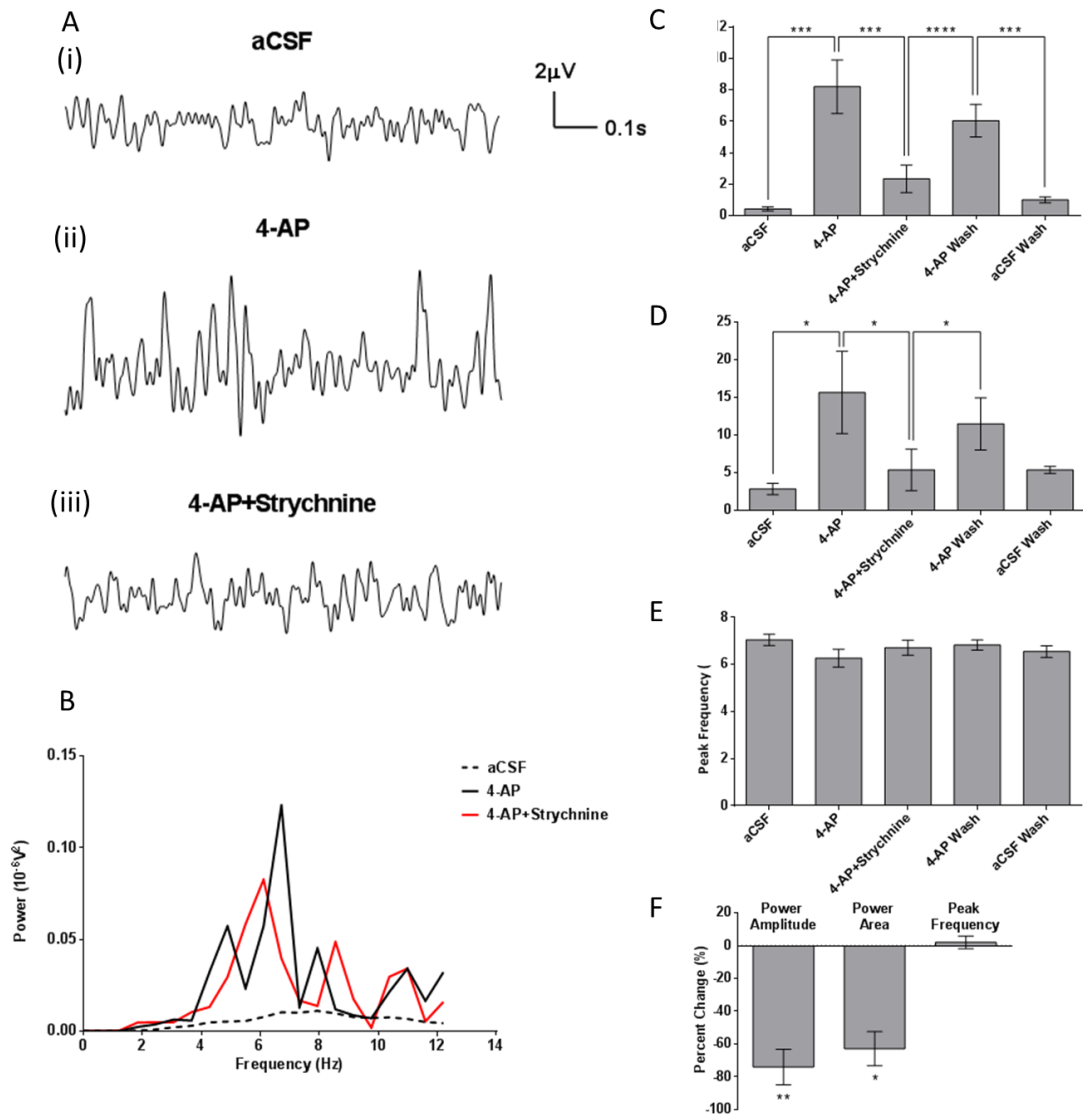


Figure 5.24 The effects of glycine receptor antagonist strychnine on 4-AP-induced activity in the SG of spinal cord slices recorded from using single electrode extracellular recording technique. (A) Sections of a recording during perfusion of (i) aCSF alone, (ii) aCSF with 4-AP and (iii) aCSF with 4-AP and strychnine (10 μ M). (B) The power spectra generated for each of the sections of the recording described in part (A). (C) The mean power amplitude values for each section of the slice recordings as indicated. (D) The power area values for each section of the slice recordings. (E) The peak frequency values for each section of these slice recordings. (F) The percent change in each of the rhythmic activity parameters, comparing the 4-AP activity to that with 4-AP and strychnine. (N=3, n=8)

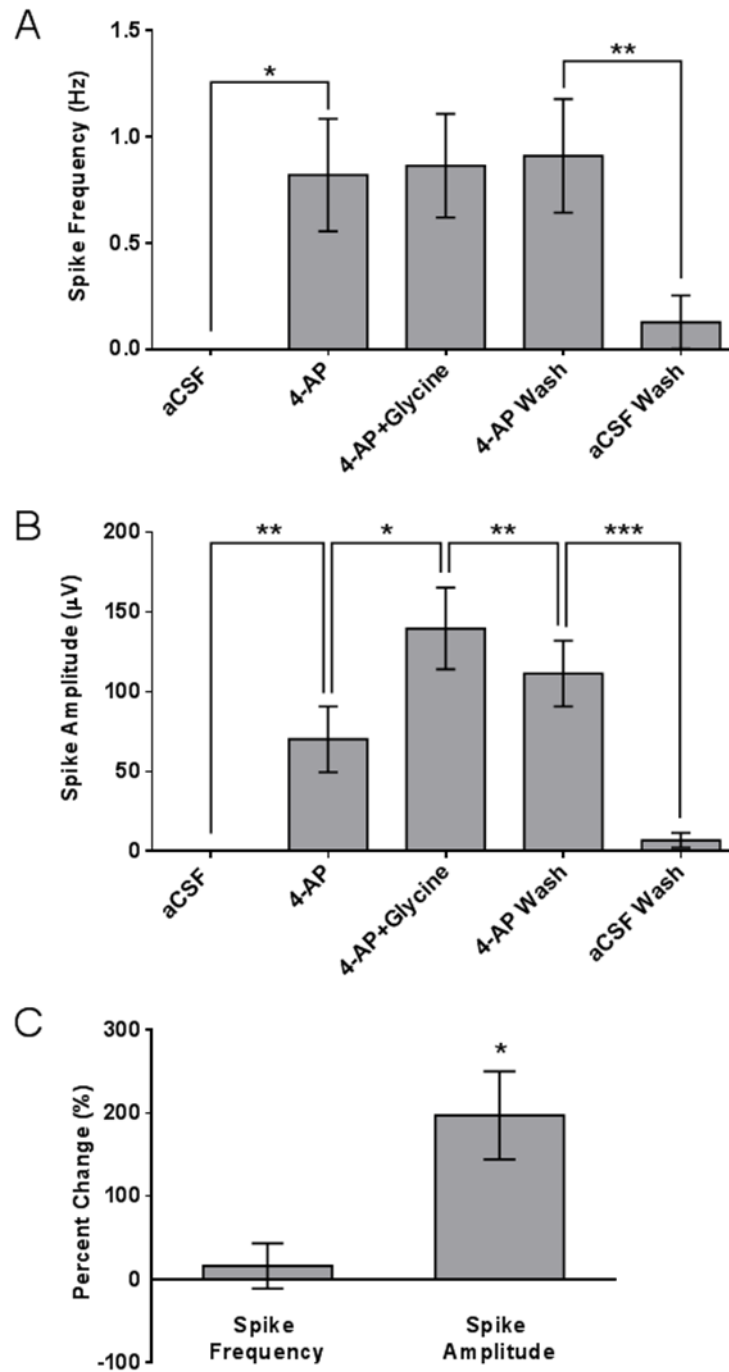


Figure 5.25 The changes in 4-AP-induced population spike frequency and amplitude in the SG of spinal cord slices by glycine (2 mM). (A) The mean population spike frequencies measured during perfusion of standard aCSF, aCSF with 4-AP and aCSF with 4-AP and glycine, followed by a wash with 4-AP then a wash with aCSF to show recovery of activity. (B) The mean spike amplitudes measured during each of the same sections of the recording as indicated. (C) The percent change in spike frequency and amplitude from those recorded during 4-AP perfusion and 4-AP with glycine. (N=3, n=11)

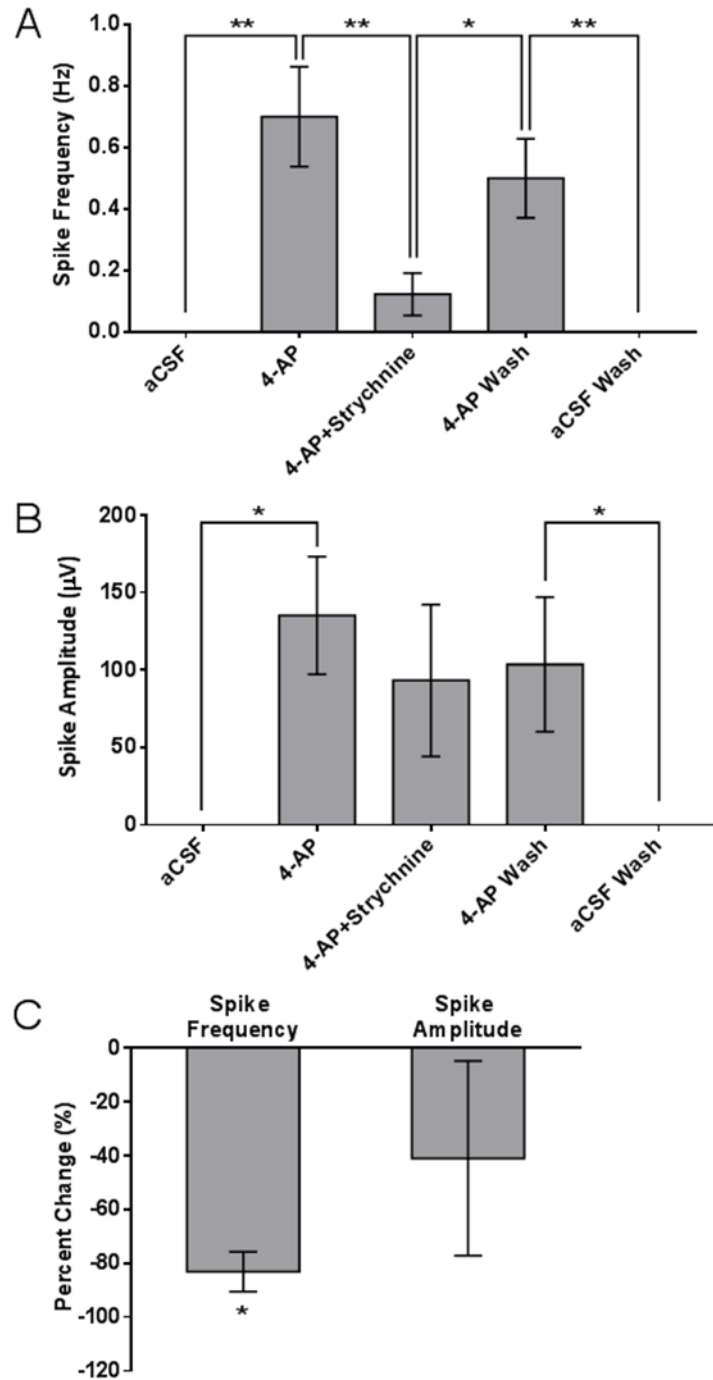


Figure 5.26 The changes in 4-AP-induced population spike frequency and amplitude in the SG of spinal cord slices by glycine receptor antagonist strychnine (10 μ M). (A) The mean population spike frequencies measured during perfusion of standard aCSF, aCSF with 4-AP and aCSF with 4-AP and strychnine, followed by a wash with 4-AP then a wash with aCSF to show recovery of activity. (B) The mean spike amplitudes measured during each of the same sections of the recording as indicated. (C) The percent change in spike frequency and amplitude from those recorded during 4-AP perfusion and 4-AP with strychnine. (N=3, n=8)

Table 5.6 A summary of the effects of the glycine and strychnine on the 4-AP-induced rhythmic activity in the SG. The symbols ↑ and ↓ indicated a significant increase or decrease respectively, n.s. indicates no significant change.

Compound	Effect on 4-AP-Induced Rhythmic Activity		
	Power Amplitude	Power Area	Peak Frequency
Glycine	↑	↑	n.s
Strychnine	↓	↓	n.s

Table 5.7 A summary of the effects of the glycine and strychnine on the 4-AP-induced population spike activity in the SG. The symbols ↑ and ↓ indicated a significant increase or decrease respectively, n.s. indicates no significant change.

Compound	Effect on 4-AP-Induced Population Spikes	
	Spike Frequency	Spike Amplitude
Glycine	n.s	↑
Strychnine	↓	n.s

Tables 5.8 and 5.9 display a comprehensive list of the effects of all the compounds tested on the spinal cord slices against the 4-AP-induced rhythmic activity (Table 5.8) and population spike activity (Table 5.9) in the SG of the spinal DH.

Table 5.8 Summary of the actions of each compound applied on the 4-AP-induced rhythmic activity in the SG of the spinal cord slices. ↑ signifies a significant increase in that parameter compared to 4-AP alone. ↓ signifies a significant decrease in the parameter compared to 4-AP, and n.s. signifies no significant change in the parameter.

Receptor Selectivity and Action	Compound	Effect on 4-AP-Induced Rhythmic Activity		
		Power Amplitude	Power Area	Peak Frequency
GABA_A Agonist	GABA	n.s.	n.s.	n.s.
GABA_A Agonist	Muscimol	↓	n.s.	n.s.
GABA_A Agonist	THIP	↓	↓	n.s.
GABA_A PAM	L-838,417	↓	↓	n.s.
GABA_A Antagonist	Bicuculline	↓	↓	↑
GABA_A Antagonist	Gabazine	↓	↓	↑
GABA_B Agonist	Baclofen	↓	↓	n.s.
GABA_B Antagonist	2-Hydroxysaclofen	↑	↑	n.s.
Glycine Agonist	Glycine	↑	↑	n.s.
Glycine Antagonist	Strychnine	↓	↓	n.s.

Table 5.9 Summary of the actions of each compound applied on the 4-AP-induced population spike amplitude and frequency in the SG of the spinal cord slices. ↑ signifies a significant increase in that parameter compared to 4-AP alone. ↓ signifies a significant decrease in the parameter compared to 4-AP, and n.s. signifies no significant change in the parameter.

Receptor Selectivity and Action	Compound	Effect on 4-AP-Induced Population Spikes	
		Spike Frequency	Spike Amplitude
GABA_A Agonist	GABA	↑	↑
GABA_A Agonist	Muscimol	↓	↓
GABA_A Agonist	THIP	↓	n.s.
GABA_A PAM	L-838,417	n.s.	n.s.
GABA_A Antagonist	Bicuculline	↓	↓
GABA_A Antagonist	Gabazine	↓	↓
GABA_B Agonist	Baclofen	↓	↓
GABA_B Antagonist	2-Hydroxysaclofen	↑	↑
Glycine Agonist	Glycine	n.s.	↑
Glycine Antagonist	Strychnine	↓	n.s.

5.4 Discussion

The first aim of this chapter was to record hyperexcitability induced by 4-AP in the SG of transverse spinal cord slices using extracellular single electrode recordings and then perfuse GABA_A, GABA_B and glycine receptor compounds. There were no spikes recorded prior to perfusing the slices with 4-AP, and there was no dominant rhythmic activity frequency. 4-AP (25 μM) produced reliable hyperexcitability in the SG recordings, but not at maximal activity, therefore allowing for further increases in activity with the perfusion of other compounds to be detected, as well as decreases in activity. The second aim of this study was to analyse the rhythmic activity of the recordings induced by 4-AP, which changed following perfusion of many of the compounds investigated. The third aim was to analyse the population spikes that occurred in the presence of 4-AP and determine if these were affected by any of the compounds investigated. All but one of the compounds applied to the spinal cord slices affected the population spikes recorded in the SG.

5.4.1 4-AP Activity and LTP

Increases in rhythmic activity and population spike parameters could be the result of plasticity of the synapses in the network. LTP of synapses has long been known to result from an increased frequency or prolonged stimulation at a synapse (Bliss and Lomo, 1973). This can arise from an increase in expression of AMPA receptors at the synapse as a result of excessive NMDA receptor activation, and/or an increase in AMPA receptor conductance and open probability (Manabe et al., 1992, Shi et al., 1999, Lu et al., 2001, Collingridge et al., 2004). Synaptic strength can occur through an increase in the probability of neurotransmitter release or an increase in the amount of neurotransmitter released at the synapse (Benke et al., 1998, Banke et al., 2000, Tomita et al., 2005). As explained in Chapter 1, rhythmic activity in the

spinal DH is thought to be generated through an intrinsically active neuron or by a specific network of interneurons. Enhancing depolarisation of the intrinsically active neuron or of a network of interneurons in the DH by blocking the potassium channels with 4-AP could lead to LTP by alleviating the voltage-dependent block of NMDA receptors. This increased NMDA receptor activation would lead to LTP as described above. The addition of compounds to the slices could either result in further LTP or reverse the process by long-term depression (LTD), which results from a reduction in stimulation of a synapse and internalisation of AMPA receptors. The two components of the 4-AP-induced activity, population spikes and rhythmic activity could occur due to the different components of LTP. For example, an increase in rhythmic activity could be the effect of an increase in AMPA receptor expression while an increase in population spikes could be due to the increased neurotransmitter release. L-838,417, glycine and strychnine only affected the rhythmic activity or one of the population spike parameters, which could result from their influence in specific components of LTD or LTP. For example, the inhibitory effect of stimulating the GABA_A or glycine receptors with agonists is likely to reduce NMDA receptor activity by repolarisation of the cell membrane. Consequently, this could result in the internalisation of AMPA receptors and therefore LTD of the synapses within the network of the spinal DH. The effect may predominantly affect the rhythmic activity more than the population spike activity of the network.

5.4.2 GABA_A Receptor Agonists Decrease Rhythmic Activity and Population Spikes with the Exception of GABA

Perfusion of GABA_A receptor agonists muscimol, THIP and PAM L-838,417 reduced either power amplitude or power area parameters, or both of the 4-AP-induced rhythmic activity parameters. Only GABA did not significantly change these

parameters. The effects of these compounds on the population spikes mostly concur with their effects on the rhythmic activity, which suggests that the two components of the 4-AP-induced activity are associated. This includes GABA, which did not instigate a significant increase the rhythmic activity parameters, but did increase population spike amplitude and frequency. However, L-838,417 did not have any significant effect on the population spike parameters but did significantly decrease both power amplitude and area of the rhythmic activity.

GABA and agonists of the GABA receptors are typically known for producing an inhibitory, hyper-polarising effect in the CNS. However, it is widely accepted that in neurons where there is a higher expression of the sodium-potassium-chloride cotransporter 1 (NKCC1) and lower KCC2 the effects of GABA are depolarising, producing excitation rather than inhibition (Zhang et al., 2006). NKCC1 accumulates chloride ions inside the cell, along with sodium and potassium ions to balance the electrical charge. KCC2 transporters export a chloride ion along with a potassium ion to balance the charge. During early development there is a higher expression of NKCC1 and lower expression of KCC2. It has been shown in rats that from postnatal day 14 (P14) the expression of NKCC1 increases until P28, where it starts to decline and remains low in adult rats. Whereas in mature neurons there is a higher expression of KCC2 and a lower expression of NKCC1, as KCC2 expression increases more slowly after birth and remains high in adult rats (Coull et al., 2003, Zhang et al., 2006, Asiedu et al., 2012). Changing the expression levels of KCC2 is sufficient to switch GABA polarity between inhibitory and excitatory (Lee et al., 2005, Ben-Ari et al., 2007). In an immature state, when the GABA_A receptor channels are opened there is an efflux of chloride ions, which depolarises the cell, enhancing excitability. In mature, adult rats this is reversed and opening of GABA_A receptor channels causes inhibition, due to an influx of chloride ions (Figure 5.27). The age at which the switch in GABA occurs from being excitatory to inhibitory has

not been consistently verified. Furthermore, it has been published that the GABA switch is complete at different ages in different regions of the CNS. For example, in the rat brainstem the switch in GABA has been reported to occur by P8 (Balakrishnan et al., 2003). In the rat spinal cord, GABA becomes hyperpolarising by P6-7 (Baccei and Fitzgerald, 2004). In the retina there is evidence that the GABA switch does not happen until P14-18 (Fischer et al., 1998). In this study the rats used were P14, therefore according to previously published data in the spinal cord the GABA switch should have occurred and therefore GABA should produce an inhibitory effect. This is consistent with the GABA_A receptor agonists investigated in this study, and the PAM L-838,417, reducing the rhythmic activity and population spikes.

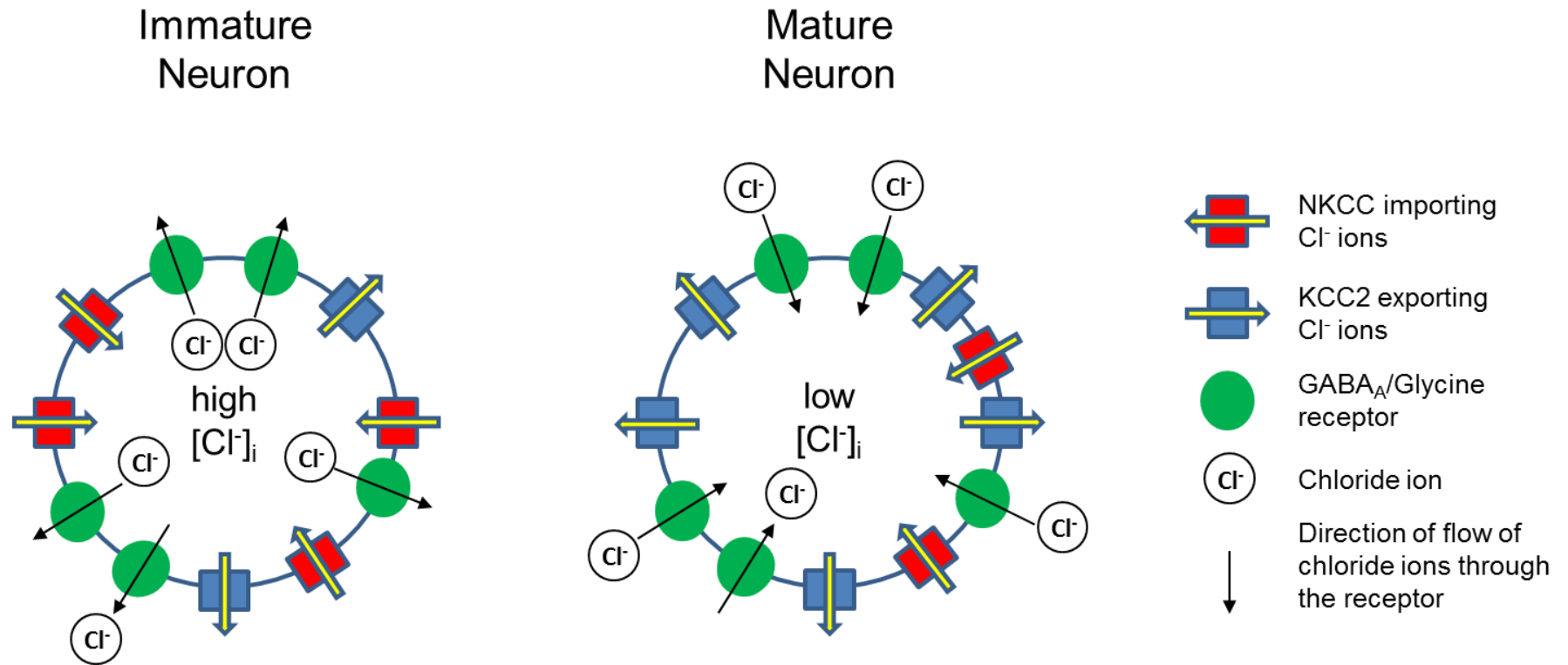


Figure 5.27 A schematic diagram of the switch in direction of chloride ion flux between immature and mature neurons as a result of a change in the expression of the transporters KCC2 and NKCCs. Immature neurons have a higher expression of NKCCs and a lower expression of KCC2s, which causes an accumulation of chloride ions inside the neuron. Therefore an opening of GABA_A and or glycine receptor channels produces a net efflux of chloride ions. The opposite occurs in the mature system where there is a low intracellular chloride ions concentration as a result of an increased KCC2 expression and a decreased NKCC expression.

The different effect on activity observed with GABA compared to the other GABA_A receptor agonists could be because it is the endogenous agonist of both the GABA_A and GABA_B receptors. While GABA_A receptors tend to be located post-synaptically, GABA_B receptors are located both pre- and post-synaptically (Essrich et al., 1998, Yang et al., 2002). Therefore GABA_B receptors can either exert their effects by inhibiting release of neurotransmitter pre-synaptically or by hyperpolarising the post-synaptic cell, preventing propagation of action potentials. Therefore, depending on the expression of GABA_A and GABA_B receptors in excitatory and inhibitory neurons within the spinal DH network their activation could either produce an overall inhibition or excitation of the network. This could explain the different outcome observed with perfusion of GABA with the other GABA_A receptor agonists which are more specific to GABA_A than GABA_B. The selective GABA_A agonists only exert their influence on the GABA_A receptors while GABA influences the activity of both GABA_A and GABA_B receptors when perfused across the slices. Since GABA perfusion increased the population spike frequency and amplitude this could suggest that the activation of those GABA_A and GABA_B receptors located on inhibitory interneurons dominated over the actions of GABA at these receptors located on excitatory interneurons.

Alternatively, the perfusion of GABA on the spinal cord slices could result in desensitisation of the GABA_A and GABA_B receptors from excessive stimulation due to the high GABA concentration. There is evidence that desensitisation of GABA_B receptors results in their internalisation (Guetg et al., 2010). A desensitisation of GABA_B receptors would reduce GABA inhibition as there would be fewer receptors for GABA to bind, which could lead to disinhibition in the spinal DH network and increase excitability. There is also evidence that excessive GABA_A receptor activation leads to membrane depolarisation as a result of a collapse in the chloride concentration gradient, changing the flux of chloride ions through the GABA_A

receptors (Staley et al., 1995). This was suggested to result in a depolarisation of the membrane and therefore remove the voltage-dependent block of NMDA receptors by magnesium. The opening of NMDA receptors would then cause the increase in excitability, which was observed with the perfusion of GABA in this study. The depolarisation of the membrane by excessive GABA_A receptor activation has also been shown to be dependent on an efflux of bicarbonate ions, due to the increase in intracellular chloride ions from the excessive activation of GABA_A receptors (Kaila et al., 1997). GABA_A receptors are also permeable to bicarbonate ions (Kaila and Voipio, 1987). The efflux of bicarbonate ions through the GABA_A receptors would lead to the depolarisation of the membrane.

GABA, muscimol, THIP and L-838,417 also exerts an analgesic effect in *in vivo* and *in vitro* studies. GABA exerts prolonged analgesia following nerve injury *in vivo* (Eaton et al., 1999). Muscimol also has analgesic effects for both thermal and mechanical pain (Miletic et al., 2003). Intrathecal administration of muscimol reduces inflammatory pain and allodynia that result from spinal nerve ligation (Hwang and Yaksh, 1997, Kaneko and Hammond, 1997). Furthermore, THIP and muscimol administration decreases mechanical allodynia following nerve injury (Malan et al., 2002, Rode et al., 2005). THIP is selective for extrasynaptic GABA_A receptors, which typically contain a δ -subunit, particularly receptors composed of $\alpha 4\beta 3\delta$ subunits (Nusser et al., 1998, Brown et al., 2002, Krosgaard-Larsen et al., 2004, Shen et al., 2005). In the neocortex and cerebellum THIP increases δ -subunit containing GABA_A receptor current, producing tonic inhibition (Brickley et al., 1996, Drasbek and Jensen, 2006). Since THIP was the only GABA_A agonist which did not induce any effect on the population spike amplitude in this study, perhaps this is related to this compound primarily binding extrasynaptic receptors. Extrasynaptic GABA_A receptor subtypes have longer decay kinetics, slower desensitisation and a higher affinity for GABA which results in a prolonged, tonic inhibition of the neuron

(Brickley et al., 1996, Saxena and Macdonald, 1996, Devor et al., 2001, Nusser and Mody, 2002). These properties make these extrasynaptic receptors ideal targets for novel analgesics, as there is the potential that a lower dose and/or frequency of dose could be required reducing treatment-associated side-effects.

L-838,417 binds to the benzodiazepine site on GABA_A receptors. The development of this compound was considered a breakthrough in GABA receptor pharmacology due to its high subtype-selective efficacy. L-838,417 does not modulate α 1-containing GABA_A receptors but enhances GABA response in α 2-, α 3- and α 5-containing receptors (McKernan et al., 2000). This is highly beneficial for the analgesic properties of this compound, as without the efficacy at α 1-containing GABA_A receptors this compound does not display sedative effects like many other compounds but retains its properties as an analgesic and anxiolytic. *In vivo* application of L-838,417 has been shown to exert anti-hyperalgesic effects in inflammatory and neuropathic pain models (Knabl et al., 2008). Despite the numerous advantages of this compound, L-838,417 could not undergo clinical trials due to its pharmacokinetic limitations. Since the development of this compound others have been designed based on its structure, including CTP-354, which retains the advantageous properties of L-838,417 and has improved pharmacokinetics (Knabl et al., 2008). CTP-354 is currently undergoing clinical trials for the treatment of pain and spasticity resulting from spinal cord injury or multiple sclerosis (CoNCERT Pharmaceuticals Inc, 2015). The results presented in this study show that L-838,417 application to the spinal cord causes a decrease in the power amplitude and area of the rhythmic activity, without affecting the population spikes in the spinal DH. Therefore, the analgesic properties of L-838,417 are likely to be the result of the change in rhythmic activity of the network. Consequently it could be beneficial to design novel analgesics which exert the same effects on these rhythmic activity parameters.

5.4.3 *GABA_A Receptor Antagonists Decrease 4-AP-Induced Rhythmic Activity and Population Spikes in the SG of the Spinal Cord*

GABA_A receptor antagonists bicuculline and gabazine both decreased the power amplitude and area, and increased peak frequency of the rhythmic activity. These were the only compounds to affect the peak frequency of the rhythmic activity. The explanation of the GABA_A agonists utilized in this study cannot be extended to the antagonist bicuculline and gabazine. These antagonists produced an inhibitory effect on the 4-AP-induced hyperexcitability, which is consistent with previously published data that have also used this 4-AP model in the spinal DH (Ruscheweyh and Sandkuhler, 2003, Chapman et al., 2009). Additionally, bicuculline reduced 4-AP-induced activity in the neocortex, where similarly almost all spikes were inhibited (Aram et al., 1991). The circuitry of the superficial DH network could explain the phenomenon of the GABA_A agonists and antagonists both producing an inhibitory effect on the 4-AP-induced hyperexcitability. There is evidence of synapses between two inhibitory interneurons within the spinal DH, as well as synapses between excitatory and inhibitory interneurons (Zheng et al., 2010). Figure 5.28 illustrates two hypothetical series of interneurons in the superficial spinal DH which both exist, according to previous reports, on the synapses between interneurons in the DH. This explanation relies on GABA_A antagonists acting only to inhibit those receptors on the second inhibitory interneuron in Figure 5.28B. There is considerable evidence for inhibitory interneurons in the spinal cord co-releasing GABA and glycine (Bohlhalter et al., 1994). Furthermore, a group of interneurons predominantly bicuculline-sensitive (GABA-dominant) and another group primarily glycine-dominant have been identified in the superficial spinal DH (Takazawa and MacDermott, 2010). If the first inhibitory interneuron in the hypothetical model is GABA-dominant and the second is glycine-dominant, this would concur with the effects observed with bicuculline and gabazine. The inhibition of the GABA_A

receptors at the first inhibitory synapse would prevent the second inhibitory interneuron being inhibited. However, at the second synapse, inhibition of the GABA_A receptors would not prevent the inhibition of the postsynaptic excitatory interneuron as glycine would be released at this synapse inhibiting the post-synaptic interneuron leading to inhibition of the network activity. Inhibitory interneurons in laminae I-IIo may be GABA-dominant while those at the lamina II-III border are mainly glycine-dominant (Inquimbert et al., 2007). The recordings made in this study were from lamina II, which is a likely region where there is a crossover, such that there are some GABA- and some glycine-dominant interneurons.

Alternatively the effects of the antagonists could be explained by a depolarising block. The blocking of inhibition by the GABA_A receptor antagonists could result in excessive excitation by the glutamatergic interneurons to the point where the glutamatergic receptors reach a depolarising block (Bianchi et al., 2012). However, no initial increase in oscillations or population spikes was observed in the recordings with these antagonists from the time-point when they were applied to the slices.

There is evidence that application of 4-AP causes a downregulation of KCC2 (Rivera et al., 2004). A downregulation of KCC2 in the spinal DH would result in an accumulation of chloride ions inside the interneurons, reverting the neurons back to a state similar to that of an immature neuron as illustrated in Figure 5.27. Consequently this would result in GABA_A receptor activation having a depolarising effect and therefore blocking this with an antagonist would have an inhibitory effect. This would be consistent with the antagonists bicuculline and gabazine exerting an inhibitory effect and with the perfusion of GABA having an excitatory effect. However, the inhibition of activity seen with the other GABA_A receptor agonists does not fit with this notion. It is possible that as mentioned previously the actions of these compounds could depend on the location of the GABA_A receptors at which these compounds are effective and the synapses between the interneurons, as

proposed in Figure 5.28. If 4-AP does cause a change in the KCC2 expression and therefore the intracellular chloride ion concentration switching GABA signalling from inhibitory to excitatory, the hypothetical model circuitry proposed in Figure 5.28 would have to be switched so that the agonists and antagonists actions are exchanged compared to those described.

Bicuculline increases allodynia and produces hypersensitivity, lowering pain thresholds (Yaksh, 1989, Sivilotti and Woolf, 1994, Green and Dickenson, 1997, Reeve et al., 1998, Sorkin et al., 1998, Malan et al., 2002). In spinal cord slice *in vitro* studies bicuculline has been shown to produce hypersensitivity in DH neurons. If bicuculline does produce a decrease in excitability *in vivo* as has been shown in the results presented here then the mechanism by which this effect results in enhanced nociception remains to be understood. In understanding this mechanism the development of novel analgesics could be revolutionised.

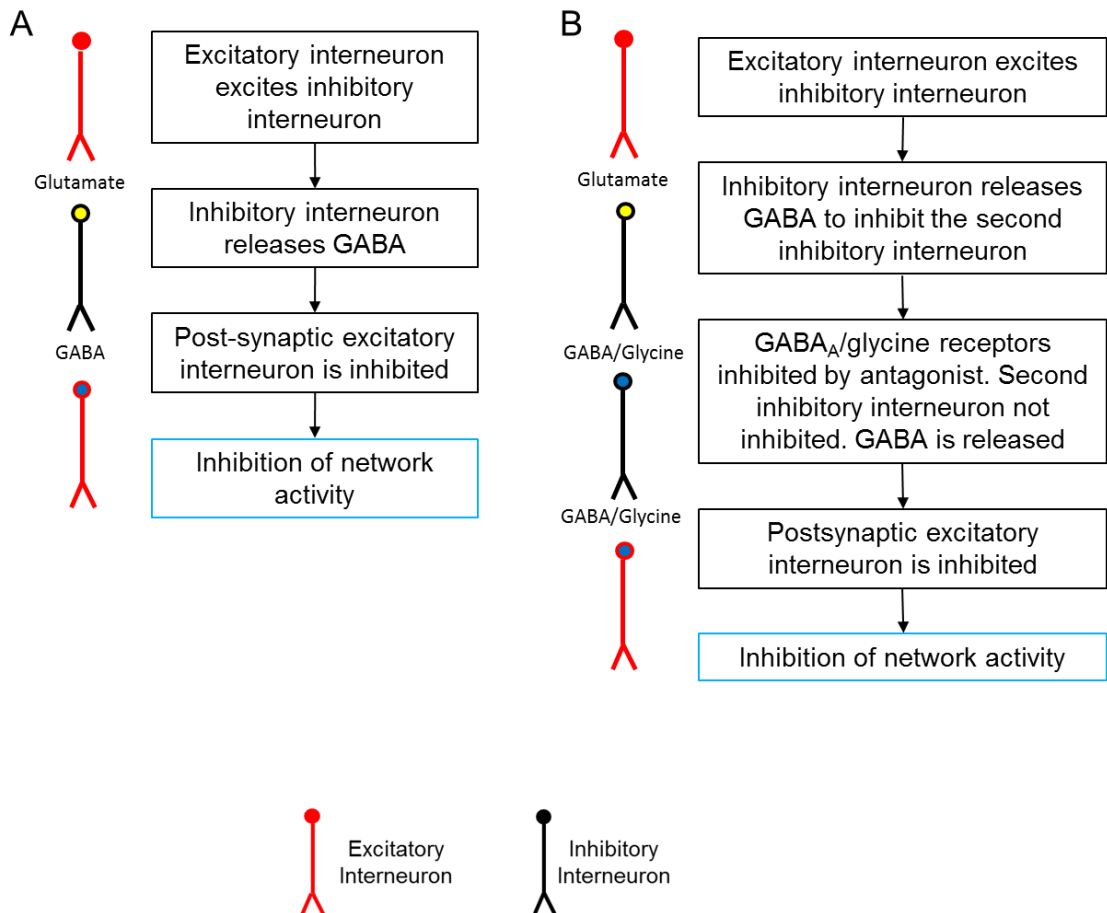


Figure 5.28 Hypothetical models to account for the effects observed with the GABA_A receptor agonists and antagonists. (A) The circuit of two excitatory interneurons intercepted by an inhibitory interneuron. In the presence of a GABA_A receptor agonist this series of interneurons would cause inhibition of the network activity. (B) A circuit where there are two inhibitory interneurons in series. Activation of the first inhibitory interneuron would inhibit the second preventing the second inhibitory interneuron from inhibiting the post-synaptic excitatory interneuron thereby causing an increase in the activity. However, in the presence of an antagonist of GABA_A receptors, the inhibition of the second interneuron would be prevented by the blocking of the GABA_A receptors at the synapse. Thereby the second inhibitory interneuron can inhibit the postsynaptic excitatory interneuron and thus inhibit network excitability. This assumes that the antagonist of the GABA_A receptors only works at those receptors located on the inhibitory interneuron and not the final postsynaptic excitatory interneuron.

5.4.4 *GABA_B Receptor Agonist Inhibits and Antagonist Enhances 4-AP-Induced Rhythmic Activity and Population Spikes*

The GABA_B receptor agonist baclofen produced an inhibitory effect on both the rhythmic activity and population spikes. Additionally, the antagonist of the GABA_B receptor increased the activity. These results correlate with activation of GABA_B receptor producing hyperpolarisation, by inhibiting calcium channel conductance and increasing potassium channel conductance (Chronwall et al., 2001). GABA_B receptors are located both pre- and post-synaptically, and are predominantly expressed in lamina I and II of the spinal DH. Pre-synaptically they inhibit calcium channels and therefore prevent the release of neurotransmitters into the synaptic cleft while post-synaptically they hyperpolarise the membrane by opening potassium channels (Yang et al., 2001). The data of this study imply GABA_B receptors are involved in modulating the rhythmic activity within the spinal DH as well as the population spikes. Baclofen has anti-nociceptive effects in rat models of neuropathic pain and has been used clinically as an analgesic and anti-spastic drug (Sokal and Chapman, 2003). Baclofen and PAM of GABA_B CGP7930 act as analgesics to mechanically induced visceral pain (Brusberg et al., 2009). In addition, it is effective in the treatment of headache, migraines and trigeminal neuralgia (Hering-Hanit, 1999, Hering-Hanit and Gadoth, 2000, 2001). Interestingly, the CNS actions of baclofen have a more significant role for its analgesic effects than in the periphery (Gangadharan et al., 2009). Therefore, the effects of GABA_B receptor signalling on the spinal DH rhythm and spikes could explain the higher effectiveness of baclofen in the CNS as opposed to the periphery.

The GABA_B antagonist 2-hydroxysaclofen can reverse the inhibition and anti-nociceptive actions of baclofen *in vivo* (Yajima et al., 2000). There is evidence of GABA_B receptors controlling the release of transmitter from primary afferents in the spinal DH (Marvizon et al., 1999, Ataka et al., 2000). Since GABA_B receptors are G-

protein coupled receptors (GPCRs), they modulate the DH rhythmic activity and population spikes by a different mechanism to the ionotropic GABA_A receptors. This could explain the differences observed between the antagonists of the GABA_A receptors and the GABA_B antagonist 2-hydroxysaclofen. The GABA_B receptors control the release of GABA from inhibitory interneurons in the spinal DH by regulating P/Q-type calcium channels (Yang et al., 2015). Therefore, baclofen inhibiting the activity in the DH could act through preventing the inhibition of a postsynaptic excitatory interneuron, as illustrated in Figure 5.28A.

5.4.5 Glycine receptor compound effects on spinal dorsal horn activity

As well as GABA, glycine is known as one of the main inhibitory neurotransmitters in the CNS. Similarly to GABA, glycine produced an increase in the 4-AP-induced rhythmic activity with the effects being significant for power amplitude and area. Glycine also increased population spike amplitude but did not significantly increase the frequency. Moreover, the potent glycine receptor antagonist strychnine reduced power amplitude and area of the 4AP-induced rhythmic activity. The population spike frequency and amplitude were also decreased. This is consistent with the GABA_A receptor antagonist effects. Therefore, it appears likely that the electrochemical gradient of chloride ions is not the same as would be expected in an adult. However, glycine is also a co-agonist of the NMDA receptor along with glutamate (Papouin et al., 2012). Therefore, application of glycine is likely to increase the activity of NMDA receptors which will in turn increase excitation. The blocking of the glycine transporters has an analgesic effect *in vivo* (Haranishi et al., 2010). By inhibiting glycine transporters the extracellular concentration of glycine would increase, creating a similar state to that of applying glycine directly as done in this study. This could suggest the mechanism of analgesia in the spinal DH is more

complicated than that proposed in the hypothetical models in Figure 5.28. Alternatively the notion that the chloride electrochemical gradient in the slice is altered by 4-AP could similarly explain this phenomenon of glycine increasing rhythmic activity and population spikes, which concurs with the inhibitory effects of strychnine. The study of the role of glycine receptors is difficult due to the lack of specific compounds acting at this receptor. Strychnine has long been used to separate the effects of GABA from glycine due to its ability to selectively bind the glycine receptor. Strychnine causes pain-like behaviour in animals when applied to the spinal cord (Yaksh, 1989). Co-release of GABA and glycine from a single neuron is known to occur in the superficial spinal DH (Keller et al., 2001). The combined release of these neurotransmitters in the DH could be required for their optimal effects.

5.4.6 *Extracellular Recordings from Spinal Cord Slice Dorsal Horn as a Model for Investigating the Network*

This study has illustrated that this model of 4-AP activity in spinal cord slices, recorded with extracellular recordings, can be utilised to record rhythmic activity in the spinal DH as well as population spikes. The effects of the GABA_A, GABA_B and glycine receptor drugs could also be determined. This recording technique is not amenable to fast high-throughput screening, which does hamper its use in the initial screening of multiple novel drugs. However, this model does provide a more intact DH network platform which is more suited to investigating the physiology of the spinal DH, and studying the rhythmic activity. Although the circuitry cannot be identified through using extracellular recordings it does provide a mechanism in which to study the network as a whole, which is more transferrable to *in vivo*

studies. The spinal DH circuitry is unknown and its complexity limits the predictive power of this assay.

6 Multi-Electrode Array with Spinal Cord Slices and Cultured Dorsal Horn Cells

6.1 Introduction

A MEA typically consists of an arrangement of 60 titanium nitride electrodes embedded in a glass base-plate recording area. MEAs come with various arrangements of electrodes which can be of different sizes, distances apart and arrangements (Multi Channel Systems, Germany). The electrodes on the base recording area are surrounded so that there is a chamber in which cells can be cultured or slices can be perfused. Each electrode on a MEA detects the extracellular field potentials of the surrounding population of cells. Fast voltage transients can be detected, which correspond to the combined action potentials of a number of neurons in contact with the electrode. This recording technique can be done over longer periods of time compared to intracellular recording methods (Spira and Hai, 2013). The development of MEA technology is centred on improving our understanding of neuronal network connectivity and their physiological function. The research of neuronal networks has been limited by the electrophysiological techniques available. While extracellular recordings are stable for long duration recordings from large populations of cells, intracellular recordings can measure subthreshold membrane oscillations and individual cell EPSPs or IPSPs but are less stable recordings (Spira and Hai, 2013, Kruskal et al., 2015). Intracellular recording from hundreds of individual neurons simultaneously, where individual neurons could be stimulated by current injection, would be the ideal technique to facilitate our understanding of the involvement of individual neurons in network activity. Currently there are a number of approaches which are tackling the development of such a technique (Ojovan et al., 2015). Until the development of this technique is finalised, MEA technology with slices or cultured cells provides a method by which the activity of a neuronal network can be measured simultaneously at multiple sites across the slice or cultured cell network (Streit et al., 2001, Xiang et al., 2007, Hill et al., 2010, Baltz and Voigt, 2015). The electrodes of an MEA can cover an area of between

700 μm^2 to 5 mm^2 depending on electrode arrangement and electrode size (Multi Channel Systems, Germany). Therefore, the firing behaviour across different brain regions or multiple spinal laminae of a rodent tissue slice section can be detected simultaneously. Furthermore, the synchronicity of activity across a slice or a cultured network of cells can also be determined from MEA recordings. The primary advantage of this type of extracellular recording over the single electrode recordings is that the activity at 60 distinct locations on a tissue slice or culture is recorded simultaneously, which enables comparisons to be made between multiple regions.

As used previously with the single electrode recordings from spinal cord slices, in this chapter 4-AP was used to induce activity in the spinal cord slices with the MEA recording technique. The 4-AP model of epilepsy has been investigated with MEA technology with brain slices (Hill et al., 2010). MEA recordings from hippocampal slices have shown that synchronous firing occurs with application of 4-AP (Grosser et al., 2014). Grosser *et al* (2014) also confirmed that GABAergic interneurons synchronously fire in these slices. These synchronously firing GABAergic interneurons were proposed to be what gave rise to the recorded inhibitory local field potentials (LFPs). In this study GABA_A, GABA_B and glycine receptor agonists and antagonists were applied to the acute spinal cord slices and cultured DH cells during MEA recordings to explore the roles of these receptors in the spinal DH network and provide an indication of the utility of the MEA assay with the two *in vitro* models for screening novel compounds.

In this chapter MEA spinal cord slice recordings have been compared with the single electrode recordings from the DH of spinal cord slices. Consequently, this allows for validation of both data sets as well as allowing for a comparison of the recordings from the superficial DH with that from the deeper DH laminae and the VH. MEA recordings using the cultured DH cells provide a non-invasive electrophysiological technique to directly record the electrical activity of the culture

network. The MEA recordings from the spinal DH cell culture can be compared with that of the spinal cord slices, which will help to determine the potential of this cell culture model for investigating the activity of the network of the superficial DH and its potential as a screening platform for novel analgesics. Furthermore, the MEA recordings performed using the cultured DH cells can also be compared with the data obtained from the calcium imaging assays with the culture. The calcium imaging experiments provided an indirect method to measure the whole network activity and its responses to pharmacological compounds, while the DH culture MEA recordings directly measure the electrical activity at multiple sites across the culture.

6.1.1 Aims

The aims of this investigation using MEA methodology, as applied to both acute spinal cord slices and cultured DH cells, were:

1. To determine whether 4-AP-induced hyperexcitability recorded within SG using the single microelectrode method in acute spinal cord slices can be replicated under MEA recording conditions.
2. To use MEA technology to determine more fully the extent and spread of 4-AP-induced hyperexcitability manifest across superficial and deep DH and VH.
3. To compare and contrast the effects of glycinergic and GABA-ergic pharmacological tools on 4-AP-induced hyperexcitability recorded using either the single microelectrode technique or MEA technology
4. To determine whether inhibition of the potassium chloride cotransporter KCC2 can modify 4-AP-induced hyperexcitability under MEA conditions
5. To determine whether spontaneous activity of the cultured DH cells detected using the calcium imaging assay additionally manifests as electrical events that can be recorded as population field activity using MEA technology.

6. To evaluate the effects of glycinergic and GABAergic pharmacological tools on spontaneous electrical activity recorded from cultured DH cells using MEA technology.

6.2 Methods

6.2.1 Multi-Electrode Extracellular Spinal Cord Slice Recordings

Transverse lumbar spinal cord slices from Wistar rats (12-16 days old) were cut to a thickness of 350 μm and incubated at 32°C in standard, oxygenated aCSF for one hour as described previously in Chapter 5. After the incubation period a slice was placed into the well of a perforated multi-electrode array (MEA) (Multi Channel Systems, Germany). The MEA has 60 3-D microelectrodes arranged on an 8 x 8 grid, with an internal reference electrode (

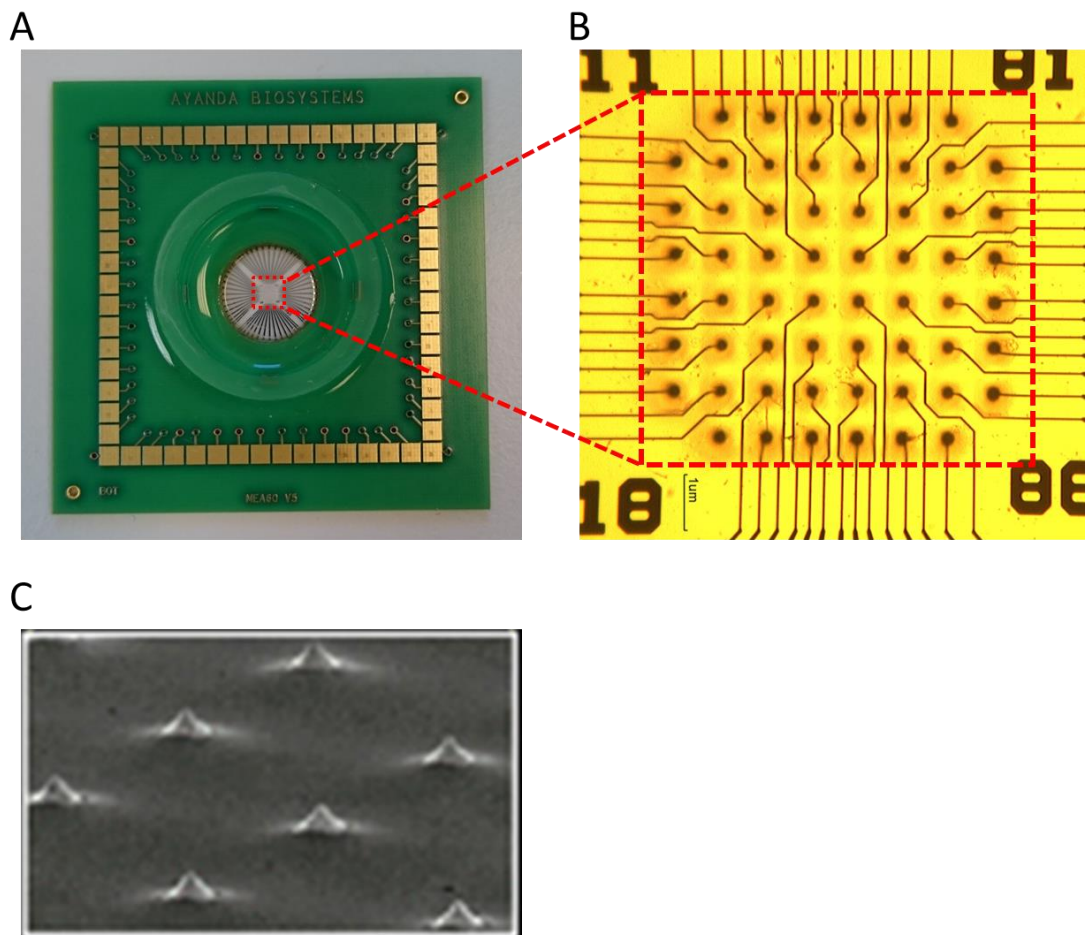


Figure 6.1). The microelectrodes were of low density (electrodes spaced 200 μm apart, diameter 40 μm , height 45 μm) and titanium nitrate-coated. Placing the MEA

onto the preamplifier headstage platform in the rig the slice could then be seen using an inverted CK40 Olympus microscope (Figure 6.2). The slice could be moved around the base of the MEA using a pasture pipette with standard aCSF solution to push the slice without damaging it and keeping it moist. The slice was positioned so that as many electrodes as possible were located on the SG region (Figure 6.3). To prevent the slice moving during the perfusion of the aCSF a harp slice grid (ALA Scientific Instruments, USA) was placed on top of the slice using fine forceps (Figure 6.3). This improves the contact of the slice with the electrodes thereby reducing the noise of the recordings at the electrodes. The MEA was clamped to the headstage between a heating element and the MEA1060-Inv-BC-PA amplifier. The MEA1060-Inv-BC-PA amplifier was connected to a FA60SBC filter amplifier, which in turn was linked to the computer with MC Rack software (Multi Channel Systems, Germany) so that the signal can be digitised and the data captured for analysis. The temperature of the heating element under the MEA chip and that of an inline PH01 perfusion cannula was controlled by a TC02 temperature control unit. The temperature of the perfusing solution and the bath solution could therefore be maintained at 37°C. A Minipuls 3 peristaltic pump (Gilson, Middleton, USA) was used to perfuse the slice at a rate of 1.5-2 ml/min. The perfusion outlet was operated by a constant vacuum pump (CVP), with the cannula outlet submerged in the bath solution to remove aCSF. Therefore there was a continuous flow of fresh, oxygenated aCSF either with or without a compound depending on the stage of the experiment in progress. For each slice recording the baseline activity was measured for one minute, followed by recording for 25 minutes with aCSF containing 4-AP (25 µM). Each compound tested on the slices was perfused for a subsequent 25 minutes, made in the aCSF with 4-AP solution. A list of the compounds applied and their concentrations can be found in Table 6.1. Each compound was typically tested on 6 slices (n) from at least two different rats (N).

Compound	Concentration (μM)	Supplier	Solvent
GABA	50	Sigma	dH ₂ O
THIP (Gaboxadol Hydrochloride)	50	Sigma	dH ₂ O
Muscimol	10	Sigma	dH ₂ O
Bicuculline methiodide	50	Sigma	dH ₂ O
Gabazine (SR-95531)	10	Sigma	dH ₂ O
Baclofen hydrochloride	10	Sigma	dH ₂ O
2-Hydroxysaclofen	10	Alfa Aesar	DMSO
Glycine	1000	Sigma	dH ₂ O
Strychnine	10	Sigma	DMSO
Gelsemine hydrochloride	30	Extrasynthese	DMSO
VU0240551	30	Sigma	DMSO

Table 6.1 List of compounds applied to the spinal cord slices during the MEA recordings, with their concentrations, supplier and the solvent utilised to dissolve the substance.

6.2.2 MC Rack MEA Data Analysis

The MC Rack software was used for the analysis of the MEA recordings. Electrodes were selected for analysis based on their location on the slice. Those electrodes positioned in the SG region of the superficial spinal DH were used in the analysis and compared with the data from electrodes in the deep DH laminae and ventral horn (VH) according to the images taken for each recording. The recorded data was initially run through a low pass filter with a cut-off frequency of 50 Hz. A spike sorter was used to detect spikes, set at pre-trigger of 100 ms, post-trigger of 200 ms and a dead time of 200 ms. The spike threshold level was set at $-15 \mu\text{V}$, spike analysers could then be set up to determine the peak to peak amplitude and rate of firing.

Values for these parameters were determined for the data during perfusion of 4-AP and during perfusion of 4-AP with the drug of interest added to demonstrate the change in activity as a result of the drug applied. Statistical analysis of the data sets was performed using Graph Pad Prism 6 (GraphPad Software Inc., California, USA). Two-tailed, paired t-tests were used to calculate significance probability between the activity with 4-AP application to that with 4-AP and drug. A one-way ANOVA with a Tukey post-hoc comparison was utilised to compare data sets of each region of the spinal cord, the SG, deep DH and VH. The number of rats utilised per compound tested is denoted N, with the number of individual slices recorded from for each compound is denoted n.

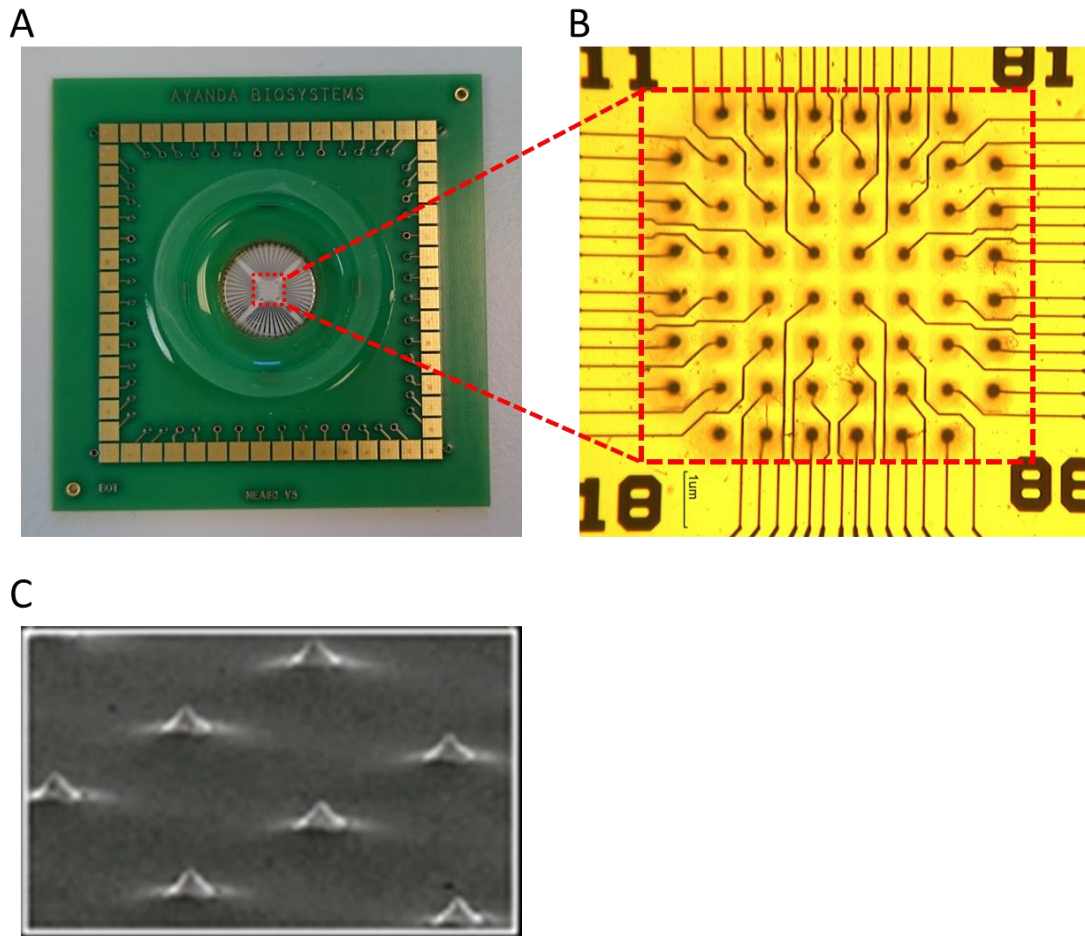


Figure 6.1 (A) A photograph of a perforated MEA probe demonstrating the green plastic base plate with a circular glass centre, enclosed within a well. The electrodes are embedded within the glass and connected to the gold plates that surround the central well. The pins on the headstage of the MEA connect with the gold plates of the array. The photograph was taken with an Xperia Z3 camera (Sony, UK). (B) A photograph of the electrodes on the central glass base of the MEA, taken with Moticam 100 camera (Motic, Barcelona, Spain). (C) An image of the MEA electrodes upon which the slice sits (image is modified from Multi Channel Systems, Japan).

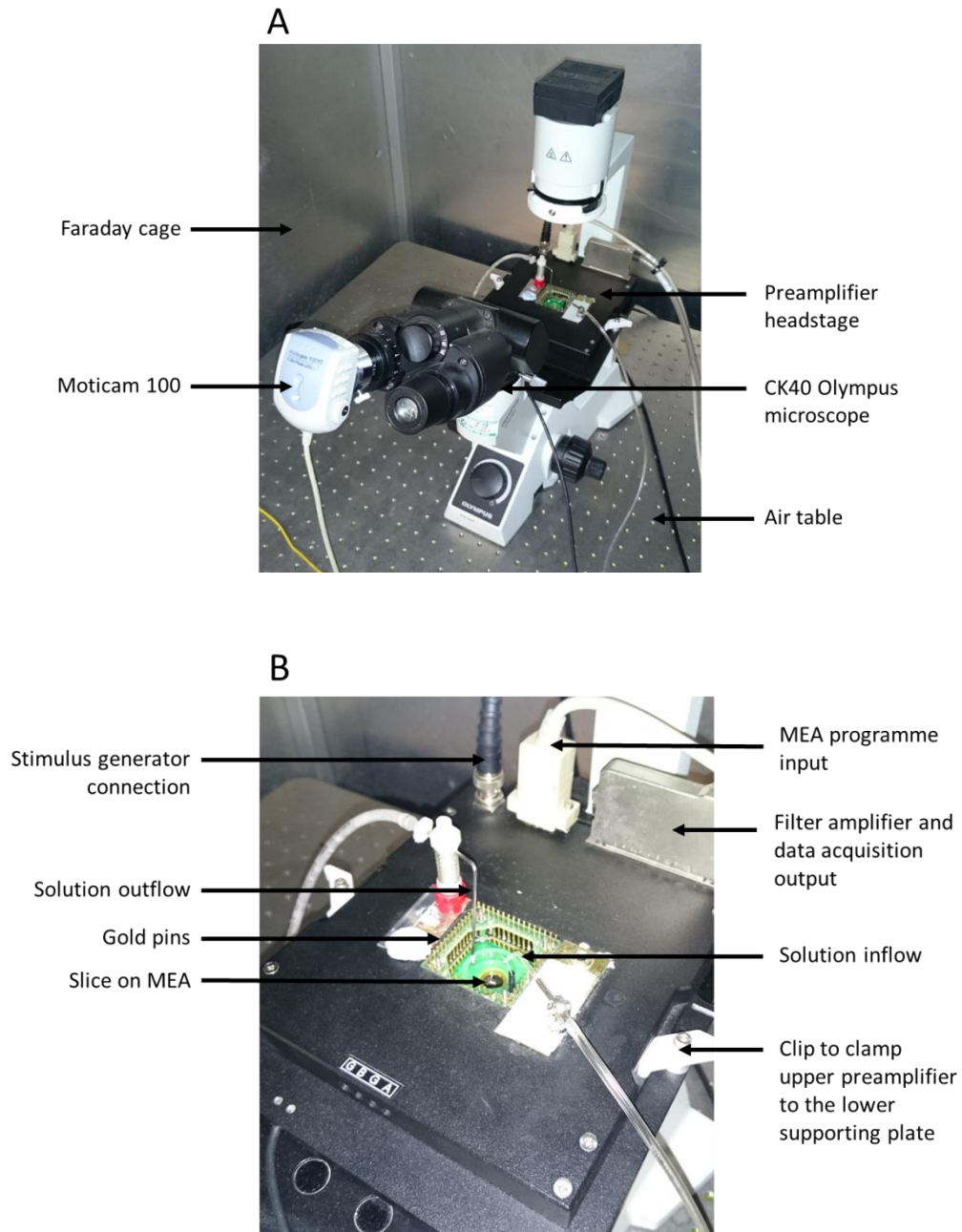


Figure 6.2 Photographs of the MEA rig setup taken with an Xperia Z3 (Sony, UK). (A) The inverted microscope with the preamplifier headstage and Moticam attached. This camera is placed in one of the eye pieces of the inverted CK40 Olympus microscope (Olympus, UK) in the rig on which the MEA preamplifier is situated. This camera was connected to the computer, where Motic Images software was used for image capture. (B) A photograph of the preamplifier headstage, consisting of the lower supporting plate and upper amplifier with the connecting gold pins which are pressed down on to the MEA probe. The probe is placed in the between the supporting plate and the upper preamplifier. The metal plate upon which the MEA probe sits is temperature controlled, and set to 37°C.

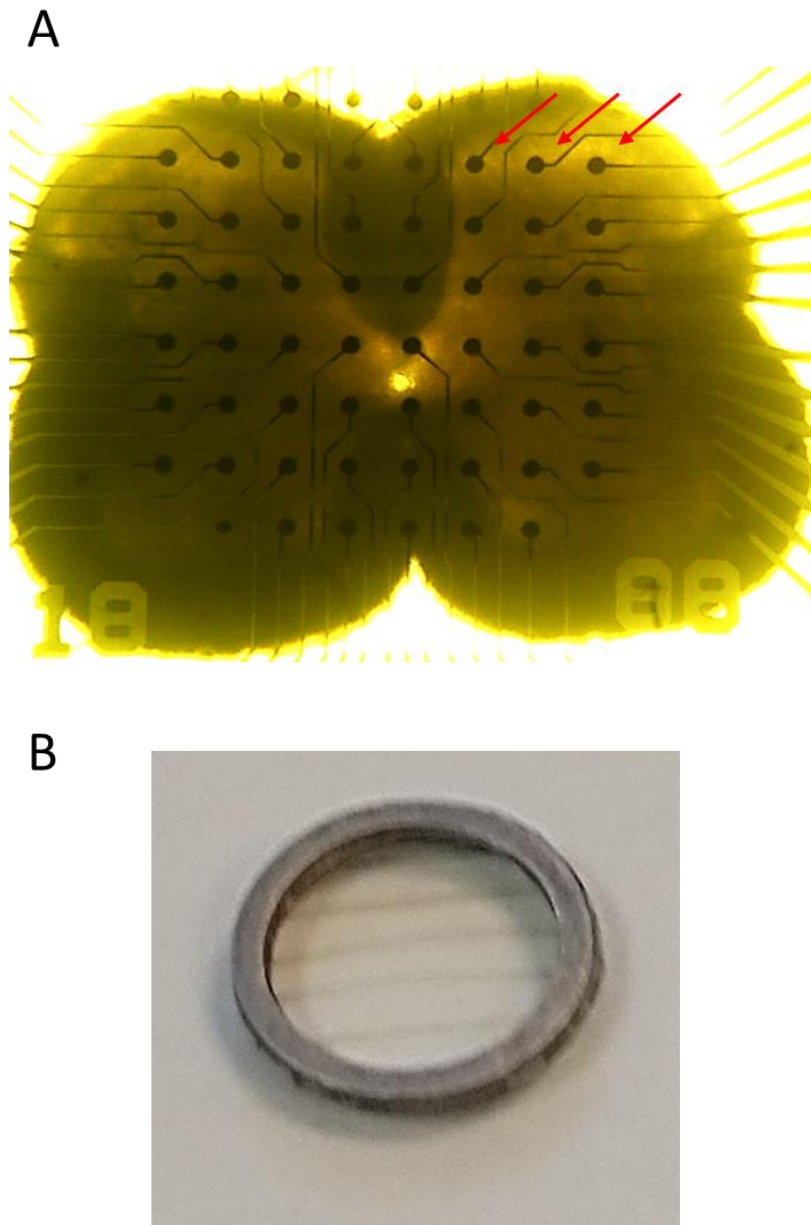


Figure 6.3 (A) A photograph of a lumbar spinal cord slice on an 8x8 MEA probe, taken with the Moticam 100 camera (Motic, Barcelona, Spain). The SG laminae can be seen as more transparent compared to the other laminae and is innervated by three electrodes in each hemisphere of the slice which is indicated by arrows. (B) An image of the harp grid used as a weight to hold the slice in place over the electrodes on the MEA. The harp weighs approximately 0.4 g, consisting of glass-coated steel ring with polyimide-coated silica fibers at 1mm spacing. This photograph was taken using an Xperia Z3 camera (Sony, UK).

6.2.3 *Culturing Embryonic Dorsal Horn Cells on the MED64 Arrays*

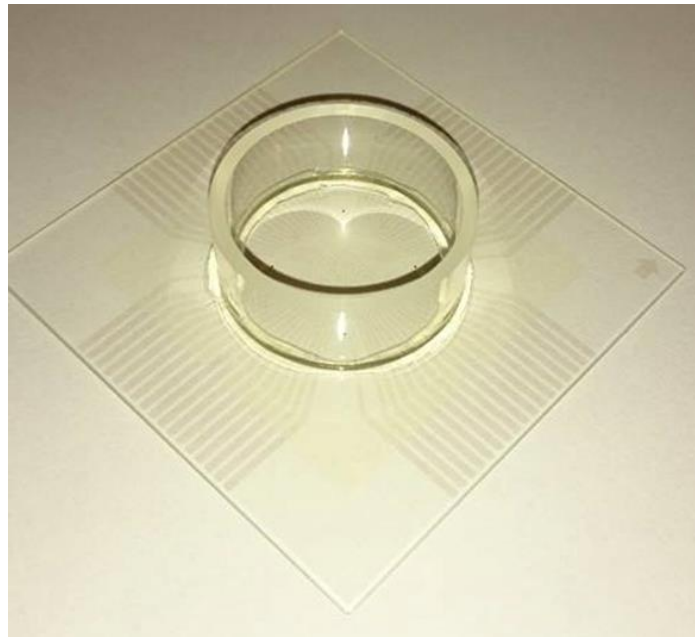
The MEA probes used for cell culture were MED64 probes (Alpha MED Scientific Incorporated, Japan) (Figure 6.4). These were cleaned, sterilised and coated before being used for cell culture. The probes were first treated with 0.1% polyethylenimine (Fulka Analytical) diluted in 28 mM Borate Buffer (Fulka Analytical) at pH 8.4 overnight at room temperature. They were then rinsed with sterile distilled water 3 times before incubation with PBS (Sigma) containing 10% FBS Gold (PAA) and 10% horse serum for 1 hour at 37°C. The probes were rinsed with ethanol and left to dry in a sterile hood, and then further sterilised by exposure to UV light for one hour. Once sterilised the probes were kept in sterile 6 cm petri dishes (Thermo Fisher Scientific, UK). As done previously for the plates, the MED64 probes were coated with poly-D-lysine (>300,000 MW) for a minimum of 24 hours before use, and coated with mouse laminin (0.01 mM) for at least 3 hours before the cells were added and kept at 37°C. The tissue dissection from the embryos at E14 and the processing for the DH tissue was performed as described previously in Chapter 2. Once the cells were added to the MED64 probes with a cell density of 1.5×10^6 cells/probe, the probes were then pulse spun to 1000 rpm using an eppendorf centrifuge (Eppendorf AG, USA). The MED64 probes were kept in the sterile 6 cm petri dishes and incubated at 37°C. The same procedure of media changes were performed as described for culturing the cells on 96-well plates for up to 14 days.

6.2.4 *MED64 Recordings with Cultured Dorsal Horn Cells*

The cultured DH cells on the MED64 probes were recorded at day 12-14 in culture. The media was removed and replaced with 1 ml HBSS (-/-) with added calcium chloride (1.8 mM) and 1% HEPES, adjusted to pH 7.4 with sodium hydroxide and warmed to 37°C. The MED64 array is placed on the MED connector headstage,

which has gold contact pins to pick up the signals from the electrodes and transfer them to the amplifier (Panasonic SU-MED640). The amplifier is connected to a computer with Mobius software (version Win 7 0.3.9) (Alpha MED Scientific Inc., Japan) with the Spike Sorter package for data acquisition and analysis. Baseline data was recorded for up to 5 minutes at which point a compound was directly pipetted into the well of the MEA probe. The signals were then recorded for a further 5 minutes in the presence of the compound. This time frame was found to be sufficiently long enough for all the compounds to exert their effects on the activity of the culture and stabilise to allow time of the effects of the compounds on the activity of the culture to be recorded. Further compound additions were done in the same way, without washing out of the first compound. The compounds utilised in this assay were GABA, muscimol, bicuculline, glycine, taurine, strychnine and gelsemine. These are the same as those used in the slice MEA recordings as listed in Table 6.1, with the addition of taurine which was supplied by Sigma, dissolved in dH₂O and applied to the cultures at 1 mM. All compounds were diluted in HBSS (-/-) to the required concentration so that the final concentration in the well of the MED64 probe was as stated in the results. The MEA probe DH culture data for each compound were obtained from a minimum of two different culture preparations from different sets of embryos, except in the case of muscimol where only one of the DH cultures on the MEA tested with muscimol displayed spontaneous activity.

A



B

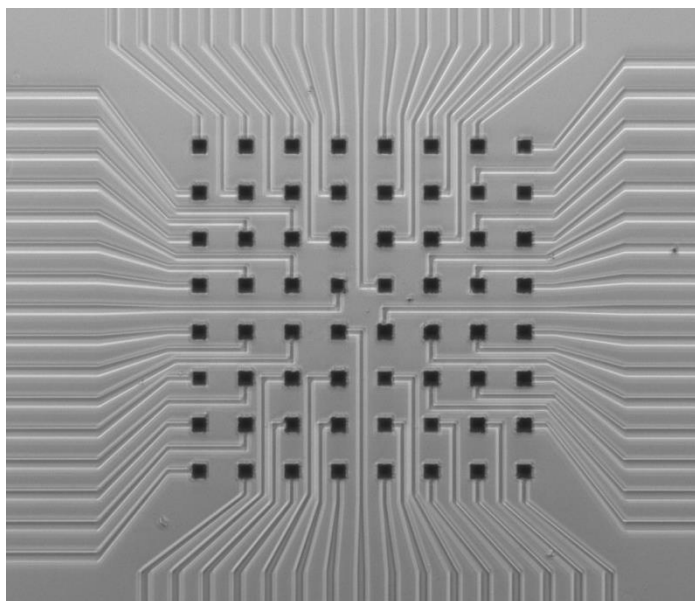


Figure 6.4 (A) A MED64 probe used to culture the DH cells. It consists of a glass base plate with 64 embedded electrodes, which are enclosed in a well. Photograph taken with a Xperia Z3 camera (Sony, UK). (B) A photograph of the array of electrodes on the base of the MED64 probe, this was taken with an EVOS digital inverted microscope (AMG, Fisher Scientific).

6.2.5 Analysis of MED64 Recordings with Cultured Dorsal Horn Cells

All analysis was completed offline with a pre-defined workflow template in the Spike Sorter software. Only those electrode channels in which spikes were observed either before or after compounds were applied were analysed. Furthermore where multiple electrodes were recording from the same cluster of cells, only two of the neighbouring electrodes were analysed as they were considered to be identical recordings from the same cells. These data were filtered with a 50 Hz filter. Using the analysis template, spikes were detected according to a chosen threshold and grouped according to their waveform similarity. For a distinct waveform type to be classified as a cluster there had to be a minimum of 5 spikes that meet the same waveform criteria determined by the software programme script. The threshold for spike detection was between $\pm 10 \mu\text{V}$. The spike frequency was determined for the baseline data and in the presence of each compound. The effects of the compounds on the cells was found to occur within 30 seconds following addition, therefore the full 5 minutes of recording in the presence of the compound was used to determine the spike frequency. On the MED64 system the compounds could not be washed off, therefore the activity of the culture during consecutive compound additions is overcoming the effects of the previous compound. The spike frequencies between the baseline section and those sections of the recording with compounds were compared with a paired one-way ANOVA followed by Tukey's multiple comparisons test using GraphPad Prism 6 (GraphPad Software, Inc.). The graphs are displayed with significance stars, where * indicates $p < 0.05$, ** signifies $p < 0.01$ and *** indicates $p < 0.001$. All graphs are plotted with the mean \pm S.E.M. The number of individual preparations is denoted N, with the number of MEA recordings from the cultured DH cells is denoted n. The total number of electrodes from all the MEA recordings for each experiment included in the analysis is denoted e.

6.3 Results

6.3.1 MEA Recordings Show 4-AP Induces Population Spikes throughout the Dorsal Horn and Ventral Horn of Spinal Cord Slices

The MEA recordings from acute spinal cord slices illustrate that 4-AP induces population spikes, similar to those observed in the single electrode extracellular recordings. The 4-AP activity across the spinal cord slices was compared by combining data from 28 MEA slice recordings. The mean spike amplitudes and spike frequencies were determined for the SG, deep DH and VH for the 4-AP-induced activity (Figure 6.5). The spike amplitude and frequency in the SG region were not significantly different to those found in the deep DH. However, the mean population spike frequency and amplitude in the VH were significantly lower than that recorded in the SG and deep DH. The MEA slice recordings demonstrated that the population spikes have a highly synchronised firing pattern across each of the hemispheres of the slice. Typically it could be seen that the right and left DH hemispheres of the slice had their own synchronous activity but are not synchronous with each other (Figure 6.6).

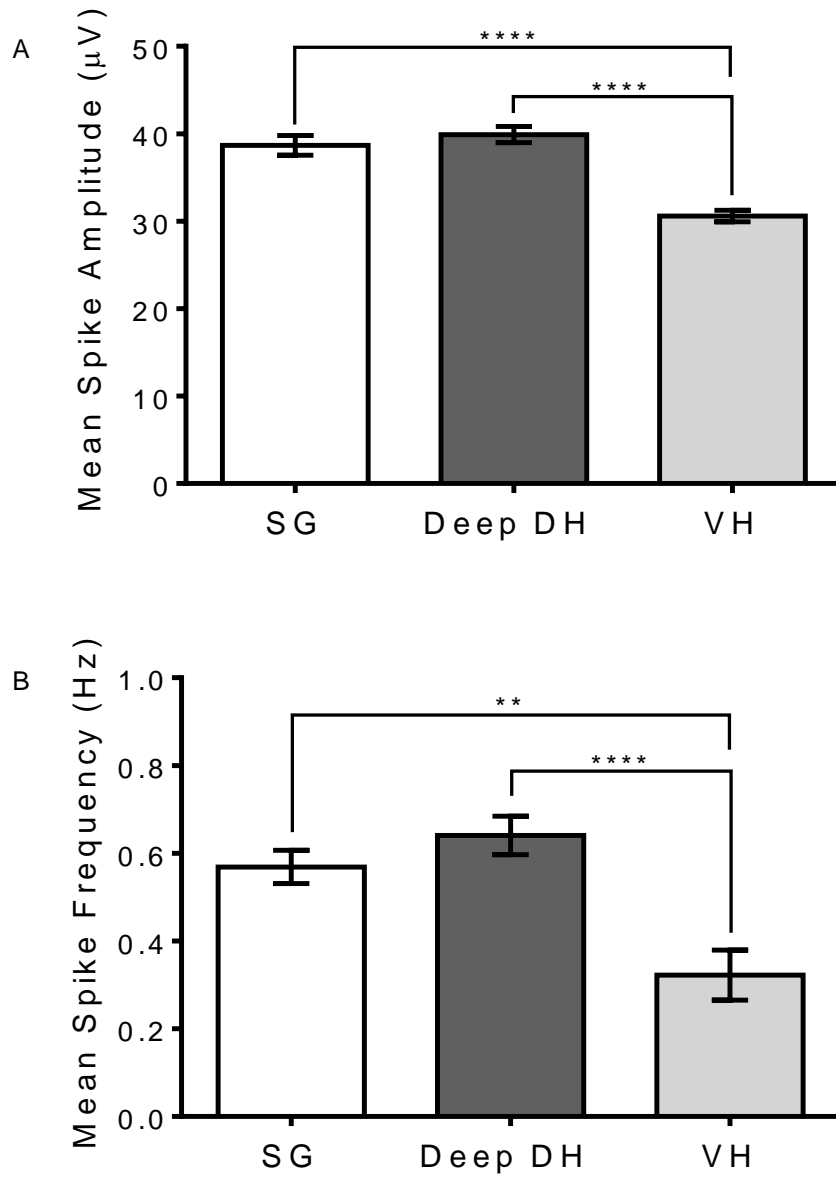


Figure 6.5 4-AP-induced activity in the SG, deep DH and VH of spinal cord slices on the MEA (N=15, n=28). The mean population spike amplitude (A), and the mean population spike frequency (B), calculated for the SG, deep DH and VH.

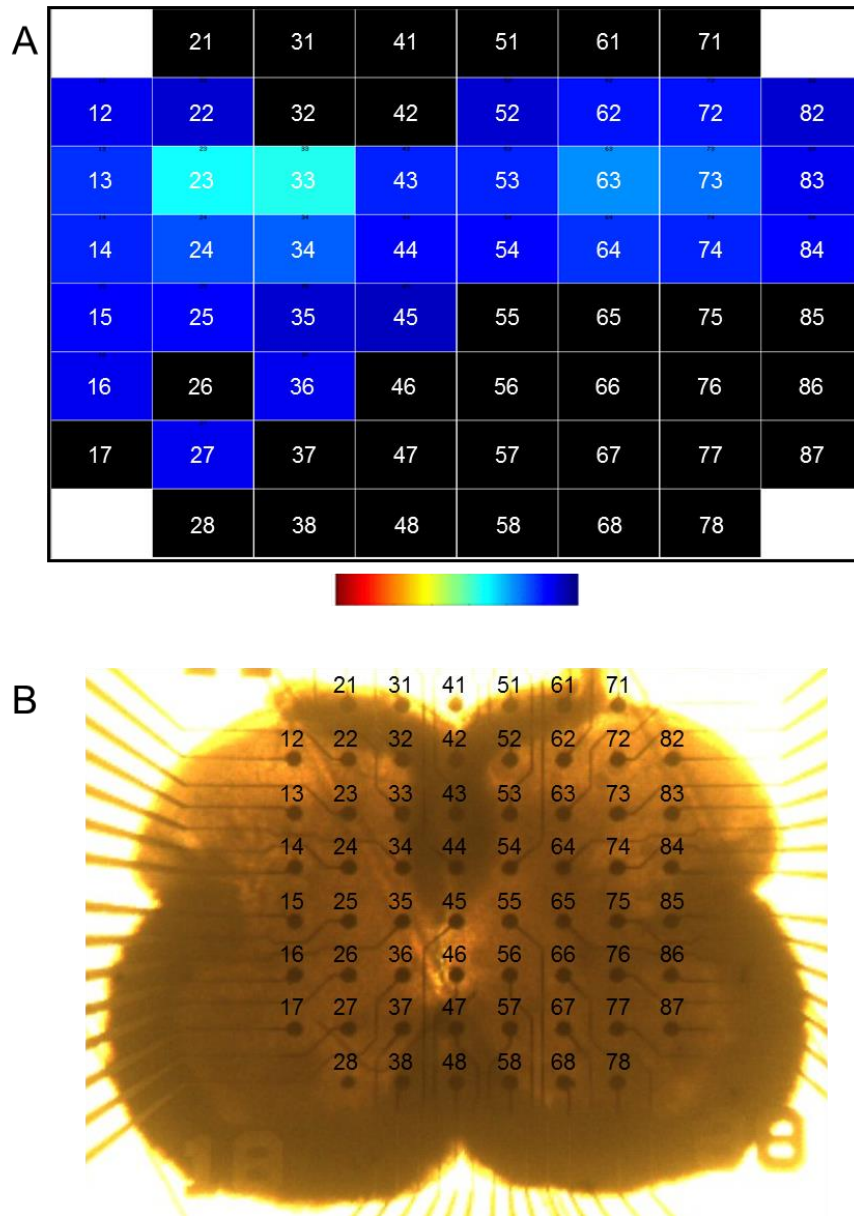


Figure 6.6 The incidence of spikes at each electrode at a single 1 second time point in a MEA recording from a spinal cord slice perfused with 4-AP. (A) Each box represents one electrode of the MEA array, which is numbered according to the column and row in which it is situated. For example electrode 34 is located in column 3, row 4 of the array. The location of each electrode on the spinal cord slice from which the recording was made can be seen in (B). When a spike is detected at an electrode according to a set threshold, the corresponding box becomes coloured according to the pseudo-colour map shown. The larger the spike amplitude, the further to the right of the pseudo-colour map the box becomes (A). At the 1 second time point of this example, the electrodes recording from the SG (12, 22, 32, 52, 62, 72 and 82) and deeper DH laminae (electrodes 13-84) have each detected a population spike. Therefore, this illustrates the synchronous firing across the DH networks, which are not synchronous with the VH.

6.1.1.1 *GABA_A Receptor Agonists and Antagonists Modulate the 4-AP-Induced Activity*

Pharmacological tools were used to probe whether GABA_A receptor signalling contributes to the 4-AP-induced activity within the SG, seep DH and VH. This was investigated using the agonists GABA, muscimol and THIP and the antagonists bicuculline and gabazine. Perfusion of GABA (50 µM) significantly increased the amplitude and spike frequency induced by 4-AP in the SG, deep DH and VH (Figure 6.7). Similarly application of THIP (gaboxadol) (50 µM) significantly increased the 4-AP-induced spike amplitude and frequency in each of the three regions analysed, except the spike frequency in the VH (Figure 6.8). The GABA_A receptor agonist muscimol (10 µM) significantly decreased 4-AP-induced spike amplitude and frequency across the spinal cord slices in the DH and VH (Figure 6.9). The GABA_A receptor antagonist bicuculline (50 µM) significantly decreased the 4-AP-induced population spike amplitude and frequency in the SG and deep DH, but had no significant effect in the VH (Figure 6.10). Gabazine exerted similar effects to bicuculline, significantly decreasing the 4-AP-induced spike frequency and amplitude in the SG and deep DH. Additionally, gabazine decreased the spike frequency and amplitude in the VH (Figure 6.11).

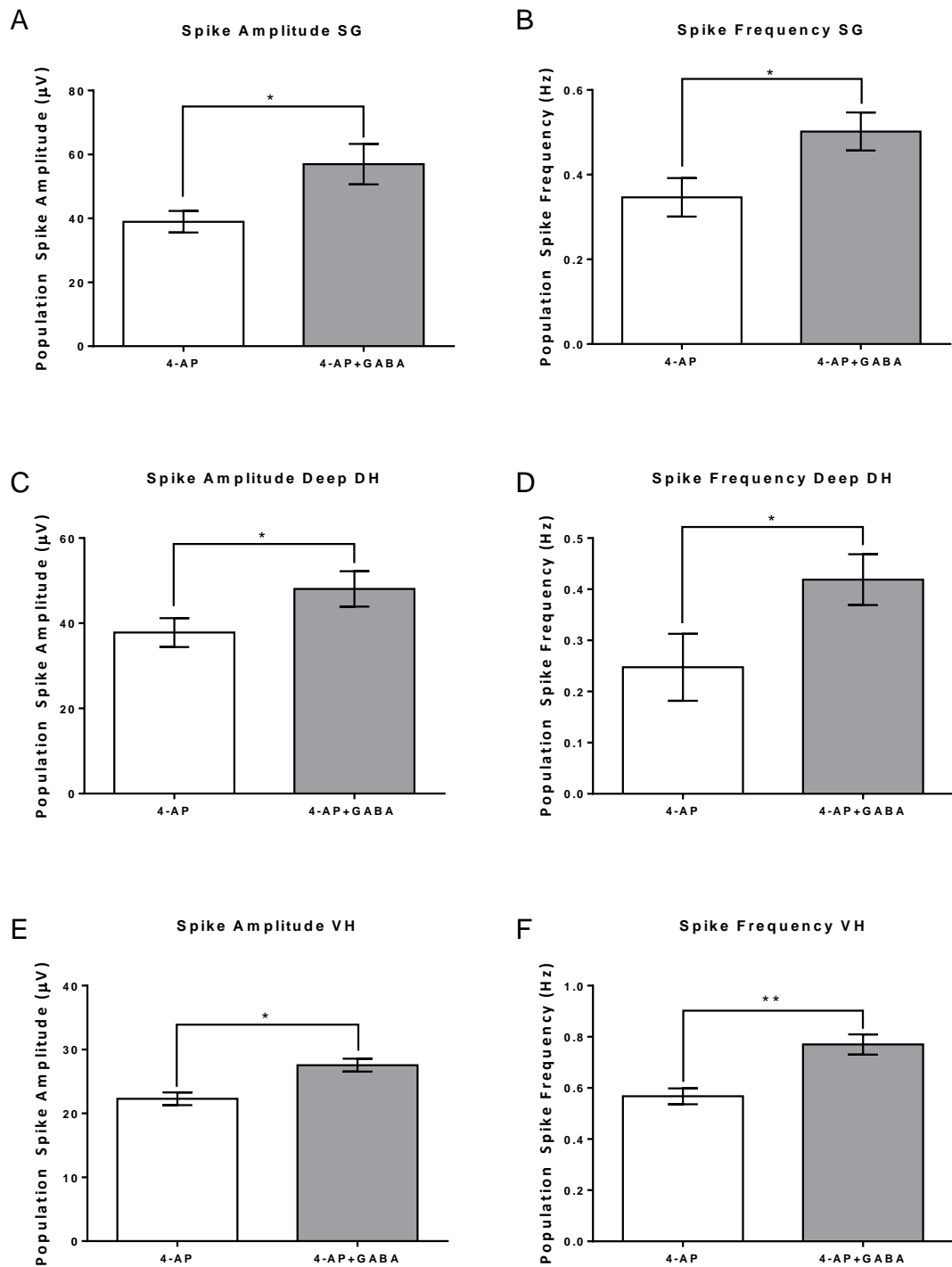


Figure 6.7 The average spike amplitudes and frequencies in the SG, deep DH and VH regions of the spinal cord slices determined from MEA recordings during the perfusion of 4-AP and 4-AP with GABA (50 μ M) (N=3, n=6). (A), (C) and (E) illustrate the population spike amplitudes in the SG, deep DH and VH respectively during the perfusion of 4-AP and 4-AP with GABA. (B), (D) and (F) show the spike frequency data in the SG, deep DH and VH respectively during the perfusion of 4-AP and 4-AP with GABA.

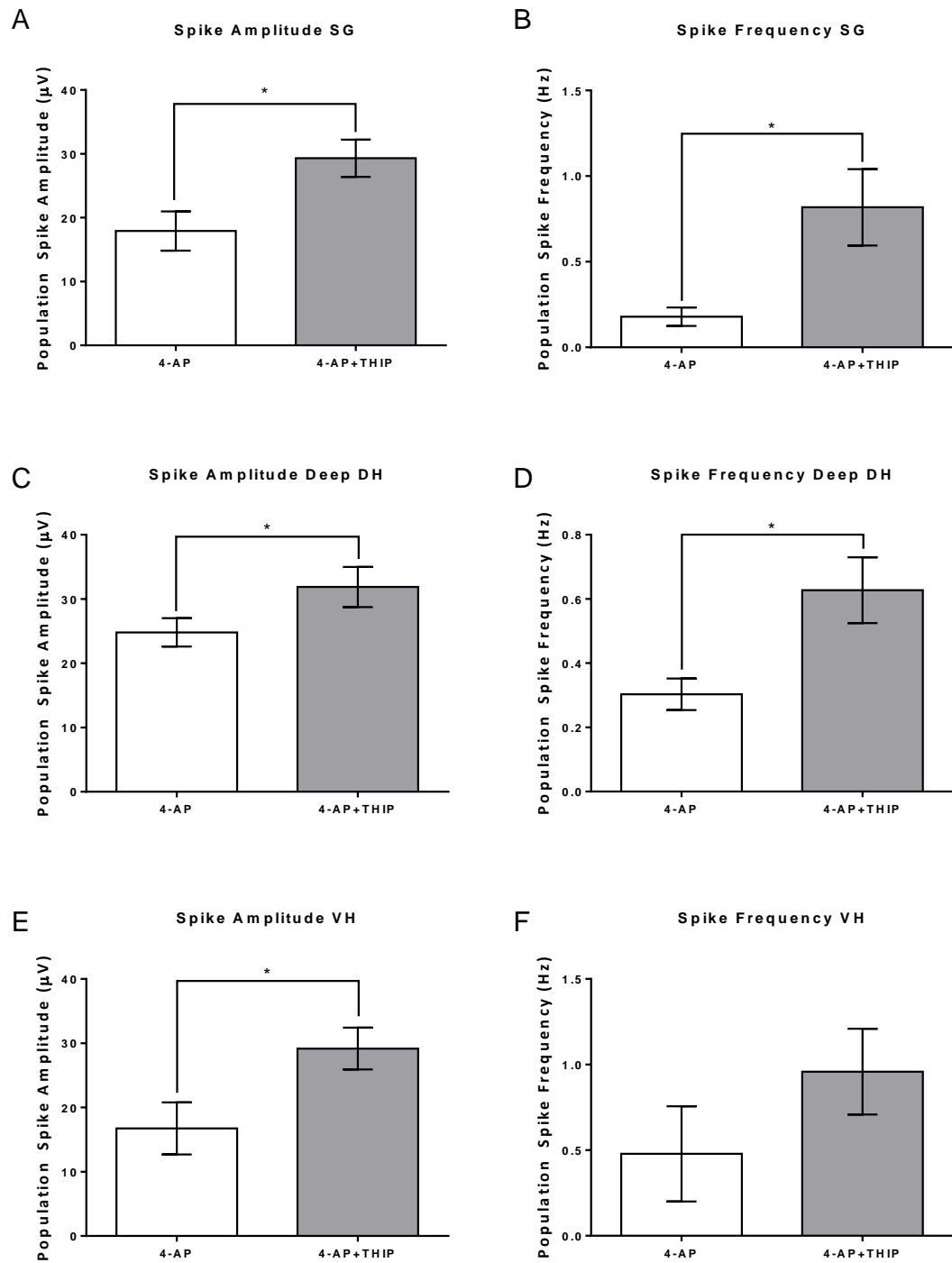


Figure 6.8 The mean population spike amplitude and frequency in the SG, deep DH and VH of the spinal cord slices determined from MEA recordings during the perfusion of 4-AP and 4-AP with THIP (50 μM) (N=3, n=7). (A), (C) and (E) demonstrate the spike amplitude data in the SG, deep DH and VH respectively during the perfusion of 4-AP and subsequent perfusion of 4-AP with THIP. (B), (D) and (F) show the population spike frequency data in the SG, deep DH and VH respectively during the perfusion of 4-AP and then with 4-AP with THIP.

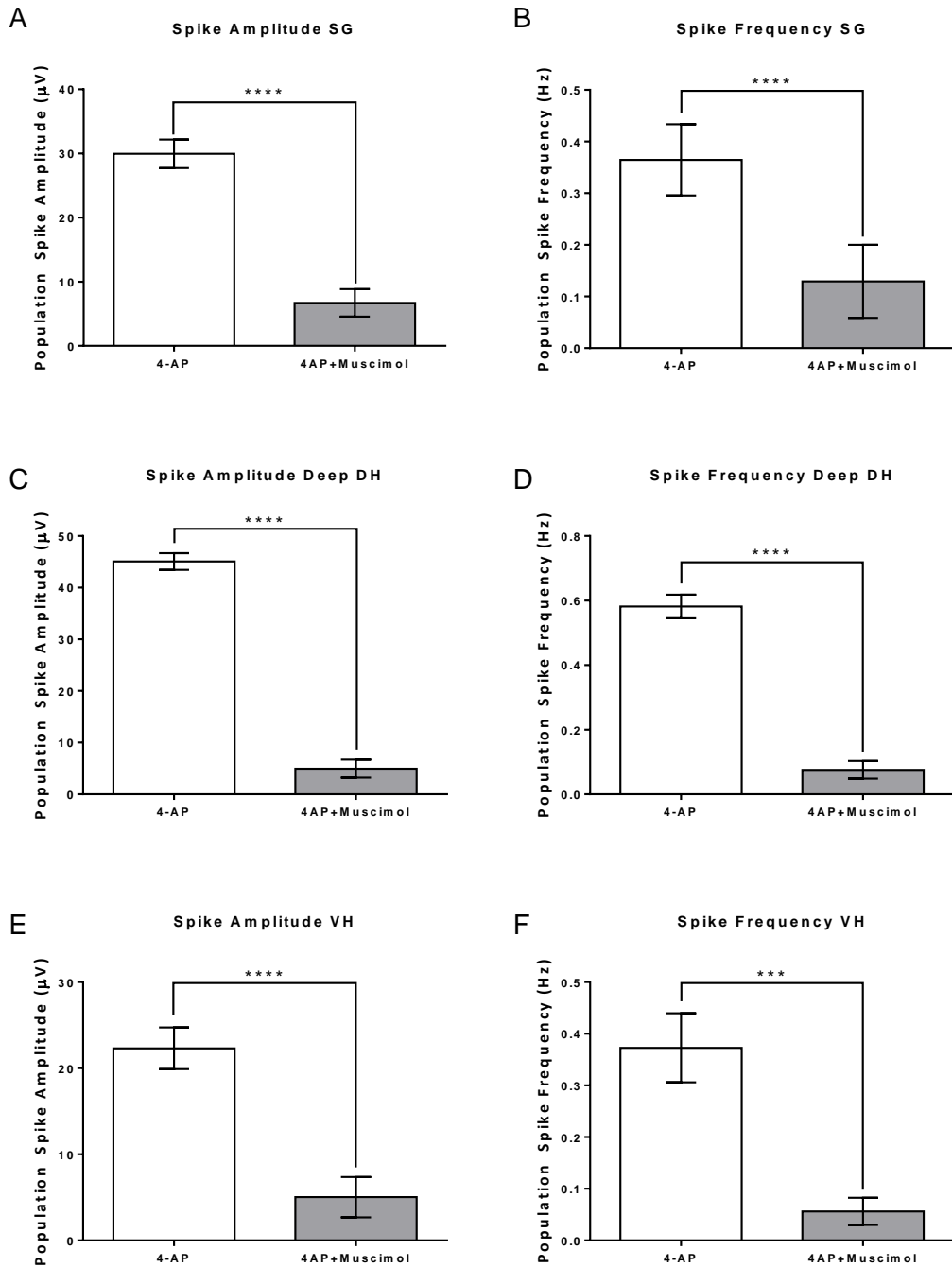


Figure 6.9 The average population spike amplitude and frequency during the perfusion of 4-AP and 4-AP with muscimol (10 μ M) in the SG, deep DH and VH of the spinal cord slices measured from MEA recordings (N=3, n=6). (A) The mean spike amplitude and (B) the mean spike frequency in the SG of the spinal DH during 4-AP perfusion and during the subsequent perfusion of 4-AP with muscimol. In the deep DH region of the spinal cord slice (C) the mean spike amplitude and (D) spike frequency in the presence of 4-AP and 4-AP with muscimol. The 4-AP and 4-AP with muscimol mean population spike amplitude (E) and spike frequency (F).

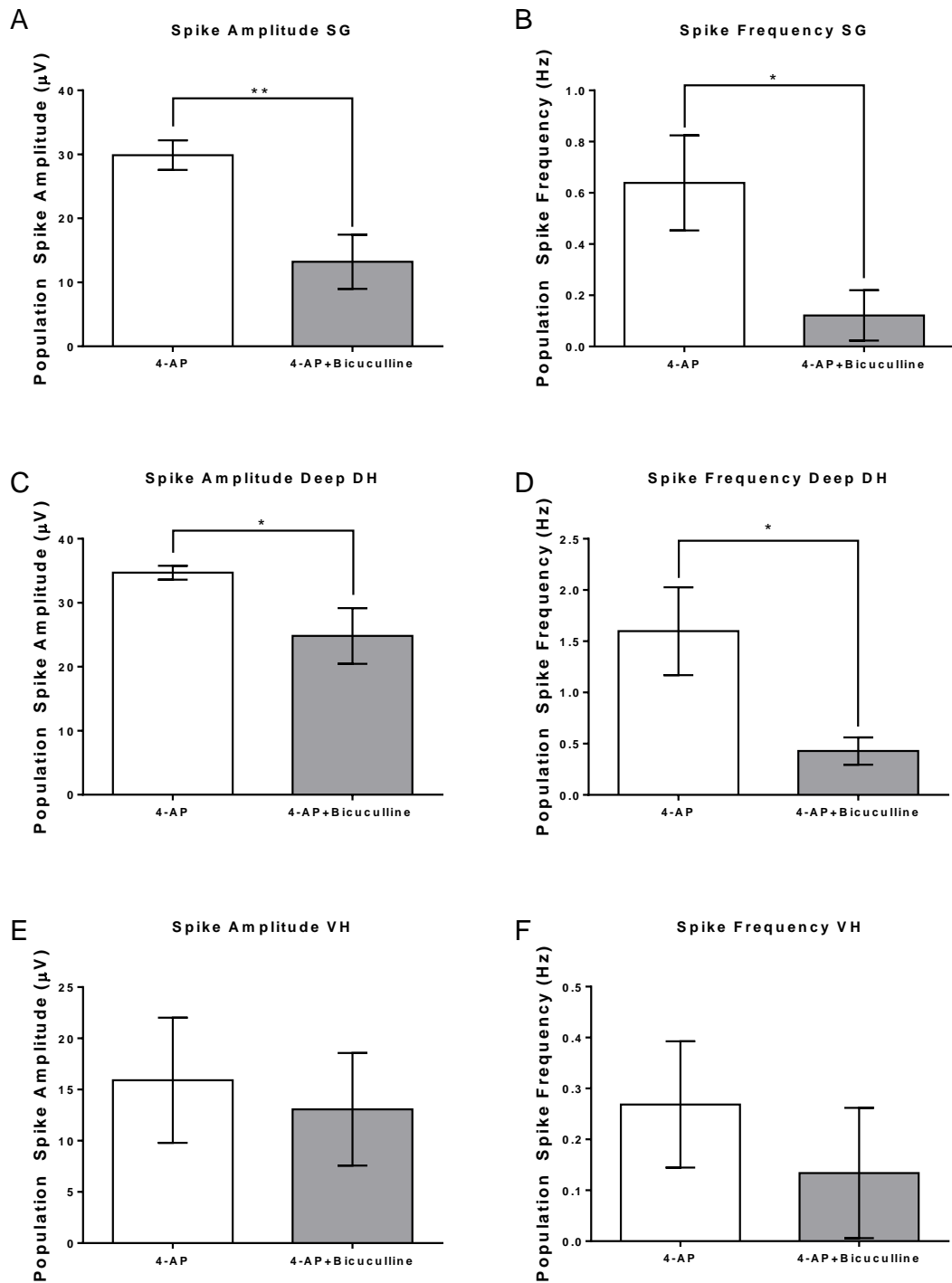


Figure 6.10 The average population spike amplitude and frequency in the SG, deep DH and VH of spinal cord slices recorded using the MEA during the perfusion of 4-AP and then with 4-AP with bicuculline (50 μM) (N=4, n=8). (A), (C) and (E) show the population spike amplitudes in the SG, deep DH and VH respectively. (B), (D) and (F) show the population spike frequencies in the SG, deep DH and VH respectively.

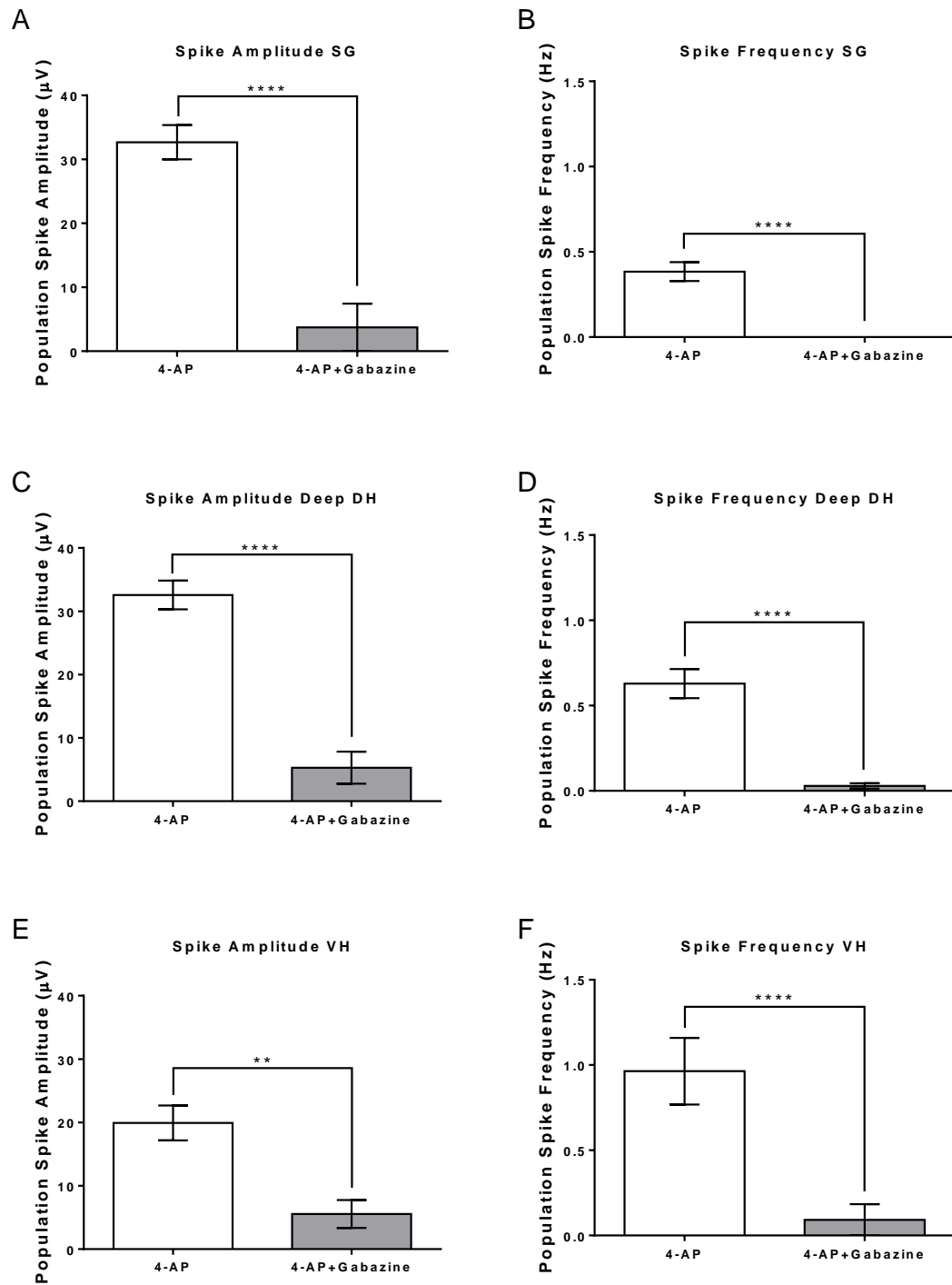


Figure 6.11 The average population spike amplitude and frequency recorded from the SG, deep DH and VH of spinal cord slices on the MEA during perfusion of 4-AP and 4-AP with gabazine (10 μM) (N=2, n=4). (A), (C) and (E) illustrate the spike amplitude data in the SG, deep DH and VH respectively. (B), (D) and (F) demonstrate the spike frequency data in the SG, deep DH and VH regions respectively.

6.1.1.2 GABA_B Receptor Agonist and Antagonist Modulate the 4-AP-Induced Activity

GABA_B agonist baclofen and antagonist 2-hydroxysaclofen were applied to the slices on the MEA probes to determine if GABA_B receptor signalling is involved in controlling the hyperexcitability in the spinal DH. Baclofen significantly reduced the amplitude and frequency of the population spikes induced by 4-AP in the SG and deep DH (Figure 6.12). In the VH, baclofen significantly reduced amplitude but had no effect on spike frequency. The antagonist 2-hydroxysaclofen significantly increased the spike amplitudes in the SG, deep DH and VH. However, 2-hydroxysaclofen did not change the frequency in any of these regions (Figure 6.13).

6.1.1.3 Glycine Receptor Agonists and Antagonists Modulate the 4-AP-Induced Activity

Glycine (1 mM) significantly increased the spike amplitude and rate in the superficial SG region, deep DH and in the VH (Figure 6.14). The glycine receptor antagonist strychnine, highly selective for glycine receptors over GABA receptors, also significantly increased population spike amplitude and rate in all these three regions of the spinal cord slices (Figure 6.15). Gelsemine produced a significant decrease in 4-AP-induced population spike amplitude and frequency in the SG region of the spinal DH. In the deep DH the frequency was also significantly reduced, however the spike amplitude was significantly increased. Furthermore, gelsemine did not have any effects on the 4-AP activity in the VH of the spinal cord slices (Figure 6.16).

6.1.1.4 KCC2 Inhibitor VU0240551 Increases 4-AP-Induced Activity

The application of the KCC2 inhibitor VU0240551 to the spinal cord slices increased spike amplitude in the SG, deep DH and VH regions. However this inhibitor had no influence on the rate of spike firing in the DH. VU0240551 increased the frequency of firing in the VH although the firing frequencies here were very low. There were no spikes in the VH with 4-AP perfusion alone in these slices, and the addition of VU0240551 only increased firing frequency to between 0.02 and 0.08 Hz in 6 of the VH electrodes (Figure 6.17).

A summary of the effects of all the GABA_A and GABA_B receptor compounds on the 4-AP-induced activity recorded from the spinal cord slices on the MEA can be found in Table 6.2. A summary of the effects of the glycine receptor agonist and antagonist, and the KCC2 inhibitor VU 024551 on the 4-AP-induced activity in the spinal cord slices on the MEA can be found in Table 6.3.

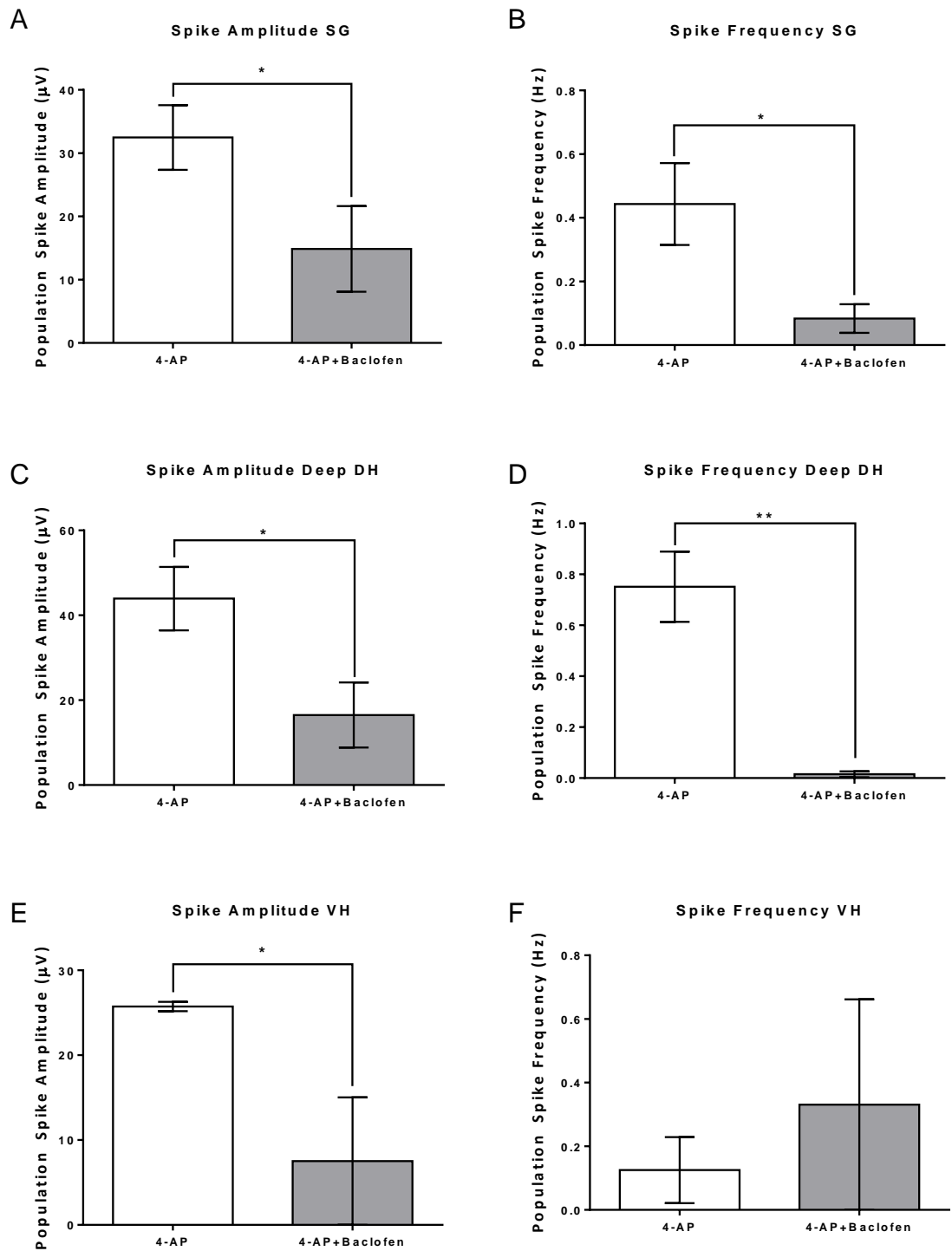


Figure 6.12 The mean population spike amplitude and frequency in the SG, deep DH and VH during perfusion of 4-AP and 4-AP with baclofen (10 μM) recorded with the MEA (N=3, n=7). (A) and (B) show the data for the SG during perfusion of 4-AP and then 4-AP with baclofen. (C) and (D) illustrate the data for the deep DH and (E) and (F) show the data for the VH.

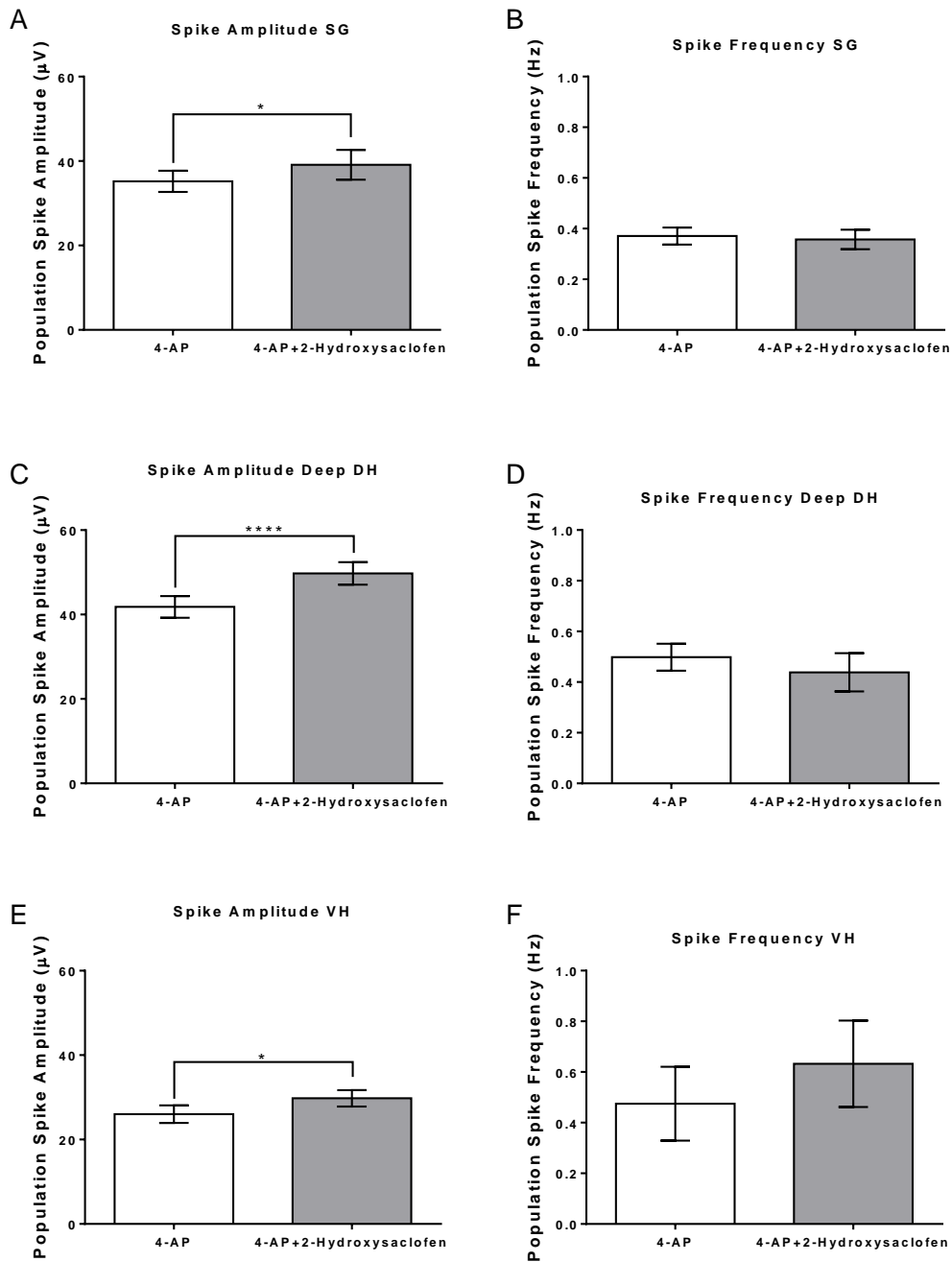


Figure 6.13 The mean population spike amplitude and frequency during perfusion of 4-AP and 4-AP with 2-hydroxysaclofen (10 μM) in SG, deep DH and VH of the spinal cord slice during the MEA recordings (N=2, n=4). (A), (C) and (E) show the mean spike amplitude values in the SG, deep DH and VH during the perfusion of 4-AP and 4-AP with 2-hydroxysaclofen. (B), (D) and (F) demonstrate the spike frequency data in the SG, deep DH and VH during perfusion of 4-AP and 4-AP with 2-hydroxysaclofen. 2-hydroxysaclofen only influenced the spike amplitude and not the frequency of the 4-AP-induced activity.

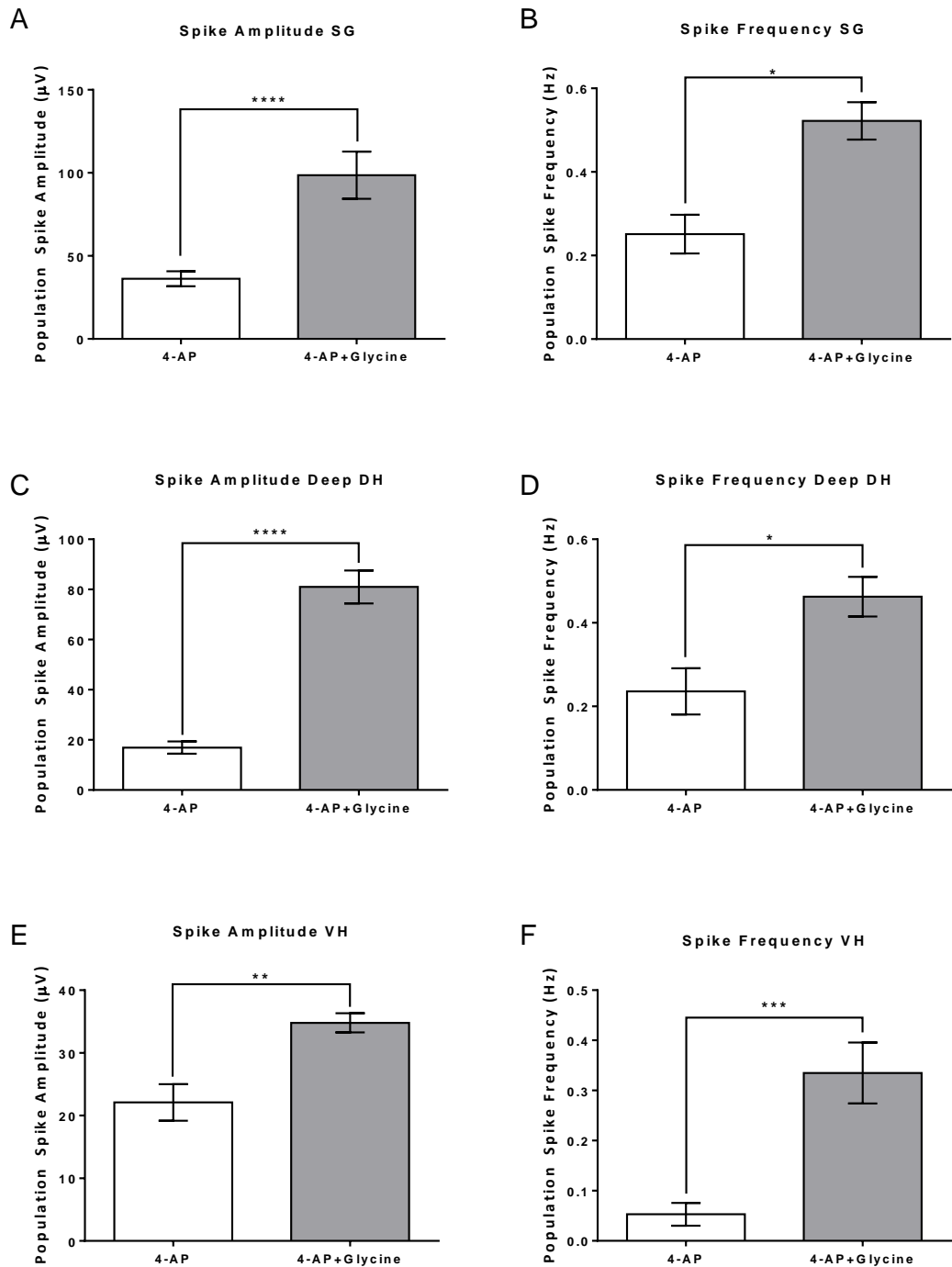


Figure 6.14 The mean population spike amplitude and frequency in the spinal cord slices recorded with the MEA during the perfusion of 4-AP and 4-AP with glycine (1 mM) (N=2, n=6). (A), (C) and (E) illustrate the spike amplitude data in the SG, deep DH and VH respectively, during perfusion of 4-AP and then 4-AP with glycine. (B), (D) and (F) show the mean spike frequency values in the SG, deep DH and VH during the perfusion of 4-AP and 4-AP with glycine.

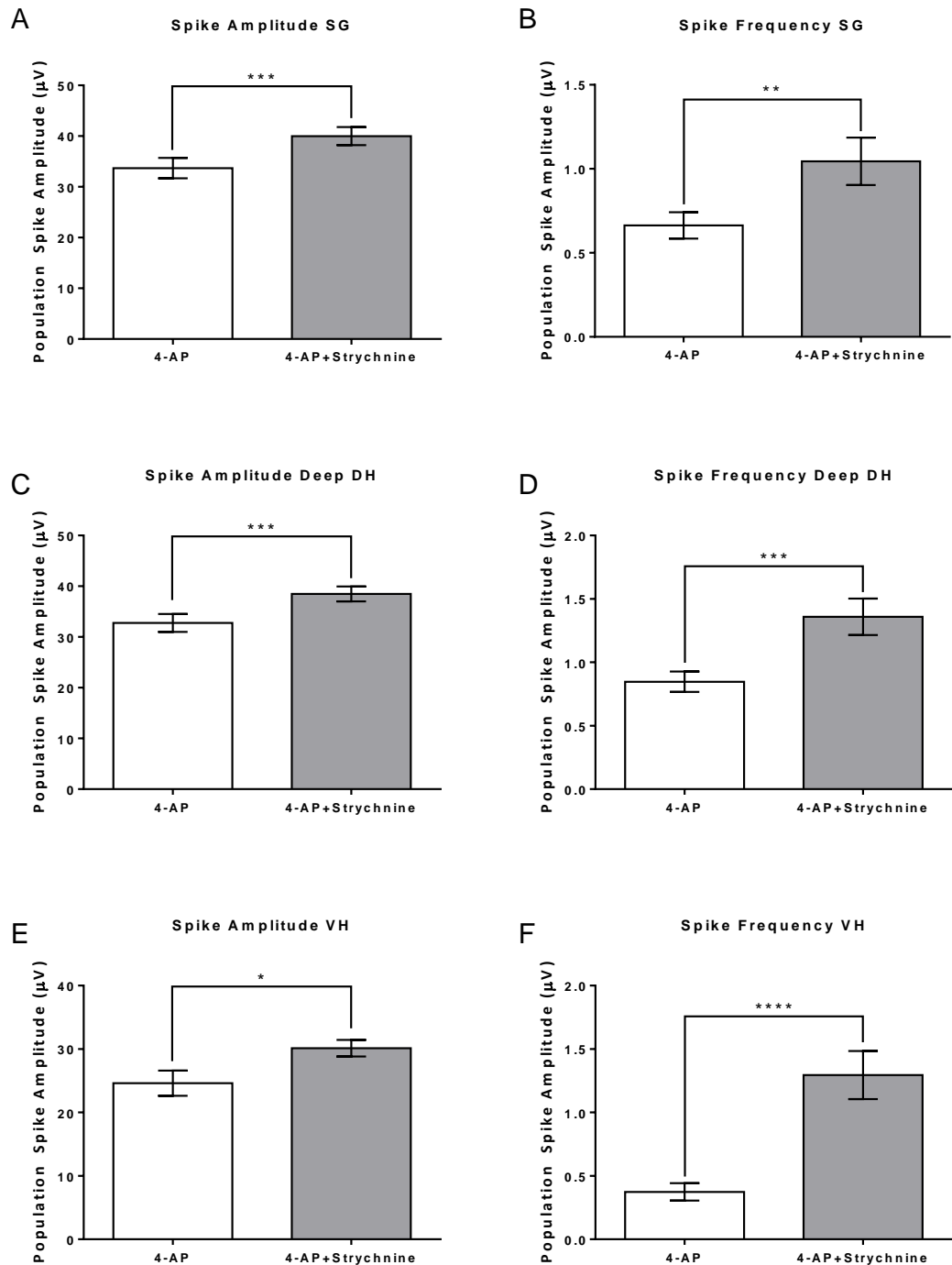


Figure 6.15 The mean population spike amplitudes and frequencies in the SG, deep DH and VH regions of the spinal cord slices during perfusion of 4-AP and 4-AP with strychnine (10 μM) recorded using the MEA (N=4, n=10). (A), (C) and (E) illustrate the spike amplitude data for the SG, deep DH and VH during the perfusion of 4-AP and then 4-AP with strychnine. (B), (D) and (F) shown the spike frequency values in the SG, deep DH and VH during perfusion of 4-AP and then with 4-AP and strychnine. Strychnine increased both spike frequency and amplitude across the spinal cord slices.

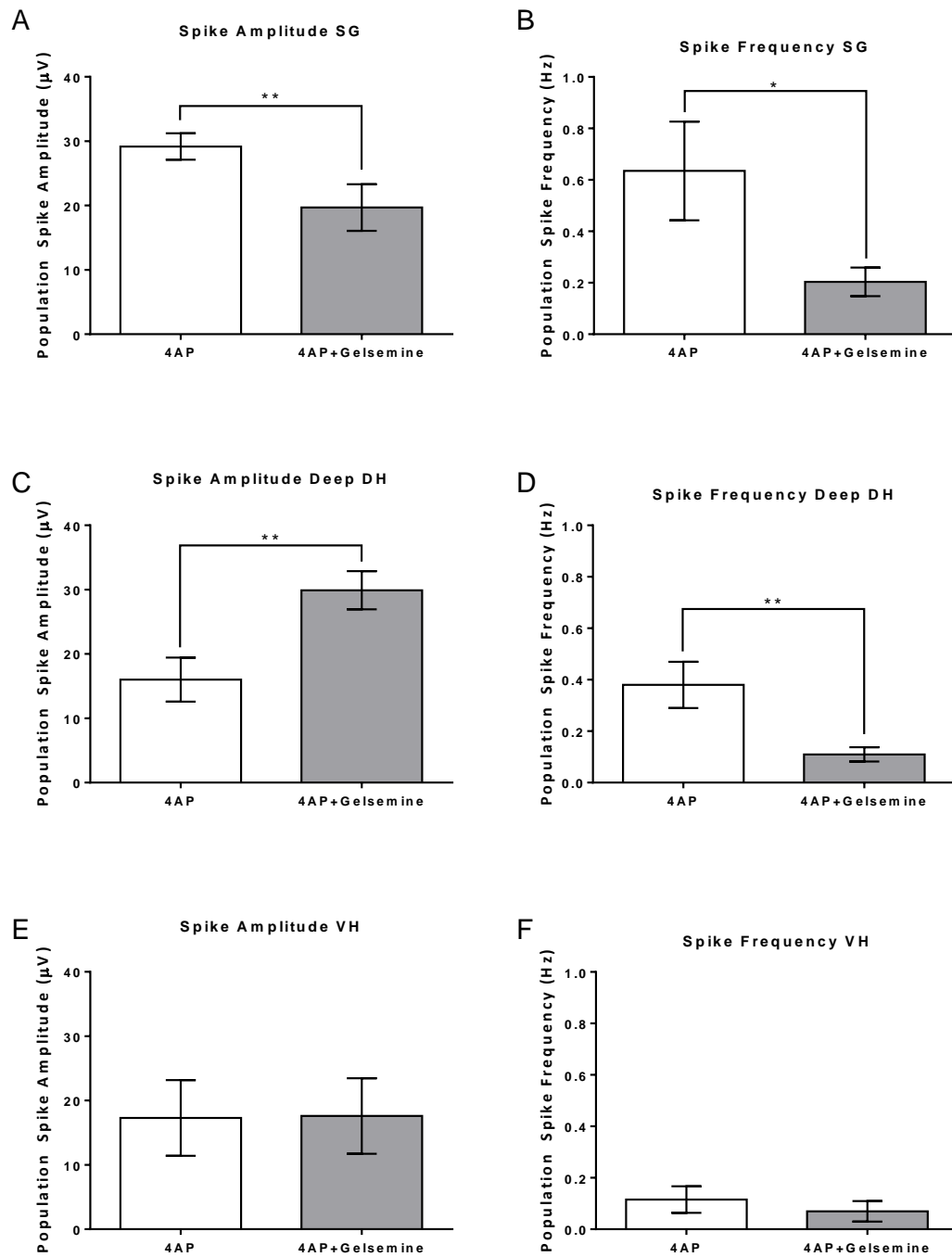


Figure 6.16 The mean population spike amplitudes and frequencies recorded from spinal cord slices using the MEA during perfusion of 4-AP and 4-AP with gelsemine (30 μ M) (N=2, n=4). (A) and (B) show the spike amplitude and frequency respectively in the SG region of the spinal cord slices. (C) and (D) show the mean spike amplitude and frequency, respectively, in the deep DH. (E) and (F) illustrate the mean spike amplitude and frequency, respectively, in the VH of the spinal cord slices.

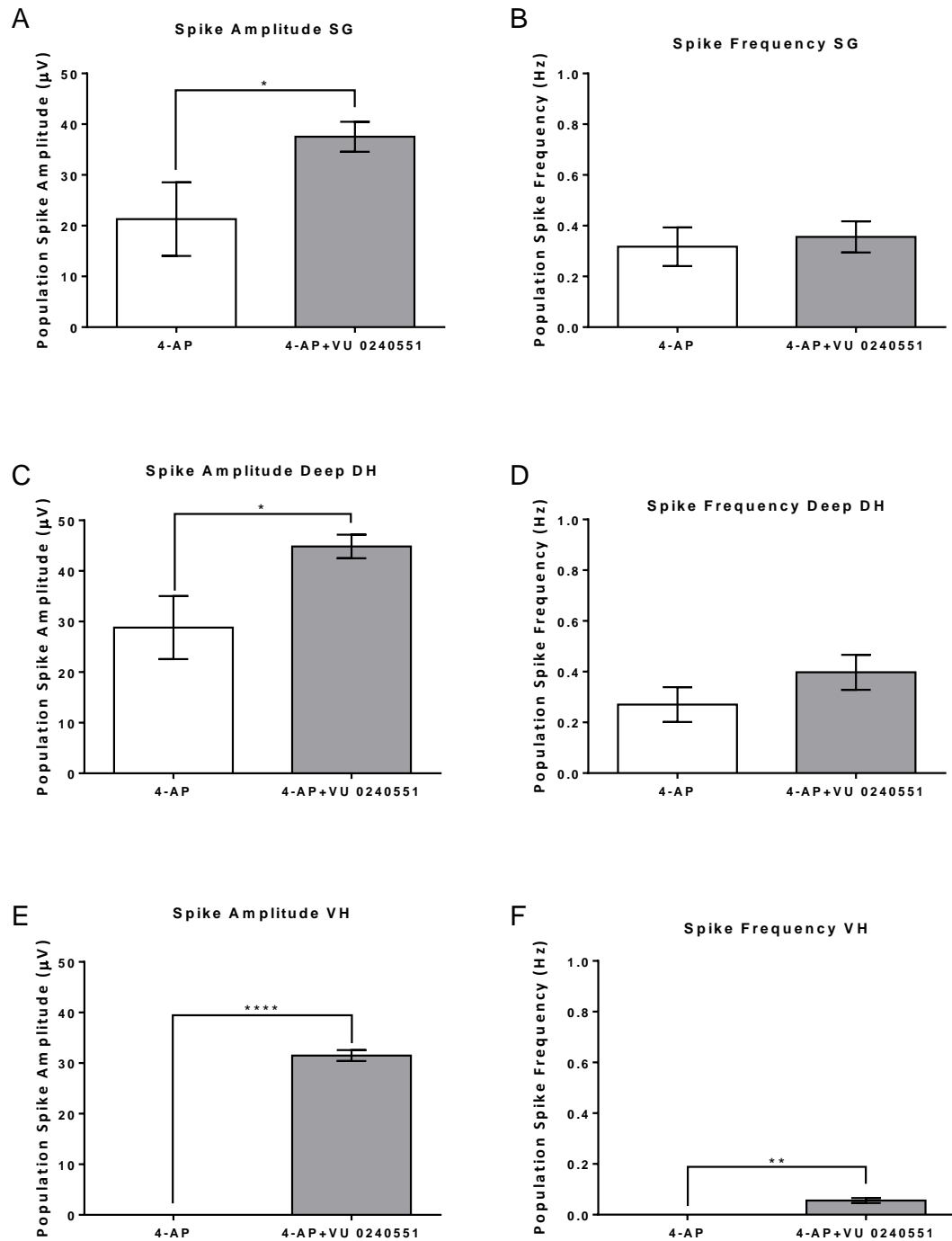


Figure 6.17 The mean population spike amplitudes and frequencies from the SG, deep DH and VH regions of spinal cord slices recorded from using the MEA during perfusion of 4-AP and 4-AP with VU 0240551 (30 μM) (N=2, n=5). (A), (C) and (E) show the population spike amplitude data in the SG, deep DH and VH during the perfusion of 4-AP and 4-AP with VU 0240551. (B), (D) and (F) illustrate the population spike frequency data in the SG, deep DH and VH during perfusion of 4-AP and then 4-AP with VU 0240551.

	SG		Deep DH		VH	
	Amplitude	Frequency	Amplitude	Frequency	Amplitude	Frequency
GABA	↑	↑	↑	↑	↑	↑
THIP	↑	↑	↑	↑	↑	n.s
Muscimol	↓	↓	↓	↓	↓	↓
Bicuculline	↓	↓	↓	↓	n.s	n.s
Gabazine	↓	↓	↓	↓	↓	↓
Baclofen	↓	↓	↓	↓	↓	n.s
2-Hydroxysaclofen	↑	n.s	↑	n.s	↑	n.s

Table 6.2 A summary of the effects on the 4-AP induced activity by the GABA_A and GABA_B receptor agonists and antagonists applied to the spinal cord slices on the MEA. ↑ indicates a significant increase, ↓ is a significant decrease and n.s stands for no significant change in the 4-AP activity.

	SG		Deep DH		VH	
	Amplitude	Frequency	Amplitude	Frequency	Amplitude	Frequency
Glycine	↑	↑	↑	↑	↑	↑
Strychnine	↑	↑	↑	↑	↑	↑
Gelsemine	↓	↓	↑	↓	n.s	n.s
VU0240551	↑	n.s	↑	n.s	↑	↑

Table 6.3 A summary of the effect of the glycine receptor agonist and antagonists and the KCC2 inhibitor on the 4-AP-induced population spikes in the SG, deep DH and VH of the spinal cord slices recorded from using the MEA. ↑ indicates a significant increase, ↓ is a significant decrease and n.s stands for no significant change in the 4-AP activity.

6.3.2 *MEA Recordings with Cultured Dorsal Horn Cells Detect Spontaneous Activity*

It was exceptionally challenging to achieve healthy, spontaneously firing cells when culturing the DH cells on the MED64 probes. One of the main problems was that a large proportion of the cells did not adhere to the surface of the probes. A number of factors were optimised to solve this issue. Firstly, centrifugation of the probes after plating the cells improved adhesion of the cells to the base of the arrays. Secondly, a higher molecular weight poly-D-lysine coating was utilised, which also aided cell adhesion. As observed with the spinal DH culture on the 96-well plates, the density of cells in the wells has a huge impact on the health of the culture and the spontaneous firing. Therefore it was difficult to obtain spontaneous firing of the cultures on the MED64 probes, as after 12-14 days in culture there were often significantly fewer cells remaining due to poor cell adhesion. Despite these complications, there were a number of healthy cultures on the MED64 probes which did display spontaneous firing (Figure 6.18). An example of the spontaneous activity of the DH cultures recorded with the MED64 MEA is illustrated in Figure 6.19.

6.3.2.1 *The Spontaneous Activity of the Spinal Dorsal Horn Culture was Modulated by GABA_A and Glycine Receptor Agonists and Antagonists*

The spike frequency detected from the baseline spontaneous firing of the culture on the MED64 was variable between different cultures. The mean frequency of spontaneous firing determined from combining all recordings from the MED64 was 0.45 ± 0.08 Hz (N=9, n=13). Due to the limited number of MED64 probes with successful cultures only a select number of compounds were investigated. GABA receptor agonist GABA (50 μ M) significantly reduced the spontaneous firing frequency by 60.3% from 0.96 ± 0.05 to 0.38 ± 0.05 Hz. Subsequent addition of

bicuculline (50 μ M) to the culture increased spike frequency by $71 \pm 9.82\%$ compared to the frequency observed during GABA alone (Figure 6.20). The GABA_A receptor-specific agonist muscimol (10 μ M) was also applied to the culture. This abolished almost all spontaneous spikes from 921 spikes in 300 seconds of baseline recording, to 5 spikes in the following 300 seconds in the presence of muscimol. Bicuculline (100 μ M) was applied after the addition of muscimol and which restored some of the spike firing (538 spikes) (Figure 6.21). Table 6.4 summarises the results from the spinal DH cultures on the MED64 and the effects of the GABA_A receptor compounds.

To investigate the role of glycine receptor signalling on the DH culture electrical activity, agonists glycine and taurine, and antagonists strychnine and gelsemine were applied. Glycine (1 mM) significantly reduced spontaneous firing frequency by $64.6 \pm 0.03\%$ (Figure 6.22). Subsequent addition of gelsemine increased spike frequency by $56.5 \pm 0.06\%$ to a frequency that was not significantly different to the baseline firing rate (Figure 6.22). Taurine (1 mM) did not significantly change the spike frequency, but did decrease the baseline frequency by $14 \pm 0.04\%$. Strychnine (10 μ M) significantly increased spike frequency by $52.4 \pm 0.11\%$ compared to the frequency in the presence of taurine (Figure 6.23). Table 6.5 summarises the results of the glycine receptor agonists and antagonists on the spinal DH cultures on the MED64 probes.

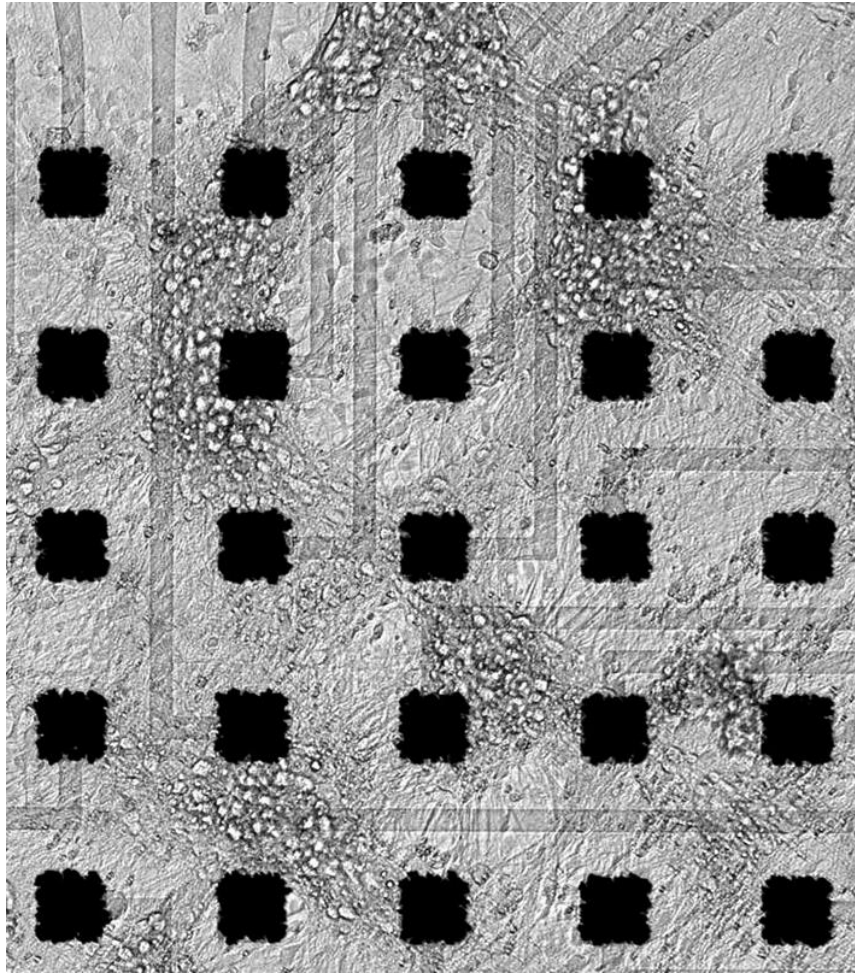


Figure 6.18 An image of the embryonic spinal DH culture on a MED64 probe after 13 DIV. Despite the clustering of the cells, spontaneous electrical activity was detected from those electrodes in direct contact or located next to the cell clusters. The image was taken with an EVOS inverted microscope (AMG, Fisher Scientific).

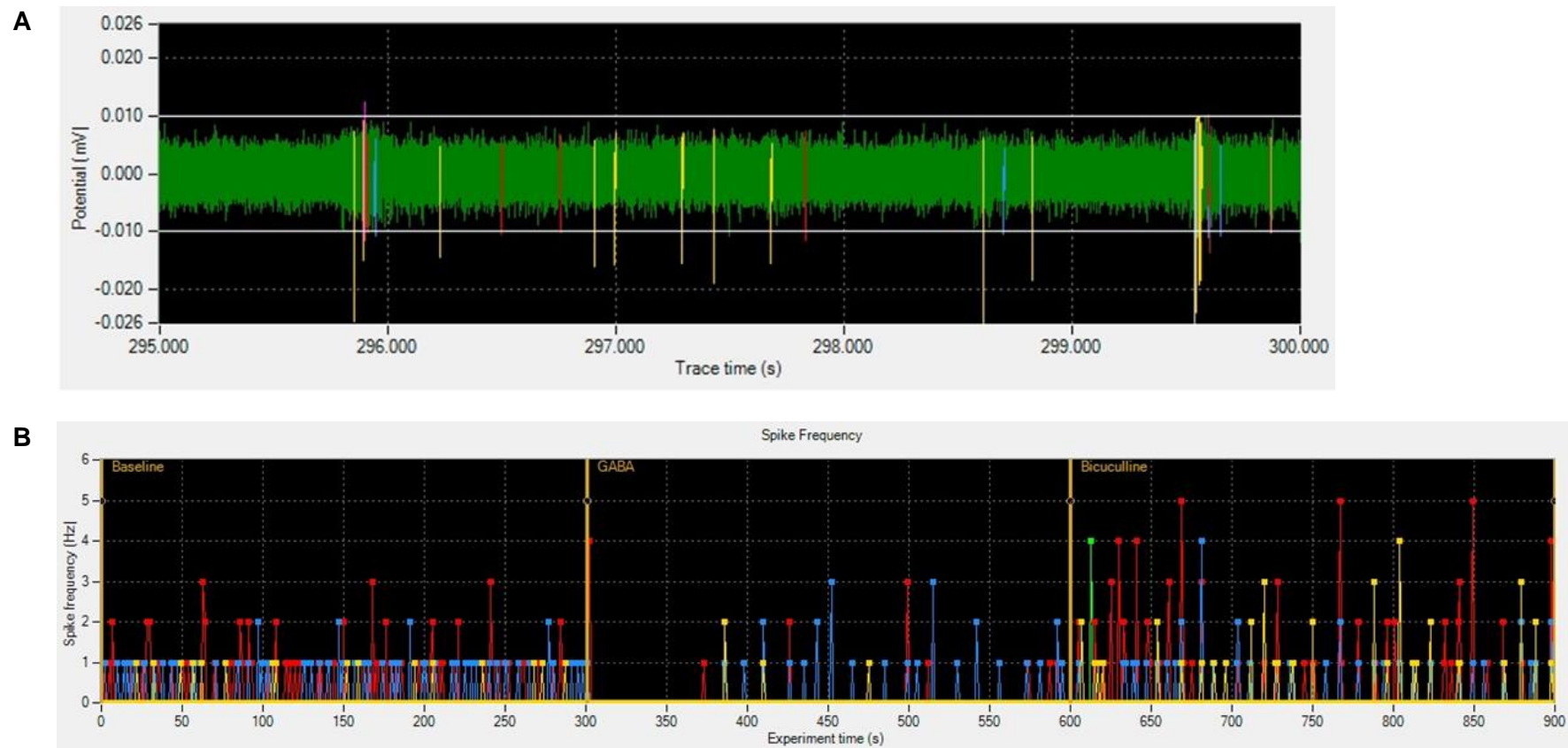


Figure 6.19 (A) A section of a recording from a MED64 probe with the DH culture at day 12, showing the baseline spontaneous activity. The two horizontal white lines indicate the threshold level for spike detection ($10\ \mu\text{V}$). The vertical coloured lines are those highlighted spikes that have reached the threshold level. The different colours represent each of the different classes of spikes, categorised according to their waveform similarity. (B) The spike frequency profile throughout a full recording from the DH cells on the MED64. Each dot represents the number of spikes at that time point. The colours correspond to the different classes of spikes as shown in (A). Each section of the recording is indicated by the vertical yellow lines at which point the compounds were added, in this case GABA ($50\ \mu\text{M}$) at 300 seconds and bicuculline ($50\ \mu\text{M}$) at 600 seconds.

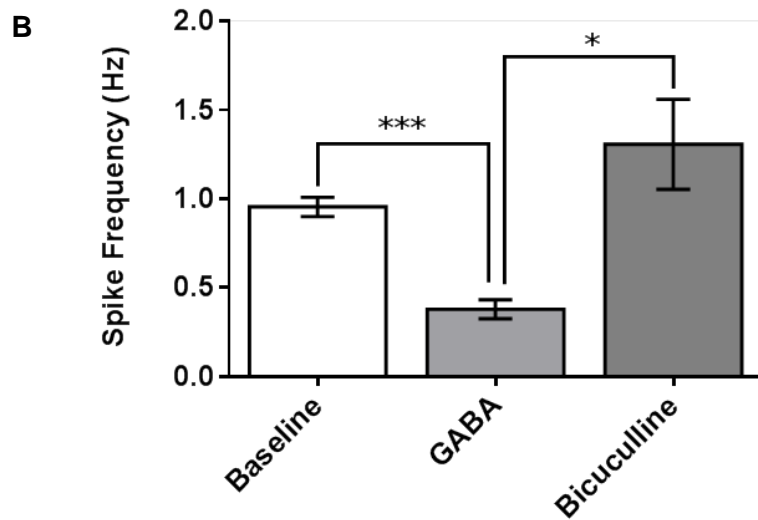
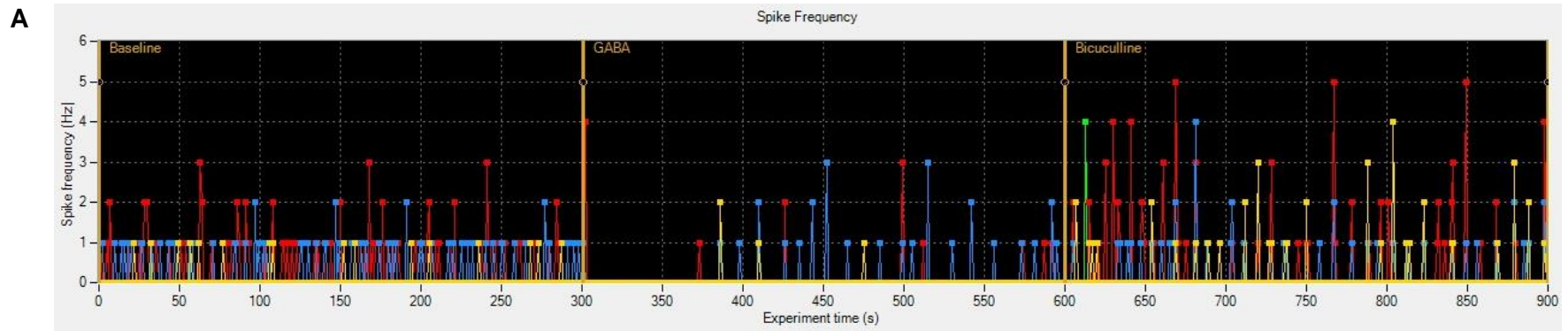


Figure 6.20 Embryonic spinal DH culture recording on the MED64, with GABA receptor agonist and antagonist application. (A) A trace of spike frequency against time from one electrode of a MED64 probe with cultured DH cells at 12 DIV. The first 300 seconds show the spontaneous firing activity. Each dot represents the number of spikes occurring at that time point. The colours represent the different classes of spikes, grouped according to their waveform similarity. The following 300 seconds demonstrates the reduction of spikes in the presence of GABA (50 μ M) which was added at the 300 second time point. The final 300 seconds shows the activity with addition of bicuculline (50 μ M) which was applied at the 600 second time point, without washing off the previously applied GABA. (B) The mean spike frequency (\pm SEM) during each of the sections illustrated in (A) (N=2, n=3, e=8).

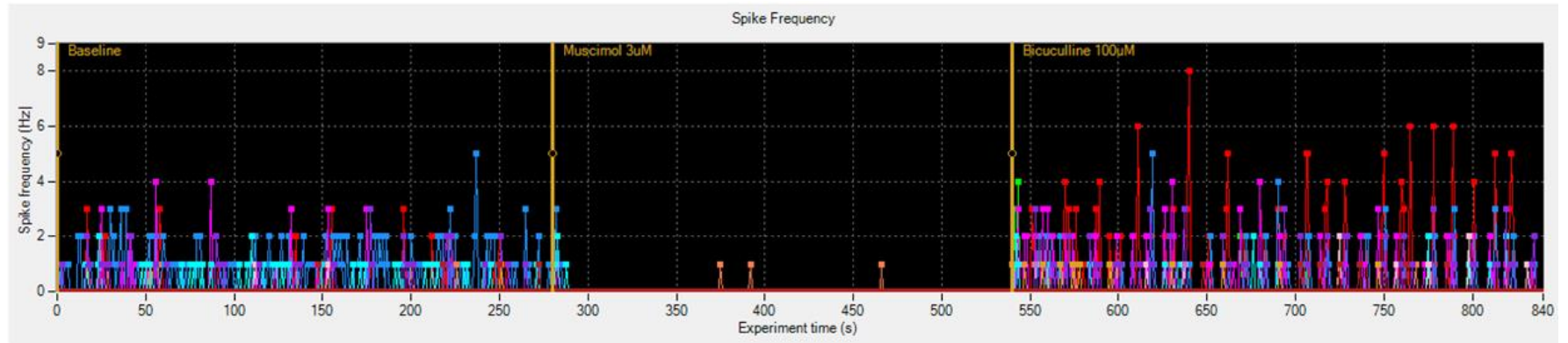
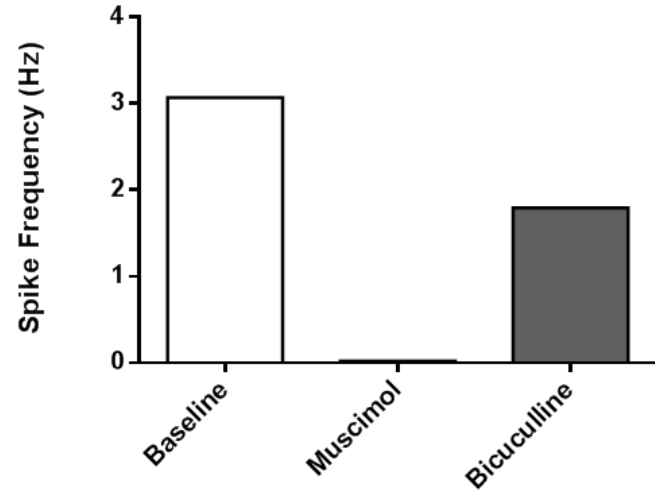
A**B**

Figure 6.21 A MED64 recording with the spinal DH culture where muscimol and bicuculline are applied to the culture. (A) The spike frequency profile against time of a recording from the DH culture on the MED64. The first section of the recording shows the baseline spontaneous activity, which is followed by the addition of muscimol (3 μ M). Therefore, the second section of the recording is the activity of the culture in the presence of muscimol. The final section is in the presence of bicuculline (100 μ M), which restores the population spikes. (B) The spike frequency of each of the sections of the data shown in (A) (N=1, e=1).

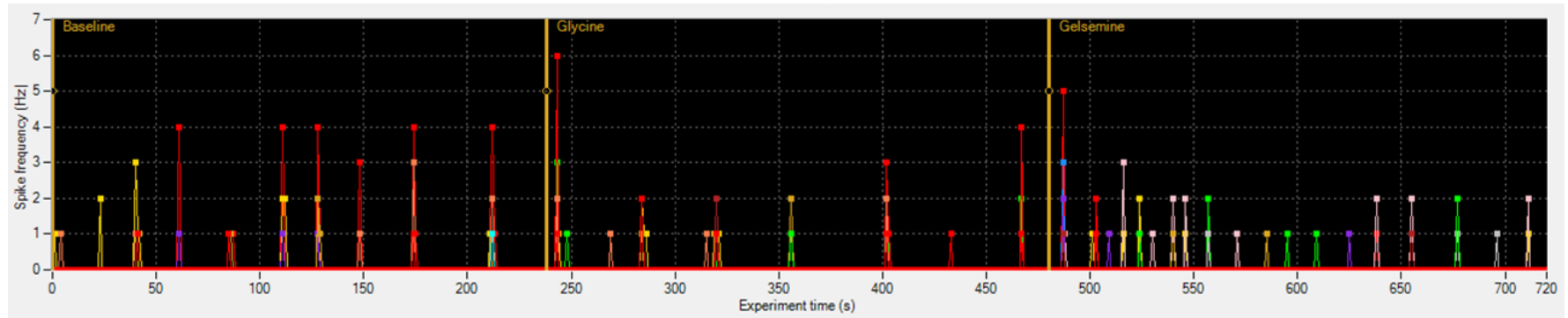
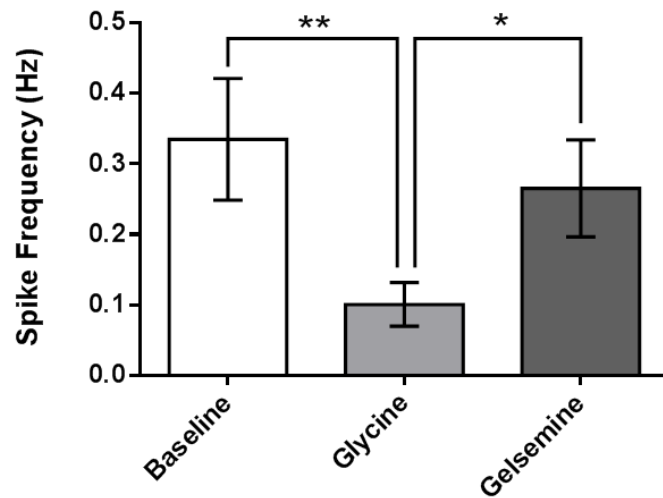
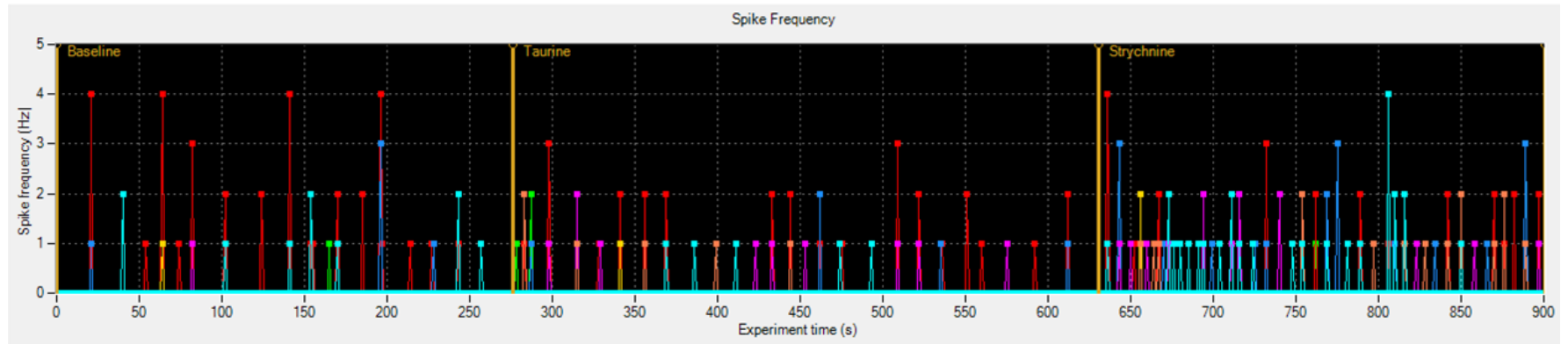
A**B**

Figure 6.22 The effect of glycine and gelsemine on the spinal DH culture electrical activity using the MED64. (A) An example from one electrode of the MED65 probe of the profile of the spike frequency against time. The first section of the recording illustrates the DH culture baseline activity. The second section of the recording illustrates the DH culture activity in the presence of glycine (1 mM) and the final section is the activity in the presence of gelsemine (50 μ M). (B) The mean spike frequencies recorded for each of the sections of the recordings described in (A) from the DH cultures on the MED64. (N=4, n=6, e=35).

A



B

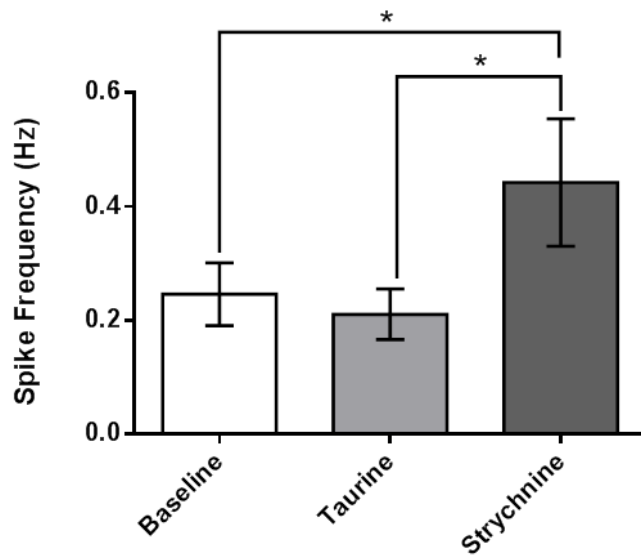


Figure 6.23 The effect of taurine and strychnine on the DH cultures on the MED64. (A) An example profile from one electrode of a recording with taurine and strychnine. The spontaneous baseline activity is shown in the initial section, followed by the spike frequency of the culture in the presence of taurine (1 mM). The final section of the trace is the spinal DH culture activity in the presence of strychnine (10 μ M). (B) The mean spike frequencies of the DH culture recorded at each electrode for the three sections of the recordings described in (A) (N=2, n=3, e=8).

Spike Frequency	
GABA	↓
Muscimol	↓
Bicuculline	↑

Table 6.4 A summary table of the effects of the GABA_A receptor agonist and antagonists applied to the spinal DH cultures on the MED64 probes. ↑ signifies a significant increase in spike frequency and ↓ indicates a significant decrease in spike frequency.

Spike Frequency	
Glycine	↓
Taurine	n.s
Strychnine	↑
Gelsemine	↑

Table 6.5 A summary table of the effects of the glycine receptor agonists and antagonists on the spinal DH culture activity recorded using the MED64. ↑ signifies a significant increase in the DH culture spike frequency, ↓ indicates a significant decrease in spike frequency and n.s signifies no significant change in spike frequency.

6.4 Discussion

6.4.1 MEA Spinal Cord Slice Recordings Detected 4-AP-Induced Activity Throughout all Laminae of the Dorsal and Ventral Horns Hyperexcitability

Utilising MEA technology with the acute spinal cord slices enabled the measurement of activity to be made at multiple sites from within a single laminae of the slice and across many different lamina simultaneously. Therefore the activity from the SG, deep DH and VH of the spinal cord slices could be measured simultaneously. Furthermore, obtaining data from multiple recording sites within the SG results in greater statistical power of the data compared to the single electrode recordings as described in Chapter 5. As shown previously in Chapter 5, there was no spontaneous firing in the spinal cord slices recorded during the baseline period prior to 4-AP perfusion. This is consistent with previous reports from spinal cord slice recordings where there was a very low incidence of spontaneous activity or none at all (Ruscheweyh and Sandkuhler, 2003, Taccola and Nistri, 2005). The results presented in this chapter illustrate that 4-AP can be used to induce a hyperexcitable state comparable to that which occurs in *in vivo* pain models (Takaishi et al., 1996, Chapman et al., 1998b, Ruscheweyh and Sandkuhler, 2003, Urch and Dickenson, 2003, Quinn et al., 2010). This hyperexcitability was similarly observed in the single electrode recordings from the spinal cord slices as presented in Chapter 5. Importantly, the MEA slice recordings completed for this chapter demonstrate that the activity induced by 4-AP in the spinal cord slices manifests more prominently in the DH than the VH (Figure 6.5). In the VH, 4-AP has been previously demonstrated to induce repetitive firing which has been identified to not be influenced by the DH 4-AP-induced activity but can be modulated by the locomotor central pattern generator network activity (Taccola and Nistri, 2005). Furthermore, synchronicity of the 4-AP-induced activity was detected within one DH

region but little coherence between the two DH regions. Additionally, there was little synchronicity between the DH and VH. These findings are consistent with previous reports from hemisected spinal cord slices (Taccola and Nistri, 2005).

The subsequent increase in release of GABA from inhibitory interneurons activates postsynaptic GABA_A receptors, and an influx of chloride ions. The increase in intracellular chloride ion concentration activates KCC2 co-transporters, which causes an efflux of potassium and chloride ions (Viitanen et al., 2010). This potassium ion efflux increases the extracellular potassium ion concentration, which has been detected following 4-AP application to hippocampal slices (Morris et al., 1996). Transient increases in extracellular potassium ion concentration have been suggested to initiate the depolarisation of neighbouring neurons as well as shifting the reversal potential of GABA_A receptors to a more positive potential resulting in weaker GABAergic inhibition (Avoli and de Curtis, 2011). Therefore, these mechanisms increase neuronal excitability, and suggest how 4-AP initiates epileptiform activity in CNS networks. By linking this mechanism with the previously described ING and PING networks for generating rhythmic oscillations, the increase in neuronal excitability by 4-AP could be the drive for these networks which then synchronise neuronal firing and generate the oscillations.

The higher spike frequency and amplitude recorded from the DH compared to the VH of the lumbar spinal cord slices could be the result of a lower expression of KCC2 in the VH (Javdani et al., 2015). A lower expression of KCC2 in the VH would result in less efflux of chloride and potassium ions following application of 4-AP and consequently less neighbouring neurons in the network would be depolarised, lessening the excitatory drive for the generation of rhythmic activity. Alternatively, there is a lower expression of a number of GABA_A receptor subunits in the VH compared to the DH (Paul et al., 2012). This could similarly be the cause of the reduced 4-AP-induced activity in the VH as there would be less influx of chloride

ions through the reduced number of GABA_A receptors resulting in a diminished activation of KCC2 co-transporters. Therefore, there would be a smaller increase in extracellular potassium ion concentration and a smaller excitatory drive for the generation of rhythmic oscillations in the VH.

6.4.2 4-AP-Induced Activity in Spinal Cord Slices is Modulated by GABA_A Receptor Agonists and Antagonists

The GABA_A receptor agonist GABA and the partial agonist THIP both enhanced the 4-AP-induced population spike frequency and amplitude in the SG, deep DH and VH. The increase in excitability observed with the application of these GABA receptor agonists could be the result of an increase in activity of the KCC2 co-transporter as a result of a large increase in intracellular chloride ions following GABA_A receptor stimulation by the applied GABA_A receptor agonists. As described previously this may result in an increase in extracellular potassium ion concentration which subsequently depolarises neighbouring neurons (Avoli and Jefferys, 2015). Furthermore, blocking GABA_A receptors with antagonists would have the opposite effect, as was observed in the bicuculline and gabazine recordings. However, there is evidence that 4-AP downregulates KCC2 expression (Rivera et al., 2004). A downregulation of KCC2 would result in an accumulation of chloride ions inside the neurons, consequently causing the activation of GABA_A receptors to produce an efflux of chloride ions and therefore depolarisation and an increased excitability. This downregulation of KCC2 by 4-AP could similarly explain the decrease in 4-AP-induced activity observed with GABA_A receptor antagonists bicuculline and gabazine. In the case of a downregulation of KCC2 and consequently an increase in intracellular chloride ions, the blocking of GABA_A receptors would prevent the efflux of chloride ions and therefore decrease neuronal excitability. Under normal *in vivo*

conditions bicuculline has been shown to cause hypersensitivity and allodynia in rats (Yaksh, 1989). Assuming that the effects of the currently investigated GABA_A compounds are reversed in the *in vitro* spinal cord slice model due to changes in the chloride electrochemical gradient by 4-AP, the results could be considered equivalent to the published *in vivo* data.

Interestingly the GABA_A receptor agonist muscimol significantly decreased population spike frequency and amplitude in the SG, deep DH and VH. This is opposite to the effects of GABA application, which could be explained through GABA also binding to the GABA_B receptor. Alternatively, as GABA is the endogenous agonist, dramatically increasing the concentration of GABA extracellularly could initiate changes intracellularly to prevent further production or increase uptake and degradation of GABA which may over compensate and prevent any GABA inhibition. Muscimol and bicuculline have previously been shown to both decrease spinal network activity *in vitro* (Yoon et al., 2010). Furthermore, muscimol decreases activity in the spinal cord of rats with a spinal cord injury, which can be reversed by bicuculline (Wakai et al., 2005, Miyazato et al., 2008). Therefore, there is potentially an alternative mechanism for the activation of GABA_A receptors to cause a loss of 4-AP-induced activity in the spinal cord networks. For example, a decrease in intracellular chloride ion concentration has been linked with the intrinsic pathway of apoptosis (Heimlich and Cidlowski, 2006). Therefore, an excessive block of GABA_A receptors with bicuculline could decrease the intracellular chloride ion concentration, which could lead to cell death or possibly a loss of activity of the neurons in the spinal cord slice consequently reducing activity.

6.4.3 4-AP Activity in Spinal Cord Slices is Modulated by GABA_B Receptor Agonist Baclofen and Antagonist 2-Hydroxysaclofen

GABA_B receptor agonist baclofen significantly decreased 4-AP induced spike amplitude and frequency in the SG and deep DH. In the VH, baclofen significantly decreased spike amplitude but not spike frequency. Baclofen is used clinically as an anti-spastic agent and muscle relaxant (Capek and Esplin, 1982, Miyazato et al., 2008, Kuroiwa et al., 2009). There is also evidence that GABA_B receptors are involved in the pain pathway in both the periphery and in the spinal DH (Allerton et al., 1989, Liu et al., 2014, Huang et al., 2015). Baclofen exerts an analgesic effect in rodent pain models, including orofacial formalin model and chronic constriction of the sciatic nerve (Franek et al., 2004, Nowak et al., 2013). Therefore, the results presented here are consistent with previously reported *in vivo* and *in vitro* data with baclofen reducing neuronal excitability. The GABA_B antagonist 2-hydroxysaclofen significantly increased spike amplitude in the SG, deep DH and VH, however there was no effect recorded on the spike frequency in any of these regions. This increase in excitability was reported previously where 2-hydroxysaclofen reversed the effects of baclofen (Curtis et al., 1988). Since 2-hydroxysaclofen did not affect the spike frequency and only amplitude, it is possible that there are different mechanisms that modulate these different components of the population spikes. For example, as discussed previously the frequency of the spikes could be determined by the network and the gating of activity by GABAergic and glycinergic interneurons. The amplitude of the population spikes could be dependent on synaptic strength, which has been previously illustrated for GABA_A receptor signalling (Chapman et al., 1998a).

6.4.4 4-AP Activity in Spinal Cord Slices is Modulated by Glycine Receptor Agonist and Antagonists

Application of glycine to the spinal cord slices on the MEA significantly increased the 4-AP-induced population spike amplitude and frequency in the SG, deep DH and VH. This was also shown with the single electrode recordings from the DH of spinal cord slices presented in chapter 5. Furthermore, the same effect was observed with the GABA_A receptor agonists GABA and THIP. Therefore, the increase in activity in the presence of glycine could similarly be explained by a change in the electrochemical gradient of chloride ions as a result of a downregulation of KCC2 in the presence of 4-AP. Or the increased activation of glycine receptors could add to the increased intracellular chloride ion concentration, as similarly described for GABA. This could then increase KCC2 activity to produce an increase in extracellular potassium ion concentration, which depolarises nearby neurons thus increasing network activity. Alternatively, glycine is also a co-agonist at the NMDA receptor, in addition to glutamate (Papouin et al., 2012). When activated under normal physiological conditions, NMDA receptors produce depolarisation of the cell and thus result in an increase in cell excitability (Chen et al., 1997). Therefore, the increased extracellular glycine concentration in the spinal cord slices could also produce an increase in the probability of NMDA receptor channel opening, which would consequently increase excitability which was detected with the perfusion of glycine. However, glycine is only a co-agonist of extrasynaptic NMDA receptors (Papouin et al., 2012), which could be less involved in the generation of synchronous network activity in the spinal DH. Furthermore, previous reports using this model have shown that inhibiting NMDA receptors with antagonist AP5 had no significant effect on 4-AP activity (Chapman et al., 2009). This suggests that the NMDA receptor does not have a major role in the 4-AP-induced activity within the spinal DH. Therefore, the effects of glycine perfusion

observed here may well be through its actions at glycine receptors and not through NMDA receptors.

Glycine receptor antagonist strychnine also produced a significant increase in 4-AP-induced spike amplitude and frequency in all regions of the spinal cord slices investigated. In the single electrode recordings for spinal cord slices strychnine application decreased the 4-AP-induced activity. Previous studies have shown that *in vivo* pharmacological activation of glycine receptors exerts an analgesic effect in the spinal cord, while blocking glycine receptors increases symptoms of pain, including allodynia (Beyer et al., 1985, Yaksh, 1989, Sivilotti and Woolf, 1994, Lynch and Callister, 2006, Lu et al., 2013). Furthermore, *in vivo* patch-clamp recordings from the SG have shown that strychnine blocks IPSPs (Narikawa et al., 2000). The enhanced activity with application of both glycine receptor agonist and antagonist could be explained by the circuitry of the inhibitory and excitatory interneurons. If strychnine acts on those glycine receptors located on postsynaptic glutamatergic interneurons, strychnine would prevent the inhibition of these excitatory interneurons and therefore increase excitability. Additionally, as previously explained in Chapter 5, synapses between two inhibitory interneurons have been identified in the spinal DH (Zheng et al., 2010). If the application of glycine to the spinal cord slices results in glycine predominantly activating the glycine receptors on inhibitory interneurons this would enhance the inhibition of these inhibitory interneurons. Consequently, these inhibitory interneurons would be prevented from inhibiting postsynaptic glutamatergic interneurons and thus result in further excitation.

Gelsemine binds the glycine receptor and exerts an analgesic effect as well as muscle relaxation, sedation and anxiolytic effects (Zhang and Wang, 2015). Furthermore, it is believed that gelsemine is selective for $\alpha 3$ -containing glycine receptors (Venard et al., 2008, Zhang and Wang, 2015). The data presented here

illustrate that the application of gelsemine on the spinal cord slices produces a significant decrease in 4-AP-induced population spike amplitude and frequency in the superficial DH. In the deep DH gelsemine increased spike amplitude but decreased spike frequency. While in the VH there was no significant change was observed. The different effects in the different lamina could be due to the expression of the glycine $\alpha 3$ -containing receptors being primarily in the superficial DH (Harvey et al., 2004). This would explain the lack of effect in the VH due to the absence of the $\alpha 3$ -containing glycine receptors, while gelsemine did modify the 4-AP activity in the DH where the concentration of these receptors is the highest. The decrease in activity in the presence of gelsemine is consistent with the analgesic effect of this compound *in vivo* (Wu et al., 2015a, Zhang and Wang, 2015). Gelsemine has not been used clinically due to its highly toxic and short-lived effects which limit its dosage and therefore its applications as an analgesic (Wu et al., 2015a, Zhang and Wang, 2015).

6.4.5 KCC2 Inhibitor VU0240551 Increases 4-AP Spike Amplitude in the Spinal Cord

The KCC2 inhibitor VU0240551 caused an increase in spike amplitude in the SG, deep DH and VH. However, it only increased spike frequency in the VH. Blocking the KCC2 transporters likely produced an increase in spike amplitude as a result of an increase in intracellular chloride ion concentration, as this co-transporter would not be able to export chloride ions from the DH neurons. Therefore, the electrochemical gradient chloride would be shifted and the opening of GABA_A and glycine receptor ion channels would lead to an efflux of chloride ions. Consequently these neurons depolarise, thus increasing excitability. A shift in the chloride electrochemical gradient from KCC2 downregulation similarly produces an increase

in the excitability in the hippocampus where it increases seizure susceptibility (MacKenzie and Maguire, 2015). Therefore, the results presented here are consistent with previous findings. Pharmacologically targeting the KCC2 co-transporter has been investigated in the spinal DH for the development of novel analgesics (Coull et al., 2003, Zhang et al., 2008c, Hasbargen et al., 2010, Ford et al., 2015).

6.4.6 Cultured Dorsal Horn Cells on the MEA Detects Synchronous and Non-Synchronous Electrical Activity

Once optimised, the cultured DH cells on the MEA displayed some diverse activity compared to that detected with the calcium imaging assay discussed in Chapter 3. The calcium imaging experiments demonstrated a highly synchronous, rhythmic activity of the culture. On the MEA the DH culture did have comparable synchronous spontaneous field potentials across the culture. In addition, there were non-synchronous spikes detected sporadically between the synchronous firing. These non-synchronous spikes were likely undetected in the calcium imaging assay due to these spikes exerting a smaller change in the fluorescence and the lower sensitivity of the calcium imaging assay compared to the electrophysiological recordings. However, the pharmacology was consistent with the calcium imaging data. The results presented in this chapter show that the GABA_A and glycine receptor agonists GABA, glycine and taurine all decreased spike frequency. The antagonists bicuculline, strychnine and gelsemine all increased spike frequency. These results are consistent with these receptors exerting an inhibitory effect in this network. Furthermore, these data are consistent with previous *in vivo* and *in vitro* reports of agonists decreasing excitability and producing anti-nociceptive effects and the antagonists increasing activity and causing pronociceptive effects (Beyer et

al., 1985, Narikawa et al., 2000, Harvey et al., 2004, Racz et al., 2005, Harvey et al., 2009, Haranishi et al., 2010, Wu et al., 2015a, Zhang and Wang, 2015).

6.4.7 *Comparing the Potential of the Spinal Cord Slice and Spinal Dorsal Horn Culture Models*

Extracellular recordings from spinal cord slices provide a useful platform in which to obtain information regarding the mechanisms of generating and regulating network excitability. The development of the spinal cord slice technique has improved the health of the slices and therefore the networks and recordings from them (Avoli and Jefferys, 2015). The MEA technique provides a more powerful method of investigating the slice activity compared to the single electrode recordings through being able to obtain more data from a single slice and study the network synchronicity. However, compared to the calcium imaging assay the MEA spinal cord slice technique is a lower throughput technique. Furthermore, the problem remains that the complexity of the spinal cord slice limits our understanding of the data obtained from the extracellular recordings. The simplified DH cell culture network provides an accessible model in which to gain further insight into network synchronicity and rhythmicity. However, the differences in pharmacological responses in the culture compared to the slices, which have a more intact network, suggests that both models are required for a more complete understanding of network activity. The culturing process of the DH cells could have resulted in the loss of some vital component in the DH network which has manifested as a difference in pharmacology. The DH culture network is likely to be less similar to the *in vivo* DH network compared to the *in vitro* slice model. However, the data obtained with the spinal DH culture in both the calcium imaging assay and the MEA was highly consistent, while the spinal cord slice pharmacology with the single electrode

recordings was not entirely consistent with the MEA recordings. Therefore, the spinal DH culture model is more robust, and consequently potentially more attractive for testing novel analgesics.

The MEA recording with the DH cells is extremely low throughput to test compounds and achieving the required culture conditions is challenging. Recent advancement in MEA technology has resulted in the development of multi-well plates with MEA arrays in each well (mwMEAs) (Axion Biosystems, USA). Cells can be cultured on these MEA multi-well plates and recordings from all wells made simultaneously with easy access for compound addition (McConnell et al., 2012). However, even with this innovative technology the challenge of obtaining the optimal culturing conditions for DH cells on the MEA remains. The MEA slice recordings provide a more cost-effective and reliable recording method to study the network activity. Furthermore, being able to compare the activity across the different lamina of spinal cord slices is extremely valuable. Utilising both spinal cord slice and DH culture models on the MEA also provides the opportunity to investigate the differences in the networks and their pharmacology. Consequently the value of the culture as an *in vitro* model of the DH network can be further assessed and used for the development of analgesics.

7 General Discussion

7.1 Outline

This research aimed to address the development of *in vitro* models for the screening of novel analgesics and investigate the role of GABA_A and glycine receptors on the spinal DH network activity. Currently available analgesics, including morphine and its analogues, do not provide sufficient pain relief in all patients and are well-known for their adverse side effects and abuse-liability (Stein, 2013). Therefore there is a high demand for novel analgesics with improved efficacy and fewer side effects. Over the past 20 years the greatest progress in the development of new analgesics has been limited to the reformulation of opioids, production of anticonvulsants, cyclooxygenase (COX) inhibitors and amine reuptake inhibitors (Woolf, 2010). The limited advancement in novel analgesic development is partly due to a lack of robust, reproducible, translational platforms to predict drug efficacy and investigate the feasibility of proposed hypotheses (Borsook et al., 2014). Therefore this study has utilised two *in vitro* model systems of the spinal DH, firstly the well-established spinal cord slice model and secondly a developed and optimised primary cell culture model. In addition to evaluating these two model systems as potential platforms for screening novel centrally acting analgesics, the roles and mechanisms of inhibitory GABA_A and glycine receptors in the generation and modulation of spinal DH activity were investigated. A summary of the overall effects of the compounds tested on each model with the different techniques is provided in Table 7.1.

7.2 Primary Cell Culture of the Spinal Dorsal Horn

7.2.1 Characterisation of the Spinal Dorsal Horn Culture

In this study the development and optimisation of the embryonic spinal DH cell culture has been described with the intentions of this model being utilised for

screening novel analgesics and to investigate the physiology of the spinal DH network. The spinal DH culture was characterised to determine the expression of cell types existing in the *ex-vivo* spinal cord slice, with a focus on the expression of GABA_A and glycine receptor subunit expression. Immunohistochemistry was used to illustrate proportions in the expression of neuronal cells, glia and microglia in the DH culture and as well as that of excitatory and inhibitory interneurons. The proportion of inhibitory and excitatory interneurons in the DH culture was found to be typical of the spinal DH in *ex-vivo* spinal cord slices, with 30-40% inhibitory and 60-70% excitatory (Polgar et al., 2003). Each of the GABA_A and glycine receptor α subunits were expressed in the DH culture, with the expression of the glycine receptor β subunit and glycine transporters 1 and 2 detected by RT-PCR. Absolute quantification RT-PCR revealed the expression of the glycine receptor α 1 subunit was only two-fold higher than the α 2 subunit, and approximately seventeen-fold higher than α 3 subunit expression in the DH culture. The reverse was true in the adult human spinal cord mRNA, where the expression of the glycine receptor α 3 subunit was approximately twenty-fold higher than the α 1 expression when the numbers of molecules for each α 3 splice variant are combined. The novel finding in the adult human spinal cord mRNA was that the K variant of the glycine receptor α 3 subunit is more highly expressed compared to the L variant. The expression of the two splice variants of the α 3 subunit has been investigated in the hippocampus where there is a higher expression of the α 3L variant in rodents and humans. Furthermore, in humans with temporal lobe epilepsy (TLE) the expression of the α 3K variant is increased at the expense of the α 3L variant expression (Eichler et al., 2009). This implies that glycine receptors are fundamentally required for the regulation of network rhythmic oscillations and α 3-containing glycine receptors play a key role. The K variant of the α 3 subunit is missing 15 amino acids in the intracellular loop compared to the L variant, and has faster desensitizing receptor kinetics (Nikolic et al., 1998). The frequency of rhythmic oscillations in the brain are

also influenced by GABA_A receptor kinetics (Wang and Buzsáki, 1996). Therefore, it is highly probable that differences in glycine receptor subtype kinetics could also influence the frequency of oscillations in the spinal DH network. If this is the case, the lower expression of the glycine receptor $\alpha 3$ subunit relative to the $\alpha 1$ subunit in the DH culture compared to the human spinal cord suggests a lower relative expression of the glycine receptor $\alpha 3$ K variant. Consequently, a smaller proportion of glycine receptors will have faster desensitisation kinetics which could decrease the generation and frequency of the rhythmic oscillations in the DH culture compared to the human spinal cord. These differences in the networks should be taken into account when using the DH culture model to screen novel compounds.

Further classification of the inhibitory interneurons in the spinal DH cell culture was performed to show co-localisation of the inhibitory interneurons with nNOS and PV. PV-expressing inhibitory interneurons in the brain are required for the generation of gamma oscillatory activity (Sohal et al., 2009, Volman et al., 2011). Therefore the occurrence of rhythmic activity in the DH culture could be linked to the PV-expressing inhibitory interneurons. Importantly there was also strong positive staining for KCC2 in many of the DH culture's inhibitory interneurons, implicating that these interneurons could have a similar chloride electrochemical gradient as the mature spinal DH network (Rivera et al., 1999, Coull et al., 2003). The prevalent expression of KCC2 in the DH culture implies that the embryonic neurons have matured during the 12 to 14 day period of culturing. Therefore, GABA and glycine neurotransmission in the DH culture is likely to be inhibitory.

7.2.2 GABAergic and Glycinergic Neurotransmission Regulate Spinal Dorsal Horn Culture Rhythmic Oscillations

Calcium imaging and MEA techniques were used to measure the activity of the cultured DH cells. Spontaneous, rhythmic firing of the DH culture network was detected with both these techniques. Calcium imaging is an indirect measure of neuronal activity, measuring the flux of intracellular calcium (Grienberger and Konnerth, 2012), while MEA recordings measure the extracellular electrical activity of the network (Spira and Hai, 2013). The calcium imaging with the BD Pathway system enabled visualisation of the spontaneous, highly synchronised, rhythmic network activity. This technique was invaluable during the optimisation of the culture, however, the throughput is extremely low and therefore the remaining calcium imaging data was obtained using the Flexstation microplate reader. The Flexstation assay provides a higher throughput technique to investigate the effects of compounds on the culture, although smaller oscillations in activity go undetected. The MEA recordings provide a more detailed account of the culture's activity, detecting some additional smaller spikes and measuring the duration and amplitude of population spikes. The electrical activity of the DH culture measured from 64 electrodes simultaneously across the culture using the MEA also demonstrated synchronous firing of the cells. However, culturing the cells on the MEAs was particularly problematic and it is a very low throughput assay but the cultured cells on the MEA are extremely accessible. The spontaneous activity measured using calcium imaging and MEA techniques was lessened with application of GABA_A and glycine receptor agonists including GABA, muscimol, glycine and taurine. Antagonists of these receptors, including bicuculline, gabazine, strychnine and gelsemine, all enhanced the spontaneous activity of the spinal DH cultures. This suggests the chloride electrochemical gradient is similar to mature neurons, as the stimulation of glycine and GABA_A receptors had an inhibitory effect. This is

supported by the KCC2 expression in the culture illustrated from the IF staining. Furthermore, these results illustrate that the rhythmic oscillatory activity of the spinal DH culture requires inhibitory neurotransmission. This finding is supported by previous reports of the fundamental requirement of inhibitory neurotransmission for oscillatory rhythmic activity in the brain and spinal cord in *in vitro* slice models and spinal cord cell cultures (Sandkuhler and Eblen-Zajjur, 1994, Streit et al., 2001, Chapman et al., 2009, Kim et al., 2015, Kuki et al., 2015).

7.2.3 *Glycine Receptor siRNA Gene Silencing in the Spinal Dorsal Horn Culture*

Due to the lack of glycine receptor subtype-selective compounds, I employed an siRNA gene silencing technique in the DH culture to further investigate the role of the glycine receptor subtypes in the DH network oscillatory activity. Unfortunately, the siRNAs used in this study for the glycine receptor α subunits 1-3 were not all selective, as indicated by RT-PCR results in the DH cultures transfected with each of the siRNAs. Only the glycine receptor $\alpha 3$ siRNA selectively silenced the expression of the glycine receptor $\alpha 3$ subunit, the other two siRNAs knocked-down the expression of their target subunit and the $\alpha 3$ subunit. Each of the glycine receptor siRNAs caused a significant loss of the spontaneous rhythmic oscillations in the culture. This emphasises the key role for the glycine receptor in the generation of the spontaneous rhythmic activity, and could suggest that the glycine receptor $\alpha 3$ subunit is primarily responsible as its expression was knocked down by all three siRNAs. The loss of rhythmic activity in the DH culture could be the result of the culture not reaching the same mature state as observed with untreated DH cultures, since the siRNA was transfected 3-4 days before the culture is considered to have fully matured. Glycine receptors have been linked with formation of

synapses and the maturation of networks (Ben-Ari, 2001). However, the majority of the cultures were still responsive to strychnine and glycine which produced the same effects as observed in the untreated cultures. This implicates the existence of glycine receptors within the culture and that the culture has matured to a state where glycine receptor transmission is inhibitory which occurs *in vivo* during postnatal development (Ben-Ari et al., 2007). Although the cultures transfected with each of the glycine receptor siRNAs all responded to strychnine which increased activity, the $\alpha 3$ siRNA transfected cultures were the only cultures not to respond to glycine addition in terms of the spike frequency or area under the curve. Therefore, this further indicates a prominent role for the $\alpha 3$ -containing glycine receptors in the DH over the other two receptor subtypes. This result is consistent with other reports of the $\alpha 3$ glycine receptors in the spinal DH being selectively involved in pain conditions, particularly inflammatory pain (Harvey et al., 2004, Racz et al., 2005, Harvey et al., 2009). Consequently, designing compounds that are selective for the glycine receptor $\alpha 3$ subtype could lead to the production of novel analgesics with reduced adverse side effects. Obtaining subunit-selective siRNAs are required to more definitively determine if the $\alpha 3$ -glycine receptors are truly the primary subtypes involved in the spinal DH network activity.

7.3 Spinal Cord Slice Recordings

7.3.1 GABA_A and Glycine Receptors Modulate the 4-AP-Induced Rhythmic Activity

In the spinal cord slice single electrode and MEA recordings the application of 4-AP produced hyperexcitability, which could be seen across the slice in the MEA recordings. Furthermore, the MEA recordings illustrated that the 4-AP-induced activity was highly synchronous across the DH. The 4-AP-induced activity has been

previously used as a model of epilepsy in brain slices (Gonzalez-Sulser et al., 2012) and in spinal cord slices as a model of neuropathic pain (Ruscheweyh and Sandkuhler, 2003, Asghar et al., 2005, Chapman et al., 2009). The data obtained from the dorsal and ventral horns of the spinal cord slices using the MEA recordings illustrated that the 4-AP-induced activity in the DH had a higher spike frequency and amplitude compared to that observed in the VH. An additional benefit of the MEA recordings over the single electrode slice recordings was that there are more electrodes recording from each of the laminae which produce more statistically powerful data. Therefore while the changes in 4-AP-induced activity following application of compounds to the slices using each of these techniques were the same, the MEA recordings produced the most statistically powerful data.

Antagonists of the GABA_A receptor, bicuculline and gabazine, decreased the 4-AP-induced spike frequency and amplitude in the single electrode and MEA recordings, which is consistent with previously published data in the spinal DH system (Ruscheweyh and Sandkuhler, 2003, Chapman et al., 2009). While initially this might seem counterintuitive, it is possible that the block of inhibitory neurotransmission is required for the generation of the rhythmic oscillations by synchronising the excitatory activity. The proposed models of rhythmic oscillatory activity, ING and PING described in section 1.5 of chapter 1, require inhibitory interneurons to generate the rhythmic activity. There is evidence for these models in the hippocampus, where stimulating inhibitory interneurons increased the gamma oscillations while hyperpolarising them decreased the oscillations (Cardin et al., 2009, Sohal et al., 2009). In comparison, the stimulation of excitatory interneurons is less effective in increasing the oscillations (Cardin et al., 2009). In the spinal DH culture bicuculline increased the activity, this infers potential differences in the network circuitry or the mechanisms of generation of the 4-AP activity compared to

the spontaneous firing of the culture. If this is the case, caution is required when utilizing these models to screen for novel analgesic compounds.

Interestingly the glycine receptor antagonist strychnine increased the 4-AP-induced population spike frequency and amplitude in the MEA slice recordings. The increase in activity following the application of strychnine to the spinal cord slice is consistent with the blocking of glycine inhibition resulting in increased excitation. This has been indicated in the brain, where a reduction in glycine inhibition can produce epileptiform activity (Shen et al., 2015). In agreement with the current data, a more pertinent example is that bicuculline and strychnine produce opposite effects in the spinal DH following application of 4-AP in the spinal DH (Ruscheweyh and Sandkuhler, 2003). Furthermore, glycine application to the slices also produced an increase in the 4-AP-induced spike amplitude and frequency in the recordings obtained using both techniques. The action of glycine could be explained from glycine also acting as a co-agonist at NMDA receptors (Papouin et al., 2012). NMDA receptors are typically excitatory, therefore an increase in glycine concentration is likely to increase NMDA receptor activation and consequently produce the increase activity in the DH network. The different response to application of glycine in the spinal cord slices further suggests that the networks are not the same, or that the 4-AP-induced activity involves different mechanisms of generation compared to the spontaneous firing of the DH culture.

The GABA_A receptor partial agonist L-838,417, which selectively mediates its actions through $\alpha 2$, $\alpha 3$ and $\alpha 5$ -containing GABA_A receptors reduced 4-AP-induced rhythmic activity in the spinal DH as observed using the single electrode recordings. This result demonstrates that activation of these subtypes of GABA_A receptors is sufficient to modulate the excitatory activity in the spinal DH. Therefore developing

novel compounds which selectively target these GABA_A receptor subtypes could be advantageous in minimising adverse side effects (Knabl et al., 2008). THIP and muscimol similarly decreased the rhythmic oscillatory activity in the spinal DH, as observed using single electrode recordings. THIP is an agonist of GABA_A receptors but an antagonist of GABA_{A-p} receptors. Therefore, despite the antagonism of GABA_{A-p} receptors, the 4-AP-induced activity was still reduced by THIP, which could have occurred because GABA_{A-p} receptors are not significantly involved in modulation of the spinal DH network activity.

In MEA recordings the blocking of KCC2 with VU0240551 increased the 4-AP-induced spike amplitude in the DH and VH. In theory the blocking of KCC2 would be predicted to prevent the transportation of chloride ions out of the cells to maintain a low intracellular chloride ion concentration. Therefore, the opening of the GABA_A and glycine receptor ion channels would have an efflux of chloride ions, rather than the normal influx of chloride ions which causes hyperpolarisation of the cell. The same effect was found with VU0240551 in the DH culture, which further confirms that the culture has matured to a state where GABA_A and glycine receptor neurotransmission is inhibitory. The modulation of the rhythmic activity in both the *in vitro* models investigated in this study clearly depends on the chloride ion electrochemical gradient and the signalling through GABA_A and glycine receptors.

GABA_B receptors also modulated the 4-AP-induced rhythmic activity, with the agonist baclofen decreasing the rhythmic activity and population spikes in the single electrode and MEA recordings. In contrast GABA_B receptor antagonist 2-hydroxysaclofen enhanced the 4-AP-induced activity, in the spinal cord slice recordings by single electrode and MEA techniques. Baclofen and 2-hydroxysaclofen similarly decreased and increased the DH culture activity respectively. Evidence suggests that there is no downregulation of GABA_B receptors in the spinal DH in models of neuropathic pain (Engle et al., 2006). The reduction in

the GABA_A receptor signalling in the spinal DH in pain conditions could prevent the effectiveness of analgesics targeting the GABA_A receptor. Therefore, the sustained GABA_B receptor expression in the spinal DH in pain conditions is advantageous for targeting these receptors in the design of novel analgesics. However, the limited subtypes of the GABA_B receptor family could imply a potentially large array of side effects following administration of GABA_B receptor-targeting compounds (Bowery, 2006).

7.4 Conclusions

The two *in vitro* model systems investigated in this study have been utilised to illustrate that GABA_A, GABA_B and glycine receptor signalling is able to modulate the rhythmic oscillatory activity of the spinal DH network. Furthermore, the α 3-containing glycine receptors play a key role in this mechanism of modulating the network activity, which has also been indicated in human spinal cord. Additionally, the spinal DH network activity is also dependent on KCC2 activity, which maintains the chloride electrochemical gradient and consequently the effects of GABA and glycine neurotransmission within the network. Consequently, designing novel analgesics that target these receptors could be efficacious.

The newly developed and characterised spinal DH culture model platform had many similarities with the spinal cord slice physiology in terms of the cell types present and the proportions of excitatory and inhibitory interneurons. The culture was easily transferable to be utilised in multiple techniques. However, discrepancies between the responses to a number of compounds in the spinal DH culture network and the spinal cord slice recordings indicate there are differences in the two models. This could relate to the 4-AP inducing activity that is different to the inherent, spontaneous activity of the DH culture. Alternatively the culturing of dissociated

embryonic DH cells could result in the formation of a network which is fundamentally different to the *in vivo* spinal DH, and thus also differ from the *in vitro* spinal cord slice model. The reliance of cell culture models to investigate novel analgesics could be the reason why many pharmaceutical companies have not been able to progress many of their compounds through clinical trials. However, the complexity of the spinal cord slice model prevents a complete interpretation of the data obtained from this model. Further characterisation of both these models is necessary to advance our understanding of how the spinal DH rhythmic activity is generated and modulated. These models provide initial screening platforms for analgesics, which could be utilised to indicate which compounds have the potential to be advanced to pre-clinical studies with *in vivo* animal models. Therefore, these *in vitro* models reduce the number of *in vivo* animal experiments by enabling an initial selection of the most promising compounds.

Compound	Spinal Dorsal Horn Cell Culture		Acute Spinal Cord Slice	
	Flexstation	MEA	S.E.	MEA
GABA	↓	↓	ND	↑
THIP	NA	NA	↓	↑
Muscimol	↓	↓	↓	↓
Diazepam	↓	NA	NA	NA
L-838417	NA	NA	↓	NA
Bicuculline methiodide	↑	↑	↓	↓
Gabazine (SR-95531)	↑	NA	↓	↓
Baclofen hydrochloride	↓	NA	↓	↓
2-Hydroxysaclofen	↑	NA	↑	↑
Glycine	↓	↓	↑	↑
Taurine	↓	↓	NA	NA
CP-802079 hydrochloride	↓	NA	NA	NA
Strychnine	↑	↑	↓	↑
Gelsemine hydrochloride	↑	↑	NA	ND
VU0240551	↑	NA	NA	↑

Table 7.1 A summary of the overall effect of each of the compounds tested on the spinal DH cell culture model and the acute spinal cord slice model for each technique. S.E. stands for the single electrode recording technique, ↑ indicates a significant increase in activity, ↓ indicates a significant decrease in activity, NA = not applicable or not tested and ND = not defined.

References

- Ahmad AH, Ismail Z (2002) c-fos and its Consequences in Pain. The Malaysian journal of medical sciences : MJMS 9:3-8.
- Ahmadi S, Lippross S, Neuhuber WL, Zeilhofer HU (2002) PGE2 selectively blocks inhibitory glycinergic neurotransmission onto rat superficial dorsal horn neurons. *Nature neuroscience* 5:34-40.
- Akagi H, Hirai K, Hishinuma F (1991) Cloning of a glycine receptor subtype expressed in rat brain and spinal cord during a specific period of neuronal development. *FEBS letters* 281:160-166.
- Al Ghamdi KS, Polgar E, Todd AJ (2009) Soma size distinguishes projection neurons from neurokinin 1 receptor-expressing interneurons in lamina I of the rat lumbar spinal dorsal horn. *Neuroscience* 164:1794-1804.
- Albantakis L, Lohmann C (2009) A simple method for quantitative calcium imaging in unperturbed developing neurons. *Journal of neuroscience methods* 184:206-212.
- Albéri L, Lintas A, Kretz R, Schwaller B, Villa AEP (2013) The calcium-binding protein parvalbumin modulates the firing 1 properties of the reticular thalamic nucleus bursting neurons. *Journal of neurophysiology* 109:2827-2841.
- Allain A-E, Cazenave W, Delpy A, Exertier P, Barthe C, Meyrand P, Cattaert D, Branchereau P (2015) Nonsynaptic glycine release is involved in the early KCC2 expression. *Developmental Neurobiology* n/a-n/a.
- Allerton CA, Boden PR, Hill RG (1989) Actions of the GABAB agonist, (-)-baclofen, on neurones in deep dorsal horn of the rat spinal cord in vitro. *British journal of pharmacology* 96:29-38.
- Ameres SL, Martinez J, Schroeder R (2007) Molecular basis for target RNA recognition and cleavage by human RISC. *Cell* 130:101-112.
- Amin J, Brooks-Kayal A, Weiss DS (1997) Two Tyrosine Residues on the α Subunit Are Crucial for Benzodiazepine Binding and Allosteric Modulation of γ -Aminobutyric AcidA Receptors. *Molecular pharmacology* 51:833-841.
- Andersen P, Dingledine R, Gjerstad L, Langmoen IA, Laursen AM (1980) Two different responses of hippocampal pyramidal cells to application of gamma-amino butyric acid. *The Journal of physiology* 305:279-296.
- Antal M, Petko M, Polgar E, Heizmann CW, Storm-Mathisen J (1996) Direct evidence of an extensive GABAergic innervation of the spinal dorsal horn by fibres descending from the rostral ventromedial medulla. *Neuroscience* 73:509-518.
- Aram JA, Michelson HB, Wong RK (1991) Synchronized GABAergic IPSPs recorded in the neocortex after blockade of synaptic transmission mediated by excitatory amino acids. *Journal of neurophysiology* 65:1034-1041.
- Asghar AU, Cilia La Corte PF, LeBeau FE, Al Dawoud M, Reilly SC, Buhl EH, Whittington MA, King AE (2005) Oscillatory activity within rat substantia gelatinosa in vitro: a role for chemical and electrical neurotransmission. *The Journal of physiology* 562:183-198.
- Asiedu MN, Mejia G, Ossipov MK, Malan TP, Kaila K, Price TJ (2012) Modulation of spinal GABAergic analgesia by inhibition of chloride extrusion capacity in mice. *The journal of pain : official journal of the American Pain Society* 13:546-554.
- Ataka T, Kumamoto E, Shimoji K, Yoshimura M (2000) Baclofen inhibits more effectively C-afferent than Delta-afferent glutamatergic transmission in substantia gelatinosa neurons of adult rat spinal cord slices. *Pain* 86:273-282.

- Augustine GJ (2001) How does calcium trigger neurotransmitter release? *Current Opinion in Neurobiology* 11:320-326.
- Ault B, Nadler JV (1983) Anticonvulsant-like actions of baclofen in the rat hippocampal slice. *British journal of pharmacology* 78:701-708.
- Avoli M, de Curtis M (2011) GABAergic synchronization in the limbic system and its role in the generation of epileptiform activity. *Progress in neurobiology* 95:104-132.
- Avoli M, Jefferys JGR (2015) Models of drug-induced epileptiform synchronization in vitro. *Journal of neuroscience methods*.
- Baba H, Ji R-R, Kohno T, Moore KA, Ataka T, Wakai A, Okamoto M, Woolf CJ (2003) Removal of GABAergic inhibition facilitates polysynaptic A fiber-mediated excitatory transmission to the superficial spinal dorsal horn. *Molecular and Cellular Neuroscience* 24:818-830.
- Baccei ML, Fitzgerald M (2004) Development of GABAergic and glycinergic transmission in the neonatal rat dorsal horn. *The Journal of neuroscience : the official journal of the Society for Neuroscience* 24:4749-4757.
- Baimbridge KG, Celio MR, Rogers JH (1992) Calcium-binding proteins in the nervous system. *Trends in Neurosciences* 15:303-308.
- Bakker MJ, van Dijk JG, van den Maagdenberg AM, Tijssen MA (2006) Startle syndromes. *The Lancet Neurology* 5:513-524.
- Balakrishnan V, Becker M, Lohrke S, Nothwang HG, Guresir E, Friauf E (2003) Expression and function of chloride transporters during development of inhibitory neurotransmission in the auditory brainstem. *The Journal of neuroscience : the official journal of the Society for Neuroscience* 23:4134-4145.
- Baltz T, Voigt T (2015) Interaction of electrically evoked activity with intrinsic dynamics of cultured cortical networks with and without functional fast GABAergic synaptic transmission. *Frontiers in cellular neuroscience* 9:272.
- Banke TG, Bowie D, Lee H, Huganir RL, Schousboe A, Traynelis SF (2000) Control of GluR1 AMPA receptor function by cAMP-dependent protein kinase. *The Journal of neuroscience : the official journal of the Society for Neuroscience* 20:89-102.
- Barker JL, McBurney RN, Mathers DA (1983) Convulsant-induced depression of amino acid responses in cultured mouse spinal neurones studied under voltage clamp. *British journal of pharmacology* 80:619-629.
- Barnard EA, Skolnick P, Olsen RW, Mohler H, Sieghart W, Biggio G, Braestrup C, Bateson AN, Langer SZ (1998) International Union of Pharmacology. XV. Subtypes of γ -Aminobutyric Acid A Receptors: Classification on the Basis of Subunit Structure and Receptor Function. *Pharmacological reviews* 50:291-314.
- Baron R (2006) Mechanisms of disease: neuropathic pain--a clinical perspective. *Nature clinical practice Neurology* 2:95-106.
- Basbaum AI, Bautista DM, Scherrer G, Julius D (2009) Cellular and Molecular Mechanisms of Pain. *Cell* 139:267-284.
- Becker CM, Hermans-Borgmeyer I, Schmitt B, Betz H (1986) The glycine receptor deficiency of the mutant mouse spastic: evidence for normal glycine receptor structure and localization. *The Journal of neuroscience : the official journal of the Society for Neuroscience* 6:1358-1364.
- Belelli D, Lambert JJ (2005) Neurosteroids: endogenous regulators of the GABAA receptor. *Nature reviews Neuroscience* 6:565-575.
- Ben-Ari Y (2001) Developing networks play a similar melody. *Trends in Neurosciences* 24:353-360.
- Ben-Ari Y, Gaiarsa JL, Tyzio R, Khazipov R (2007) GABA: a pioneer transmitter that excites immature neurons and generates primitive oscillations. *Physiological reviews* 87:1215-1284.

- Benke TA, Luthi A, Isaac JT, Collingridge GL (1998) Modulation of AMPA receptor unitary conductance by synaptic activity. *Nature* 393:793-797.
- Berridge MJ, Lipp P, Bootman MD (2000) The versatility and universality of calcium signalling. *Nat Rev Mol Cell Biol* 1:11-21.
- Berrocal YA, Almeida VW, Puentes R, Knott EP, Hechtman JF, Garland M, Pearse DD (2014) Loss of central inhibition: implications for behavioral hypersensitivity after contusive spinal cord injury in rats. *Pain research and treatment* 2014:178278.
- Beyer C, Roberts LA, Komisaruk BR (1985) Hyperalgesia induced by altered glycinergic activity at the spinal cord. *Life sciences* 37:875-882.
- Bianchi D, Marasco A, Limongiello A, Marchetti C, Marie H, Tirozzi B, Migliore M (2012) On the mechanisms underlying the depolarization block in the spiking dynamics of CA1 pyramidal neurons. *Journal of computational neuroscience* 33:207-225.
- Bliss TV, Lomo T (1973) Long-lasting potentiation of synaptic transmission in the dentate area of the anaesthetized rabbit following stimulation of the perforant path. *The Journal of physiology* 232:331-356.
- Bohlhalter S, Mohler H, Fritschy JM (1994) Inhibitory neurotransmission in rat spinal cord: co-localization of glycine- and GABAA-receptors at GABAergic synaptic contacts demonstrated by triple immunofluorescence staining. *Brain research* 642:59-69.
- Bohlhalter S, Weinmann O, Mohler H, Fritschy JM (1996) Laminar compartmentalization of GABAA-receptor subtypes in the spinal cord: an immunohistochemical study. *The Journal of neuroscience : the official journal of the Society for Neuroscience* 16:283-297.
- Boileau AJ, Evers AR, Davis AF, Czajkowski C (1999) Mapping the Agonist Binding Site of the GABAAR receptor: Evidence for a β -Strand. *The Journal of Neuroscience* 19:4847-4854.
- Bormann J (2000) The 'ABC' of GABA receptors. *Trends in Pharmacological Sciences* 21:16-19.
- Bormann J, Rundstrom N, Betz H, Langosch D (1993) Residues within transmembrane segment M2 determine chloride conductance of glycine receptor homo- and hetero-oligomers. *The EMBO journal* 12:3729-3737.
- Borsook D, Hargreaves R, Bountra C, Porreca F (2014) Lost but making progress—Where will new analgesic drugs come from? *Science Translational Medicine* 6:249sr243-249sr243.
- Bowery NG (2006) GABAB receptor: a site of therapeutic benefit. *Current opinion in pharmacology* 6:37-43.
- Bragin A, Jando G, Nadasdy Z, Hetke J, Wise K, Buzsaki G (1995) Gamma (40-100 Hz) oscillation in the hippocampus of the behaving rat. *The Journal of neuroscience : the official journal of the Society for Neuroscience* 15:47-60.
- Brejck K, van Dijk WJ, Smit AB, Sixma TK (2002) The 2.7 Å structure of AChBP, homologue of the ligand-binding domain of the nicotinic acetylcholine receptor. *Novartis Foundation symposium* 245:22-29; discussion 29-32, 165-168.
- Bremner L, Fitzgerald M, Baccei M (2006) Functional GABAA-Receptor-Mediated Inhibition in the Neonatal Dorsal Horn. *Journal of neurophysiology* 95:3893-3897.
- Brickley SG, Cull-Candy SG, Farrant M (1996) Development of a tonic form of synaptic inhibition in rat cerebellar granule cells resulting from persistent activation of GABAA receptors. *The Journal of physiology* 497 (Pt 3):753-759.
- Brickley SG, Cull-Candy SG, Farrant M (1999) Single-Channel Properties of Synaptic and Extrasynaptic GABAA Receptors Suggest Differential

- Targeting of Receptor Subtypes. *The Journal of Neuroscience* 19:2960-2973.
- Brown N, Kerby J, Bonnert TP, Whiting PJ, Wafford KA (2002) Pharmacological characterization of a novel cell line expressing human alpha(4)beta(3)delta GABA(A) receptors. *British journal of pharmacology* 136:965-974.
- Brusberg M, Ravnefjord A, Martinsson R, Larsson H, Martinez V, Lindstrom E (2009) The GABA(B) receptor agonist, baclofen, and the positive allosteric modulator, CGP7930, inhibit visceral pain-related responses to colorectal distension in rats. *Neuropharmacology* 56:362-367.
- Buckwalter MS, Cook SA, Davisson MT, White WF, Camper SA (1994) A frameshift mutation in the mouse alpha 1 glycine receptor gene (Glr1) results in progressive neurological symptoms and juvenile death. *Human molecular genetics* 3:2025-2030.
- Buskila Y, Breen PP, Tapson J, van Schaik A, Barton M, Morley JW (2014) Extending the viability of acute brain slices. *Scientific Reports* 4:5309.
- Butt SJB, Harris-Warrick RM, Kiehn O (2002) Firing Properties of Identified Interneuron Populations in the Mammalian Hindlimb Central Pattern Generator. *The Journal of Neuroscience* 22:9961-9971.
- Buzsáki G, Anastassiou CA, Koch C (2012) The origin of extracellular fields and currents — EEG, ECoG, LFP and spikes. *Nature reviews Neuroscience* 13:407-420.
- Buzsaki G, Buhl DL, Harris KD, Csicsvari J, Czeh B, Morozov A (2003) Hippocampal network patterns of activity in the mouse. *Neuroscience* 116:201-211.
- Buzsaki G, Draguhn A (2004) Neuronal oscillations in cortical networks. *Science* 304:1926-1929.
- Caillard O, Moreno H, Schwaller B, Llano I, Celio MR, Marty A (2000) Role of the calcium-binding protein parvalbumin in short-term synaptic plasticity. *Proceedings of the National Academy of Sciences* 97:13372-13377.
- Cancedda L, Fiumelli H, Chen K, Poo M-m (2007) Excitatory GABA Action Is Essential for Morphological Maturation of Cortical Neurons In Vivo. *The Journal of Neuroscience* 27:5224-5235.
- Candeletti S, Lopetuso G, Cannarsa R, Cavina C, Romualdi P (2006) Effects of prolonged treatment with the opiate tramadol on prodynorphin gene expression in rat CNS. *J Mol Neurosci* 30:341-347.
- Capek R, Esplin B (1982) Baclofen-induced decrease of excitability of primary afferents and depression of monosynaptic transmission in cat spinal cord. *Canadian journal of physiology and pharmacology* 60:160-166.
- Cardin JA, Carlen M, Meletis K, Knoblich U, Zhang F, Deisseroth K, Tsai L-H, Moore CI (2009) Driving fast-spiking cells induces gamma rhythm and controls sensory responses. *Nature* 459:663-667.
- Castro-Lopes JM, Tavares I, Coimbra A (1993) GABA decreases in the spinal cord dorsal horn after peripheral neurectomy. *Brain research* 620:287-291.
- Celio MR (1990) Calbindin D-28k and parvalbumin in the rat nervous system. *Neuroscience* 35:375-475.
- Celio MR, Heizmann CW (1982) Calcium-binding protein parvalbumin is associated with fast contracting muscle fibres. *Nature* 297:504-506.
- Chang Y, Wang R, Barot S, Weiss DS (1996) Stoichiometry of a Recombinant GABAA Receptor. *The Journal of Neuroscience* 16:5415-5424.
- Chapman CA, Perez Y, Lacaille JC (1998a) Effects of GABA(A) inhibition on the expression of long-term potentiation in CA1 pyramidal cells are dependent on tetanization parameters. *Hippocampus* 8:289-298.
- Chapman RJ, Cilia La Corte PF, Asghar AU, King AE (2009) Network-based activity induced by 4-aminopyridine in rat dorsal horn in vitro is mediated by both chemical and electrical synapses. *The Journal of physiology* 587:2499-2510.

- Chapman V, Suzuki R, Dickenson AH (1998b) Electrophysiological characterization of spinal neuronal response properties in anaesthetized rats after ligation of spinal nerves L5-L6. *The Journal of physiology* 507:881-894.
- Chen QX, Perkins KL, Choi DW, Wong RKS (1997) Secondary Activation of a Cation Conductance Is Responsible for NMDA Toxicity in Acutely Isolated Hippocampal Neurons. *The Journal of Neuroscience* 17:4032-4036.
- Chen R, Okabe A, Sun H, Sharopov S, Hanganu-Opatz IL, Kolbaev SN, Fukuda A, Luhmann HJ, Kilb W (2014) Activation of glycine receptors modulates spontaneous epileptiform activity in the immature rat hippocampus. *The Journal of physiology* 592:2153-2168.
- Chen ST, Iida A, Guo L, Friedmann T, Yee JK (1996) Generation of packaging cell lines for pseudotyped retroviral vectors of the G protein of vesicular stomatitis virus by using a modified tetracycline inducible system. *Proceedings of the National Academy of Sciences of the United States of America* 93:10057-10062.
- Chen X, Johnston D (2005) Constitutively active G-protein-gated inwardly rectifying K⁺ channels in dendrites of hippocampal CA1 pyramidal neurons. *The Journal of neuroscience : the official journal of the Society for Neuroscience* 25:3787-3792.
- Chéry N, De Koninck Y (2000) GABAB Receptors Are the First Target of Released GABA at Lamina I Inhibitory Synapses in the Adult Rat Spinal Cord. *Journal of neurophysiology* 84:1006-1011.
- Chiara DC, Jayakar SS, Zhou X, Zhang X, Savechenkov PY, Bruzik KS, Miller KW, Cohen JB (2013) Specificity of Intersubunit General Anesthetic-binding Sites in the Transmembrane Domain of the Human $\alpha 1\beta 3\gamma 2$ γ -Aminobutyric Acid Type A (GABA(A)) Receptor. *The Journal of biological chemistry* 288:19343-19357.
- Choi I-S, Cho J-H, Jeong S-G, Hong J-S, Kim S-J, Kim J, Lee M-G, Choi B-J, Jang I-S (2008) GABAB receptor-mediated presynaptic inhibition of glycinergic transmission onto substantia gelatinosa neurons in the rat spinal cord. *Pain* 138:330-342.
- Christensen BN, Perl ER (1970) Spinal neurons specifically excited by noxious or thermal stimuli: marginal zone of the dorsal horn. *Journal of neurophysiology* 33:293-307.
- Chronwall BM, Davis TD, Severidit MW, Wolfe SE, McCarron KE, Beatty DM, Low MJ, Morris SJ, Enna SJ (2001) Constitutive expression of functional GABA(B) receptors in mIL-tsA58 cells requires both GABA(B(1)) and GABA(B(2)) genes. *Journal of neurochemistry* 77:1237-1247.
- Chu Y-C, Guan Y, Skinner J, Raja SN, Johns RA, Tao Y-X (2005) Effect of genetic knockout or pharmacologic inhibition of neuronal nitric oxide synthase on complete Freund's adjuvant-induced persistent pain. *Pain* 119:113-123.
- Chub N, O'Donovan MJ (1998) Blockade and recovery of spontaneous rhythmic activity after application of neurotransmitter antagonists to spinal networks of the chick embryo. *The Journal of neuroscience : the official journal of the Society for Neuroscience* 18:294-306.
- Clavier N, Lombard MC, Besson JM (1992) Benzodiazepines and pain: effects of midazolam on the activities of nociceptive non-specific dorsal horn neurons in the rat spinal cord. *Pain* 48:61-71.
- Collingridge GL (1995) The brain slice preparation: a tribute to the pioneer Henry McIlwain. *Journal of neuroscience methods* 59:5-9.
- Collingridge GL, Isaac JT, Wang YT (2004) Receptor trafficking and synaptic plasticity. *Nature reviews Neuroscience* 5:952-962.
- Collingridge GL, Olsen RW, Peters J, Spedding M (2009) A nomenclature for ligand-gated ion channels. *Neuropharmacology* 56:2-5.

- Coltman BW, Earley EM, Shahar A, Dudek FE, Ide CF (1995) Factors influencing mossy fiber collateral sprouting in organotypic slice cultures of neonatal mouse hippocampus. *The Journal of comparative neurology* 362:209-222.
- Contini M, Raviola E (2003) GABAergic synapses made by a retinal dopaminergic neuron. *Proceedings of the National Academy of Sciences of the United States of America* 100:1358-1363.
- Cooper EJ, Johnston GAR, Edwards FA (1999) Effects of a naturally occurring neurosteroid on GABA(A) IPSCs during development in rat hippocampal or cerebellar slices. *The Journal of physiology* 521:437-449.
- Coull JA, Beggs S, Boudreau D, Boivin D, Tsuda M, Inoue K, Gravel C, Salter MW, De Koninck Y (2005) BDNF from microglia causes the shift in neuronal anion gradient underlying neuropathic pain. *Nature* 438:1017-1021.
- Coull JA, Boudreau D, Bachand K, Prescott SA, Nault F, Sik A, De Koninck P, De Koninck Y (2003) Trans-synaptic shift in anion gradient in spinal lamina I neurons as a mechanism of neuropathic pain. *Nature* 424:938-942.
- Cox PJ, Pitcher T, Trim SA, Bell CH, Qin W, Kinloch RA (2008) The effect of deletion of the orphan G - protein coupled receptor (GPCR) gene MrgE on pain-like behaviours in mice. *Molecular pain* 4:2.
- Cuellar JM, Antognini JF, Carstens E (2004) An in vivo method for recording single unit activity in lumbar spinal cord in mice anesthetized with a volatile anesthetic. *Brain Research Protocols* 13:126-134.
- Cunningham MO, Whittington MA, Bibbig A, Roopun A, LeBeau FEN, Vogt A, Monyer H, Buhl EH, Traub RD (2004) A role for fast rhythmic bursting neurons in cortical gamma oscillations in vitro. *Proceedings of the National Academy of Sciences of the United States of America* 101:7152-7157.
- Curtis DR, Duggan AW, Felix D, Johnston GAR (1970) Bicuculline and Central GABA Receptors. *Nature* 228:676-677.
- Curtis DR, Gynther BD, Beattie DT, Kerr DIB, Prager RH (1988) Baclofen antagonism by 2-hydroxy-saclofen in the cat spinal cord. *Neuroscience letters* 92:97-101.
- Cutting GR, Lu L, O'Hara BF, Kasch LM, Montrose-Rafizadeh C, Donovan DM, Shimada S, Antonarakis SE, Guggino WB, Uhl GR (1991) Cloning of the gamma-aminobutyric acid (GABA) rho 1 cDNA: a GABA receptor subunit highly expressed in the retina. *Proceedings of the National Academy of Sciences* 88:2673-2677.
- Czarnecki A, Magloire V, Streit J (2008) Local oscillations of spiking activity in organotypic spinal cord slice cultures. *The European journal of neuroscience* 27:2076-2088.
- Das P, Bell-Horner CL, Machu TK, Dillon GH (2003) The GABA(A) receptor antagonist picrotoxin inhibits 5-hydroxytryptamine type 3A receptors. *Neuropharmacology* 44:431-438.
- De Simoni A, Yu LM (2006) Preparation of organotypic hippocampal slice cultures: interface method. *Nature protocols* 1:1439-1445.
- DeFazio RA, Keros S, Quick MW, Hablitz JJ (2000) Potassium-Coupled Chloride Cotransport Controls Intracellular Chloride in Rat Neocortical Pyramidal Neurons. *The Journal of Neuroscience* 20:8069-8076.
- Devor A, Fritschy JM, Yarom Y (2001) Spatial distribution and subunit composition of GABA(A) receptors in the inferior olivary nucleus. *Journal of neurophysiology* 85:1686-1696.
- Diaz A, Dickenson AH (1997) Blockade of spinal N- and P-type, but not L-type, calcium channels inhibits the excitability of rat dorsal horn neurones produced by subcutaneous formalin inflammation. *Pain* 69:93-100.
- Dixon C, Sah P, Lynch JW, Keramidis A (2014) GABA(A) Receptor α and γ Subunits Shape Synaptic Currents via Different Mechanisms. *The Journal of biological chemistry* 289:5399-5411.

- Drasbek KR, Jensen K (2006) THIP, a hypnotic and antinociceptive drug, enhances an extrasynaptic GABAA receptor-mediated conductance in mouse neocortex. *Cereb Cortex* 16:1134-1141.
- Duncalfe LL, Carpenter MR, Smillie LB, Martin IL, Dunn SM (1996) The major site of photoaffinity labeling of the gamma-aminobutyric acid type A receptor by [3H]flunitrazepam is histidine 102 of the alpha subunit. *The Journal of biological chemistry* 271:9209-9214.
- Eaton MJ, Martinez MA, Karmally S (1999) A single intrathecal injection of GABA permanently reverses neuropathic pain after nerve injury. *Brain research* 835:334-339.
- Eaton MJ, Plunkett JA, Karmally S, Martinez MA, Montanez K (1998) Changes in GAD- and GABA- immunoreactivity in the spinal dorsal horn after peripheral nerve injury and promotion of recovery by lumbar transplant of immortalized serotonergic precursors. *Journal of Chemical Neuroanatomy* 16:57-72.
- Ebert B, Storustovu S, Mortensen M, Frølund B (2002) Characterization of GABA(A) receptor ligands in the rat cortical wedge preparation: evidence for action at extrasynaptic receptors? *British journal of pharmacology* 137:1-8.
- Eblen-Zajjur AA, Sandkuhler J (1997) Synchronicity of nociceptive and non-nociceptive adjacent neurons in the spinal dorsal horn of the rat: stimulus-induced plasticity. *Neuroscience* 76:39-54.
- Eglen R, Reisine T (2010) Primary Cells and Stem Cells in Drug Discovery: Emerging Tools for High-Throughput Screening. *ASSAY and Drug Development Technologies* 9:108-124.
- Eichler SA, Förstera B, Smolinsky B, Jüttner R, Lehmann T-N, Fählung M, Schwarz G, Legendre P, Meier JC (2009) Splice-specific roles of glycine receptor $\alpha 3$ in the hippocampus. *European Journal of Neuroscience* 30:1077-1091.
- Elbashir SM, Harborth J, Lendeckel W, Yalcin A, Weber K, Tuschl T (2001a) Duplexes of 21-nucleotide RNAs mediate RNA interference in cultured mammalian cells. *Nature* 411:494-498.
- Elbashir SM, Lendeckel W, Tuschl T (2001b) RNA interference is mediated by 21- and 22-nucleotide RNAs. *Genes & development* 15:188-200.
- Emamghoreishi M, Keshavarz M, Nekooeian AA (2015) Acute and chronic effects of lithium on BDNF and GDNF mRNA and protein levels in rat primary neuronal, astroglial and neuroastroglia cultures. *Iranian Journal of Basic Medical Sciences* 18:240-246.
- Engle MP, Gassman M, Sykes KT, Bettler B, Hammond DL (2006) Spinal Nerve Ligation Does Not Alter the Expression or Function of GABA(B) Receptors in Spinal Cord and Dorsal Root Ganglia of the Rat. *Neuroscience* 138:1277-1287.
- Essrich C, Lorez M, Benson JA, Fritschy JM, Luscher B (1998) Postsynaptic clustering of major GABAA receptor subtypes requires the gamma 2 subunit and gephyrin. *Nature neuroscience* 1:563-571.
- Farrar SJ, Whiting PJ, Bonnert TP, McKernan RM (1999) Stoichiometry of a Ligand-gated Ion Channel Determined by Fluorescence Energy Transfer. *Journal of Biological Chemistry* 274:10100-10104.
- Fee MS (2000) Active Stabilization of Electrodes for Intracellular Recording in Awake Behaving Animals. *Neuron* 27:461-468.
- Fischer KF, Lukasiewicz PD, Wong RO (1998) Age-dependent and cell class-specific modulation of retinal ganglion cell bursting activity by GABA. *The Journal of neuroscience : the official journal of the Society for Neuroscience* 18:3767-3778.
- Fisher RS, Webber WR, Lesser RP, Arroyo S, Uematsu S (1992) High-frequency EEG activity at the start of seizures. *Journal of clinical neurophysiology : official publication of the American Electroencephalographic Society* 9:441-448.

- Ford A, Castonguay A, Cottet M, Little JW, Chen Z, Symons-Liguori AM, Doyle T, Egan TM, Vanderah TW, De Konnick Y, Tosh DK, Jacobson KA, Salvemini D (2015) Engagement of the GABA to KCC2 Signaling Pathway Contributes to the Analgesic Effects of A(3)AR Agonists in Neuropathic Pain. *The Journal of Neuroscience* 35:6057-6067.
- Franek M, Vaculin S, Rokyta R (2004) GABA(B) receptor agonist baclofen has non-specific antinociceptive effect in the model of peripheral neuropathy in the rat. *Physiological research / Academia Scientiarum Bohemoslovaca* 53:351-355.
- Fritschy JM, Mohler H (1995) GABAA-receptor heterogeneity in the adult rat brain: differential regional and cellular distribution of seven major subunits. *The Journal of comparative neurology* 359:154-194.
- Fucile S (2004) Ca²⁺ permeability of nicotinic acetylcholine receptors. *Cell Calcium* 35:1-8.
- Fujita M, Sato K, Sato M, Inoue T, Kozuka T, Tohyama M (1991) Regional distribution of the cells expressing glycine receptor beta subunit mRNA in the rat brain. *Brain research* 560:23-37.
- Galimberti I, Gogolla N, Alberi S, Santos AF, Muller D, Caroni P (2006) Long-term rearrangements of hippocampal mossy fiber terminal connectivity in the adult regulated by experience. *Neuron* 50:749-763.
- Galzi J-L, Changeux J-P (1994) Neurotransmitter-gated ion channels as unconventional allosteric proteins. *Current Opinion in Structural Biology* 4:554-565.
- Gangadharan V, Agarwal N, Brugger S, Tegeder I, Bettler B, Kuner R, Kurejova M (2009) Conditional gene deletion reveals functional redundancy of GABAB receptors in peripheral nociceptors in vivo. *Molecular pain* 5:68.
- Gao YJ, Ji RR (2009) c-Fos and pERK, which is a better marker for neuronal activation and central sensitization after noxious stimulation and tissue injury? *The open pain journal* 2:11-17.
- Garthwaite J (2008) Concepts of neural nitric oxide-mediated transmission. *European Journal of Neuroscience* 27:2783-2802.
- Ge LH, Lee SC, Liu J, Yang XL (2007) Glycine receptors are functionally expressed on bullfrog retinal cone photoreceptors. *Neuroscience* 146:427-434.
- Gingrich KJ, Roberts WA, Kass RS (1995) Dependence of the GABAA receptor gating kinetics on the alpha-subunit isoform: implications for structure-function relations and synaptic transmission. *The Journal of physiology* 489 (Pt 2):529-543.
- Gonzalez-Sulser A, Wang J, Queenan BN, Avoli M, Vicini S, Dzakpasu R (2012) Hippocampal neuron firing and local field potentials in the in vitro 4-aminopyridine epilepsy model. *Journal of neurophysiology* 108:2568-2580.
- Gordon J, Amini S, White MK (2013) General overview of neuronal cell culture. *Methods in molecular biology (Clifton, NJ)* 1078:1-8.
- Graham BA, Brichta AM, Callister RJ (2007) Moving From an Averaged to Specific View of Spinal Cord Pain Processing Circuits. *Journal of neurophysiology* 98:1057-1063.
- Green GM, Dickenson A (1997) GABA-receptor control of the amplitude and duration of the neuronal responses to formalin in the rat spinal cord. *Eur J Pain* 1:95-104.
- Grenier F, Timofeev I, Steriade M (2003) Neocortical very fast oscillations (ripples, 80-200 Hz) during seizures: intracellular correlates. *Journal of neurophysiology* 89:841-852.
- Grenningloh G, Pribilla I, Prior P, Multhaup G, Beyreuther K, Taleb O, Betz H (1990) Cloning and expression of the 58 kd β subunit of the inhibitory glycine receptor. *Neuron* 4:963-970.

- Grienberger C, Konnerth A (2012) Imaging Calcium in Neurons. *Neuron* 73:862-885.
- Griffon N, Büttner C, Nicke A, Kuhse J, Schmalzing G, Betz H (1999) Molecular determinants of glycine receptor subunit assembly. *The EMBO journal* 18:4711-4721.
- Grognet A, Hertz F, DeFeudis FV (1983) Comparison of the analgesic actions of THIP and morphine. *General pharmacology* 14:585-589.
- Grosser S, Queenan BN, Lalchandani RR, Vicini S (2014) Hilar somatostatin interneurons contribute to synchronized GABA activity in an in vitro epilepsy model. *PloS one* 9:e86250.
- Grudt TJ, Perl ER (2002) Correlations between neuronal morphology and electrophysiological features in the rodent superficial dorsal horn. *The Journal of physiology* 540:189-207.
- Grudzinska J, Schemm R, Haeger S, Nicke A, Schmalzing G, Betz H, Laube B (2005) The beta subunit determines the ligand binding properties of synaptic glycine receptors. *Neuron* 45:727-739.
- Guan Y, Yaster M, Raja S, Tao Y-X (2007) Genetic knockout and pharmacologic inhibition of neuronal nitric oxide synthase attenuate nerve injury-induced mechanical hypersensitivity in mice. *Molecular pain* 3:29.
- Guertin PA (2012) Central Pattern Generator for Locomotion: Anatomical, Physiological, and Pathophysiological Considerations. *Frontiers in Neurology* 3:183.
- Guetg N, Abdel Aziz S, Holbro N, Turecek R, Rose T, Seddik R, Gassmann M, Moes S, Jenoe P, Oertner TG, Casanova E, Bettler B (2010) NMDA receptor-dependent GABAB receptor internalization via CaMKII phosphorylation of serine 867 in GABAB1. *Proceedings of the National Academy of Sciences of the United States of America* 107:13924-13929.
- Gurley D, Amin J, Ross PC, Weiss DS, White G (1995) Point mutations in the M2 region of the alpha, beta, or gamma subunit of the GABAA channel that abolish block by picrotoxin. *Receptors & channels* 3:13-20.
- Han L, Talwar S, Wang Q, Shan Q, Lynch JW (2013) Phosphorylation of $\alpha 3$ Glycine Receptors Induces a Conformational Change in the Glycine-Binding Site. *ACS Chemical Neuroscience* 4:1361-1370.
- Hantman AW, van den Pol AN, Perl ER (2004) Morphological and Physiological Features of a Set of Spinal Substantia Gelatinosa Neurons Defined by Green Fluorescent Protein Expression. *The Journal of Neuroscience* 24:836-842.
- Haranishi Y, Hara K, Terada T, Nakamura S, Sata T (2010) The antinociceptive effect of intrathecal administration of glycine transporter-2 inhibitor ALX1393 in a rat acute pain model. *Anesthesia and analgesia* 110:615-621.
- Harvey RJ, Depner UB, Wassle H, Ahmadi S, Heindl C, Reinold H, Smart TG, Harvey K, Schutz B, Abo-Salem OM, Zimmer A, Poisbeau P, Welzl H, Wolfer DP, Betz H, Zeilhofer HU, Muller U (2004) GlyR $\alpha 3$: an essential target for spinal PGE2-mediated inflammatory pain sensitization. *Science* 304:884-887.
- Harvey RJ, Schmieden V, Von Holst A, Laube B, Rohrer H, Betz H (2000) Glycine receptors containing the $\alpha 4$ subunit in the embryonic sympathetic nervous system, spinal cord and male genital ridge. *European Journal of Neuroscience* 12:994-1001.
- Harvey VL, Caley A, Muller UC, Harvey RJ, Dickenson AH (2009) A Selective Role for $\alpha 3$ Subunit Glycine Receptors in Inflammatory Pain. *Frontiers in molecular neuroscience* 2:14.
- Hasbargen T, Ahmed MM, Miranpuri G, Li L, Kahle KT, Resnick D, Sun D (2010) Role of NKCC1 and KCC2 in the development of chronic neuropathic pain

- following spinal cord injury. *Annals of the New York Academy of Sciences* 1198:168-172.
- Heaulme M, Chambon J-P, Leyris R, Molimard J-C, Wermuth CG, Biziere K (1986) Biochemical characterization of the interaction of three pyridazinyl-GABA derivatives with the GABAA receptor site. *Brain research* 384:224-231.
- Heimlich G, Cidlowski JA (2006) Selective Role of Intracellular Chloride in the Regulation of the Intrinsic but Not Extrinsic Pathway of Apoptosis in Jurkat T-cells. *Journal of Biological Chemistry* 281:2232-2241.
- Heinke B, Ruscheweyh R, Forsthuber L, Wunderbaldinger G, Sandkuhler J (2004) Physiological, neurochemical and morphological properties of a subgroup of GABAergic spinal lamina II neurones identified by expression of green fluorescent protein in mice. *The Journal of physiology* 560:249-266.
- Hendrich J, Bauer CS, Dolphin AC (2012a) Chronic pregabalin inhibits synaptic transmission between rat dorsal root ganglion and dorsal horn neurons in culture. *Channels (Austin)* 6:124-132.
- Hendrich J, Bauer CS, Dolphin AC (2012b) Chronic pregabalin inhibits synaptic transmission between rat dorsal root ganglion and dorsal horn neurons in culture. *Channels* 6:124-132.
- Hering-Hanit R (1999) Baclofen for prevention of migraine. *Cephalalgia : an international journal of headache* 19:589-591.
- Hering-Hanit R, Gadoth N (2000) Baclofen in cluster headache. *Headache* 40:48-51.
- Hering-Hanit R, Gadoth N (2001) The use of baclofen in cluster headache. *Current pain and headache reports* 5:79-82.
- Hill AJ, Jones NA, Williams CM, Stephens GJ, Whalley BJ (2010) Development of multi-electrode array screening for anticonvulsants in acute rat brain slices. *Journal of neuroscience methods* 185:246-256.
- Hinckley C, Seebach B, Ziskind-Conhaim L (2005) Distinct roles of glycinergic and GABAergic inhibition in coordinating locomotor-like rhythms in the neonatal mouse spinal cord. *Neuroscience* 131:745-758.
- Hoehn-Saric R (1983) Effects of THIP on chronic anxiety. *Psychopharmacology* 80:338-341.
- Hsieh MT, Donaldson LF, Lumb BM (2015) Differential contributions of A- and C-nociceptors to primary and secondary inflammatory hypersensitivity in the rat. *Pain* 156:1074-1083.
- Huang D, Huang S, Peers C, Du X, Zhang H, Gamper N (2015) GABAB receptors inhibit low-voltage activated and high-voltage activated Ca²⁺ channels in sensory neurons via distinct mechanisms. *Biochemical and Biophysical Research Communications* 465:188-193.
- Hubner CA, Holthoff K (2013) Anion transport and GABA signaling. *Frontiers in cellular neuroscience* 7:177.
- Hughes DI, Sikander S, Kinnon CM, Boyle KA, Watanabe M, Callister RJ, Graham BA (2012) Morphological, neurochemical and electrophysiological features of parvalbumin-expressing cells: a likely source of axo-axonic inputs in the mouse spinal dorsal horn. *The Journal of physiology* 590:3927-3951.
- Humpel C (2015) Organotypic brain slice cultures: A review. *Neuroscience* 305:86-98.
- Hutvagner G, Zamore PD (2002) A microRNA in a multiple-turnover RNAi enzyme complex. *Science* 297:2056-2060.
- Hwang JH, Yaksh TL (1997) The effect of spinal GABA receptor agonists on tactile allodynia in a surgically-induced neuropathic pain model in the rat. *Pain* 70:15-22.
- Ibuki T, Hama AT, Wang XT, Pappas GD, Sagen J (1996) Loss of GABA-immunoreactivity in the spinal dorsal horn of rats with peripheral nerve injury

- and promotion of recovery by adrenal medullary grafts. *Neuroscience* 76:845-858.
- Ikeda H, Stark J, Fischer H, Wagner M, Drdla R, Jager T, Sandkuhler J (2006) Synaptic amplifier of inflammatory pain in the spinal dorsal horn. *Science* 312:1659-1662.
- Infante C, Diaz M, Hernandez A, Constandil L, Pelissier T (2007) Expression of nitric oxide synthase isoforms in the dorsal horn of monoarthritic rats: effects of competitive and uncompetitive N-methyl-D-aspartate antagonists. *Arthritis Research & Therapy* 9:R53.
- Inquimbert P, Rodeau JL, Schlichter R (2007) Differential contribution of GABAergic and glycinergic components to inhibitory synaptic transmission in lamina II and laminae III-IV of the young rat spinal cord. *The European journal of neuroscience* 26:2940-2949.
- Ito S, Yeh F-C, Hiolski E, Rydygier P, Gunning DE, Hottowy P, Timme N, Litke AM, Beggs JM (2014) Large-Scale, High-Resolution Multielectrode-Array Recording Depicts Functional Network Differences of Cortical and Hippocampal Cultures. *PloS one* 9:e105324.
- Javdani F, Holló K, Hegedűs K, Kis G, Hegyi Z, Dócs K, Kasugai Y, Fukazawa Y, Shigemoto R, Antal M (2015) Differential expression patterns of K⁺/Cl⁻ cotransporter 2 in neurons within the superficial spinal dorsal horn of rats. *Journal of Comparative Neurology* 523:1967-1983.
- Jenkins A, Greenblatt EP, Faulkner HJ, Bertaccini E, Light A, Lin A, Andreasen A, Viner A, Trudell JR, Harrison NL (2001) Evidence for a common binding cavity for three general anesthetics within the GABAA receptor. *The Journal of neuroscience : the official journal of the Society for Neuroscience* 21:RC136.
- Jia F, Pignataro L, Harrison NL (2007) GABAA receptors in the thalamus: $\alpha 4$ subunit expression and alcohol sensitivity. *Alcohol* 41:177-185.
- Jin N, Narasaraaju T, Kolliputi N, Chen J, Liu L (2005) Differential expression of GABAA receptor π subunit in cultured rat alveolar epithelial cells. *Cell and tissue research* 321:173-183.
- Jonsson S, Morud J, Pickering C, Adermark L, Ericson M, Söderpalm B (2012) Changes in glycine receptor subunit expression in forebrain regions of the Wistar rat over development. *Brain research* 1446:12-21.
- Kahle KT, Khanna A, Clapham DE, Woolf CJ (2014) Therapeutic restoration of spinal inhibition via druggable enhancement of potassium-chloride cotransporter KCC2-mediated chloride extrusion in peripheral neuropathic pain. *JAMA neurology* 71:640-645.
- Kaila K, Lamsa K, Smirnov S, Taira T, Voipio J (1997) Long-lasting GABA-mediated depolarization evoked by high-frequency stimulation in pyramidal neurons of rat hippocampal slice is attributable to a network-driven, bicarbonate-dependent K⁺ transient. *The Journal of neuroscience : the official journal of the Society for Neuroscience* 17:7662-7672.
- Kaila K, Voipio J (1987) Postsynaptic fall in intracellular pH induced by GABA-activated bicarbonate conductance. *Nature* 330:163-165.
- Kaneko M, Hammond DL (1997) Role of spinal gamma-aminobutyric acidA receptors in formalin-induced nociception in the rat. *The Journal of pharmacology and experimental therapeutics* 282:928-938.
- Kato G, Kawasaki Y, Ji RR, Strassman AM (2007) Differential wiring of local excitatory and inhibitory synaptic inputs to islet cells in rat spinal lamina II demonstrated by laser scanning photostimulation. *The Journal of physiology* 580:815-833.
- Keefer EW, Gramowski A, Gross GW (2001) NMDA Receptor-Dependent Periodic Oscillations in Cultured Spinal Cord Networks. *Journal of neurophysiology* 86:3030-3042.

- Keller AF, Breton J-D, Schlichter R, Poisbeau P (2004) Production of 5 α -Reduced Neurosteroids Is Developmentally Regulated and Shapes GABAA Miniature IPSCs in Lamina II of the Spinal Cord. *The Journal of Neuroscience* 24:907-915.
- Keller AF, Coull JA, Chery N, Poisbeau P, De Koninck Y (2001) Region-specific developmental specialization of GABA-glycine cosynapses in laminae I-II of the rat spinal dorsal horn. *The Journal of neuroscience : the official journal of the Society for Neuroscience* 21:7871-7880.
- Kern DS, Maclean KN, Jiang H, Synder EY, Sladek JJR, Bjugstad KB (2011) Neural Stem Cells Reduce Hippocampal Tau and Reelin Accumulation in Aged Ts65Dn Down Syndrome Mice. *Cell Transplantation* 20:371-379.
- Kibaly C, Meyer L, Patte-Mensah C, Mensah-Nyagan AG (2008) Biochemical and functional evidence for the control of pain mechanisms by dehydroepiandrosterone endogenously synthesized in the spinal cord. *The FASEB Journal* 22:93-104.
- Kilic G, Moran O, Cherubini E (1991) N-methyl-D-aspartate receptor-mediated spontaneous activity in cerebellar granule cells in culture. *Neuroscience Letters* 130:263-266.
- Kim T, Thankachan S, McKenna JT, McNally JM, Yang C, Choi JH, Chen L, Kocsis B, Deisseroth K, Strecker RE, Basheer R, Brown RE, McCarley RW (2015) Cortically projecting basal forebrain parvalbumin neurons regulate cortical gamma band oscillations. *Proceedings of the National Academy of Sciences of the United States of America* 112:3535-3540.
- Kim TK, Eberwine JH (2010) Mammalian cell transfection: the present and the future. *Analytical and Bioanalytical Chemistry* 397:3173-3178.
- Kling C, Koch M, Saul B, Becker CM (1997) The frameshift mutation oscillator (Glr1(spdl-ot)) produces a complete loss of glycine receptor alpha1-polypeptide in mouse central nervous system. *Neuroscience* 78:411-417.
- Knabl J, Witschi R, Hosl K, Reinold H, Zeilhofer UB, Ahmadi S, Brockhaus J, Sergejeva M, Hess A, Brune K, Fritschy JM, Rudolph U, Mohler H, Zeilhofer HU (2008) Reversal of pathological pain through specific spinal GABAA receptor subtypes. *Nature* 451:330-334.
- Kneussel M, Betz H (2000) Receptors, gephyrin and gephyrin-associated proteins: novel insights into the assembly of inhibitory postsynaptic membrane specializations. *The Journal of physiology* 525 Pt 1:1-9.
- Korpi ER, Koikkalainen P, Vekovischeva OY, Mäkelä R, Kleinz R, Uusi-Oukari M, Wisden W (1999) Cerebellar granule-cell-specific GABAA receptors attenuate benzodiazepine-induced ataxia: evidence from $\alpha 6$ -subunit-deficient mice. *European Journal of Neuroscience* 11:233-240.
- Koutsikou S, Parry DM, MacMillan FM, Lumb BM (2007) Laminar organization of spinal dorsal horn neurones activated by C- vs. A-heat nociceptors and their descending control from the periaqueductal grey in the rat. *The European journal of neuroscience* 26:943-952.
- Kovalchuk Y, Eilers J, Lisman J, Konnerth A (2000) NMDA Receptor-Mediated Subthreshold Ca²⁺ Signals in Spines of Hippocampal Neurons. *The Journal of Neuroscience* 20:1791-1799.
- Krogsgaard-Larsen P, Frolund B, Liljefors T, Ebert B (2004) GABA(A) agonists and partial agonists: THIP (Gaboxadol) as a non-opioid analgesic and a novel type of hypnotic. *Biochemical pharmacology* 68:1573-1580.
- Krosnowski K, Ashby S, Sathyanesan A, Luo W, Ogura T, Lin W (2012) Diverse populations of intrinsic cholinergic interneurons in the mouse olfactory bulb. *Neuroscience* 213:161-178.
- Kruskal Peter B, Jiang Z, Gao T, Lieber Charles M (2015) Beyond the Patch Clamp: Nanotechnologies for Intracellular Recording. *Neuron* 86:21-24.

- Kuhse J, Laube B, Magalei D, Betz H (1993) Assembly of the inhibitory glycine receptor: identification of amino acid sequence motifs governing subunit stoichiometry. *Neuron* 11:1049-1056.
- Kuhse J, Schmieden V, Betz H (1990) A single amino acid exchange alters the pharmacology of neonatal rat glycine receptor subunit. *Neuron* 5:867-873.
- Kuki T, Fujihara K, Miwa H, Tamamaki N, Yanagawa Y, Mushiake H (2015) Contribution of parvalbumin and somatostatin-expressing GABAergic neurons to slow oscillations and the balance in beta-gamma oscillations across cortical layers. *Frontiers in Neural Circuits* 9:6.
- Kullmann PH, Ene FA, Kandler K (2002) Glycinergic and GABAergic calcium responses in the developing lateral superior olive. *The European journal of neuroscience* 15:1093-1104.
- Kumazawa T, Perl ER (1978) Excitation of marginal and substantia gelatinosa neurons in the primate spinal cord: indications of their place in dorsal horn functional organization. *The Journal of comparative neurology* 177:417-434.
- Kuroiwa M, Kitano Y, Takasuna K, Manabe S, Saito T (2009) Muscle relaxant and neurotoxic activities of intrathecal baclofen in rats. *Pharmacological Research* 60:392-396.
- Labrakakis C, Lorenzo LE, Bories C, Ribeiro-da-Silva A, De Koninck Y (2009) Inhibitory coupling between inhibitory interneurons in the spinal cord dorsal horn. *Molecular pain* 5:24.
- Labrakakis C, Rudolph U, De Koninck Y (2014) The heterogeneity in GABAA receptor-mediated IPSC kinetics reflects heterogeneity of subunit composition among inhibitory and excitatory interneurons in spinal lamina II. *Frontiers in cellular neuroscience* 8:424.
- Lange MD, Doengi M, Lesting J, Pape HC, Jungling K (2012) Heterosynaptic long-term potentiation at interneuron-principal neuron synapses in the amygdala requires nitric oxide signalling. *The Journal of physiology* 590:131-143.
- Lau BK, Vaughan CW (2014) Descending modulation of pain: the GABA disinhibition hypothesis of analgesia. *Curr Opin Neurobiol* 29:159-164.
- Le Blon D, Hoornaert C, Daans J, Santermans E, Hens N, Goossens H, Berneman Z, Ponsaerts P (2014) Distinct spatial distribution of microglia and macrophages following mesenchymal stem cell implantation in mouse brain. *Immunol Cell Biol* 92:650-658.
- Lee H, Chen CX, Liu YJ, Aizenman E, Kandler K (2005) KCC2 expression in immature rat cortical neurons is sufficient to switch the polarity of GABA responses. *The European journal of neuroscience* 21:2593-2599.
- Legendre P, McKenzie JS, Dupouy B, Vincent JD (1985) Evidence for bursting pacemaker neurones in cultured spinal cord cells. *Neuroscience* 16:753-767.
- Lein PJ, Barnhart CD, Pessah IN (2011) Acute hippocampal slice preparation and hippocampal slice cultures. *Methods Mol Biol* 758:115-134.
- Lewis TM, Schofield PR, McClellan AML (2003) Kinetic determinants of agonist action at the recombinant human glycine receptor. *The Journal of physiology* 549:361-374.
- Li CL, Mc IH (1957) Maintenance of resting membrane potentials in slices of mammalian cerebral cortex and other tissues in vitro. *The Journal of physiology* 139:178-190.
- Li J, Baccei ML (2011) Pacemaker neurons within newborn spinal pain circuits. *The Journal of neuroscience : the official journal of the Society for Neuroscience* 31:9010-9022.
- Li J, Blankenship ML, Baccei ML (2013) Inward-rectifying potassium (Kir) channels regulate pacemaker activity in spinal nociceptive circuits during early life. *The Journal of neuroscience : the official journal of the Society for Neuroscience* 33:3352-3362.

- Li J, Kritzer E, Ford NC, Arbabi S, Baccei ML (2014) Connectivity of pacemaker neurons in the neonatal rat superficial dorsal horn. *The Journal of comparative neurology*.
- Light AR, Perl ER (1979) Reexamination of the dorsal root projection to the spinal dorsal horn including observations on the differential termination of coarse and fine fibers. *The Journal of comparative neurology* 186:117-131.
- Lindstrom SH, Azizi N, Weller C, Wilson M (2010) Retinal input to efferent target amacrine cells in the avian retina. *Visual neuroscience* 27:103-118.
- Liu P, Guo W-Y, Zhao X-N, Bai H-P, Wang Q, Wang X-L, Zhang Y-Z (2014) Intrathecal baclofen, a GABAB receptor agonist, inhibits the expression of p-CREB and NR2B in the spinal dorsal horn in rats with diabetic neuropathic pain. *Canadian journal of physiology and pharmacology* 92:655-660.
- Lodge DJ, Behrens MM, Grace AA (2009) A loss of parvalbumin-containing interneurons is associated with diminished oscillatory activity in an animal model of schizophrenia. *The Journal of neuroscience : the official journal of the Society for Neuroscience* 29:2344-2354.
- Loeser JD, Ward AA, Jr. (1967) Some effects of deafferentation on neurons of the cat spinal cord. *Archives of neurology* 17:629-636.
- Lombard MC, Nashold BS, Jr., Albe-Fessard D, Salman N, Sakr C (1979) Deafferentation hypersensitivity in the rat after dorsal rhizotomy: a possible animal model of chronic pain. *Pain* 6:163-174.
- Lossi L, Alasia S, Salio C, Merighi A (2009) Cell death and proliferation in acute slices and organotypic cultures of mammalian CNS. *Progress in neurobiology* 88:221-245.
- Lovitt CJ, Shelper TB, Avery VM (2014) *Advanced Cell Culture Techniques for Cancer Drug Discovery*. *Biology* 3:345-367.
- Lu VB, Biggs JE, Stebbing MJ, Balasubramanyan S, Todd KG, Lai AY, Colmers WF, Dawbarn D, Ballanyi K, Smith PA (2009) Brain-derived neurotrophic factor drives the changes in excitatory synaptic transmission in the rat superficial dorsal horn that follow sciatic nerve injury. *The Journal of physiology* 587:1013-1032.
- Lu W, Man H, Ju W, Trimble WS, MacDonald JF, Wang YT (2001) Activation of synaptic NMDA receptors induces membrane insertion of new AMPA receptors and LTP in cultured hippocampal neurons. *Neuron* 29:243-254.
- Lu Y, Dong H, Gao Y, Gong Y, Ren Y, Gu N, Zhou S, Xia N, Sun Y-Y, Ji R-R, Xiong L (2013) A feed-forward spinal cord glycinergic neural circuit gates mechanical allodynia. *The Journal of clinical investigation* 123:4050-4062.
- Lu Y, Perl ER (2005) Modular organization of excitatory circuits between neurons of the spinal superficial dorsal horn (laminae I and II). *The Journal of neuroscience : the official journal of the Society for Neuroscience* 25:3900-3907.
- Lynch JW (2004) Molecular Structure and Function of the Glycine Receptor Chloride Channel. *Physiological reviews* 84:1051-1095.
- Lynch JW, Callister RJ (2006) Glycine receptors: a new therapeutic target in pain pathways. *Curr Opin Investig Drugs* 7:48-53.
- MacKenzie G, Maguire J (2015) Chronic stress shifts the GABA reversal potential in the hippocampus and increases seizure susceptibility. *Epilepsy research* 109:13-27.
- Magnuson DSK, Johnson R, Peet MJ, Curry K, McLennan H (1987) A novel spinal cord slice preparation from the rat. *Journal of neuroscience methods* 19:141-145.
- Majumdar S, Wässle H, Jusuf PR, Haverkamp S (2008) Mirror-symmetrical populations of wide-field amacrine cells of the macaque monkey retina. *The Journal of comparative neurology* 508:13-27.

- Maksay G, Laube B, Betz H (2001) Subunit-specific modulation of glycine receptors by neurosteroids. *Neuropharmacology* 41:369-376.
- Malan TP, Mata HP, Porreca F (2002) Spinal GABA(A) and GABA(B) receptor pharmacology in a rat model of neuropathic pain. *Anesthesiology* 96:1161-1167.
- Malet M, Vieytes CA, Lundgren KH, Seal RP, Tomasella E, Seroogy KB, Hokfelt T, Gebhart GF, Brumovsky PR (2013) Transcript expression of vesicular glutamate transporters in lumbar dorsal root ganglia and the spinal cord of mice - effects of peripheral axotomy or hindpaw inflammation. *Neuroscience* 248:95-111.
- Malin SA, Davis BM, Molliver DC (2007) Production of dissociated sensory neuron cultures and considerations for their use in studying neuronal function and plasticity. *Nat Protocols* 2:152-160.
- Malosio ML, Grenningloh G, Kuhse J, Schmieden V, Schmitt B, Prior P, Betz H (1991a) Alternative splicing generates two variants of the alpha 1 subunit of the inhibitory glycine receptor. *Journal of Biological Chemistry* 266:2048-2053.
- Malosio ML, Marqueze-Pouey B, Kuhse J, Betz H (1991b) Widespread expression of glycine receptor subunit mRNAs in the adult and developing rat brain. *The EMBO journal* 10:2401-2409.
- Manabe T, Renner P, Nicoll RA (1992) Postsynaptic contribution to long-term potentiation revealed by the analysis of miniature synaptic currents. *Nature* 355:50-55.
- Mangan PS, Sun C, Carpenter M, Goodkin HP, Sieghart W, Kapur J (2005) Cultured Hippocampal Pyramidal Neurons Express Two Kinds of GABAA Receptors. *Molecular pharmacology* 67:775-788.
- Maniataki E, Mourelatos Z (2005) A human, ATP-independent, RISC assembly machine fueled by pre-miRNA. *Genes & development* 19:2979-2990.
- Maric H-M, Mukherjee J, Tretter V, Moss SJ, Schindelin H (2011) Gephyrin-mediated γ -Aminobutyric Acid Type A and Glycine Receptor Clustering Relies on a Common Binding Site. *Journal of Biological Chemistry* 286:42105-42114.
- Marksteiner J, Humpel C (2007) Beta-amyloid expression, release and extracellular deposition in aged rat brain slices. *Mol Psychiatry* 13:939-952.
- Marvizon JC, Grady EF, Stefani E, Bunnett NW, Mayer EA (1999) Substance P release in the dorsal horn assessed by receptor internalization: NMDA receptors counteract a tonic inhibition by GABA(B) receptors. *The European journal of neuroscience* 11:417-426.
- Marvizon JC, Martinez V, Grady EF, Bunnett NW, Mayer EA (1997) Neurokinin 1 receptor internalization in spinal cord slices induced by dorsal root stimulation is mediated by NMDA receptors. *The Journal of neuroscience : the official journal of the Society for Neuroscience* 17:8129-8136.
- Massobrio P, Tessadori J, Chiappalone M, Ghirardi M (2015) In Vitro Studies of Neuronal Networks and Synaptic Plasticity in Invertebrates and in Mammals Using Multielectrode Arrays. *Neural Plasticity* 2015:196195.
- Matrai J, Chuah MKL, VandenDriessche T (2010) Recent Advances in Lentiviral Vector Development and Applications. *Mol Ther* 18:477-490.
- Matranga C, Tomari Y, Shin C, Bartel DP, Zamore PD (2005) Passenger-strand cleavage facilitates assembly of siRNA into Ago2-containing RNAi enzyme complexes. *Cell* 123:607-620.
- Matthews EA, Dickenson AH (2001a) Effects of ethosuximide, a T-type Ca²⁺ channel blocker, on dorsal horn neuronal responses in rats. *European journal of pharmacology* 415:141-149.

- Matthews EA, Dickenson AH (2001b) Effects of spinally delivered N- and P-type voltage-dependent calcium channel antagonists on dorsal horn neuronal responses in a rat model of neuropathy. *Pain* 92:235-246.
- Matzenbach B, Maulet Y, Sefton L, Courtier B, Avner P, Guénet JL, Betz H (1994) Structural analysis of mouse glycine receptor alpha subunit genes. Identification and chromosomal localization of a novel variant. *Journal of Biological Chemistry* 269:2607-2612.
- Maxwell DJ, Belle MD, Cheunsuang O, Stewart A, Morris R (2007) Morphology of inhibitory and excitatory interneurons in superficial laminae of the rat dorsal horn. *The Journal of physiology* 584:521-533.
- McCaffrey AP, Meuse L, Pham TT, Conklin DS, Hannon GJ, Kay MA (2002) RNA interference in adult mice. *Nature* 418:38-39.
- McConnell ER, McClain MA, Ross J, LeFew WR, Shafer TJ (2012) Evaluation of multi-well microelectrode arrays for neurotoxicity screening using a chemical training set. *Neurotoxicology* 33:1048-1057.
- McKernan RM, Rosahl TW, Reynolds DS, Sur C, Wafford KA, Atack JR, Farrar S, Myers J, Cook G, Ferris P, Garrett L, Bristow L, Marshall G, Macaulay A, Brown N, Howell O, Moore KW, Carling RW, Street LJ, Castro JL, Ragan CI, Dawson GR, Whiting PJ (2000) Sedative but not anxiolytic properties of benzodiazepines are mediated by the GABA(A) receptor alpha1 subtype. *Nature neuroscience* 3:587-592.
- Meier JC, Henneberger C, Melnick I, Racca C, Harvey RJ, Heinemann U, Schmieden V, Grantyn R (2005) RNA editing produces glycine receptor [alpha]3P185L, resulting in high agonist potency. *Nature neuroscience* 8:736-744.
- Meisner JG, Marsh AD, Marsh DR (2010) Loss of GABAergic interneurons in laminae I-III of the spinal cord dorsal horn contributes to reduced GABAergic tone and neuropathic pain after spinal cord injury. *Journal of neurotrauma* 27:729-737.
- Melzack R, Wall PD (1965) Pain mechanisms: a new theory. *Science* 150:971-979.
- Mergenthaler P, Wendland K, Meisel A (2014) A versatile tool for the analysis of neuronal survival. *Methods* 66:325-329.
- Meyer G, Kirsch J, Betz H, Langosch D (1995a) Identification of a gephyrin binding motif on the glycine receptor beta subunit. *Neuron* 15:563-572.
- Meyer G, Kirsch J, Betz H, Langosch D (1995b) Identification of a gephyrin binding motif on the glycine receptor β subunit. *Neuron* 15:563-572.
- Miletic G, Draganic P, Pankratz MT, Miletic V (2003) Muscimol prevents long-lasting potentiation of dorsal horn field potentials in rats with chronic constriction injury exhibiting decreased levels of the GABA transporter GAT-1. *Pain* 105:347-353.
- Miletic V, Randic M (1981) Neonatal rat spinal cord slice preparation: postsynaptic effects of neuropeptides on dorsal horn neurons. *Brain research* 254:432-438.
- Milligan CJ, Buckley NJ, Garret M, Deuchars J, Deuchars SA (2004) Evidence for Inhibition Mediated by Coassembly of GABAA and GABAC Receptor Subunits in Native Central Neurons. *The Journal of Neuroscience* 24:7241-7250.
- Mirza NR, Nielsen EO (2006) Do subtype-selective gamma-aminobutyric acid A receptor modulators have a reduced propensity to induce physical dependence in mice? *The Journal of pharmacology and experimental therapeutics* 316:1378-1385.
- Mitchell SJ, Silver RA (2003) Shunting Inhibition Modulates Neuronal Gain during Synaptic Excitation. *Neuron* 38:433-445.
- Miyazato M, Sasatomi K, Hiragata S, Sugaya K, Chancellor MB, de Groat WC, Yoshimura N (2008) GABA-RECEPTOR ACTIVATION IN THE

- LUMBOSACRAL SPINAL CORD REDUCES DETRUSOR OVERACTIVITY IN SPINAL CORD INJURED RATS. *The Journal of urology* 179:1178-1183.
- Moore KA, Kohno T, Karchewski LA, Scholz J, Baba H, Woolf CJ (2002) Partial peripheral nerve injury promotes a selective loss of GABAergic inhibition in the superficial dorsal horn of the spinal cord. *The Journal of neuroscience : the official journal of the Society for Neuroscience* 22:6724-6731.
- Morris ME, Obrocea GV, Avoli M (1996) Extracellular K⁺ accumulations and synchronous GABA-mediated potentials evoked by 4-aminopyridine in the adult rat hippocampus. *Exp Brain Res* 109:71-82.
- Mortensen M, Smart TG (2006) Extrasynaptic $\alpha\beta$ subunit GABA(A) receptors on rat hippocampal pyramidal neurons. *The Journal of physiology* 577:841-856.
- Murase K, Nedeljkov V, Randic M (1982) The actions of neuropeptides on dorsal horn neurons in the rat spinal cord slice preparation: an intracellular study. *Brain research* 234:170-176.
- Narikawa K, Furue H, Kumamoto E, Yoshimura M (2000) In Vivo Patch-Clamp Analysis of IPSCs Evoked in Rat Substantia Gelatinosa Neurons by Cutaneous Mechanical Stimulation. *Journal of neurophysiology* 84:2171-2174.
- Nayeem N, Green TP, Martin IL, Barnard EA (1994) Quaternary Structure of the Native GABAA Receptor Determined by Electron Microscopic Image Analysis. *Journal of neurochemistry* 62:815-818.
- Neal MJ, Shah MA (1989) Baclofen and phaclofen modulate GABA release from slices of rat cerebral cortex and spinal cord but not from retina. *British journal of pharmacology* 98:105-112.
- Neher E, Sakaba T (2008) Multiple Roles of Calcium Ions in the Regulation of Neurotransmitter Release. *Neuron* 59:861-872.
- Nickolls S, Mace H, Fish R, Edye M, Gurrell R, Ivarsson M, Pitcher T, Tanimoto-Mori S, Richardson D, Sweatman C, Nicholson J, Ward C, Jinks J, Bell C, Young K, Rees H, Moss A, Kinloch R, McMurray G (2011) A Comparison of the $\alpha 2/3/5$ Selective Positive Allosteric Modulators L-838,417 and TPA023 in Preclinical Models of Inflammatory and Neuropathic Pain. *Advances in pharmacological sciences* 2011:608912.
- Nikolic Z, Laube B, Weber RG, Lichter P, Kioschis P, Poustka A, Mülhardt C, Becker C-M (1998) The Human Glycine Receptor Subunit $\alpha 3$: GLRA3 GENE STRUCTURE, CHROMOSOMAL LOCALIZATION, AND FUNCTIONAL CHARACTERIZATION OF ALTERNATIVE TRANSCRIPTS. *Journal of Biological Chemistry* 273:19708-19714.
- Nowak P, Kowalińska-Kania M, Nowak D, Kostrzewa RM, Malinowska-Borowska J (2013) Antinociceptive Effects of H(3) (R-Methylhistamine) and GABA(B) (Baclofen)-Receptor Ligands in an Orofacial Model of Pain in Rats. *Neurotoxicity Research* 24:258-264.
- Nusser Z, Mody I (2002) Selective modulation of tonic and phasic inhibitions in dentate gyrus granule cells. *Journal of neurophysiology* 87:2624-2628.
- Nusser Z, Sieghart W, Somogyi P (1998) Segregation of different GABAA receptors to synaptic and extrasynaptic membranes of cerebellar granule cells. *The Journal of neuroscience : the official journal of the Society for Neuroscience* 18:1693-1703.
- Obien MEJ, Deligkaris K, Bullmann T, Bakkum DJ, Frey U (2015) Revealing Neuronal Function through Microelectrode Array Recordings. *Frontiers in Neuroscience* 8.
- Ojovan SM, Rabieh N, Shmoel N, Erez H, Maydan E, Cohen A, Spira ME (2015) A feasibility study of multi-site, intracellular recordings from mammalian neurons by extracellular gold mushroom-shaped microelectrodes. *Scientific Reports* 5:14100.

- Oliveira AL, Hydling F, Olsson E, Shi T, Edwards RH, Fujiyama F, Kaneko T, Hokfelt T, Cullheim S, Meister B (2003) Cellular localization of three vesicular glutamate transporter mRNAs and proteins in rat spinal cord and dorsal root ganglia. *Synapse* 50:117-129.
- Olsen RW, Sieghart W (2008) International Union of Pharmacology. LXX. Subtypes of γ -Aminobutyric Acid(A) Receptors: Classification on the Basis of Subunit Composition, Pharmacology, and Function. Update. *Pharmacological reviews* 60:243-260.
- Olsen RW, Sieghart W (2009) GABAA receptors: Subtypes provide diversity of function and pharmacology. *Neuropharmacology* 56:141-148.
- Owens DF, Boyce LH, Davis MBE, Kriegstein AR (1996) Excitatory GABA Responses in Embryonic and Neonatal Cortical Slices Demonstrated by Gramicidin Perforated-Patch Recordings and Calcium Imaging. *The Journal of Neuroscience* 16:6414-6423.
- Pan Z-H, Zhang D, Zhang X, Lipton SA (2000) Evidence for coassembly of mutant GABACp1 with GABA α 2S, glycine α 1 and glycine α 2 receptor subunits in vitro. *European Journal of Neuroscience* 12:3137-3145.
- Pandamooz S, Nabiuni M, Miyan J, Ahmadiani A, Dargahi L (2015) Organotypic Spinal Cord Culture: a Proper Platform for the Functional Screening. *Mol Neurobiol* 1-16.
- Papouin T, Ladepeche L, Ruel J, Sacchi S, Labasque M, Hanini M, Groc L, Pollegioni L, Mothet JP, Oliet SH (2012) Synaptic and extrasynaptic NMDA receptors are gated by different endogenous coagonists. *Cell* 150:633-646.
- Paul J, Zeilhofer HU, Fritschy J-M (2012) Selective distribution of GABAA receptor subtypes in mouse spinal dorsal horn neurons and primary afferents. *Journal of Comparative Neurology* 520:3895-3911.
- Perreault P, Avoli M (1991) Physiology and pharmacology of epileptiform activity induced by 4-aminopyridine in rat hippocampal slices. *Journal of neurophysiology* 65:771-785.
- Ploner M, Gross J, Timmermann L, Pollok B, Schnitzler A (2006) Oscillatory activity reflects the excitability of the human somatosensory system. *NeuroImage* 32:1231-1236.
- Poisbeau P, Patte-Mensah C, Keller AF, Barrot M, Breton J-D, Luis-Delgado OE, Freund-Mercier MJ, Mensah-Nyagan AG, Schlichter R (2005) Inflammatory Pain Upregulates Spinal Inhibition via Endogenous Neurosteroid Production. *The Journal of Neuroscience* 25:11768-11776.
- Polgar E, Durrieux C, Hughes DI, Todd AJ (2013) A quantitative study of inhibitory interneurons in laminae I-III of the mouse spinal dorsal horn. *PLoS one* 8:e78309.
- Polgar E, Hughes DI, Arham AZ, Todd AJ (2005) Loss of neurons from laminae I-III of the spinal dorsal horn is not required for development of tactile allodynia in the spared nerve injury model of neuropathic pain. *The Journal of neuroscience : the official journal of the Society for Neuroscience* 25:6658-6666.
- Polgar E, Hughes DI, Riddell JS, Maxwell DJ, Puskar Z, Todd AJ (2003) Selective loss of spinal GABAergic or glycinergic neurons is not necessary for development of thermal hyperalgesia in the chronic constriction injury model of neuropathic pain. *Pain* 104:229-239.
- Polgár E, Sardella TCP, Tiong SYX, Locke S, Watanabe M, Todd AJ (2013) Functional differences between neurochemically defined populations of inhibitory interneurons in the rat spinal dorsal horn. *PAIN®* 154:2606-2615.
- Poulter M, Barker J, O'Carroll A, Lolait S, Mahan L (1992) Differential and transient expression of GABAA receptor alpha-subunit mRNAs in the developing rat CNS. *The Journal of Neuroscience* 12:2888-2900.

- Pratten M, Ahir BK, Smith-Hurst H, Memon S, Mutch P, Cumberland P (2012) Primary cell and micromass culture in assessing developmental toxicity. *Methods Mol Biol* 889:115-146.
- Prescott SA, Sejnowski TJ, De Koninck Y (2006) Reduction of anion reversal potential subverts the inhibitory control of firing rate in spinal lamina I neurons: towards a biophysical basis for neuropathic pain. *Molecular pain* 2:32-32.
- Pribilla I, Takagi T, Langosch D, Bormann J, Betz H (1992) The atypical M2 segment of the beta subunit confers picrotoxinin resistance to inhibitory glycine receptor channels. *The EMBO journal* 11:4305-4311.
- Punnakkal P, von Schoultz C, Haenraets K, Wildner H, Zeilhofer HU (2014) Morphological, biophysical and synaptic properties of glutamatergic neurons of the mouse spinal dorsal horn. *The Journal of physiology* 592:759-776.
- Quadrato G, Elnaggar MY, Duman C, Sabino A, Forsberg K, Di Giovanni S (2014) Modulation of GABAA receptor signaling increases neurogenesis and suppresses anxiety through NFATc4. *The Journal of neuroscience : the official journal of the Society for Neuroscience* 34:8630-8645.
- Quinn KP, Dong L, Golder FJ, Winkelstein BA (2010) Neuronal hyperexcitability in the dorsal horn after painful facet joint injury. *Pain* 151:414-421.
- Racz I, Schutz B, Abo-Salem OM, Zimmer A (2005) Visceral, inflammatory and neuropathic pain in glycine receptor alpha 3-deficient mice. *Neuroreport* 16:2025-2028.
- Rand TA, Ginalski K, Grishin NV, Wang X (2004) Biochemical identification of Argonaute 2 as the sole protein required for RNA-induced silencing complex activity. *Proceedings of the National Academy of Sciences of the United States of America* 101:14385-14389.
- Ransom BR, Neale E, Henkart M, Bullock PN, Nelson PG (1977) Mouse spinal cord in cell culture. I. Morphology and intrinsic neuronal electrophysiologic properties. *Journal of neurophysiology* 40:1132-1150.
- Ravikumar M, Jain S, Miller RH, Capadona JR, Selkirk SM (2012) An organotypic spinal cord slice culture model to quantify neurodegeneration. *Journal of neuroscience methods* 211:280-288.
- Rees MI, Lewis TM, Kwok JB, Mortier GR, Govaert P, Snell RG, Schofield PR, Owen MJ (2002) Hyperekplexia associated with compound heterozygote mutations in the beta-subunit of the human inhibitory glycine receptor (GLRB). *Human molecular genetics* 11:853-860.
- Reeve AJ, Dickenson AH, Kerr NC (1998) Spinal effects of bicuculline: modulation of an allodynia-like state by an A1-receptor agonist, morphine, and an NMDA-receptor antagonist. *Journal of neurophysiology* 79:1494-1507.
- Rexed B (1952) The cytoarchitectonic organization of the spinal cord in the cat. *The Journal of comparative neurology* 96:414-495.
- Richardson JE, Garcia PS, O'Toole KK, Derry JM, Bell SV, Jenkins A (2007) A conserved tyrosine in the beta2 subunit M4 segment is a determinant of gamma-aminobutyric acid type A receptor sensitivity to propofol. *Anesthesiology* 107:412-418.
- Rivera C, Li H, Thomas-Crusells J, Lahtinen H, Viitanen T, Nanobashvili A, Kokaia Z, Airaksinen MS, Voipio J, Kaila K, Saarma M (2002) BDNF-induced TrkB activation down-regulates the K⁺-Cl⁻ cotransporter KCC2 and impairs neuronal Cl⁻ extrusion. *The Journal of cell biology* 159:747-752.
- Rivera C, Voipio J, Payne JA, Ruusuvaari E, Lahtinen H, Lamsa K, Pirvola U, Saarma M, Kaila K (1999) The K⁺/Cl⁻ co-transporter KCC2 renders GABA hyperpolarizing during neuronal maturation. *Nature* 397:251-255.
- Rivera C, Voipio J, Thomas-Crusells J, Li H, Emri Z, Sipila S, Payne JA, Minichiello L, Saarma M, Kaila K (2004) Mechanism of activity-dependent downregulation of the neuron-specific K-Cl cotransporter KCC2. *The Journal*

- of neuroscience : the official journal of the Society for Neuroscience 24:4683-4691.
- Rode F, Jensen DG, Blackburn-Munro G, Bjerrum OJ (2005) Centrally-mediated antinociceptive actions of GABA(A) receptor agonists in the rat spared nerve injury model of neuropathic pain. *European journal of pharmacology* 516:131-138.
- Rossi DJ, Hamann M (1998) Spillover-Mediated Transmission at Inhibitory Synapses Promoted by High Affinity $\alpha 6$ Subunit GABAA Receptors and Glomerular Geometry. *Neuron* 20:783-795.
- Ruscheweyh R, Sandkuhler J (2003) Epileptiform activity in rat spinal dorsal horn in vitro has common features with neuropathic pain. *Pain* 105:327-338.
- Ruscheweyh R, Sandkuhler J (2005) Long-range oscillatory Ca^{2+} waves in rat spinal dorsal horn. *The European journal of neuroscience* 22:1967-1976.
- Ruscheweyh R, Wilder-Smith O, Drdla R, Liu XG, Sandkuhler J (2011) Long-term potentiation in spinal nociceptive pathways as a novel target for pain therapy. *Molecular pain* 7:20.
- Russo D, Clavenzani P, Sorteni C, Bo Minelli L, Botti M, Gazza F, Panu R, Ragionieri L, Chiocchetti R (2013) Neurochemical features of boar lumbosacral dorsal root ganglion neurons and characterization of sensory neurons innervating the urinary bladder trigone. *The Journal of comparative neurology* 521:342-366.
- Samad TA, Moore KA, Sapirstein A, Billet S, Allchorne A, Poole S, Bonventre JV, Woolf CJ (2001) Interleukin-1[β]-mediated induction of Cox-2 in the CNS contributes to inflammatory pain hypersensitivity. *Nature* 410:471-475.
- Sandkühler J (2009) Models and Mechanisms of Hyperalgesia and Allodynia. *Physiological reviews* 89:707-758.
- Sandkuhler J, Eblen-Zajjur AA (1994) Identification and characterization of rhythmic nociceptive and non-nociceptive spinal dorsal horn neurons in the rat. *Neuroscience* 61:991-1006.
- Sardella TCP, Polgár E, Watanabe M, Todd AJ (2011) A quantitative study of neuronal nitric oxide synthase expression in laminae I–III of the rat spinal dorsal horn. *Neuroscience* 192:708-720.
- Sarnthein J, Stern J, Aufenberg C, Rousson V, Jeanmonod D (2006) Increased EEG power and slowed dominant frequency in patients with neurogenic pain. *Brain : a journal of neurology* 129:55-64.
- Sato K, Zhang JH, Saika T, Sato M, Tada K, Tohyama M (1991) Localization of glycine receptor $\alpha 1$ subunit mRNA-containing neurons in the rat brain: An analysis using in situ hybridization histochemistry. *Neuroscience* 43:381-395.
- Saxena NC, Macdonald RL (1996) Properties of putative cerebellar gamma-aminobutyric acid A receptor isoforms. *Molecular pharmacology* 49:567-579.
- Schmidtko A, Tegeder I, Geisslinger G (2009) No NO, no pain? The role of nitric oxide and cGMP in spinal pain processing. *Trends in Neurosciences* 32:339-346.
- Schmieden V, Betz H (1995) Pharmacology of the inhibitory glycine receptor: agonist and antagonist actions of amino acids and piperidine carboxylic acid compounds. *Molecular pharmacology* 48:919-927.
- Schmieden V, Grenningloh G, Schofield PR, Betz H (1989) Functional expression in *Xenopus* oocytes of the strychnine binding 48 kd subunit of the glycine receptor. *The EMBO journal* 8:695-700.
- Schmieden V, Kuhse J, Betz H (1993) Mutation of glycine receptor subunit creates beta-alanine receptor responsive to GABA. *Science* 262:256-258.
- Schoenen J (1982) The dendritic organization of the human spinal cord: the dorsal horn. *Neuroscience* 7:2057-2087.

- Schofield PR, Darlison MG, Fujita N, Burt DR, Stephenson FA, Rodriguez H, Rhee LM, Ramachandran J, Reale V, Glencorse TA, Seeburg PH, Barnard EA (1987) Sequence and functional expression of the GABAA receptor shows a ligand-gated receptor super-family. *Nature* 328:221-227.
- Scholz J, Broom DC, Youn DH, Mills CD, Kohno T, Suter MR, Moore KA, Decosterd I, Coggeshall RE, Woolf CJ (2005) Blocking caspase activity prevents transsynaptic neuronal apoptosis and the loss of inhibition in lamina II of the dorsal horn after peripheral nerve injury. *The Journal of neuroscience : the official journal of the Society for Neuroscience* 25:7317-7323.
- Seelke AMH, Dooley JC, Krubitzer LA (2013) Differential changes in the cellular composition of the developing marsupial brain. *Journal of Comparative Neurology* 521:2602-2620.
- Sejnowski TJ, Destexhe A (2000) Why do we sleep? *Brain research* 886:208-223.
- Shen H-Y, van Vliet Erwin A, Bright K-A, Hanthorn M, Lytle NK, Gorter J, Aronica E, Boison D (2015) Glycine transporter 1 is a target for the treatment of epilepsy. *Neuropharmacology* 99:554-565.
- Shen H, Gong QH, Yuan M, Smith SS (2005) Short-term steroid treatment increases delta GABAA receptor subunit expression in rat CA1 hippocampus: pharmacological and behavioral effects. *Neuropharmacology* 49:573-586.
- Sherman SE, Loomis CW (1994) Morphine insensitive allodynia is produced by intrathecal strychnine in the lightly anesthetized rat. *Pain* 56:17-29.
- Shi SH, Hayashi Y, Petralia RS, Zaman SH, Wenthold RJ, Svoboda K, Malinow R (1999) Rapid spine delivery and redistribution of AMPA receptors after synaptic NMDA receptor activation. *Science* 284:1811-1816.
- Sieghart W, Sperk G (2002) Subunit composition, distribution and function of GABA(A) receptor subtypes. *Current topics in medicinal chemistry* 2:795-816.
- Silva LR, Amitai Y, Connors BW (1991) Intrinsic oscillations of neocortex generated by layer 5 pyramidal neurons. *Science* 251:432-435.
- Simon J, Wakimoto H, Fujita N, Lalande M, Barnard EA (2004) Analysis of the Set of GABAA Receptor Genes in the Human Genome. *Journal of Biological Chemistry* 279:41422-41435.
- Sivilotti L, Woolf CJ (1994) The contribution of GABAA and glycine receptors to central sensitization: disinhibition and touch-evoked allodynia in the spinal cord. *Journal of neurophysiology* 72:169-179.
- Smith C, Kongsamut S, Wang H, Ji J, Kang J, Rampe D (2009) In Vitro electrophysiological activity of nerispiridine, a novel 4-aminopyridine derivative. *Clinical and Experimental Pharmacology and Physiology* 36:1104-1109.
- Smith DAS, Connick JH, Stone TW (1989) Effect of changing extracellular levels of magnesium on spontaneous activity and glutamate release in the mouse neocortical slice. *British Journal of Pharmacology* 97:475-482.
- Smith GB, Olsen RW (1995) Functional domains of GABAA receptors. *Trends in Pharmacological Sciences* 16:162-168.
- Smith KM, Boyle KA, Madden JF, Dickinson SA, Jobling P, Callister RJ, Hughes DI, Graham BA (2015) Functional heterogeneity of calretinin-expressing neurons in the mouse superficial dorsal horn: implications for spinal pain processing. *The Journal of physiology* 593:4319-4339.
- Sohal VS, Keist R, Rudolph U, Huguenard JR (2003) Dynamic GABA(A) receptor subtype-specific modulation of the synchrony and duration of thalamic oscillations. *The Journal of neuroscience : the official journal of the Society for Neuroscience* 23:3649-3657.
- Sohal VS, Zhang F, Yizhar O, Deisseroth K (2009) Parvalbumin neurons and gamma rhythms enhance cortical circuit performance. *Nature* 459:698-702.

- Sokal D, Chapman V (2003) Inhibitory effects of spinal baclofen on spinal dorsal horn neurones in inflamed and neuropathic rats in vivo. *Brain research* 987:67-75.
- Soltesz I, Deschenes M (1993) Low- and high-frequency membrane potential oscillations during theta activity in CA1 and CA3 pyramidal neurons of the rat hippocampus under ketamine-xylazine anesthesia. *Journal of neurophysiology* 70:97-116.
- Somers DL, Clemente FR (2002) Dorsal horn synaptosomal content of aspartate, glutamate, glycine and GABA are differentially altered following chronic constriction injury to the rat sciatic nerve. *Neuroscience letters* 323:171-174.
- Sorkin LS, Puig S, Jones DL (1998) Spinal bicuculline produces hypersensitivity of dorsal horn neurons: effects of excitatory amino acid antagonists. *Pain* 77:181-190.
- Spencer SS, Lee SA (2000) Invasive EEG in neocortical epilepsy: seizure onset. *Advances in neurology* 84:275-285.
- Spira ME, Hai A (2013) Multi-electrode array technologies for neuroscience and cardiology. *Nature nanotechnology* 8:83-94.
- Staley KJ, Soldo BL, Proctor WR (1995) Ionic mechanisms of neuronal excitation by inhibitory GABA_A receptors. *Science* 269:977-981.
- Stein C (2013) Opioids, sensory systems and chronic pain. *European journal of pharmacology* 716:179-187.
- Stórustovu S, Ebert B (2003) Gaboxadol: in vitro interaction studies with benzodiazepines and ethanol suggest functional selectivity. *European journal of pharmacology* 467:49-56.
- Streit J (1993) Regular oscillations of synaptic activity in spinal networks in vitro. *Journal of neurophysiology* 70:871-878.
- Streit J, Tscherter A, Heuschkel MO, Renaud P (2001) The generation of rhythmic activity in dissociated cultures of rat spinal cord. *The European journal of neuroscience* 14:191-202.
- Succol F, Fiumelli H, Benfenati F, Cancedda L, Barberis A (2012) Intracellular chloride concentration influences the GABA_A receptor subunit composition. *Nature communications* 3:738.
- Swerdlow M (1984) Anticonvulsant drugs and chronic pain. *Clinical neuropharmacology* 7:51-82.
- Taccola G, Nistri A (2005) Characteristics of the electrical oscillations evoked by 4-aminopyridine on dorsal root fibers and their relation to fictive locomotor patterns in the rat spinal cord in vitro. *Neuroscience* 132:1187-1197.
- Taccola G, Nistri A (2006) Oscillatory circuits underlying locomotor networks in the rat spinal cord. *Critical reviews in neurobiology* 18:25-36.
- Takaishi K, Eisele JH, Jr., Carstens E (1996) Behavioral and electrophysiological assessment of hyperalgesia and changes in dorsal horn responses following partial sciatic nerve ligation in rats. *Pain* 66:297-306.
- Takazawa T, MacDermott AB (2010) Glycinergic and GABAergic tonic inhibition fine tune inhibitory control in regionally distinct subpopulations of dorsal horn neurons. *The Journal of physiology* 588:2571-2587.
- Takehara A, Hosokawa M, Eguchi H, Ohigashi H, Ishikawa O, Nakamura Y, Nakagawa H (2007) γ -Aminobutyric Acid (GABA) Stimulates Pancreatic Cancer Growth through Overexpressing GABA_A Receptor π Subunit. *Cancer Research* 67:9704-9712.
- Tao YX, Hassan A, Haddad E, Johns RA (1999) Expression and action of cyclic GMP-dependent protein kinase I α in inflammatory hyperalgesia in rat spinal cord. *Neuroscience* 95:525-533.
- Teyler TJ (1980) Brain slice preparation: hippocampus. *Brain research bulletin* 5:391-403.

- Tibau E, Valencia M, Soriano J (2013) Identification of neuronal network properties from the spectral analysis of calcium imaging signals in neuronal cultures. *Frontiers in Neural Circuits* 7:199.
- Tiesinga P, Sejnowski TJ (2009) Cortical enlightenment: are attentional gamma oscillations driven by ING or PING? *Neuron* 63:727-732.
- Todd AJ (2010) Neuronal circuitry for pain processing in the dorsal horn. *Nature reviews Neuroscience* 11:823-836.
- Todd AJ, Hughes DI, Polgar E, Nagy GG, Mackie M, Ottersen OP, Maxwell DJ (2003) The expression of vesicular glutamate transporters VGLUT1 and VGLUT2 in neurochemically defined axonal populations in the rat spinal cord with emphasis on the dorsal horn. *The European journal of neuroscience* 17:13-27.
- Todd AJ, McKenzie J (1989) GABA-immunoreactive neurons in the dorsal horn of the rat spinal cord. *Neuroscience* 31:799-806.
- Todd AJ, Spike RC (1993) The localization of classical transmitters and neuropeptides within neurons in laminae I-III of the mammalian spinal dorsal horn. *Progress in neurobiology* 41:609-645.
- Todd AJ, Sullivan AC (1990) Light microscope study of the coexistence of GABA-like and glycine-like immunoreactivities in the spinal cord of the rat. *The Journal of comparative neurology* 296:496-505.
- Tohidi V, Nadim F (2009) Membrane resonance in bursting pacemaker neurons of an oscillatory network is correlated with network frequency. *The Journal of neuroscience : the official journal of the Society for Neuroscience* 29:6427-6435.
- Tomita S, Stein V, Stocker TJ, Nicoll RA, Brecht DS (2005) Bidirectional synaptic plasticity regulated by phosphorylation of stargazin-like TARPs. *Neuron* 45:269-277.
- Tong CK, MacDermott AB (2014) Synaptic GluN2A and GluN2B containing NMDA receptors within the superficial dorsal horn activated following primary afferent stimulation. *The Journal of neuroscience : the official journal of the Society for Neuroscience* 34:10808-10820.
- Treede RD, Kenshalo DR, Gracely RH, Jones AK (1999) The cortical representation of pain. *Pain* 79:105-111.
- Tretter V, Ehya N, Fuchs K, Sieghart W (1997) Stoichiometry and Assembly of a Recombinant GABAA Receptor Subtype. *The Journal of Neuroscience* 17:2728-2737.
- Urch CE, Dickenson AH (2003) In vivo single unit extracellular recordings from spinal cord neurones of rats. *Brain Research Protocols* 12:26-34.
- Valtschanoff JG, Weinberg RJ, Rustioni A, Schmidt HH (1992) Nitric oxide synthase and GABA colocalize in lamina II of rat spinal cord. *Neuroscience letters* 148:6-10.
- Venard C, Boujedaini N, Belon P, Mensah-Nyagan AG, Patte-Mensah C (2008) Regulation of neurosteroid allopregnanolone biosynthesis in the rat spinal cord by glycine and the alkaloidal analogs strychnine and gelsemine. *Neuroscience* 153:154-161.
- Venard C, Boujedaini N, Mensah-Nyagan AG, Patte-Mensah C (2011) Comparative Analysis of Gelsemine and Gelsemium sempervirens Activity on Neurosteroid Allopregnanolone Formation in the Spinal Cord and Limbic System. *Evidence-Based Complementary and Alternative Medicine* 2011.
- Viitanen T, Ruusuvuori E, Kaila K, Voipio J (2010) The K⁺-Cl⁻ cotransporter KCC2 promotes GABAergic excitation in the mature rat hippocampus. *The Journal of physiology* 588:1527-1540.
- Vikman KS, Hill RH, Backstrom E, Robertson B, Kristensson K (2003) Interferon-gamma induces characteristics of central sensitization in spinal dorsal horn neurons in vitro. *Pain* 106:241-251.

- Vikman KS, Kristensson K, Hill RH (2001) Sensitization of dorsal horn neurons in a two-compartment cell culture model: wind-up and long-term potentiation-like responses. *The Journal of neuroscience : the official journal of the Society for Neuroscience* 21:RC169.
- Visockis V, King AE (2013) M-channels modulate network excitatory activity induced by 4-aminopyridine in immature rat substantia gelatinosa in vitro. *Brain research* 1513:9-16.
- Volman V, Behrens MM, Sejnowski TJ (2011) Downregulation of Parvalbumin at Cortical GABA Synapses Reduces Network Gamma Oscillatory Activity. *The Journal of neuroscience : the official journal of the Society for Neuroscience* 31:18137-18148.
- Voss J, Sanchez C, Michelsen S, Ebert B (2003) Rotarod studies in the rat of the GABAA receptor agonist gaboxadol: lack of ethanol potentiation and benzodiazepine cross-tolerance. *European journal of pharmacology* 482:215-222.
- Wafford KA, Ebert B (2006) Gaboxadol--a new awakening in sleep. *Current opinion in pharmacology* 6:30-36.
- Wakai A, Kohno T, Yamakura T, Okamoto M, Ataka T, Baba H (2005) Action of isoflurane on the substantia gelatinosa neurons of the adult rat spinal cord. *Anesthesiology* 102:379-386.
- Waldvogel HJ, Baer K, Snell RG, During MJ, Faull RLM, Rees MI (2003) Distribution of gephyrin in the human brain: an immunohistochemical analysis. *Neuroscience* 116:145-156.
- Wang X-J, Buzsáki G (1996) Gamma Oscillation by Synaptic Inhibition in a Hippocampal Interneuronal Network Model. *The Journal of Neuroscience* 16:6402-6413.
- Wang X, Sun Q-Q (2012) Characterization of axo-axonic synapses in the piriform cortex of *Mus musculus*. *The Journal of comparative neurology* 520:832-847.
- Watanabe E, Akagi H (1995) Distribution patterns of mRNAs encoding glycine receptor channels in the developing rat spinal cord. *Neuroscience Research* 23:377-382.
- Watanabe M, Fukuda A (2015) Development and regulation of chloride homeostasis in the central nervous system. *Frontiers in cellular neuroscience* 9:371.
- Watts AE, Jefferys JG (1993) Effects of carbamazepine and baclofen on 4-aminopyridine-induced epileptic activity in rat hippocampal slices. *British journal of pharmacology* 108:819-823.
- Whitehead KA, Langer R, Anderson DG (2009) Knocking down barriers: advances in siRNA delivery. *Nature reviews Drug discovery* 8:129-138.
- Whittington MA, Traub RD, Kopell N, Ermentrout B, Buhl EH (2000) Inhibition-based rhythms: experimental and mathematical observations on network dynamics. *International Journal of Psychophysiology* 38:315-336.
- Wisden W, Cope D, Klausberger T, Hauer B, Sinkkonen ST, Tretter V, Lujan R, Jones A, Korpi ER, Mody I, Sieghart W, Somogyi P (2002) Ectopic expression of the GABAA receptor $\alpha 6$ subunit in hippocampal pyramidal neurons produces extrasynaptic receptors and an increased tonic inhibition. *Neuropharmacology* 43:530-549.
- Wolfrum C, Shi S, Jayaprakash KN, Jayaraman M, Wang G, Pandey RK, Rajeev KG, Nakayama T, Charrise K, Ndungo EM, Zimmermann T, Kotliansky V, Manoharan M, Stoffel M (2007) Mechanisms and optimization of in vivo delivery of lipophilic siRNAs. *Nature biotechnology* 25:1149-1157.
- Woolf CJ (2010) Overcoming obstacles to developing new analgesics. *Nat Med* 16:1241-1247.
- Wu Y-e, Li Y-d, Luo Y-j, Wang T-x, Wang H-j, Chen S-n, Qu W-m, Huang Z-l (2015a) Gelsemine alleviates both neuropathic pain and sleep disturbance in

- partial sciatic nerve ligation mice. *Acta pharmacologica Sinica* 36:1308-1317.
- Wu YE, Li YD, Luo YJ, Wang TX, Wang HJ, Chen SN, Qu WM, Huang ZL (2015b) Gelsemine alleviates both neuropathic pain and sleep disturbance in partial sciatic nerve ligation mice. *Acta pharmacologica Sinica*.
- Wu Z, Guo Z, Gearing M, Chen G (2014) Tonic inhibition in dentate gyrus impairs long-term potentiation and memory in an Alzheimer's [corrected] disease model. *Nature communications* 5:4159.
- Xia J, Pan R, Gao X, Meucci O, Hu H (2014) Native store-operated calcium channels are functionally expressed in mouse spinal cord dorsal horn neurons and regulate resting calcium homeostasis. *The Journal of physiology* 592:3443-3461.
- Xiang G, Pan L, Huang L, Yu Z, Song X, Cheng J, Xing W, Zhou Y (2007) Microelectrode array-based system for neuropharmacological applications with cortical neurons cultured in vitro. *Biosensors and Bioelectronics* 22:2478-2484.
- Yajima Y, Narita M, Tsuda M, Imai S, Kamei J, Nagase H, Suzuki T (2000) Modulation of NMDA- and (+)TAN-67-induced nociception by GABA(B) receptors in the mouse spinal cord. *Life sciences* 68:719-725.
- Yaksh TL (1989) Behavioral and autonomic correlates of the tactile evoked allodynia produced by spinal glycine inhibition: effects of modulatory receptor systems and excitatory amino acid antagonists. *Pain* 37:111-123.
- Yamamoto C, McIlwain H (1966) Electrical activities in thin sections from the mammalian brain maintained in chemically-defined media in vitro. *Journal of neurochemistry* 13:1333-1343.
- Yamamoto T, Yaksh TL (1993) Effects of intrathecal strychnine and bicuculline on nerve compression-induced thermal hyperalgesia and selective antagonism by MK-801. *Pain* 54:79-84.
- Yang K, Ma R, Wang Q, Jiang P, Li YQ (2015) Optoactivation of parvalbumin neurons in the spinal dorsal horn evokes GABA release that is regulated by presynaptic GABAB receptors. *Neuroscience letters* 594:55-59.
- Yang K, Ma WL, Feng YP, Dong YX, Li YQ (2002) Origins of GABA(B) receptor-like immunoreactive terminals in the rat spinal dorsal horn. *Brain research bulletin* 58:499-507.
- Yang K, Wang D, Li YQ (2001) Distribution and depression of the GABA(B) receptor in the spinal dorsal horn of adult rat. *Brain research bulletin* 55:479-485.
- Yang Z, Cromer BA, Harvey RJ, Parker MW, Lynch JW (2007) A proposed structural basis for picrotoxinin and picrotin binding in the glycine receptor pore. *Journal of neurochemistry* 103:580-589.
- Yasaka T, Tiong SY, Hughes DI, Riddell JS, Todd AJ (2010) Populations of inhibitory and excitatory interneurons in lamina II of the adult rat spinal dorsal horn revealed by a combined electrophysiological and anatomical approach. *Pain* 151:475-488.
- Yee JK, Miyanochara A, LaPorte P, Bouic K, Burns JC, Friedmann T (1994) A general method for the generation of high-titer, pantropic retroviral vectors: highly efficient infection of primary hepatocytes. *Proceedings of the National Academy of Sciences of the United States of America* 91:9564-9568.
- Yoon YJ, Gokin AP, Martin-Caraballo M (2010) Pharmacological manipulation of GABA-driven activity in ovo disrupts the development of dendritic morphology but not the maturation of spinal cord network activity. *Neural Development* 5:11-11.
- Youn D-h, Gerber G, Sather WA (2013) Ionotropic Glutamate Receptors and Voltage-Gated Ca(2+) Channels in Long-Term Potentiation of Spinal Dorsal Horn Synapses and Pain Hypersensitivity. *Neural Plasticity* 2013:654257.

- Young-Pearse TL, Ivic L, Kriegstein AR, Cepko CL (2006) Characterization of mice with targeted deletion of glycine receptor alpha 2. *Molecular and cellular biology* 26:5728-5734.
- Young AB, Snyder SH (1973) Strychnine Binding Associated with Glycine Receptors of the Central Nervous System. *Proceedings of the National Academy of Sciences of the United States of America* 70:2832-2836.
- Zafrakas M, Chorovicer M, Klamann I, Kristiansen G, Wild P-J, Heindrichs U, Knüchel R, Dahl E (2006) Systematic characterisation of GABRP expression in sporadic breast cancer and normal breast tissue. *International Journal of Cancer* 118:1453-1459.
- Zeilhofer HU, Möhler H, Di Lio A (2009) GABAergic analgesia: new insights from mutant mice and subtype-selective agonists. *Trends in Pharmacological Sciences* 30:397-402.
- Zeilhofer HU, Wildner H, Yevenes GE (2012) Fast synaptic inhibition in spinal sensory processing and pain control. *Physiological reviews* 92:193-235.
- Zelano J, Berg A, Thams S, Hailer NP, Cullheim S (2009) SynCAM1 expression correlates with restoration of central synapses on spinal motoneurons after two different models of peripheral nerve injury. *The Journal of comparative neurology* 517:670-682.
- Zhang J, Xue F, Chang Y (2008a) Structural Determinants for Antagonist Pharmacology That Distinguish the $\rho 1$ GABAC Receptor from GABAA Receptors. *Molecular pharmacology* 74:941-951.
- Zhang JY, Gong N, Huang JL, Guo LC, Wang YX (2013) Gelsemine, a principal alkaloid from *Gelsemium sempervirens* Ait., exhibits potent and specific antinociception in chronic pain by acting at spinal $\alpha 3$ glycine receptors. *Pain* 154:2452-2462.
- Zhang JY, Wang YX (2015) Gelsemium analgesia and the spinal glycine receptor/allopregnanolone pathway. *Fitoterapia* 100:35-43.
- Zhang LL, Fina ME, Vardi N (2006) Regulation of KCC2 and NKCC during development: membrane insertion and differences between cell types. *The Journal of comparative neurology* 499:132-143.
- Zhang M, Møller M, Broman J, Sukiasyan N, Wienecke J, Hultborn H (2008b) Expression of calcium channel CaV1.3 in cat spinal cord: Light and electron microscopic immunohistochemical study. *The Journal of comparative neurology* 507:1109-1127.
- Zhang W, Liu LY, Xu TL (2008c) Reduced potassium-chloride co-transporter expression in spinal cord dorsal horn neurons contributes to inflammatory pain hypersensitivity in rats. *Neuroscience* 152:502-510.
- Zhang XC, Zhang YQ, Zhao ZQ (2005) Involvement of nitric oxide in long-term potentiation of spinal nociceptive responses in rats. *Neuroreport* 16:1197-1201.
- Zheng J, Lu Y, Perl ER (2010) Inhibitory neurones of the spinal substantia gelatinosa mediate interaction of signals from primary afferents. *Journal of Physiology* 588:2065-2075.
- Zhou C, Huang Z, Ding L, Deel ME, Arain FM, Murray CR, Patel RS, Flanagan CD, Gallagher MJ (2013) Altered cortical GABAA receptor composition, physiology, and endocytosis in a mouse model of a human genetic absence epilepsy syndrome. *The Journal of biological chemistry* 288:21458-21472.